CRANFIELD UNIVERSITY
SCHOOL OF MECHANICAL ENGINEERING
DEPARTMENT OF APPLIED ENERGY

PhD Thesis

Academic Year 1993-94

RAJNISH KAUR CALAY

ELECTROMAGNETIC HEATING PROCESSES - ANALYSES AND SIMULATIONS

SUPERVISOR: Dr. M.NEWBOROUGH

August-1994

This thesis is submitted in partial fulfilment for the degree of Doctor of Philosophy

ABSTRACT

Electromagnetic heating (EMH) processes are being increasingly used in the industrial and domestic sectors, yet they receive relatively little attention in the thermal engineering domain. Time-temperature characteristics in EMH are qualitatively different from those in conventional heating techniques due to the additional parameters (viz dielectric properties of the material, size and shape of the product and process frequency). From a unified theory perspective, a multi-purpose model has been developed in order to obtain the heating characteristics for an arbitrary processing situation. Theoretical analyses of various EMH processes in materials of various regular geometries and a range of physical properties have been undertaken.

Despite the wide spread usage of microwave energy in the food engineering sector, few understand microwaves and their interactions with foods. Much of the published research is largely focussed from the view point of an electrical engineer and aimed at the oven designer. However, trial-and-error methods are usually employed when developing microwavable food products and when using microwave ovens. The presented thesis is focussed from the view-point of the thermal engineer and aimed primarily at food developers and end users.

The multi-purpose model was then modified specifically for simulating the heating of food materials in a microwave oven. The validity of the commonly made assumptions was investigated; in particular the variation of dielectric properties during the heating processes and their likely influence on the model's predictions. Experimental data available in the literature were compiled and analysed to form a set of equations for predicting the dielectric properties of various food materials. Also available correlations for thermal properties were evaluated for a selected set of experimental data of different food materials. Analyses were undertaken to demonstrate and evaluate the effects of various parameters on the heating characteristics of different food materials commonly heated/cooked in microwave ovens. A qualitative comparison of

model predictions and experimental measurements is provided to validate the physical basis of the model. Findings from the model lead to a better understanding of the interactions between foods and microwaves.

Another dilemma, for the product developer and the user alike, is the difference in the actual output power of MW ovens when heating different foods in varying quantities and in different containers. Variations in test methods adopted by different oven manufacturers and the need to define and standardise effective test procedures are discussed. The suitability of a synthetic hydrophilic material as a food simulator for testing microwave ovens has been investigated. It was found that hydrophilic polymeric gels of different water uptakes can be employed successfully as test loads for measuring power output and heating uniformity in certain foods of various geometries and dielectric properties in microwave ovens. The hydrophilic materials were found to provide reproducible results, so their use would eliminate one cause of variations in the present test methods. Although these synthetic materials can not simulate certain qualitative aspects of real foods (e.g. shrinkage of meat fibres or volumetric expansion of cakes and breads), good agreement was found between the cooking of meat and hydrophilic polymeric material of 60%-80% water uptake (by mass). Moisture was expressed out of both materials on heating. To the author's knowledge no other model material has been reported to have exhibited similar behaviour. Another attraction of using these materials is their reusability. The material can be fully recovered by drying and no physical and chemical degradation occurs during subsequent uses .

(Following research papers were derived from this work;

1. Multi-purpose mathematical model for EM heating processes, Applied Energy, 44(1993) 337-386
2. Predictive equations for the dielectric properties of foods, accepted for publication in International Journal of Food Science & Technology 1995(30))

ACKNOWLEDGEMENTS

I wish to express my gratitude to Dr.M.Newborough for his valuable advice and guidance throughout the course of this project. My sincere thanks are due to Mr.Charlie Knight for his much needed assistance in the laboratory, the administrative staff of Applied Energy Group and all friends for their help and pleasant nature.

I would also like to thank the scientists and researchers of the various institutes who kindly responded to my queries in connection with this study and offered their kind advice and consultations.

Thanks are due to the Science and Engineering Research Council who provided financial support for the project.

Finally, I must thank my husband Pargat and son Ranbir for their infinite patience, continued support and encouragement over the past few years.

CONTENTS

Page

CHAPTER 1

1 INTRODUCTION

1.1 HISTORICAL BACKGROUND 1
1.2 ELECTROMAGNETIC HEATING 1
1.2.1 Direct resistance heating 3
1.2.2 Induction heating 3
1.2.3 Radio-frequency and microwave heating 4
1.3 OBJECTIVES OF THE STUDY 4
1.4 ORGANISATION OF THE DISSERTATION 8

CHAPTER 2

2 MULTI-PURPOSE MODEL FOR EMH PROCESSES

2.1 THEORY OF EMH 9
2.1.1 Conductive dielectrics 9
2.1.2 Basic electromagnetic equations 10
2.1.3 Attenuation factor and skin depth 14
2.1.4 Power generation in a material 15
2.1.5 Power penetration depth 16
2.1.6 Energy coupling by a material from microwaves 19
2.2 HEAT TRANSFER 26
2.3 SIMULATING ELECTRO-THERMAL PROCESSES 27
2.4 MULTI-PURPOSE THERMAL MODEL 30
2.4.1 One-dimensional model 30
2.4.2 Two-dimensional model 31
2.4.3 Varying material properties 32
2.4.4 Boundary conditions 35
2.5 PARAMETRIC ANALYSIS OF EMH PROCESSES 39
2.6 RESULTS AND DISCUSSION 40
2.6.1 Attenuation factor 51
2.6.2 Thermal conductivity 52
2.6.3 Specific heat capacity and density 52
2.6.4 Surface heat transfer 53
2.7 USING A THERMAL MODEL FOR PRODUCT DEVELOPMENT 54
2.7.1 Input power levels and intermittent heating 61
2.7.2 Multi-layered heterogeneous materials 62
2.8 Temperature dependent material properties 69
2.9 Two-dimensional simulations 69
2.10 CONCLUSIONS 69

CHAPTER 3

3 DIELECTRIC PROPERTIES OF FOODS

3.1 INTRODUCTION 71
3.2 PHYSICAL BASIS OF DIELECTRIC LOSS 73
3.3 MEASURING METHODS 80
3.4 PREDICTIVE MODELS 80

3.4.1 Physiochemical model 80
3.4.2 Models based on experimental data 81
3.5 REVIEW OF EXPERIMENTAL DATA 82
3.5.1 Moisture content 83
3.5.2 Frequency 84
3.5.3 Temperature 84
3.5.4 Fat content 88
3.5.5 Other factors 89
3.6 REGRESSION ANALYSIS 90
3.7 DISCUSSION 91
3.8 CONCLUSIONS 93

CHAPTER 4

4 THERMOPHYSICAL PROPERTIES OF FOODS

4.1 INTRODUCTION 98
4.2 REVIEW 99
4.2.1 Measuring method 99
4.2.2 Experimental data 100
4.3 PREDICTIVE EQUATIONS 101
4.4 Comparison of available predictive equation 103
4.4.1 Specific heat capacity 103
4.4.2 Thermal conductivity 107
4.4.3 Thermal diffusivity 107
4.5 MASS DIFFUSIVITY 108
4.6 FROZEN FOODS 108
4.7 CONCLUSION 110

CHAPTER 5

5 MICROWAVE HEATING OF FOODS

5.1 INTRODUCTION 112
5.2 THEORETICAL BACKGROUND 112
5.2.1 Plane Waves and multi-mode cavity 116
5.2.2 Power Density patterns in Food loads 116
5.3 MATHEMATICAL ANALYSIS 123
5.3.1 Power distribution 126
5.3.2 Temperature distribution 127
5.3.3 Boundary conditions for microwave radiation 128
5.4 PARAMETRIC ANALYSIS 129
5.4.1 Thickness and Dielectric properties 133
5.4.2 Metallic shielding 134
5.4.3 Effect of Temperature on the Power absorption 136
5.4.4 Temperature Distribution 141
5.4.5 Multi-layered Materials 145
5.5 COMPARISON WITH EXPERIMENTAL MEASUREMENTS 145
5.5.1 Experimental details 145
5.5.2 Numerical simulations 149
5.5.3 Results and comparison 149
5.6 CONCLUSIONS 150

CHAPTER 6

6 FOOD MODELS

6.1 INTRODUCTION 151
6.2 PREVIEW 152
6.2.1 Performance Standards 152
6.2.2 Output Power 154
6.2.3 Practical Complexities 158
6.2.4 Synthetic Food models 159
6.3 MATERIALS AND METHODS 160
6.3.1 Characterisation of Real Food Behaviour 160
6.3.2 Characterisation of Hydrogel Material 161
6.4 EXPERIMENTAL PROGRAMME 163
6.4.1 Preparation of sample 163
6.4.2 Test Oven 166
6.4.3 Temperature Measurement 167
6.4.4 Other Measurements 169
6.4.5 Heating Procedure 170
6.4.6 Performance Tests 171
6.5 RESULTS AND DISCUSSIONS 172
6.5.1 Accuracy of employing the post-heating method 173
6.5.2 Cooking Apples 176
6.5.3 Carrots 176
6.5.4 Minced Beef 178
6.5.5 Cake 180
6.5.6 Hydrophilic Material (m=75%) 182
6.5.7 Hydrophilic Material (m=40%) 186
6.6 COMPARISON WITH REAL FOODS 188
6.6.1 Preliminary Tests 188
6.6.2 Performance Tests evaluation 194
6.7 EMPLOYING HYDROPHILIC MATERIALS AS TEST MATERIALS 198
6.8 REUSABILITY OF HYDROPHILIC MATERIAL 202
6.9 CONCLUSIONS 205

CHAPTER 7

7 CONCLUSIONS AND RECOMMENDATIONS

7.1 CONCLUSIONS 207
7.2.SUGGESTIONS FOR FURTHER WORK 209
7.2.1 Mathematical model 209
7.2.2 Dielectric Properties 209
7.2.3 Food Simulators 210
7.2.4 Experimental programme 211
7.3 Post-script 211

REFERENCES 213

APPENDICES

1	Nature of dielectric loss	225
2	Derivation of modified wave equation for EM heating techniques	227
3	Power generated in a dielectric	229
4	Exact solution for power generation in a thin slab for DRH process	231
5	Exact solution for power generation in a thin slab for IH process	233
6	Formulation of numerical method for 1-d calculations	235
7	Numerical method for 2-d calculations	240
8	Least squares approximation	241
9	Other empirical equations for thermal properties compared with the selected data	243
10	Mathematical model for microwave heating of foods	244
11	Hydrophilic materials	250
12	Program Listings	251

LIST OF FIGURES

CHAPTER 2

2.1	Semi-infinite slab subjected to (a) induction heating and (b) microwave heating
2.2	Semi-infinite slab configuration for EM heating
2.3	Propagation of a plane electromagnetic wave through an dielectric
2.4	Variations of electric-field intensity and power with depth for a semi-infinite slab
2.5	Energy transmission, reflection and refraction at the surface of two materials
2.6	Variation of reflection coefficient with incident angle foe TE and TM polarisations and characteristic impedance; a=200Ω; b=100Ω; c=50Ω; d=25Ω
2.7	Configuration for slab (a) heated from one side (b) heated from both sides
2.8	Configuration for (a) cylinder heated radially (b) sphere heated radially
2.9	A qualitative comparison of transient temperature profiles within (a) a slab and (b) a cylinder for different EMH processes
2.10	Temperature-profile developments for (a) a semi infinite slab, and (b) a sphere
2.11	Variation of (a) the transmitted power with respect to the distance into the material and (b) the power density for a sphere and a cylinder
2.12	For a slab, the relationship between (a) the heating effectiveness and attenuation factor and (b) the predicted heating period and the attenuation factor
2.13	Temperature distributions for a range of attenuation factors for (a) a sphere and (b) a slab
2.14	Comparison of the temperature distributions developed within a slab and a sphere

2.15 Temperature profiles for (a) spheres of different radii and (b) slabs of different thicknesses. [Base case material properties and boundary conditions apply]
2.16 Characteristic temperature difference (Tc-Ts) for spheres of various radii and attenuation factors
2.17 Variation of absorbed power with the size of a sphere
2.18 Influence of thermal conductivity on the temperature distribution achieved during microwave heating of a base-case slab
2.19 Relative heating rates for materials of different thermal mass per unit volume
2.20 Effect of the rate of radiative heat-transfer upon the temperature distribution achieved within a base-case slab for microwave heating
2.21 Effect of convective and evaporative heat losses upon the temperature distribution for a base-case
2.22 Comparison of temperature profiles achieved within a base-case slab for various power inputs
2.23 Thermal equilibrium effects during off-duty periods of an intermittent-heating cycle for a base-case
2.24 Comparison of the temperature profiles at the end of heating period for a base case slab when heated (a) continuously and (b) at different "on-off" duty cycles
2.25 Temperature profiles achieved at the end of the base-case heating period within a three-layered slab each layer of thickness 0.02m;
(a) $\alpha_1 = 25\ \bar{m}^1$, $\alpha_2 = 5\ \bar{m}^1$, $\alpha_3 = 50\ \bar{m}^1$
(b) $\alpha_1 = 25\ m^{-1}$, $\alpha_2 = 50\ m^{-1}$, $\alpha_3 = 5\ m^{-1}$
2.26 Comparison of final temperature profiles for a slab (as applies in Fig. 2.24a) with the temperature profile (b) achieved by reducing the thermal mass ($\rho_d C_p$) of the middle layer by 40%
2.27 Comparison of the final temperature profile, of a slab (as applies in Fig. 24a) with that achieved by changing the thickness of the layers y_1, y_2, y_3 to 0.03m, 0.01m and 0.02m respectively
2.28 Variation of attenuation factor and power intensity with temperature for inductively heated mild steel bar
2.29 Predicted temperature-profiles within a base-case potato slab assuming; (i) constant and (ii) temperature dependent physical properties
2.30 Two-dimensional temperature distribution in a base-case slab heated from four sides after 120 seconds
2.31 Two-dimensional temperature distribution in a base-case cylinder, heated radially and axially from the upper surface,after a period of 120 seconds

CHAPTER 3

3.1 Electromagnetic interaction (a) electronic (b) orientational and ionic (c) interfacial polarisations
3.2 Variation of dielectric constant and dielectric loss of water with temperature and frequency

3.3 Variation of permittivity of ionic-aqueous solution with temperature and frequency
3.4 Variation of dielectric constant and dielectric loss with moisture content and frequency
3.5 Variation of ε' and ε'' of various foods with temperature

CHAPTER 4

4.1 C_p of various foods in the temperature range; meats = 0-20°C; eggs = 20-40°C; other =4-30°C and Reidel's correlation
4.2 Variation of thermophysical properties of foods with temperature

CHAPTER 5

5.1 Components of a microwave oven.
5.2 Cavity standing-waves: modes in the x,y,z directions
5.3 Reflection and transmission at normal incidence transverse electromagnetic field (TEM)
5.4a Perpendicular polarisation (TE)
5.4b Parallel Polarisation (TM)
5.5 Practical illustration of edge heating in rectangular slab loads heated in MW ovens.
5.6 A practical illustration of edge heating in flat cylindrical loads heated in MW ovens
5.7 Heating of composite slab by plane waves at normal incidence.
5.8 Heating of composite slab at oblique incidence
5.9a Power density profiles for a plane slab of thicknesses: 0.017m, and 0.02m ($\alpha \approx 52 m^{-1}$)
5.9b Variation in power density profiles for a slab of thicknesses: 0.04m, 0.03m, 0.01m ($\alpha \approx m^{-1}$)
5.10 Comparison of power density profiles in 0.1m thick slabs of butter($\alpha=5m^{-1}$), potato($\alpha=52m^{-1}$), Ham($\alpha=78m^{-1}$)
5.11 Comparison of power density profiles for 0.1m thick slab ($\alpha=5m^{-1}$) calculated by Lambert's law and solving Maxwell's equations
5.12 same as 5.11 but with $\alpha=52m^{-1}$.
5.13 Power density profile for a slab ($\alpha \approx 5m^{-1}$) of thicknesses 0.1m, 0.05m, 0.025m
5.14 As for 5.13 but with $\alpha=52\ m^{-1}$
5.15 Power density pattern for normal and oblique incidence.
5.16 Power density profiles at 2min interval for a slab heated from -5°C, E =3000Vm^{-1}
5.17 Temperature distribution in the slab in Fig.5.16
5.18a Power density profile in a three layered slab (pastry, beef, pastry) 0.01m, 0.035m, and 0.005m thick respectively
5.18b Transient temperature profles for the slab in Fig.5.18a
5.19 Schematic diagram of a slab for numerical simulation
5.20a Comparison of measured temperature distribution (a) with numerical simulation in (b) after 120s
5.20b Comparison of measured temperature distribution (a) with numerical simulation in (b) after 300s

CHAPTER 6

6.1a Variation of power absorbed by a load with the load volume and dielectric properties of materials for a 500W oven.
6.1b Variation of coupling coefficient with dielectric properties and load volume for oven in Fig 6.1a
6.2 Hydrophilic polymeric material.
6.3 Free to bound water characteristics of a hydrophilic polymeric structure.
6.4 Water containment in a hydrophilic structure.
6.5a Labelling scheme for thermocouples.
6.5b Arrangement of thermocouples on a probe
6.6 Temperature profiles for apples.
6.7 Temperature profiles for carrots.
6.8 Temperature profiles for minced beef.
6.9 Temperature profiles for cake.
6.10 Temperature profiles for Hydrophilic material 75% (0.1-1mm).
6.11 Temperature profiles for Hydrophilic material 75% (1-2mm).
6.12 Temperature profiles for Hydrophilic material 40%.
6.13 Heating rates for hydrogel (75%) and apple.
6.14 Heating rates for hydrogel (75%) and carrots.
6.15 Heating rates for hydrogel (75%) and minced beef.
6.16 Heating rates for hydrogel (40%) and cake.
6.17a Temperature distribution in the test load for oven A (300kJ).
6.17b Temperature distribution in the test load for oven B (300kJ).
6.18a Temperature distribution in the test load for oven A (180kJ).
6.18b Temperature distribution in the test load for oven B (180kJ).
6.19 Apparent difference in fresh and used hydrogel.

APPENDICES

A4.1 Heating of slab of thickness 2b by DRH
A5.1 Heating of rectangular slab of thickness 2b by IH
A6.1 Interior and boundary nodes for a sphere
A7.1 Control volume for a interior node for a 2-d slab
A10.1 Heating of slab by plane waves

NOMENCLATURE

A	Ash content, %
B	Magnetic flux density, T
C	Free salt concentration, (equiv m^{-3})
c	Carbohydrate, %
C_p	Specific heat capacity, $Jkg^{-1}K^{-1}$
d	Thickness, m
D	Charge density vector, Cm^{-2}
D_p	Penetration depth, m
D_v	Mass diffusivity, m^2s^{-1}
E	Electric-field intensity, Vm^{-1}
E_o	Amplitude of electric field vector at surface, Vm^{-1}
f	Frequency, Hz
f_s	Critical frequency, Hz
F	Fat content, %
H	Magnetic-field intensity, Am^{-1}
h_c	Convection coefficient, $Wm^{-2}K^{-1}$
I	Electric current, A
j	$\sqrt{-1}$
J	Current density, Am^{-2}
L	Length, m
k	Thermal conductivity, $Wm^{-1}K^{-1}$
kv	Volumetrc coupling coefficient
K	A parameter which accounts for all losses in a dielectric ($=\varepsilon' - j\varepsilon''_e$)
m	Moisture content, %
n	Index of refraction
M	Salt content, %
P	Power, W
P_{av}	Average power density, Wm^{-3}
P_s	Power intensity at the surface, Wm^{-2}
P_v	Power density, Wm^{-3}
p	Protein, %
$\dot{q}$	Rate of heat flow, Wm^{-2}
R_n	Reflection coefficient
r	Radius of sphere/cylinder, m

r^2 Coefficient of determination, %

S Solid %

T Temperature, °C

T_K Temperature. K

T_∞ Ambient temperature, °C

T_o Initial temperature, °C

t Time, s

V Volume, m^3

X Form factor, ratio of the major to minor axis for a ellipsoid

x,y,z Unit vectors in x,y,z directions

Greek Symbols

α Attenuation factor, m^{-1}

α_T Thermal diffusivity, m^2s^{-1}

α_{TW} Thermal diffusivity of water, m^2s^{-1}

β Phase factor, $radm^{-1}$

γ Propagation factor ($=\alpha + j\beta$)

γ_o Propagation factor of free space

δ Skin depth, m

$\bar{\delta}$ Average hydration number

ε^* Permittivity, $(= \varepsilon_o \varepsilon_r)$, Fm^{-1}

ε_o Permittivity of free space, $(= 8.854 \times 10^{-12})$ Fm^{-1}

ε_r Relative permittivity, $(=\varepsilon' - j\varepsilon'')$

ε_s Static dielectric constant

ε_∞ Optical dielectric constant

ε_T Emmissivity

ε' Relative dielectric constant

ε'' Relative dipolar loss factor

η Characteristic impedance, Ω

Λ Equivalent conductivity of ionic solution, $Sm^2 equiv^{-1}$

μ Permeability, Hm^{-1}

μ_o Permeability of free space, $(= 4\pi \times 10^{-7})$ Hm^{-1}

ρ Resistivity, Ωm

ρ_d Density, kgm^{-3}

σ	Electric conductivity, Sm^{-1}
ϕ	Angle of incidence, rad
ψ	Angle of refraction, (rad)
ω	Angular frequency, $rads^{-1}$

Subscripts

c	Property of the continuous phase in a mixture
cond	Conductive
conv	Convective
I	Incident
i	Index number in y-direction
j	Index number in x-direction
m	Property of a mixture
R	Reflected
rad	Radiative
rms	Root mean square
s	Property of the solid phase in a mixture
T	Transmitted
1,2,	Corresponding to the successive elements in a material

Abbreviations

ADI	Alternating direction implicit
DRH	Direct resistance heating
EM	Electromagnetic
EMH	Electromagnetic heating
IH	Induction heating
ISM	Industrial, scientific, medical
MW	Microwave
MWH	Microwave heating
RF	Radio-frequency
TDMA	Tridiagonal matrix algorithm
TEM	Transverse electromagnetic
TE	Transverse electric

TM	Transverse magnetic
s.d.	Standard deviation
VSWR	Voltage standing wave ratio

GLOSSARY for commonly used terms not defined in text

Agar	A gel made from marine algae used to simulate properties of food.
Characteristic temperature difference	The mean bulk temperature of the sphere's inner region (Tc) minus that of the outer region (Ts) where the volume of inner and outer regions are approximately equal.
Coupling coefficient	An empirical coefficient (kv) based on a relationship between the maximum output power (P_m) of an oven and the actual power coupled by a load volume (V), i.e. $P = P_m(1-e^{-(kv)V})$.
Drichilet boundary condition	When the unknown is specified at the boundary.
Evanescent modes	Non-propagating modes.
Far field	A propagating EM wave far from its generator, when it can be assumed to be a plane wave.
Heating effectiveness	The ratio of power absorbeded by the material to the power density at the surface.
Lossy	Efficient in absorbing EM energy and converting it into heat.
Performance of MW oven	*Heating performance;* uniformity of temperature achieved in foods when heated by MW ovens.
	Cooking performance; partly subjective and evaluated in terms of speed, convenience and cooking results (IEC705).
Phantom	A substitute for a biological product in microwave heating.
Neumann boundary condition	When the normal derivative of the unknown at the boundary is specified.

CHAPTER 1

1 INTRODUCTION

1.1 HISTORICAL BACKGROUND

During the past two decades, concerns for rising unit-energy costs, depleting reserves of fossil fuels and environmental pollution have stimulated the research and development of more energy-efficient technologies, renewable sources of energy and alternative methods of energy utilization for various industrial, commercial and domestic activities. In this context, the increased application of electromagnetic-heating (EMH) techniques has improved the efficiency with which electricity is employed for thermal processing. There are four distinct techniques of EM heating: direct resistance (DRH), induction (IH) radio-frequency (RFH) and microwave (MWH) which use specific parts of the electromagnetic spectrum (Table 1.1).

The use of DRH and IH techniques for heating metals dates back to the nineteenth century [Witsenburg 1949]. The developments undertaken during the Second-World War served to demonstrate the main advantages of induction heating (i.e. low rates of heat loss and the accuracy with which heating can be located exactly where it is needed). Since 1945, progress with radio-frequency and microwave heating techniques for heating non-metals has resulted in many economically-viable drying, heating and curing processes [Perkin, 1979; Metaxas and Meredith, 1983].

1.2 ELECTROMAGNETIC HEATING

EM heating is a generic name for thermal processes wherein the specimen is stimulated with electricity directly or inductively. Applications span many industries:frequencies range from direct current to 10^{12} Hz a.c. and power inputs from a few watts to 10^{9} watts. Therefore a proper classification for electro-thermal processes is difficult to achieve [Metaxas,1987]. However, they can be divided broadly into two basic groups, those best suited to heating:

Table 1.1

Range of frequencies applicable to various EM applications

Form of Energy	Frequency Hz	Application
Light	– 10^{15} –	Optical region
Heat	– 10^{14} –	
	– 10^{13} –	Infra-red Heating
	– 10^{12} –	
Electricity	– 10^{11} –	
	– 10^{10} –	Microwave Heating
	– 10^{9} –	
	– 10^{8} –	
	– 10^{7} –	Radio-frequency Heating
	– 10^{6} –	(high frequency IH)
	– 10^{5} –	
	– 10^{4} –	Induction Heating
	– 10^{3} –	(medium frequency IH)
	– 10^{2} –	
	– 10^{1} –	Direct resistance Heating
		(low frequency IH)

(i) substances with high electrical and thermal conductivities (e.g. metals)

(ii) substances with low thermal and electrical conductivities (e.g dielectrics).

Heat travels relatively easily by electronic conduction through group (i) materials, whereas group (ii) materials can only be heated effectively by electronic, atomic and/or molecular polarisation. Direct-resistance and induction-heating techniques serve mainly to process the high-conductivity materials, whereas microwave and radio-frequency techniques are suitable for low-conductivity materials.

1.2.1 Direct-Resistance Heating

In its simplest form, direct-resistance heating (or Ohmic heating) occurs when a direct current passes through the workpiece: the heat is generated rapidly throughout the sample. Mains frequency is often applied because it requires no frequency conversion. The process is controlled by interrupting the electric current. However, to achieve adequate efficiencies, DRH is best employed for heating thin samples (e.g. wires) and applications involving metals of relatively high resistivity (e.g. the continuous heating of liquids and slurries). New applications include processing foods via DRH (e.g cooking of burgers and sterilising of liquid foods by applying the electric current directly).

1.2.2. Induction Heating

As the name implies, this utilises the transformer effect to create an alternating magnetic-field, which induces eddy currents in a conducting material and thereby dissipates heat as I^2R losses. Energy is coupled magnetically and so induction heating works well with ferromagnetic conductors such as steel. Typical operating frequencies and power consumptions range from $10^3$to 10^6Hz and from $10^3$to 10^8W respectively. One of the main advantages of induction heating is that the heating can

be confined to that part of the workpiece which is directly opposite the coil inducing the current [Witsenburg, 1949]. A metal sample may be heated superficially or throughout its bulk according to the frequency of the applied EM field.

1.2.3. Radio-frequency and Microwave Heating

It has long been established that many poor conductors or dielectrics can be heated through dipole polarisation by high frequency electromagnetic waves in the range 10 MHz to 300 GHz [Osepchuk, 1984]. Usually radio-frequency (10^7Hz<f<10^8Hz) heating is applied to materials in sheet form, whereas microwaves (10^8Hz<f<10^{11}Hz) are used for heating thick as well as laminar objects. For RFH, the material is placed between two electrodes, whereas at microwave frequencies a magnetron and waveguide are required. There are distinct bands of frequencies allocated for industrial, scientific and medical use (i.e. ISM frequencies) [Metaxas and Meredith, 1983]

1.3 OBJECTIVES OF THE STUDY

Electromagnetic heating (EMH) processes are being used increasingly in the industrial and domestic sectors, yet they receive relatively little attention in the thermal engineering domain. Thermal analyses of electromagnetic heating processes are rarely undertaken by mechanical, chemical or food engineers who have studied heat transfer at undergraduate and postgraduate level. Many numerical and analytical techniques have been developed for studying the high frequency (MWH and RFH) heating applications in biomedical and electrical engineering sectors, but a gap exists with respect to the chemical and food engineering sector. Lack of adequate understanding of EMH processes may result in numerous problems and (in the extreme) a loss of confidence in the technical and financial viabilities of the processes. For example, the basic real-life problems of applying high-frequency heating techniques include:(i) the tendency for small objects to explode, because they become super-heated due to internal hot-spot

phenomena [Kritikos and Schwan, 1975]; and (ii) the generation of irregular temperature distributions within heterogeneous or multi-layered objects due to local over-heating which, in the case of foods, could result in the continued existence of microbes in relatively cold zones. The accurate prediction of microbial lethalities in a food item depends upon a knowledge of its cross-sectional temperature distribution during heating. The development of this temperature distribution influences the process-heating period required to achieve the desired bacteriological and culinary qualities of the end product. Thus, for foods, it is particularly important to know how the cross-sectional temperature profile develops during microwave heating. Similarly, but to a lesser extent, for those processes involving metals and polymers much depends upon the temperature distribution achieved within the workpiece. Therefore the identification of cross-sectional temperature profiles in several types of electro-heat processes is highly desirable.

Temperature measurements are difficult for EM heating processes due to the lack of cheap pertinent instrumentation which is immune to electromagnetic interferences. Clearly, when developing such a process, the traditional trial-and-error technique of using actual samples is time consuming and may be expensive unless the samples geometries and properties are nearly identical. For the successful application of these processes a detailed analyses must be prepared in terms of various process parameters (which includes material properties, ambient conditions, economic considerations etc.) so as to justify their advantages against the relatively low costs of using conventional heating methods.

Multi-purpose mathematical models would thus appear to be desirable tools for predicting heating characteristics and temperature distributions and for providing a better understanding of the interactions between materials and applied electromagnetic fields. As the subject of electromagnetic heating is not taught widely, parametric analyses of cross-sectional temperature distributions, process-heating periods and super-cooling effects are rarely undertaken [Newborough and Probert, 1990]. However, some specific purpose thermal-models are

available for applications such as radio-frequency drying, diathermy, ohmic heating and microwave cooking, [Cross et al, 1982; DeWagter, 1984; De Alwis and Fryer, 1990, Datta and Liu, 1992].

The effectiveness of an electromagnetic-heating process depends upon the geometry of the workpiece, the electrical and thermal properties of the material (and hence upon its chemical composition and temperature) and the frequency and strength of the applied electromagnetic field. Therefore, a multi-purpose model should ideally be able to simulate electromagnetic-heating processes involving any material, given appropriate values for the specimen's properties and the frequency and strength of the applied EM field.

The largest consumer of microwave power is the food industry where it is used for cooking, thawing, freezing, drying and sterilization [Ayappa and Davis, 1991]. Unfortunately, microwave equipment and numerous food applications, which has been in use for 30 years and was once popular have virtually been replaced by conventional techniques. Only tempering, bacon cooking and pasta drying have retained a major foothold in the market.[Buffler, 1992].

Similarly, domestic microwave ovens have gained increasing acceptance in most countries as a supplementary cooking appliance [Platts, 1991]. This is also reflected in the increased demand within the relatively new chilled food market and the continuous introduction of new microwavable food products [Decareau, 1992]. Yet few have learned the complicated rules for scratch cooking in their microwave ovens. For the past few years great concern has been expressed regarding the capability of microwave ovens to destroy bacteria in food [Which?, May 1991]. Certain types of ovens were considered unsafe in that they failed to heat all parts of food to a temperature to kill any potential pathogens [MAFF, 1991].

There may be several reasons for the slow acceptance of using this source of energy (e.g. economic, safety, novelty), but the lack of understanding of microwaves and their interaction with food is a major obstacle. The Institute of Food Research, reported to the House of

Commons' Agriculture Committee that more investigations are needed to improve the guidelines for (i) oven testing to provide clearer instructions for reheating food and (ii) promoting greater understanding among consumers with respect to achieving acceptably-uniform temperatures [The Times, 1990].

The actual output powers of different microwave ovens rated as equal are often not true due to different sizes of the cavities, manufacturer's tolerances, testing methods etc.. Traditionally, oven manufacturers have not been willing to share power output data with other aspects of the industry. The implications of mixed power standard product lines to the food processing industry could be severe because the difference between two test procedures may indicate power output of as much as 100W [Buffler, 1991]. The food product developers have no standard by which to formulate their package labelling. The International Electrotechnical Commission (IEC) recommends that output of new microwave ovens should be measured according to the revised testing methods (IEC705 1988). The current test methods are also inadequate to evaluate the performance of an oven for the wide range of tasks which a typical oven performs during its useful life. Therefore the standards are being continuously improved. Similarly new food products with improved formulations and in different types of containers are being introduced to the market. Therefore it is important that food product development and microwave-oven testing are synchronised. Food industry and appliance manufacturers need to modify the formulation, packaging and directions for using the appliance so that a higher degree of consumer satisfaction is achieved. This investigation therefore, has three main objectives:

(1) to develop a multi-purpose mathematical model for analysing electromagnetic heating processes, so that assessments can be made of the likely thermal behaviours of a wide variety of materials.

(2) to modify the model to study the behaviours of food products subjected to microwaves, because there is a growing concern regarding the quality of foods heated in microwave ovens.

(3) to investigate the suitability of hydrophilic materials as food simulators for testing microwave ovens.

1.4 ORGANISATION OF THE DISSERTATION

Chapter 2 discusses the theoretical background of electromagnetic heating and identifies the similarities as well as the differences in the various EMH processes, in order to obtain a general-purpose mathematical model. Parametric analyses of different processes via the proposed model are then presented. From these it was possible to quantify the influence of material properties on the energy absorption as well as the energy distribution in a material. However, the order of influence of electrical and thermal properties varies for different types of processes/ materials. In order to modify the general EM model for microwave heating of foods a detailed investigation of dielectric properties of various foods and their likely effects on the model predictions is provided in Chapter 3 and a review of thermal properties and available predictive correlations is presented in Chapter 4. Commonly made assumptions concerning the power absorption for foods heated in microwave ovens are discussed in Chapter 5 and their validity is analysed for various situations. In Chapter 6, the procedures and materials used for testing microwave ovens are described. In particular the suitability of various hydrophilic materials as food simulators is established and a test procedure for assessing heating uniformity using appropriate hydrophilic samples is proposed. Conclusions and recommendations for further work are in Chapter, 7.

CHAPTER 2

2 MULTI-PURPOSE MODEL FOR ELECTROMAGNETIC HEATING PROCESSES

2.1 THEORY OF ELECTROMAGNETIC HEATING

It is desirable to identify the thermal and electrical parameters involved in electromagnetic heating, in order to understand the implications that they have upon the temperature and/or moisture distributions in the heated material. When a EM field is applied to a material, heat is generated by the dissipation of "conduction currents" and/or "displacement currents". Conduction currents ensue due to the conductivity of the material and displacement currents because of various polarisation effects occurring within the material. The theory of polarisation and conduction effects has been widely studied in the literature [Debye, 1929; Hasted, et al 1948; von Hippel, 1954]. Although the physical mechanisms governing the different types of electromagnetic heating techniques are quite distinct, a unified theoretical approach [Metaxas, 1987] is most useful. Thereby the similarities as well as the differences between the various electro-thermal processes can be identified.

2.1.1 Conductive Dielectric

The current density due to an external field, **E** in the general case of a material where both conductive and displacement current mechanisms are present may be written as:

$$\mathbf{J} = \sigma\mathbf{E} + \frac{\partial \mathbf{D}}{\partial t} \qquad (2.1)$$

the first term refers to the conduction effects and the latter represents the effects of the displacement current, **D** which is related to the applied field depending upon the material's permittivity, ε_r (=

$\varepsilon'-j\varepsilon''$). The dielectric constant, ε', is a measure of the energy stored and the loss factor, ε'', is a measure of the energy dissipated (see Appendix 1). Because with many real materials it is difficult to separate displacement and current losses, a parameter, K may be used to include all losses. K indicates the nature of the material (whether a metal or dielectric):

$$K = \varepsilon' - j \left(\frac{\sigma}{\omega \varepsilon_o} + \varepsilon'' \right) \qquad (2.2)$$

2.1.2 Basic Electromagnetic Equations

The following modified EM diffusion equation [Metaxas, 1987] can be used to compute the parameters required for heating metals and dielectrics (see Appendix 2 for the derivation of equation 2.3):

$$\nabla^2 \mathbf{E} = j\omega\mu\varepsilon_o K \frac{\partial \mathbf{E}}{\partial t} \qquad (2.3)$$

For a sinusoidally varying **E** (i.e. $= E_o e^{j\omega t}$), $\partial \mathbf{E}/\partial t = j\omega \mathbf{E}$, and so

$$\nabla^2 \mathbf{E} = -\omega^2 \mu\varepsilon_o K \mathbf{E} \qquad (2.4)$$

For a semi-infinite conductive slab (comprising a metal or a conductive dielectric) with the induced **E** field in the z direction and the induced **H** field in the x direction (see Figs. 2.1 & 2.2), equation (2.4) simplifies to:

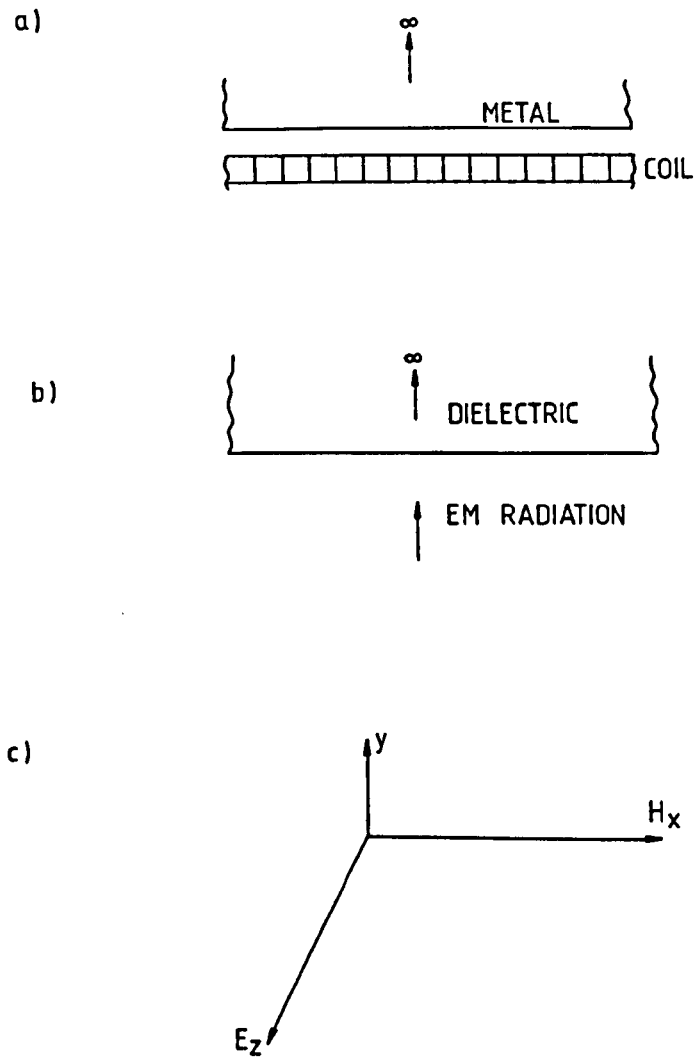

Fig.2.1 Semi-infinite slab subjected to (a) induction heating and (b) MW/RF heating with coordinate system in (c)

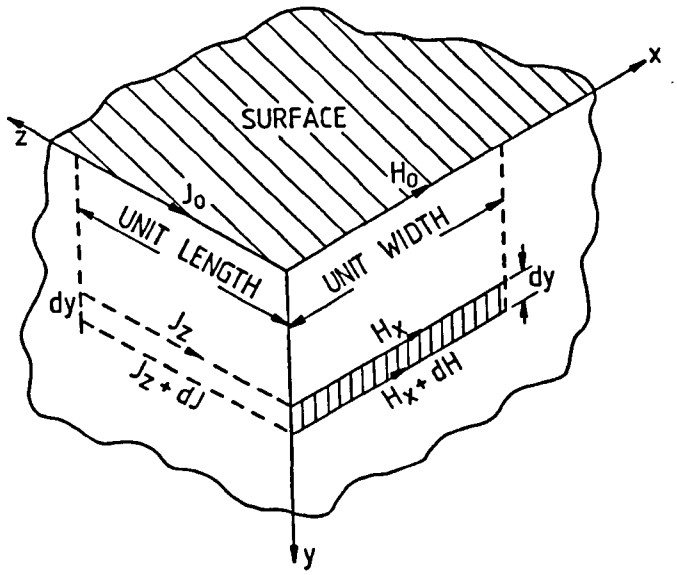

Fig.2.2 Semi-infinite slab configuraion for EM heating

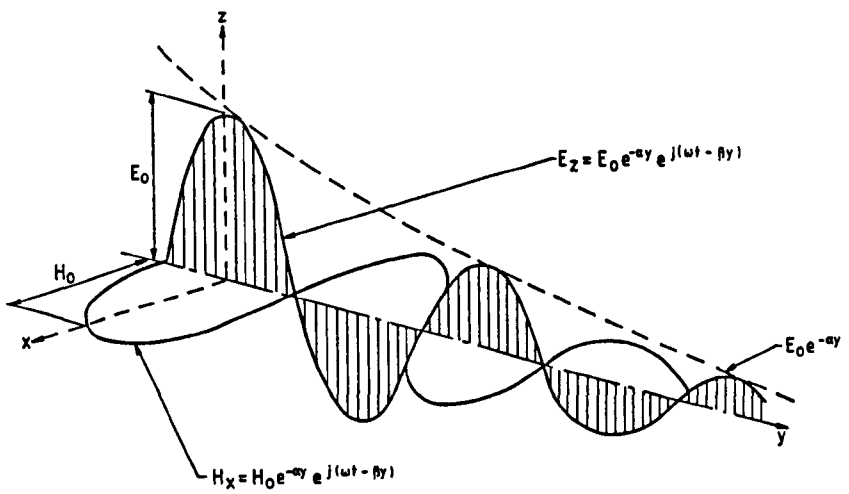

Fig.2.3 Propagation of a plane wave through a dielectric

$$\frac{\partial^2 E_z}{\partial y^2} = - \omega^2 \mu \varepsilon_o K E_z \qquad (2.5)$$

By introducing the propagation factor, γ

$$\gamma = j\omega \sqrt{\mu \varepsilon_o K} = \alpha + j\beta \qquad (2.6)$$

equation (2.5) can be simplified to

$$\frac{\partial^2 E_z}{\partial y} = \gamma^2 E_z \qquad (2.7)$$

The solution of this, including time variations and assuming that **E** remains finite when $y \to \infty$, is :

$$E_z = E_o e^{-\gamma y} e^{j\omega t} \qquad (2.8a)$$

or, taking only the real part:

$$E_z = E_o e^{-\alpha y} \cos(\omega t - \beta y) \qquad (2.8b)$$

E_o is the maximum value of the electric-field intensity, i.e. at the material/air interface. Thus, the variation of **E** within the material in y-direction is such that it changes its phase according to $e^{-j\beta y}$ and attenuates according to $e^{-\alpha y}$ (see Fig. 2.3).

Similar equations for the magnetic-field intensity and current density can be derived as follows:

$$\frac{\partial^2 H_x}{\partial y^2} = \gamma^2 H_x \quad \text{and} \quad \frac{\partial^2 J_z}{\partial y^2} = \gamma^2 J_z \tag{2.9}$$

and the solutions for sinusoidally varying H and J will be

$$H_x = H_o e^{-\gamma y} e^{\omega t} \quad \text{and,} \quad J_z = J_o e^{-\gamma y} e^{j\omega t} \tag{2.10}$$

2.1.3 Attenuation Factor and Skin Depth

The attenuation factor, α, represents a measure of the extent to which an electromagnetic field is attenuated as it penetrates a material. The reciprocal of the attenuation factor is commonly referred to as the "skin-depth", δ, which is the depth at which the magnitude of the electric-field intensity (or current density) falls to e^{-1} (i.e. ≈37%) of its value at the surface. The expression for the attenuation factor is derived from equation (2.6):

$$\alpha = \omega \sqrt{\frac{\mu_o \varepsilon_o \varepsilon'}{2}} \left[\sqrt{1+\left\{ \frac{\varepsilon''_e}{\varepsilon'} \right\}^2} - 1 \right]^{1/2} \tag{2.11}$$

2.1.4 Power absorbed in a Material

From a thermal-engineering perspective, the power absorbed (or heat generated), due to the current density, **J**, resulting from the applied EM field to is required to determine the temperature distributions and heating periods. This is given by the Poynting vector [Von Hippel, 1954]:

$$\int_s (\mathbf{E} \times \mathbf{H}^*) ds \qquad (2.12)$$

Thus the power generated can be found from the value of the surface integral. The power generated within a conductive dielectric can be estimated by substituting the value of **E** and **H** from Maxwell's equations (see Appendix 3), i.e.,

$$P_{av} = \frac{1}{2} \omega \varepsilon_o \varepsilon''_e \int_v (\mathbf{E}^* . \mathbf{E}) dV \qquad (2.13)$$

In most cases, the electric-field intensity varies within the material, but where E can be approximated by a constant value, equation (2.13) becomes (using $\mathbf{E}^*\mathbf{E} = |\mathbf{E}^2| = E^2_{rms}$):

$$P_{av} = \omega \varepsilon_o \varepsilon''_e E^2_{rms} V \qquad (2.14)$$

If the material exhibits magnetic losses, the power generated due to the effects of the magnetic-field component should be included. The modified equation then becomes:

$$P_{av} = \left[\varepsilon_o \varepsilon''_e E^2_{rms} + \mu_o \mu''_e H^2_{rms} \right] V \qquad (2.15)$$

The EM field varies exponentially with respect to the distance from the surface into the material (see eq. (2.8). Therefore, for a semi-infinite slab subjected to a sinusoidally-varying EM field, the power intensity (i.e. power per unit area) may be obtained as;

$$P_s = \frac{\omega \varepsilon_o \varepsilon''_e}{2} \int_o^y E_o^2 e^{-2\alpha y} dy \qquad (2.16)$$

$$= \frac{\omega \varepsilon_o \varepsilon''_e}{4 \alpha} E_o^2 \qquad (2.17)$$

For direct resistance heating, equation (2.17) can be modified for metals by considering the conductive effects only, so that;

$$P_s = \frac{\sigma E_o^2}{4\alpha} \qquad (2.18)$$

or, because $J = \sigma E$

$$P_s = \frac{J_o^2}{4\sigma\alpha} \qquad (2.19)$$

Similarly for IH, the current density, J, induced by the magnetic field is:

$$J_z = \nabla \times H = - \frac{\partial H_x}{\partial y} \qquad \text{(assuming } H_z = H_y = 0\text{)} \qquad (2.20)$$

By substituting from equation (2.10) into equation (2.20) and differentiating, the maximum value of current density is

$$J_o = \sqrt{2}\, H_o \alpha \qquad (2.21)$$

Then the power intensity in terms of the magnetic field intensity can be written as:

$$P_s = \frac{H_o^2\, \alpha}{2\sigma} \qquad (2.22)$$

2.1.5 Power penetration depth

The power absorbed is controlled by $|E^2|$ which decays by a factor $e^{-\alpha y}$ with depth. So the power P_y, at any depth y from the surface can be written:

$$P_y = P_o\, e^{-2\alpha y} \qquad (2.23)$$

where P_o is the power at the surface. Therefore, one can define a penetration depth, D_p, at which the power falls to e^{-1} of the value at the surface - see Fig.2.4, i.e.,

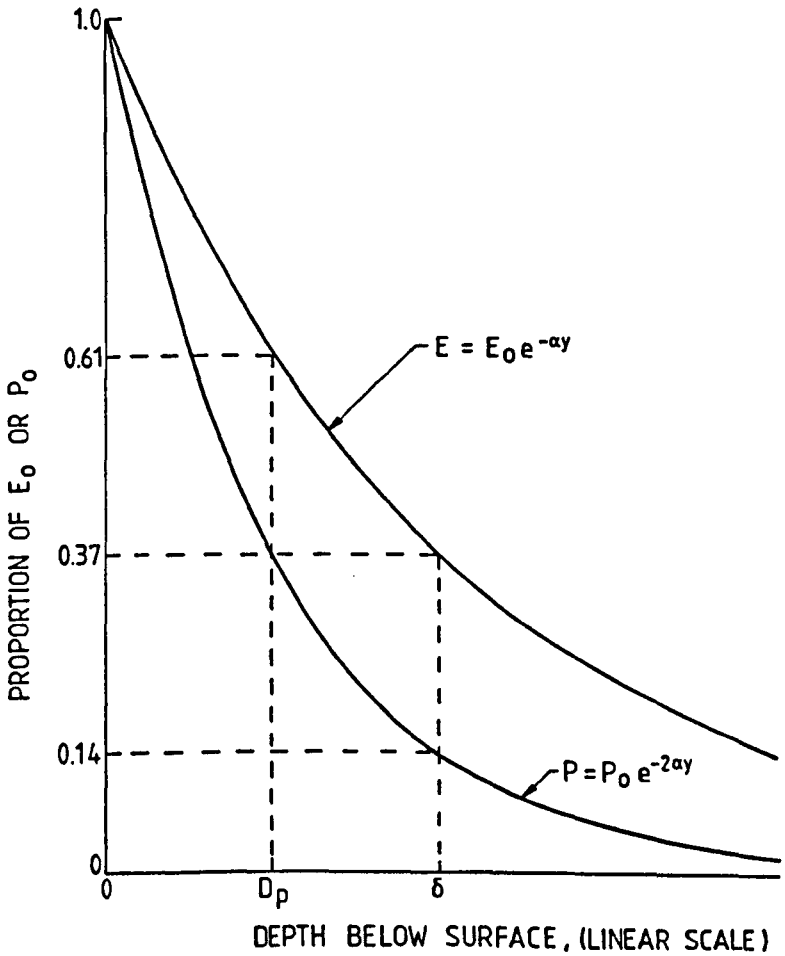

Fig.2.4 Variation of electric field intensity and power with depth in to a semi-infinite slab

$$D_p = \frac{1}{2\alpha} = \frac{\delta}{2} \qquad (2.24)$$

This is applicable to a.c. DRH and IH processes, because the effect of an alternating magnetic field is to concentrate the current in the surface layers of the conductor. For d.c. DRH processes, the current density is approximately constant throughout the material and so the power is generated more uniformly. With a.c. DRH and IH processes, it is conventional to use the concept of the workpiece's skin depth, δ, whereas in dielectric heating, one normally refers to the power penetration depth, D_p.

2.1.6 Energy Coupling by a material from microwaves

The power dissipated within the material depends upon the magnitude of the EM field developed there. In microwave ovens, this is particularly difficult to predict, because the material's introduction to the EM field influences the absolute value of the field intensity. Conceptually, a plane wave strikes the specimen's surface, it is partly reflected and partly refracted depending upon the material's properties and the angle of incidence (see Fig.2.5a). The reflection and refraction of EM waves is governed by well-known optical laws; the law of reflection and Brewster's law of polarisation by reflection:

$$\psi = \sin^{-1}(\eta/\eta_o) \sin \phi \qquad (2.25)$$

where, η_o, the characteristic impedance of free space i.e.

$$\eta_o = \left(\frac{\mu_o}{\varepsilon_o}\right)^{1/2} = 376.731\Omega \approx 377\ \Omega \qquad (2.26)$$

(a)

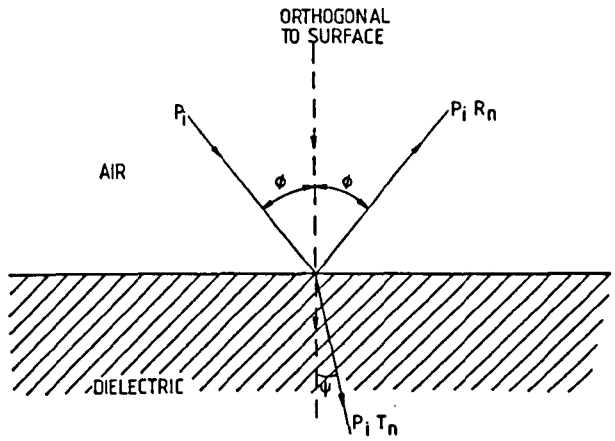

(b) TE polarisation

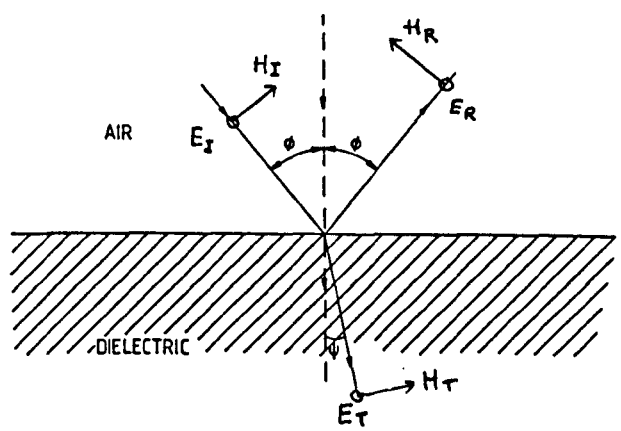

(c) TM polarisation

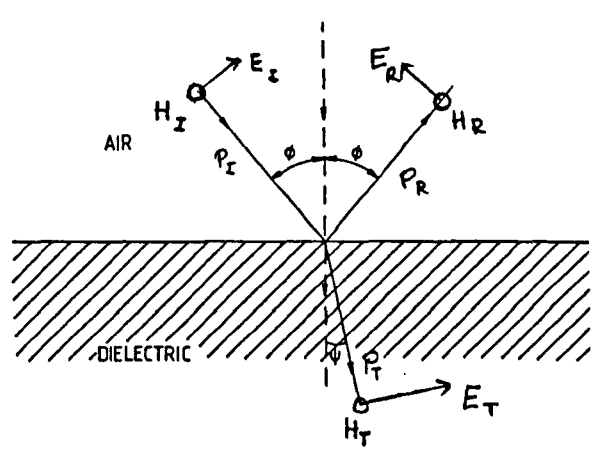

Fig.2.5 Energy transmission, reflection and refraction at the interface of two materials

and the characteristic impedance of a dielectric is:

$$\eta = \left(\frac{\mu_o \mu_r}{\varepsilon_o \varepsilon_r^*} \right)^{1/2} = \eta_o \sqrt{\frac{\mu_r}{\varepsilon_r^*}} \qquad (2.27)$$

The power reflection coefficient at the boundary of two materials for normal incidence in terms of characteristics impedances is given by (Olver, 1992).

$$R_n = \frac{P_R}{P_I} = \frac{(\eta_1 - \eta_2)^2}{(\eta_1 + \eta_2)^2} \qquad (2.28)$$

Although less used than R_n, the transmission coefficient, T_n can be similarly defined. Also $R_n + T_n = 1$.

For oblique incidence the wave may be polarised in two different ways i.e. with the electric field vector components perpendicular (TE) or parallel (TM), to the plane of incidence.

For TE polarisation:

$$R_n = \left(\frac{\eta_1 \cos \psi - \eta_2 \cos \phi}{\eta_1 \cos \psi + \eta_2 \cos \phi} \right)^2 \qquad (2.29)$$

For the parallel polarised waves (TM), R_n in terms of incident and transmission angle is ;

$$R_n = \frac{\tan^2(\phi - \psi)}{\tan^2(\phi + \psi)} \qquad (2.30)$$

There is an important difference between the TE and TM polarised waves. At a certain incident angle there is no reflected wave for parallel polarisation (TM) i.e. R_n is zero and all the incident power is transmitted and there is no reflected power (Fig.2.6a,b,c,d). From equation (2.32), this happens when $\tan(\phi+\psi) \rightarrow \infty$ (i.e. when $(\phi+\psi)=90^\circ$). This angle is known as "Brewster angle", named after Sir David Brewster (1781-1868) who discovered the effect empirically [Olver, 1992].

The difference between the characteristic impedances of two dielectrics (or air and a dielectric) results in an "impedance mismatch" and indicates the fraction of energy reflected at the interface (eq. 2.28-2.30). Many common food products have characteristic impedances of about 50Ω and so the resulting impedance-mismatch causes more than 50% of the incident power to be reflected (Fig.2.6c). To achieve efficient design of microwave heating equipment designers try to ensure that maximum energy is absorbed by a wide range of materials to be heated. In a domestic oven the reflected power re-enters the specimen in a series of multiple reflections (standing waves) between the (high R_n) walls of the oven and the specimen's surface. Thus the energy-coupling efficiencies vary with the specimen's shape and size as well as with its dielectric properties.

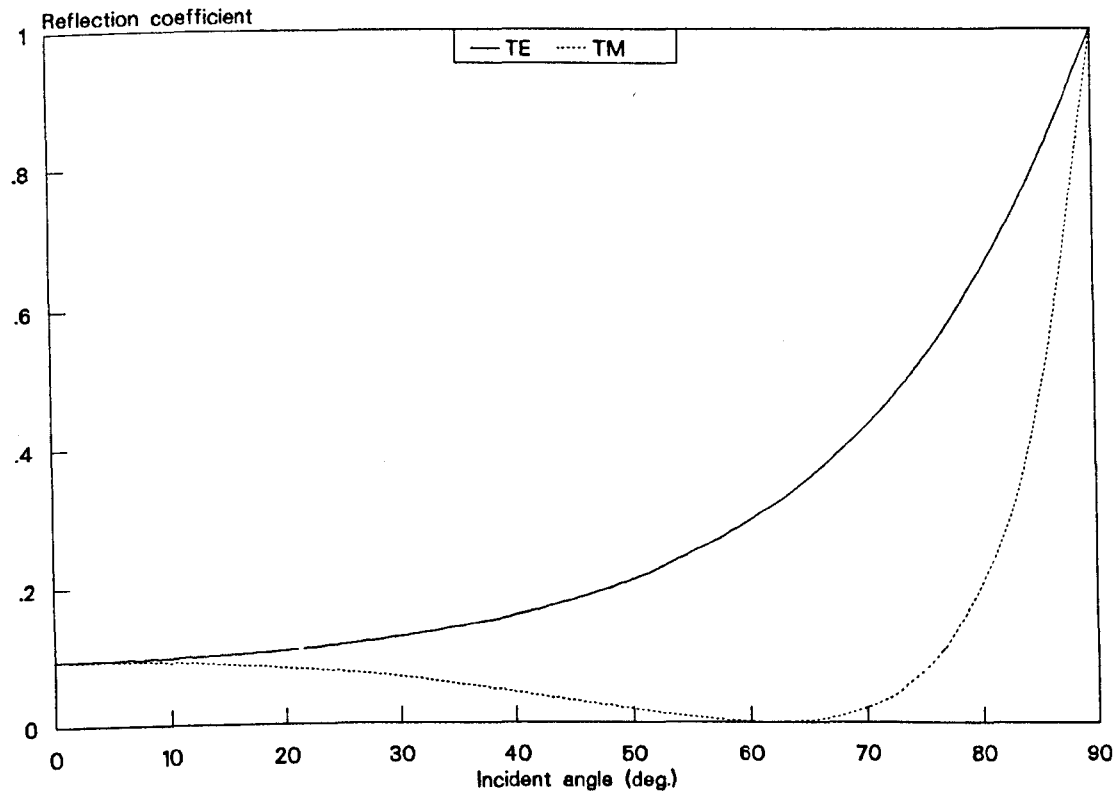

a. Characteristic Impedance = 200 Ω

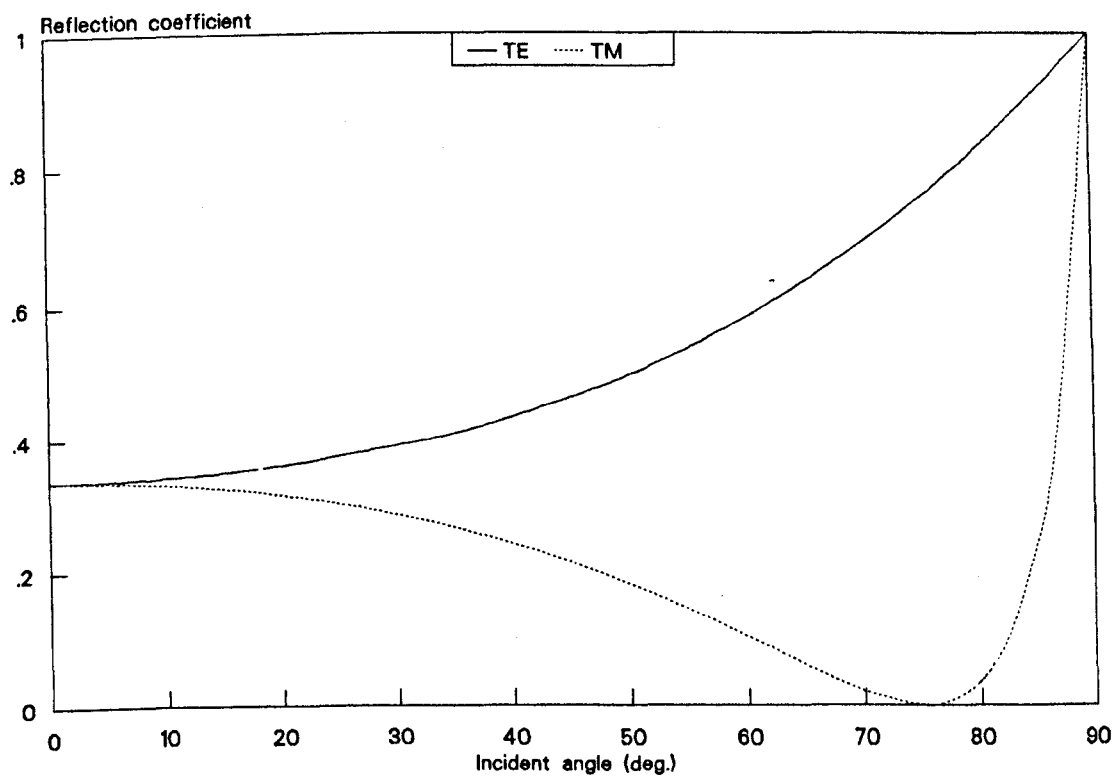

b. Characteristic Impedance = 100 Ω

Fig.2.6 Variation of reflection coefficient with incident angle for TE & TM polarisations

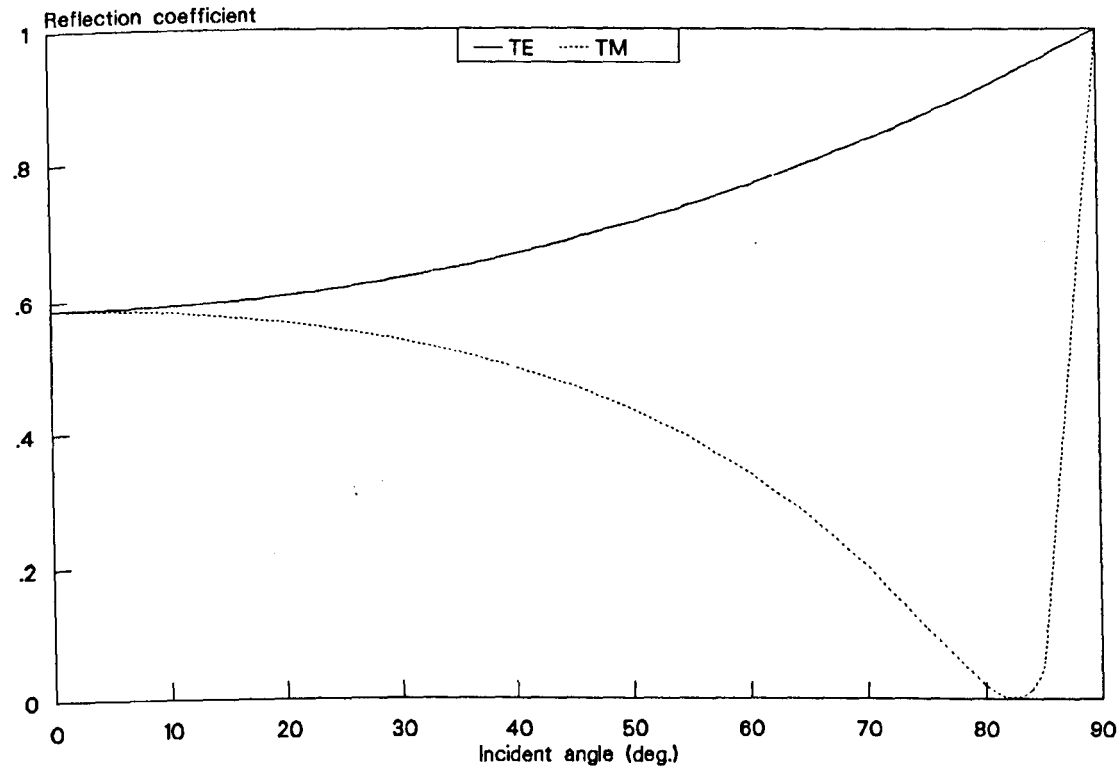

c. Characteristic Impedance = 50 Ω

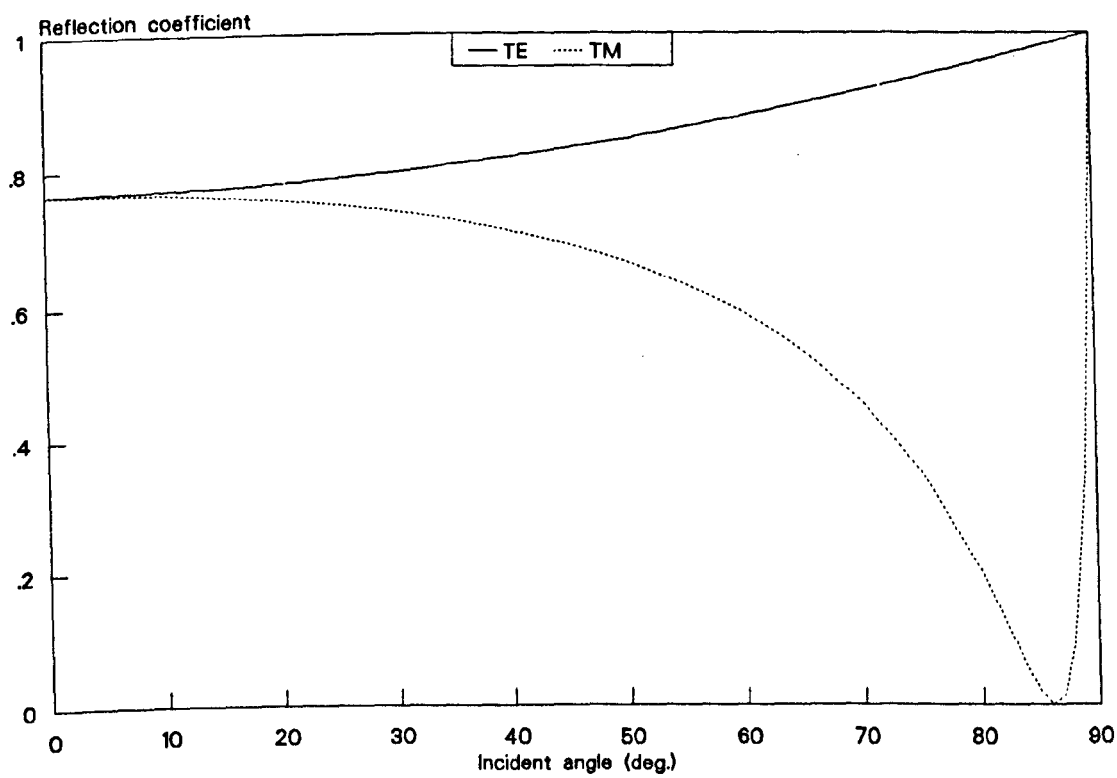

d. Characteristic Impedance = 25 Ω
Rn vs incident angle for impedances; 50Ω,25 Ω

Table 2.1

Attenuation factors and characteristic impedances of some common food materials at approxiamtely 3GHz [adapted from Kent,1987]

Food	Attenuation factor (m^{-1})	Characteristic Impedance, (Ω)
Ice	0.05	210.7
Bacon fat	2.1	238.7
Beef (frozen)	3.4	189.1
Butter	5.5	184.0
Water	38.8	42.5
Gravy	45.5	43.7
Beef	48.19	57.0
Carrot	49.2	43.1
Potato	54.4	49.3
Ham	94.8	45.5

2.2 HEAT TRANSFER

As a result of the dissipation of electrical energy within a material, it is conventional to express the rate of temperature rise as follows [Walker et al, 1976; Checcucci et al, 1983]:

$$\frac{\partial T}{\partial t} = \frac{P_v}{\rho_d C_p} \qquad (2.31)$$

The magnitude of P_v, which is the power density (in Wm^{-3}), will depend upon the properties of the material, the geometry of the specimen, the required temperature rise and the desired process-heating period. Equation (2.31) is valid for all volumetric heating concepts provided that heat losses are small (e.g. as in most DRH processes). Upon energisation, the developing temperature distribution initially resembles closely the distribution of power dissipation within the material. However, thereafter it is often influenced significantly by conductive heat-transfers within the material and by convective/radiative heat-transfers from the surface to the surroundings. The conductive heat flow is governed by Fourier's equation:

$$q''_{cond} = -k (\nabla T) \qquad (2.32)$$

The rate of convective heat-transfer can be described by Newton's equation:

$$q''_{conv} = h_c (T_\infty - T) \qquad (2.33)$$

Similarly, radiation heat transfer exchange between the specimen's surface and the surroundings follows Stefan-Boltzmann law:

$$q''_{rad} = \sigma \varepsilon_T (T_\infty^4 - T^4) \qquad (2.34)$$

(σ is Stefan-Boltzmann constant = $5.67 \times 10^{-8} W\ m^{-2} K^{-4}$)

2.3 SIMULATING EMH PROCESSES

Thermal models for EMH processes should be able to simulate:

(i) "energy coupling" from the applied electromagnetic field, and
(ii) "energy dispersion" within the specimen

Thermal analyses are less important for most DRH and IH processes and analytical methods are usually employed to estimate the necessary heating period and the bulk temperature-rise history. However, it is feasible to combine the electromagnetic field and heat-flow equations to determine the temperature distribution [Davies and Simpson, 1979]. For dielectrics, two approaches have been adopted when studying the thermal effects of EM radiation. The first is to characterise the heating of a specimen by its "heating potential" [Kritikos and Schwan, 1975; Johnson et al, 1975]. The heating potential is defined as the rate at which heat is generated in a material: it is determined by the product of the material's electrical conductivity and the electric field intensity; $|E_o^2|$. But, the electric field is not distributed uniformly within a material, so this approach does not provide a means for assessing the power generated spatially (and hence the cross-sectional temperature distribution) within the specimen. It only produces an estimate of the mean bulk temperature via equation (2.31). Alternatively, the rate of temperature rise ($\partial T/\partial t$) may be determined for a material in terms of the total absorbed power [Walker et al, 1976; Checcucci et al, 1983]. However, the total absorbed power is difficult to measure accurately, and it varies during the heating process, because the material's electrical properties are temperature-dependent. Again this route only provides an estimate of

the mean bulk temperature and offers no spatial data. Examples of empirical relationships to predict mean-bulk temperature profiles for the microwave heating of selected foods based on experimental data and using dimensional analysis also exist in the literature (Ofoli and Komolprasert, 1988; Komolprasert and Ofoli, 1989).

Various numerical methods are available in the literature to estimate the electric field distribution for high frequency applications e.g. hyperthermia, smelting, sintering, drying [Taflove, 1980; Lau and Sheppard, 1986; Yang, 1989; ; Jia and Jolly, 1992]. Although these models place great emphasis on the electrical aspects (i.e. the electric field distribution), the thermal aspects are somewhat neglected. Some models assume constant material properties and others do not allow for heat-and-mass transfer mechanisms at all. Such assumptions can often influence the predictions of a thermal model significantly

Thus the heating of a material via various EM processes is governed by a coupled system consisting of the equation (2.4) to describe the variation of power distribution in a material and the following forced heat equation:

$$\nabla (k \nabla T) + P_v = \rho_d C_p \frac{\partial T}{\partial t} \qquad (2.35)$$

where,

$$P_v = \varepsilon_o \varepsilon''_e |E^2| + \mu_o \mu''_e |H^2| \qquad (2.36)$$

The **E** and **H** field are space and time dependent, as seen earlier from the equations (2.7) and (2.9). Similarly material properties k, ρ_d, C_p, ε' and ε''_e depend upon various parameters viz. material's composition and temperature and also on process frequency as for electrical properties. Therefore, numerical techniques are desirable if the transient temperature characteristics are to be determined for a given process.

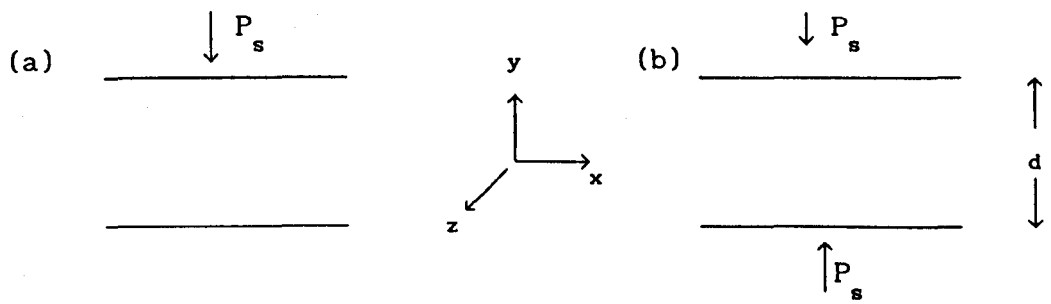

Fig.2.7 Configuration for slab (a) heated from one side (b) heated from both sides

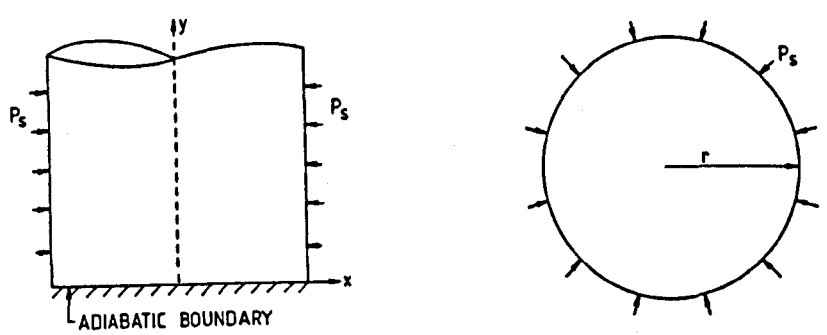

Fig.2.8 Configuration for (a) cylinder heated radially (b) sphere heated radially

2 .4 A MULTI-PURPOSE THERMAL MODEL

A general model is presented based upon the preceding discussion. The general heat transfer equation (2.35) was solved for a slab subjected to EM heating. (Fig.2.7). The model was then developed for cylinders and spheres (Fig.2.8) to study the influence of geometry on the heating of the same material under similar conditions.

2.4.1 One-dimensional Model

The heat diffusion equation with a volumetric heat generation term, in cartesian coordinates is:

$$\frac{\partial}{\partial y}\left(k(T) \frac{\partial T}{\partial y} \right) + P_v = \rho_d C_p \frac{\partial T}{\partial t} \qquad (2.37)$$

Similarly, the equation in cylindrical co-ordinates is:

$$\frac{1}{r} \frac{\partial}{\partial r}\left(k(T)\, r \frac{\partial T}{\partial r} \right) + P_v = \rho_d C_p \frac{\partial T}{\partial t} \qquad (2.38)$$

and for spheres:

$$\frac{1}{r^2} \frac{\partial}{\partial r}\left(k(T) r^2 \frac{\partial T}{\partial r} \right) + P_v = \rho_d C_p \frac{\partial T}{\partial t} \qquad (2.39)$$

The heat generation term, can be calculated assuming semi-infinite geometries. The solution depends upon the type of material and the field intensities (Section 2.1.4). Therefore, in cartesian coordinates, the power dissipated within a certain homogeneous volume between the depths, y_i and y_{i+1} from the surface is:

$$P_v = \frac{P_s \left\{ e^{-2\alpha y_i} - e^{-2\alpha y_{i+1}} \right\}}{y_{i+1} - y_i} \qquad (2.40)$$

For cylindrical and spherical geometries, P_v within a volume between the radial distances r_i and r_{i+1} from the surface was calculated using:

$$P_v = P_s \frac{\left\{ e^{-2\alpha r_i} - e^{-2\alpha r_{i+1}} \right\} + \left\{ e^{-2\alpha(2R-r_{i+1})} - e^{-2\alpha(2R-r_i)} \right\}}{r_{i+1} - r_i} \qquad (2.41)$$

(However, the analysis based on semi-infinite geometries for calculating the heat generation term does not truely hold for electrically thin geometries (i.e. for $\frac{d}{\delta} < 3$), where the effects of surface currents at both surfaces need to be considered. The analysis for the power intensity for a thin slab for DRH and IH are given in appendixes 4 and 5. The validity of this assumption for microwave heating of foods has been investigated further in Chapter 5).

The sample was divided into uniformly spaced (Δy) elements. Finite difference discretization was used for expressing spatial derivatives. The resulting temperature matrix, was solved using Gauss-elimination (see Appendix 6 for the numerical algorithm).

2.4.2 Two dimensional Model

The 2-d model was developed for rectangular and cylindrical geometries. In cartesian coordinates, equation (2.35) was written as:

$$\frac{\partial}{\partial x}\left(k(T) \frac{\partial T}{\partial x} \right) + \frac{\partial}{\partial y}\left(k(T) \frac{\partial T}{\partial y} \right) + P_v = \rho_d C_p \frac{\partial T}{\partial t} \qquad (2.42)$$

and in cylindrical coordinates:

$$\frac{1}{r}\frac{\partial}{\partial r}\left(k(T) r \frac{\partial T}{\partial r} \right) + \frac{\partial}{\partial x}\left(k(T) \frac{\partial T}{\partial x} \right) + P_v = \rho_d C_p \frac{\partial T}{\partial t} \qquad (2.43)$$

The P_v term was modified to include the variation in the other dimension. The equations (2.42) and (2.43) for slabs and cylinders respectively, were solved using the alternating direction implicit (ADI) method, whereby at each step the spatial derivatives in one dimension were evaluated explicitly, and the other was evaluated implicitly and the direction of implicit representation was changed sequentially to obtain stable solutions. This method was preferred as TDMA is applicable as in 1-d model. (see Appendix 7).

2.4.3 Varying Material Properties:

Variations in material properties due to temperature change were accommodated in the heat equation (2.37). These are generally described as linear or polynomial functions of temperature, e.g. α_T , k, and α may be written as:

$$\alpha_T(T) = b_o + b_1 T + b_2 T^2 \qquad (2.44a)$$

$$k(T) = c_o + c_1 T \qquad (2.44b)$$

$$\alpha(T) = d_o + d_1 T + d_2 T^2 + d_3 T^3 \qquad (2.44c)$$

The coefficients b's, c's and d's for different food materials were obtained from the experimental data (discussed in Chapters 3 & 4).

2.4.4 Boundary Conditions

The following initial and boundary conditions were applied for various geometries:

$$T = T_o, \quad \text{at } t = 0 \tag{2.45}$$

$$\frac{\partial T}{\partial y} = 0, \quad \text{at } y = \frac{d}{2} \tag{2.46}$$

$$\frac{\partial T}{\partial y} = 0, \quad \text{at } x = \frac{w}{2} \tag{2.47}$$

$$\frac{\partial T}{\partial r} = 0, \quad \text{at } r = R \tag{2.48}$$

Convective boundary:

$$k \frac{\partial T}{\partial y} = h_c (T_\infty - T), \quad \text{at } y = 0 \tag{2.49}$$

$$k \frac{\partial T}{\partial x} = h_c (T_\infty - T), \quad \text{at } x = 0 \tag{2.50}$$

$$k \frac{\partial T}{\partial r} = h_c (T_\infty - T), \quad \text{at } r = 0 \tag{2.51}$$

Radiative boundary:

$$k \frac{\partial T}{\partial y} = \sigma \varepsilon_T (T_\infty^4 - T^4), \quad \text{at } y = 0 \tag{2.52}$$

$$k \frac{\partial T}{\partial x} = \sigma \varepsilon_T (T_\infty^4 - T^4), \quad \text{at } x = 0 \tag{2.53}$$

$$k \frac{\partial T}{\partial r} = \sigma \varepsilon_T (T_\infty^4 - T^4), \quad \text{at } r = 0 \tag{2.54}$$

Interface Conditions

At interior interfaces, the temperature and heat flux are continuous i.e. for nodes in the y-direction.

$$T_{i1/interface} = T_{i2/interface} \tag{2.55}$$

$$-k_{i1}\left(\frac{\partial T_{i1}}{\partial y_{i1}}\right)_{interface} = -k_{i2}\left(\frac{\partial T_{i2}}{\partial y_{i2}}\right)_{interface} \tag{2.56}$$

Similarly, in the x-direction,

$$T_{j1/interface} = T_{j2/interface} \tag{2.57}$$

$$-k_{j1}\left(\frac{\partial T_{j1}}{\partial x_{j1}}\right)_{interface} = -k_{j2}\left(\frac{\partial T_{j2}}{\partial x_{j2}}\right)_{interface} \tag{2.58}$$

Interface conductivity was taken as the harmonic mean of the conductivities of the two adjacent layers [Patankar, 1980]. This eliminated any errors caused by the abrupt changes of conductivity in a composite material such that;

$$k_{i,i-1} = \frac{2k_i k_{i-1}}{k_i + k_{i-1}} \quad \text{and} \tag{2.59}$$

$$k_{i,i+1} = \frac{2k_i k_{i+1}}{k_i + k_{i+1}} \tag{2.60}$$

2.5 PARAMETRIC ANALYSES

It is desirable to consider the effect of each relevant parameter on the heating characteristics during the design of a product/process. The resistivity, ρ ($=1/\sigma$) of the material governs the rate of ohmic loss: its permittivity, ε_r^*, and permeability, μ_r, control the respective rates at which it absorbs energy from the electric and magnetic components of the applied field. The resistivities of metals are of the order of $10^{-8}\Omega m$ and are increased by impurity content and porosity, Furthermore, resistivity increases with temperature so resulting in a decrease in the attenuation factor of a metal during heating. However, biological materials, polymers and ceramics have resistivities ranging from 10^2 to $10^{19}\Omega m$ and these tend to decrease with temperature. For non-magnetic materials the relative permeability remains close to unity irrespective of the applied field intensity. However, for ferromagnetic materials $\mu_r \gg 1$ until the Curie temperature is reached whereupon $\mu_r \approx 1$.

The permittivity varies significantly with the frequency of the applied EM field, and the specimen's temperature and chemical composition. For example, the ε'' of beef decreases from 1300 to 12 as the applied frequency increases from 10MHz to 3000MHz [Metaxas and Meredith, 1983]. The combined effect of ω, ε', ε'' and ρ may be assessed from the value of the attenuation factor (Table 2.2).

The thermal diffusivity of the specimen controls the mean rate of temperature rise occurring within it. The required heating periods will tend to increase with its thermal mass ($\rho_d C_p$) and decrease with its thermal conductivity. The thermal conductivities of materials well suited to dielectric heating range from about 0.05 to 0.75 $Wm^{-1}K^{-1}$with a typical average value of 0.5 $Wm^{-1}K^{-1}$. The thermal conductivities of most metals are of the order of $50Wm^{-1}K^{-1}$ For solids, $4 \times 10^4 Jm^{-3}K^{-1} < \rho_d C_p < 4.5 \times 10^6 Jm^{-3}K^{-1}$: it has been suggested that a thermal mass value of $3 \times 10^6 Jm^{-3}K^{-1}$ can be taken as representative for most common metals and foods [Newborough and Probert, 1990].

Reference values for various parameters are given in Table 2.3. Other gross assumptions were made as follows;

i. Mean values for the physical properties (e.g. k, ρ_d,C_p, ε', ε'') apply for the base-case during the heating processes. However, for other composite materials the properties may be different for each layer and depend upon temperature.

ii. The ambient temperature was constant with respect to time. A mean value for the surface heat transfer coefficient applies during the heating period. The radiation rate equation was linearised similar to convection and radiation heat transfer coefficient was taken as $\sigma\varepsilon_T(T_s^2+T_\infty^2)(T_s+T_\infty)$ [Incropera & Dewitt, 1985]

iii For MWH processes, plane waves are incident normally at the surface.

iv the thickness d (or diameter in the case of sphere/cylinder) of the specimen is such that $d >> \delta$, so that the power may be calculated based on the assumption of semi-infinite geometries.

Table 2.2

Attenuation coefficients for some materials exposed to various electro-thermal processes: (adapted from (a) Davies,1990; and (b) Metaxas and Meredith, 1983)

Material	Temperature (°C)	Process	Frequency (Hz)	α m^{-1}
(a)				
Copper	20	DRH-IH	50	100
Steel	20	DRH-IH	50	60
Aluminium	20	DRH-IH	50	85
Aluminium	500	DRH-IH	50	47
(b)				
Maize	24	RFH	1.0×10^6	0.001
Melamine	25	RFH	1.0×10^7	0.01
Polythene	24	RFH	$\approx 10^7$	0.003
Coffee beans	50	RFH	2.0×10^7	0.02
Cotton	-	RFH	2.7×10^7	0.007
Meat	20	MWH	2.45×10^9	55.01
Carrot	20	MWH	2.8×10^9	49.2
Milk	20	MWH	2.45×10^9	46.1
Water	25	MWH	3.0×10^9	38.8
Porcelain	20	MWH	2.45×10^9	0.17
Ice	-20	MWH	3.0×10^9	0.05
Pyrex	20	MWH	2.45×10^9	0.05

Table 2.3

Base-case parameters for the heated material as employed in the model except where stated otherwise

Parameter	Unit	Value
Density	kgm^{-3}	1000
Specific heat capacity	$Jkg^{-1}K^{-1}$	3000
Thermal conductivity	$Wm^{-1}K^{-1}$	0.5
Initial temperature	°C	20
Ambient temperature	°C	20
Final mean bulk temperature	°C	75
Surface heat transfer rate	$Wm^{-2}K^{-1}$	5
Power transmitted at the surface	W	200
Attenuation coefficient	m^{-1}	50
<u>Slab</u>		
Irradiated surface area	m^{-2}	0.01
Thickness	m	0.06
<u>Sphere</u>		
Radius	m	0.03
<u>Cylinder</u>		
Radius	m	0.03
Height	m	0.1

2.6 RESULTS AND DISCUSSION

The choice of EM heating technique for processing a certain material is governed primarily by the material's physical properties and geometry and then by the user's requirements (such as the desired temperature distribution, length of heating period and cost). For example, DRH is a cheap and simple technique for achieving a near-uniform temperature distribution within a metallic material, but it is unsuitable for low-conductivity materials. Induction heating can be used preferentially to achieve high temperatures rapidly at a surface of a metal. Radio-frequency and microwave heating are only effective with low conductivity materials. However the working temperature-range, heating-period and materials involved are totally different for these EMH processes. For example with DRH, it may be required to heat 2m long, 0.01m diameter, steel rods through a temperature rise of 800°C, whereas in microwave cooking one may only need to achieve a temperature rise of 80°C in a 0.02m thick, 0.1m diameter food product such as pizza.

Fig.2.9 highlights the typical qualitative differences in the temperature profiles achieved. The effect of the alternating EM field is to concentrate the current in the surface layers which attenuates with depth into the material. The power absorbed and therefore the temperature characteristics exhibit this criterion for direct resistance, induction heating and dielectric heating. The surface temperature initially rises relatively rapidly, but, as the rate of heat losses increase at the surface, the point of maximum temperature moves progressively away from the surface towards the central region of the slab (Fig.2.9) due to the surface losses. However, as widely reported for dielectric heating, spheres and cylinders exhibit "centre heating effects" from the onset of the heating process, which can lead to dramatic cross-sectional temperature variations (Fig. 2.9 and 2.10). Centre heating effects are more pronounced in spheres, because, although the transmitted power diminishes as a wave travels towards the centre, the corresponding reduction in volume of the successive spherical, infinitesimally-thick shells causes the power dissipated per unit volume to increase dramatically as the centre is approached

(Fig.2.11). Therefore, practically the influence of geometry and material properties on heating characteristics is interdependent. However, the influence of each selected parameter was examined by varying its value while maintaining the reference for all remaining parameters.

2.6.1 Attenuation factor

Characteristic heating curves may be predicted to show the relationships between the attenuation factor, required heating period and heating effectiveness (proportion of power absorbed by the material expressed as % of the input power) for a slab of different depths (Fig. 2.11). From an energy-thrift perspective, it is desirable to achieve maximum heating effectiveness which is defined as the ratio of the power absorbed by the material to the input power. There appears to be an optimal range of attenuation factor for achieving both a maximum heating effectiveness and a minimum process heating-period (Fig.2.12). This range depends upon the shape and size of the product and the field intensity [Newborough and Probert, 1990]. At higher values of α, the heating process relies upon thermal conduction. Because the attenuation factor (or dielectric properties) of the material depend on the frequency, the optimal frequency for the process is dictated by the dielectric properties of the material involved.

The power absorbed (and heating characteristics) also depend upon the relative thickness of the material with respect to its attenuation factor. When the attenuation factor is large (or δ is small) as compared to the thickness of a material, most of the power is absorbed superficially (Fig. 2.11 & 2.13) irrespective of whether the specimen is spherical or cylindrical, and so relatively high surface temperatures result. The process of heating the interior of the specimen will depend solely upon its thermal conductivity. Some processes like surface hardening make use of this "disadvantage".

The attenuation factor changes during a heating process. For a certain geometry, a small change in the attenuation factor can alter

significantly the temperature distribution and thereby influence the heating effectiveness and the heating period required to achieve a certain mean bulk-temperature (Fig. 2.13). However, in dielectric heating for moderate to low values of α (e.g. 5-75m^{-1}) the cross-sectional temperature profile is greatly affected by the size and shape of the specimen (Fig.2.14). For example, when a 0.05m radius sphere with an attenuation factor of 50 m^{-1} is heated from a mean bulk-temperature of 20°C to 75°C, high temperatures occur near its centre. Whereas a larger sphere (with r = 0.1m) of the same material, heated under identical conditions, experiences surface heating (Fig.2.15a). Predictions for slabs of different thicknesses are illustrated in Fig.2.15b. Decisions can then be made concerning the essential parameters (such as the frequency of the EM radiation and the size of the product) so that the desired temperature distribution is achieved. For example, many approximately-spherical foods (such as potatoes and meat-balls) have typical dielectric properties at 2450 MHz, which cause core heating.

When heating in microwave ovens the total power absorbed by a load depends upon the material's dielectric properties as well as upon its size/volume. For spheres, the dependence upon radius of the power generated and cross-sectional temperature distribution achieved are shown in Fig.2.16 & 2.17. Evidently, for spheres with r >0.05m of α > 50 m^{-1} surface heating dominates. For situations where $\alpha \approx 50$ m^{-1} and $\alpha \approx 100$ m^{-1} the most uniform temperature distributions will occur in spheres of r≈0.05m and r≈0.03 mm respectively. However, for low α core-heating dominates for quasi-spherical specimens across the range under investigation (i.e. 0.005 <r< 0.125m). In general, as r and α increase the temperature difference between the inner and the outer regions (defined as characteristic temperature difference) decreases and the spheres surface becomes hotter than the centre.

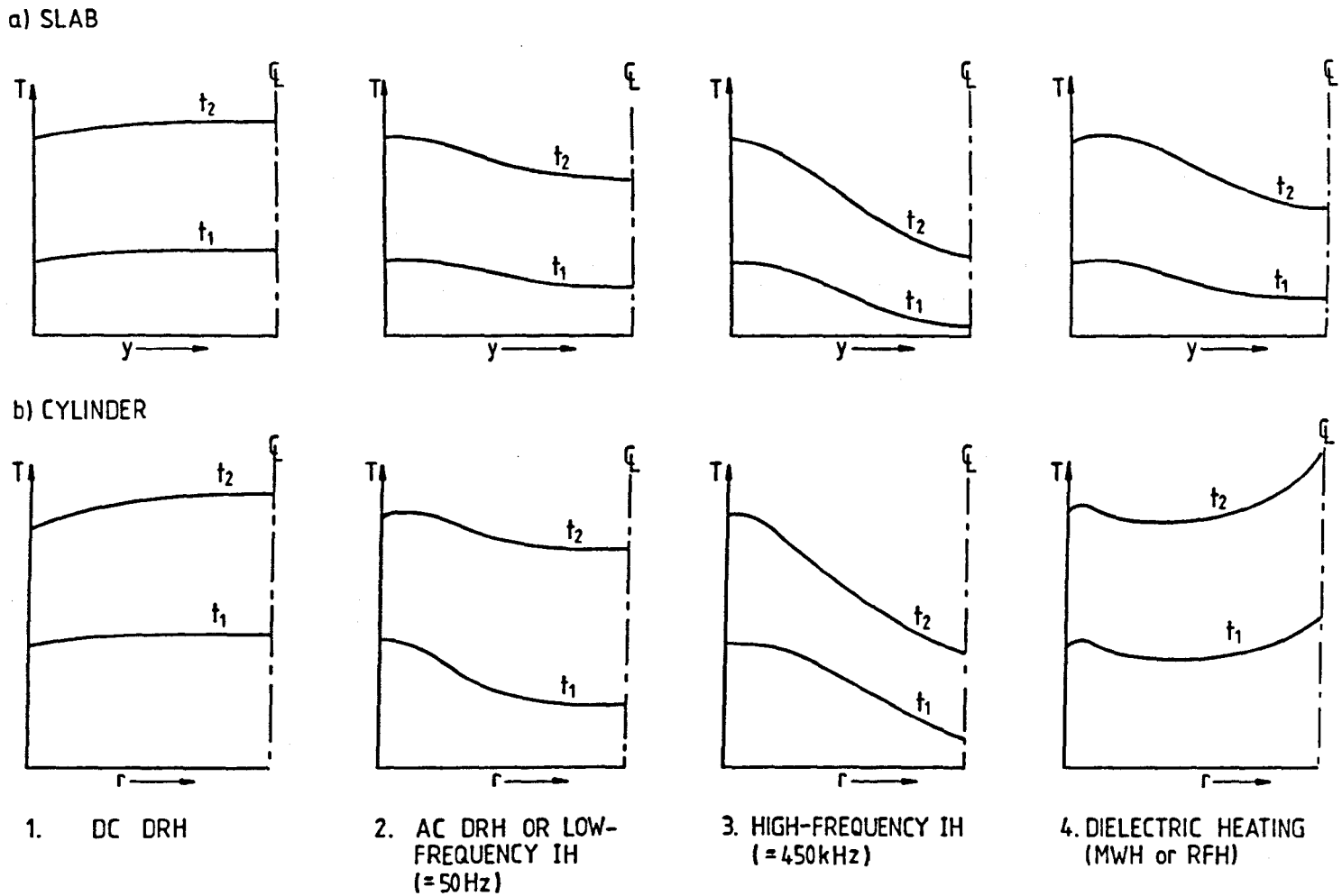

Fig.2.9 A qualitative comparison of transient temperature profiles with in (a) a slab and (b) a cylinder at time t_1 and t_2 ($t_2 > t_1$)

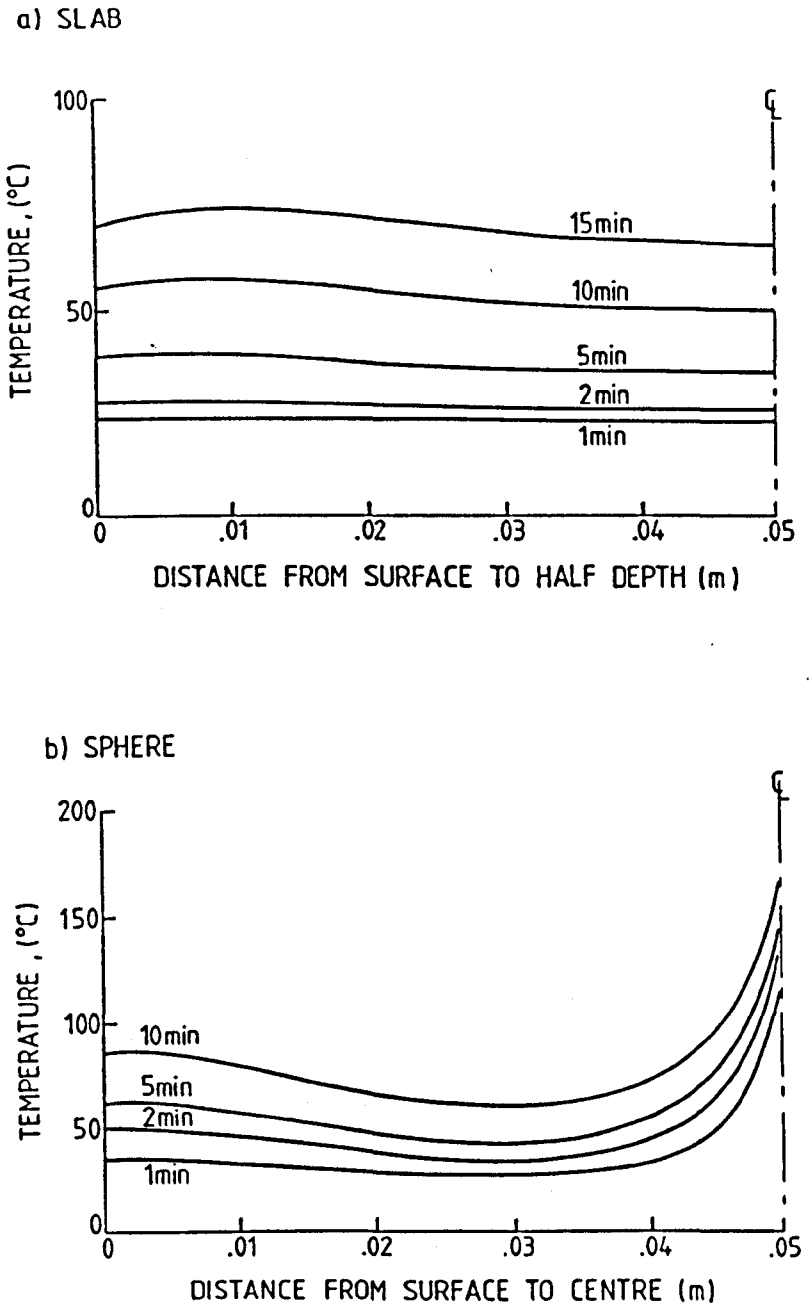

Fig.2.10 Temperature evolution due to EM heating in (a) a slab (b) a sphere. Base-case conditions apply: (Table 2.3)

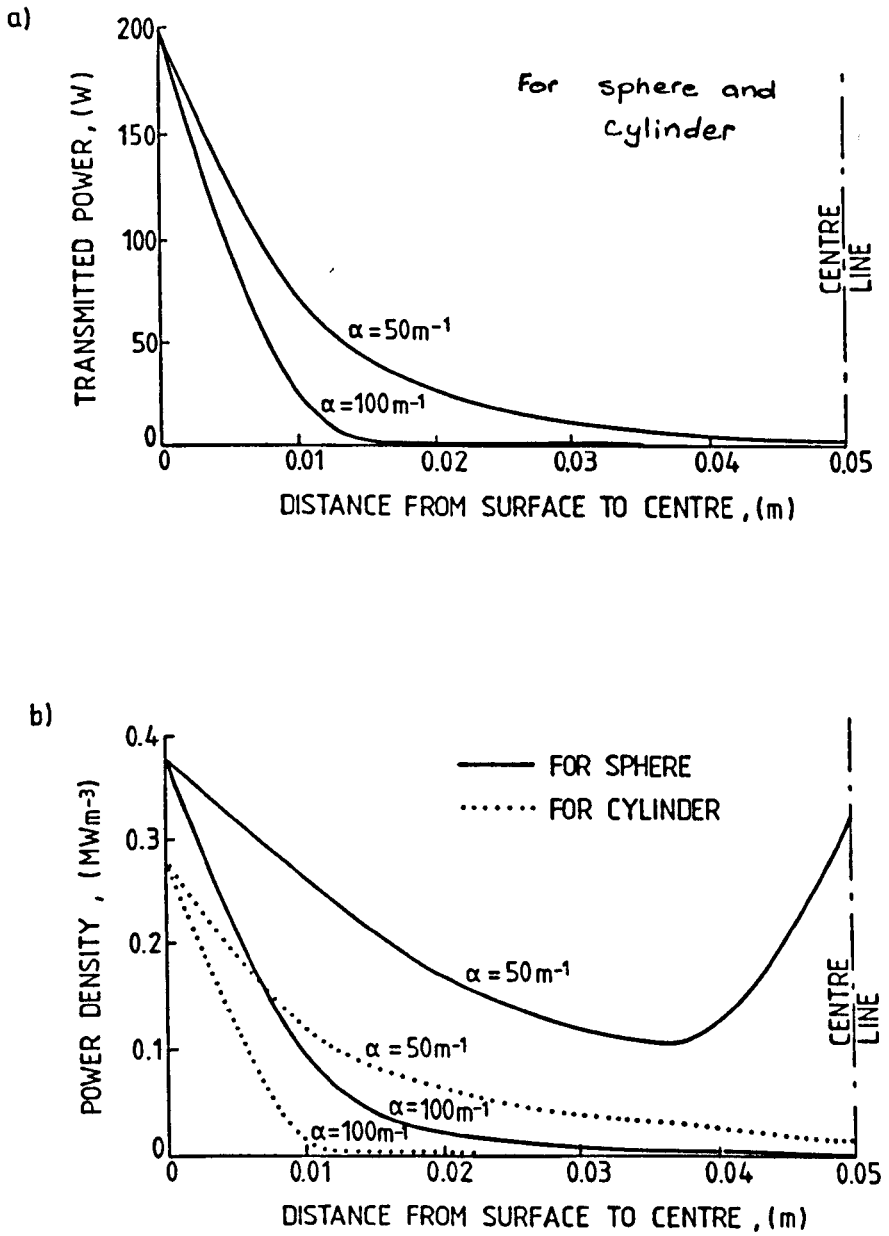

Fig.2.11 Variation of (a) Transmitted power with respect to the distance in to the material and (b) power density for a sphere and a cylinder for similar heating conditions for various attenuation factors (other parameters same as base-case slab)

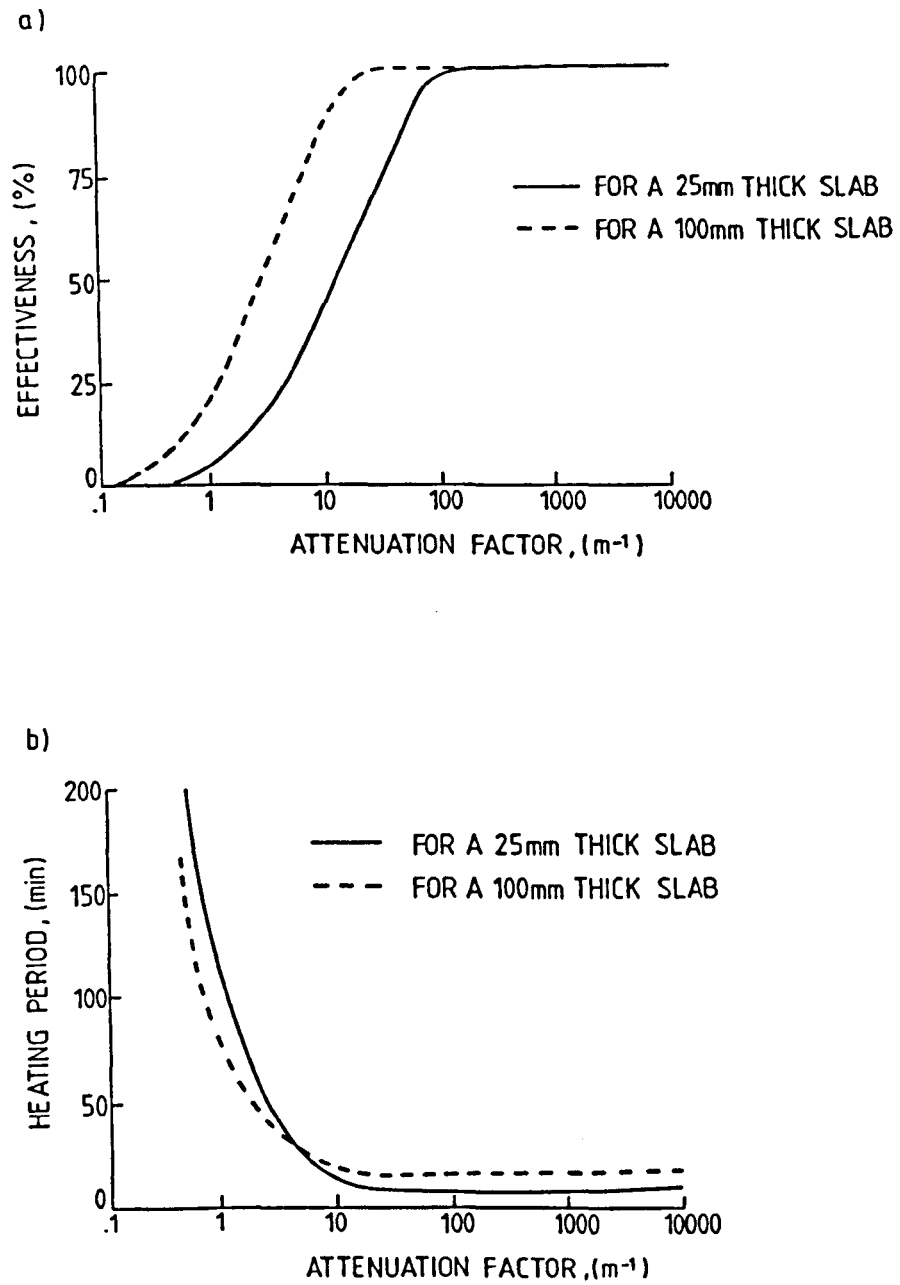

Fig.2.12 Predicted relationship between (a) the heating effectiveness and attenuation factor and (b) the required heating period and attenuation factor to achieve mean temp. 75°C

a) SPHERE

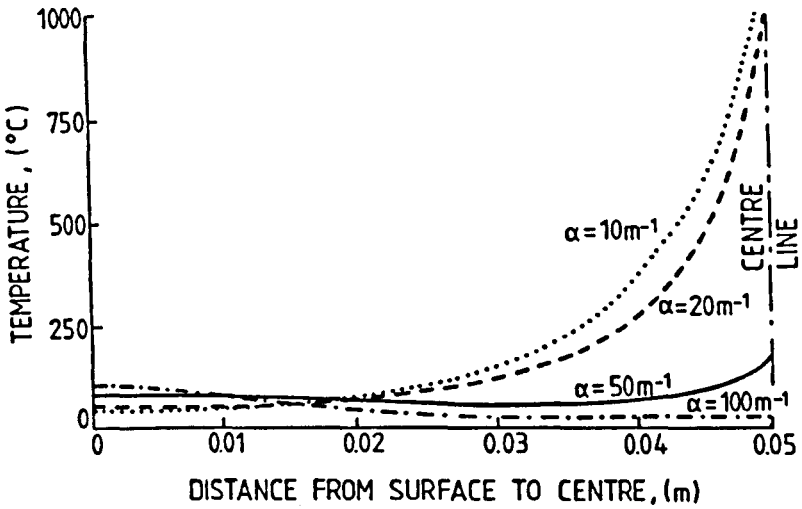

b) SLAB

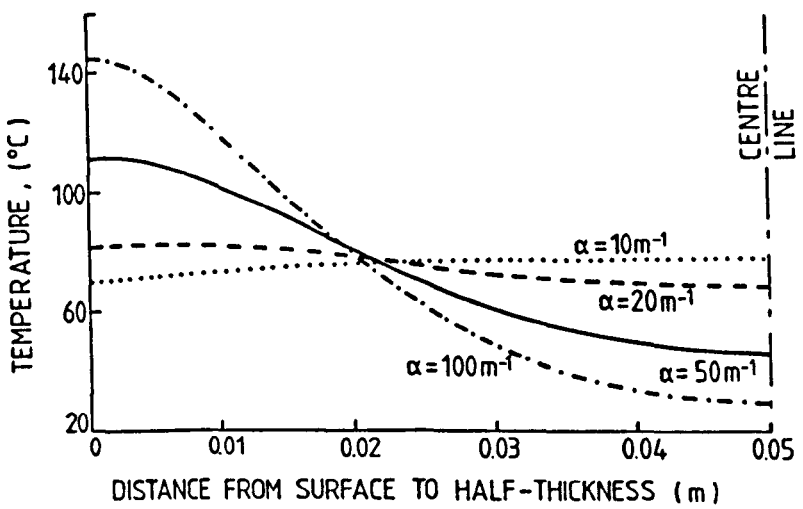

Fig.2.13 Temperature distribution for a range of attenuation factors for (a) a sphere and (b) a slab (other conditions same as base-case; temperature profiles correspond to a mean temp. =75°C)

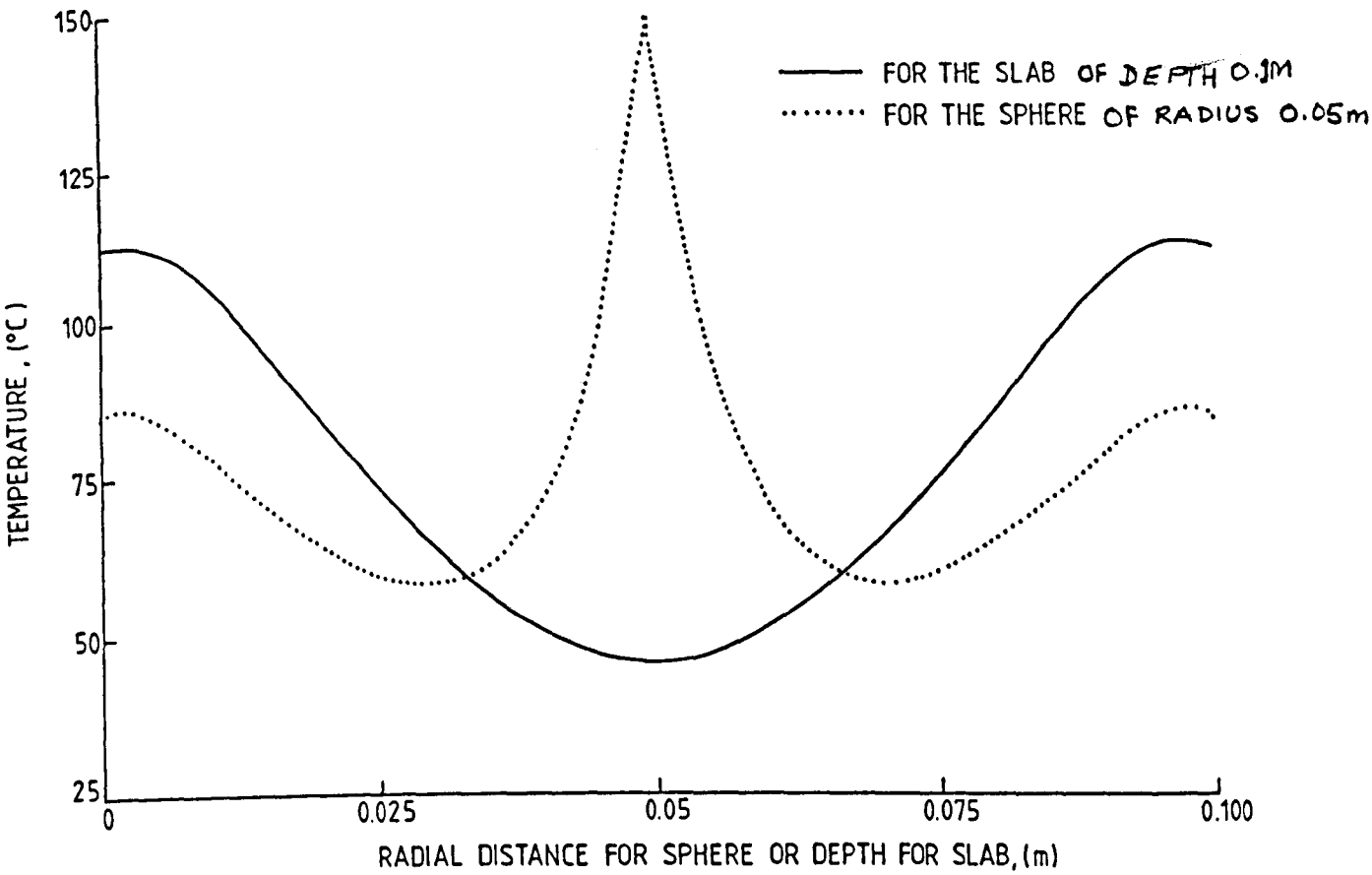

Fig.2.14 Comparison of the temperature profiles developed within a sphere and a slab heated under same conditions to achieve mean temperature =75^{o}C (other parameters same as base-case)

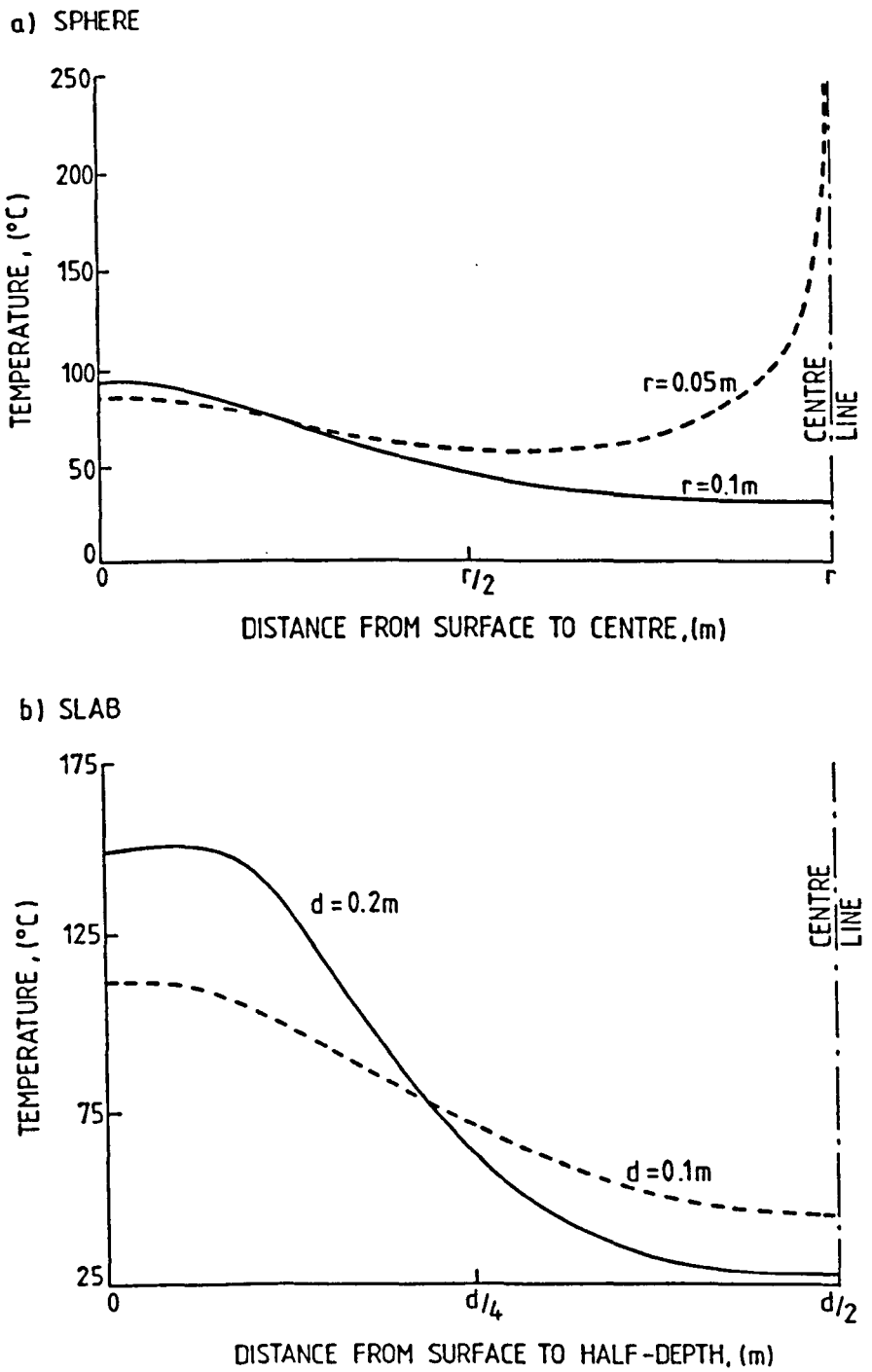

Fig.2.15 Temperature profiles represent a mean temperature=75°C within; (a) spheres of different radii and (b) slabs of different thicknesses (heated under similar conditions, other parameters same as base case)

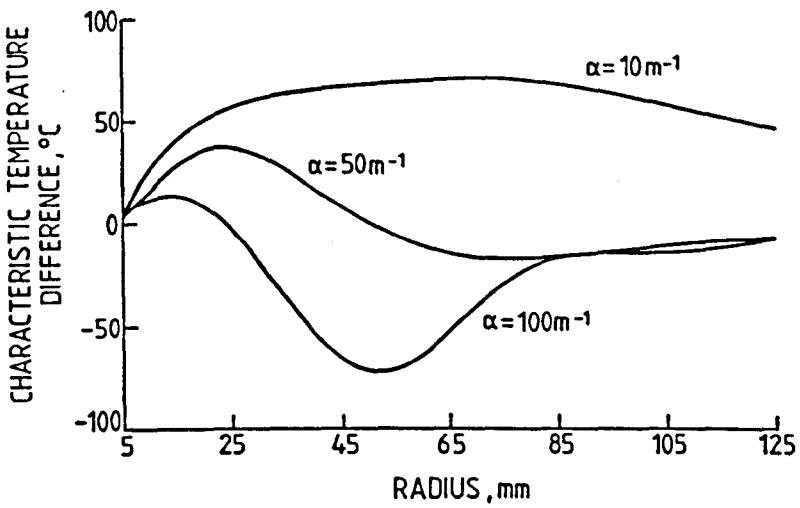

Fig.2.16 Characteristic temperature difference ($T_c - T_s$) for spheres of various sizes and attenuation factors

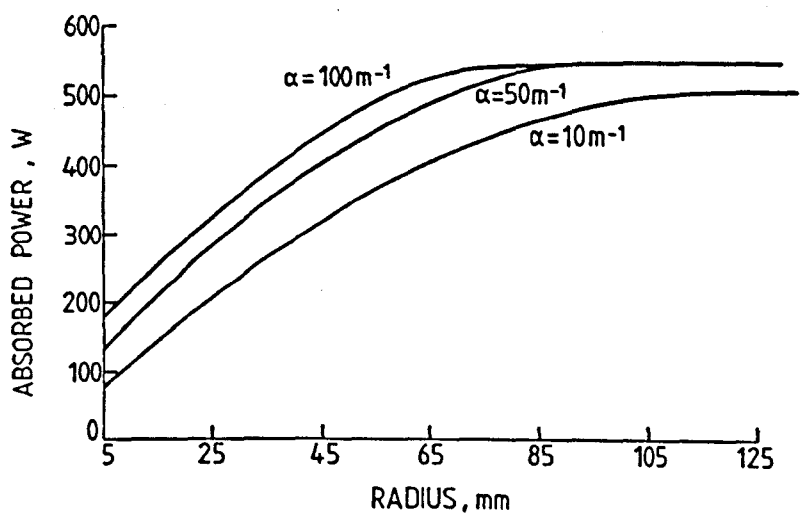

Fig.2.17 Variation of power absorbed with the size of a sphere

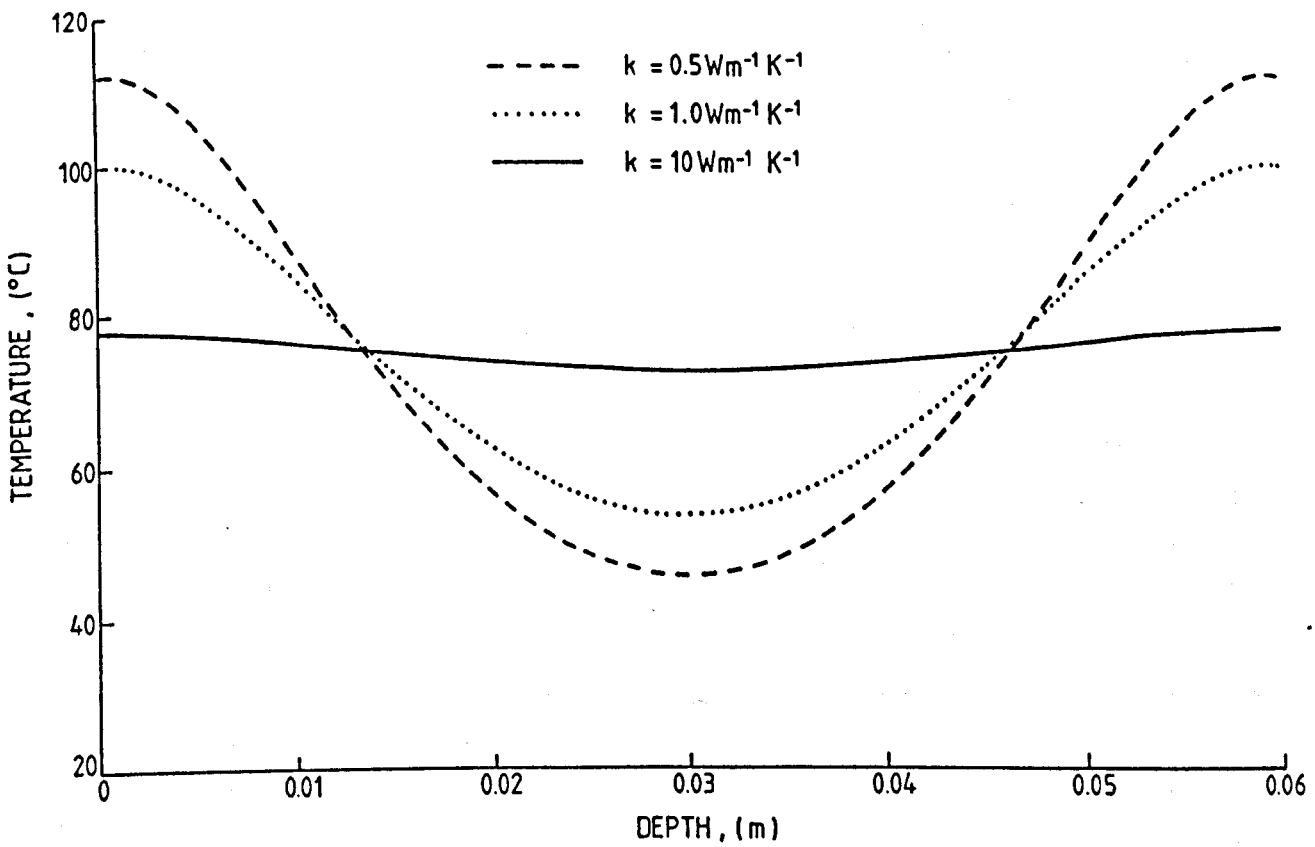

Fig.2.18 Influence of thermal conductivity on the temperature distribution achieved for microwave heating of a base case slab

2.6.2 Thermal Conductivity

For any heating process, a high thermal-conductivity will tend to lead to a more uniform temperature profiles within the material. Therefore, the thermal conductivity of a material has a significant role in achieving the desired temperature distribution within the sample (Fig. 2.18). However, the order of itsinfluence varies in different processes. For example, for DRH utilising d.c., P_v is almost invariant throughout the material and so a near uniform cross-sectional temperature can be achieved irrespective of the material's thermal conductivity. Whereas high-frequency (e.g. 450kHz) induction heating of steel, most of the heat is dissipated in a thin surface layer and the interior regions are heated only via thermal conduction.

Conversely, in microwave heating processes it is desirable, by design, to heat low-conductivity materials reasonably uniformly as the effects of thermal conduction are slight. For large attenuation factors and/or high power intensities, the effects of thermal conduction tend to be limited by the shortness of the heating process. In such cases, it may be desirable to include a 'standing period' after the period of irradiation/energisation or to heat the material intermittently (see later). Although this will improve the uniformity of temperature achieved throughout the specimen, a greater period will then be required to complete the process. If a uniform temperature distribution is desired, it may be preferable to heat the material at a different frequency - or in smaller thicknesses for flat geometries or larger diameters for quasi-spherical geometries (i.e. to reduce core-heating).

2.6.3 Specific Heat Capacity and Density

The control of specific heat-capacity and density has provided a major tool in the development of 'microwavable' food products [Schiffmann, 1986]. Oils and fats are poor absorbers of microwaves when compared with water, but due to their relatively low thermal inertia (as indicated by a low value of $\rho_d C_p$), they can be heated rapidly at high frequencies (Fig.2.19). Oils/fats also heat to higher temperatures without degradation than water. These properties of fats/oils and emulsifiers govern their selection for use in microwave food formulations. The density of a food product can be lowered by introducing more air per unit volume, which also reduces the item's effective thermal conductivity and permittivity (because the permittivity of air is unity). This tends to reduce the material's attenuation factor, which for a thick sample will help to achieve a more uniform temperature distribution. Essentially, the product's density can be altered by changing its porosity, in order to achieve a more desirable temperature distribution (see later).

2.6.4 Surface Heat Transfer

At the surface of a material, heat losses occur due to radiation, convection and evaporation. The radiative heat loss for a MWH process appears to have been neglected by many researchers [Kruhl, 1978; Mudgett, 1986] for reasons such as low emissivity and low surface temperatures. The long-wave emissivities for most biological products lie in the range of 0.8 to 0.9 [Miles, 1982] and surface temperatures (at least during cooking operations) exceed 50°C. Although the percentage error is small (Fig.2.20), it is desirable to account for radiative effects when predicting microbial lethalities in food materials.

In most metal-heating processes, emissivities are intermediate-to-high and surface temperatures of several hundred Celsius are reached, so rates of radiative heat-loss are more significant. By ignoring

radiative heat losses, the heating period will be underestimated and surface temperatures will be over-estimated. In practice, efforts are made to reduce the radiation losses. The radiative loss from a typical high emissivity work surface, increases from less than $1kWm^{-2}$ at 100°C to more than $300kWm^{-2}$ at 1300°C. Other surface-cooling effects due to convection and evaporation are more significant than radiation in RF drying and MW cooking processes, because these depend upon the local ambient temperature, the moisture content of the material, the water-vapour pressures at the surface of the specimen and in the air, the vapour permeability of the surface and also upon the local air-flow patterns within the cavity. Fig.2.21 demonstrates the influence of surface heat-transfers due to convection and evaporation upon the predicted temperature distribution in a thin low conductivity slab. Significantly higher surface-temperatures are predicted when surface evaporation is ignored.

2.7 USING A THERMAL MODEL FOR PRODUCT DEVELOPMENT

Knowing the effects of a material's properties and the frequency and intensity of the applied field upon the heating process, the model may be employed to solve the various optimisation problems (such as minimising the heating period, achieving the most uniform temperature-distribution and maximising the efficiency of the process). In most cases, the primary goals are to achieve a reasonably uniform temperature-distribution throughout the material for the least heating period. Parameters such as geometry, ambient conditions and the frequency of the EM field may be changed to achieve optimal operating conditions for a certain process or material. However, in practice the values of estimated parameters may act as an indicator only, as there are legal restrictions with respect to the use of frequencies and the most economic frequency is not necessarily the same as the optimal frequency. Sometimes it is not feasible to adjust the size, shape and physical properties of a specimen to achieve the optimal heating at the available frequency.

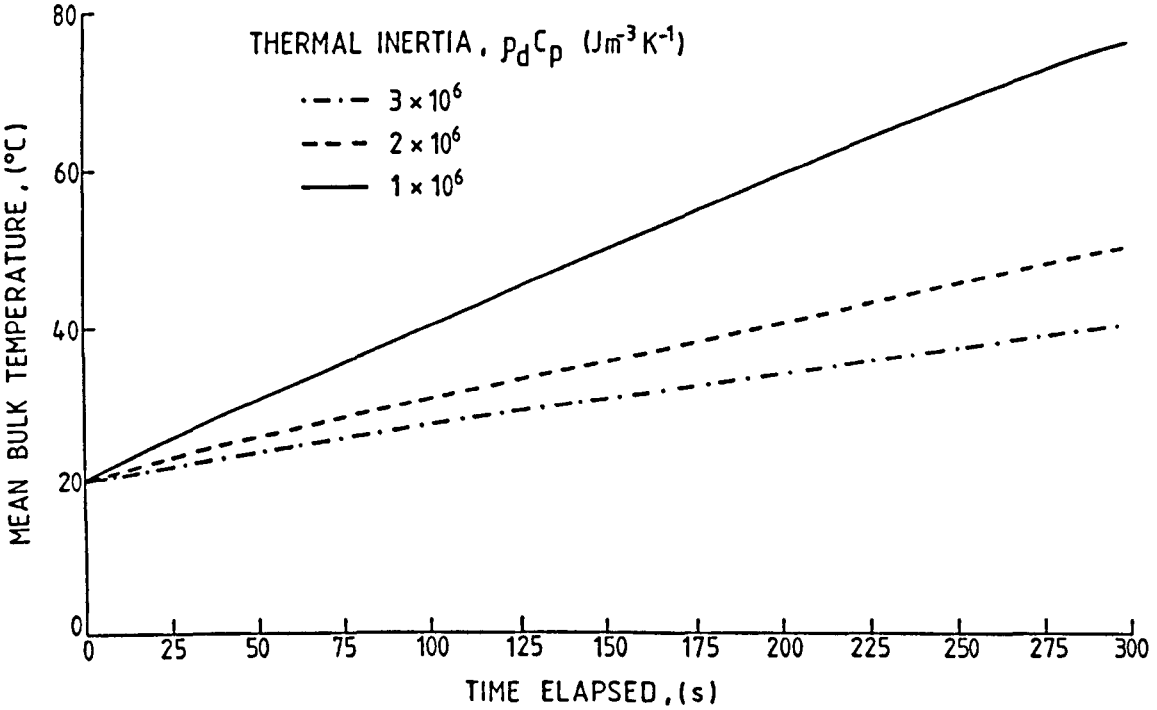

Fig.2.19 Relative heating rates for materials of different thermal mass per unit volume ($\rho_d C_p$)

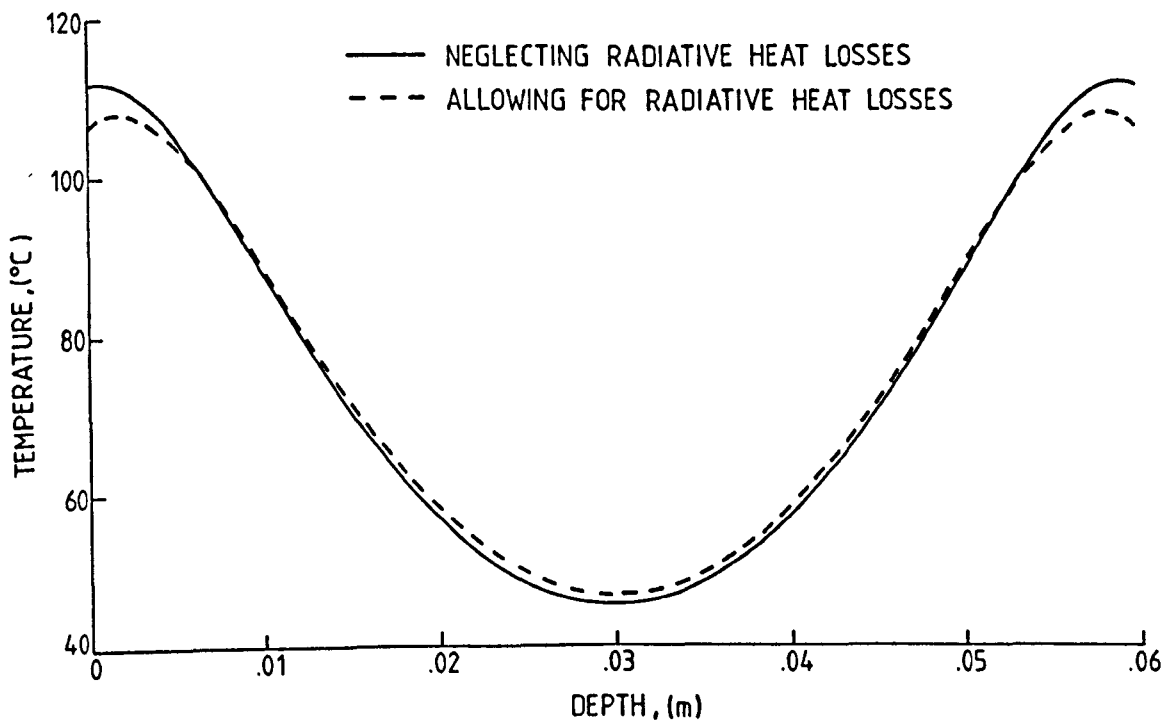

Fig.2.20 Effect of radiative heat transfer upon the temperature distribution (base case conditions apply. Profiles correspond to a mean temperature of 75°C)

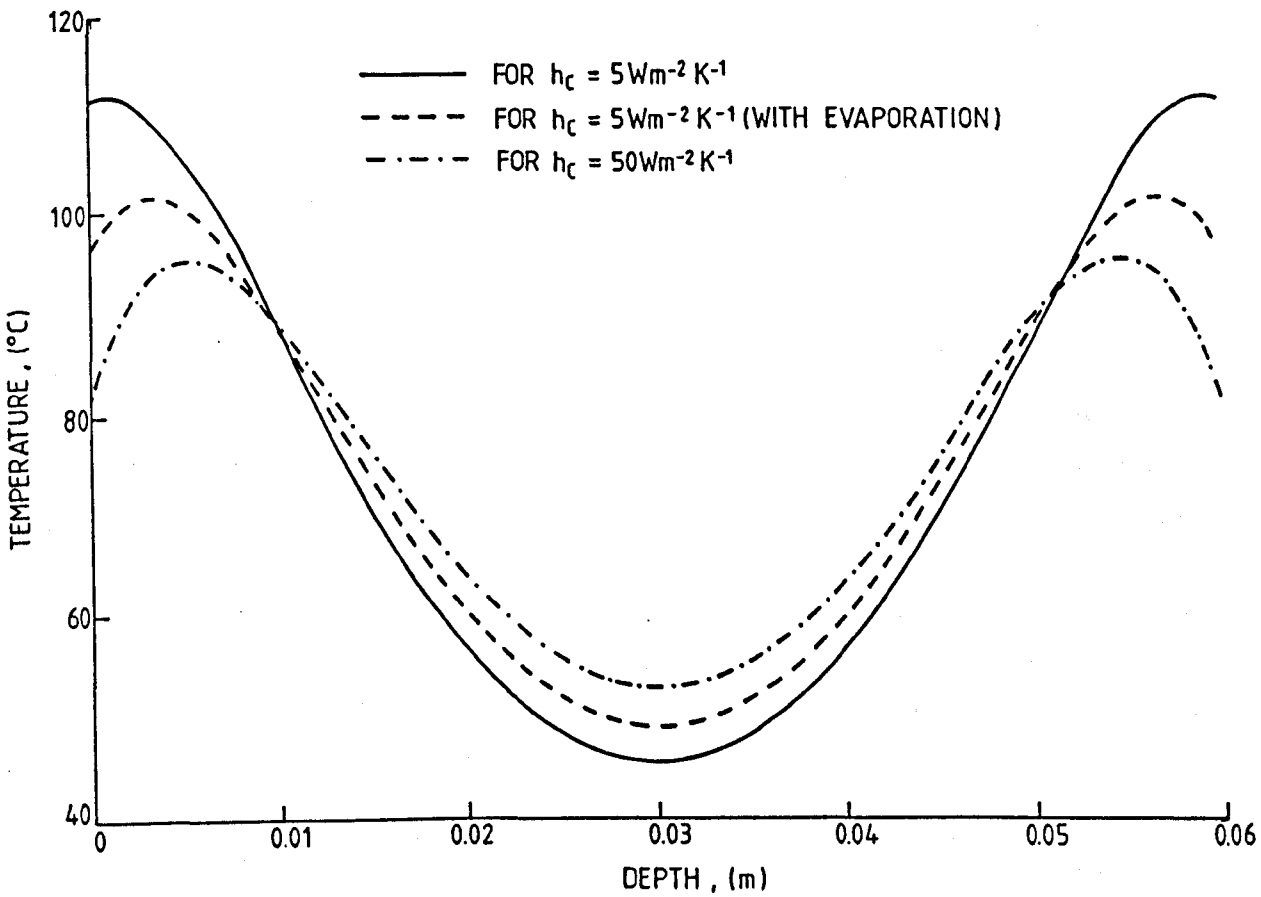

Fig.2.21 Effect of convective and evaporative heat losses upon the temperature distribution for a base-case slab to achieve mean temperature of 75°C

2.7.1. Input Power Levels and Intermittent Heating

The speed of a heating process can be increased by raising the power level: this however, in general, results in a less uniform temperature distribution (Fig. 2.22) and may not provide favourable results in sensitive processes like cooking or thawing. For example, cooking does not simply mean raising the mean-bulk temperature of a food to say 90°C but requires irreversible physio-chemical reactions to occur at suitable rates throughout the food in order to achieve a product of high culinary quality. Similarly, in a drying process, too rapid heating can cause generation of internal steam pressure faster than it can be relieved resulting in unwanted heating, over expansion or even explosion.

Expensive custom-built ovens are able to operate at variable power levels, which can be adjusted depending upon the process needs, whereas a typical domestic microwave oven only provides a means of operating the magnetron intermittently on a duty cycle to achieve a variable power level [O'Meara, 1989]. But operating with say a 5s on/5s off cycle does not achieve the same result as heating continuously at half power [O'Meara,1989]. It is expected that the temperature distribution becomes more uniform due to thermal-conduction effects during the 'off' period (Fig.2.23). By increasing the 'off' time, one can achieve a more uniform temperature distribution, but at the expense of extending considerably the heating period (Table 2.4 and Fig.2.24). The values for on-off times are chosen for illustration only. In practice these range from 2-10s for microwave ovens, because if time bases are long, it is difficult to cook sensitive foods (cakes etc.) which can not tolerate heating by high-power bursts.

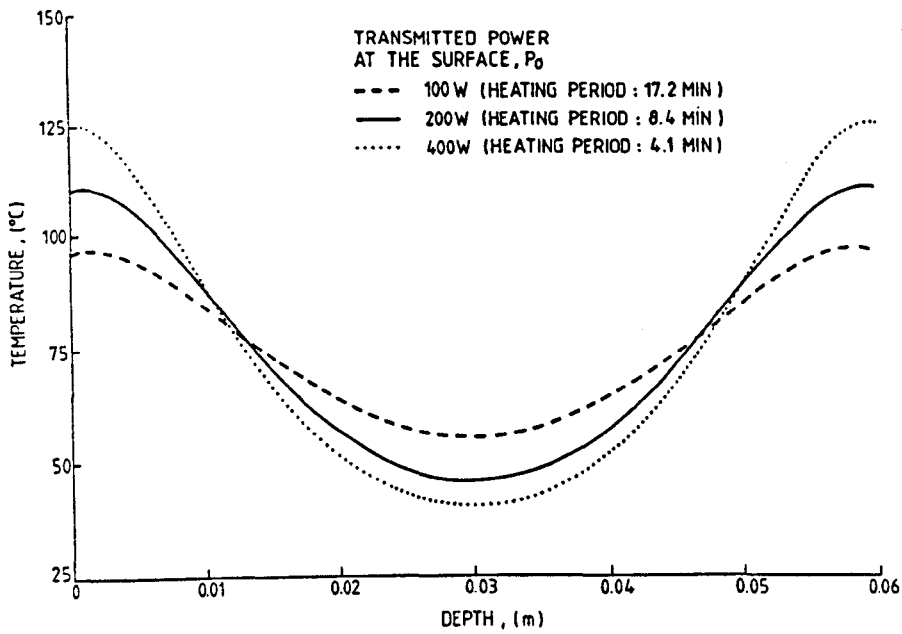

Fig.2.22 Comparison of temperature profiles achieved for base case slab for various power inputs (profiles correspond to the mean temperature of 75°C)

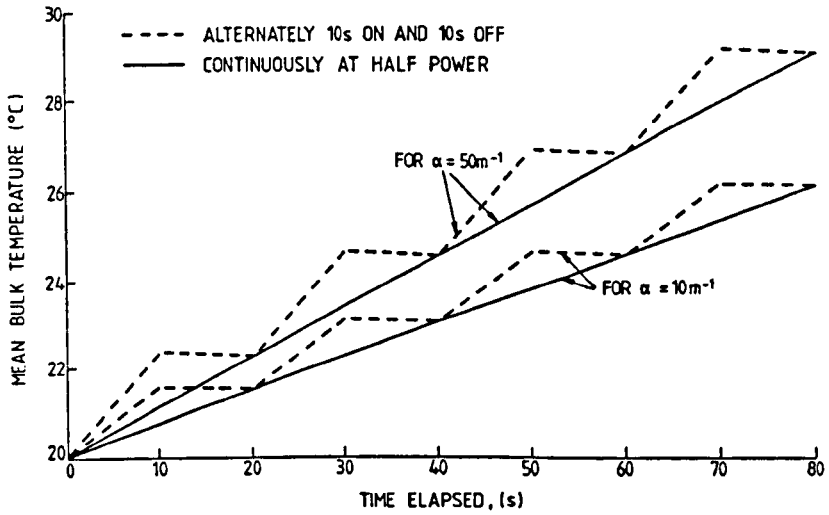

Fig.2.23 Thermal equlibrium effects during off-duty periods of an intermittent-heating cycle for a base case slab

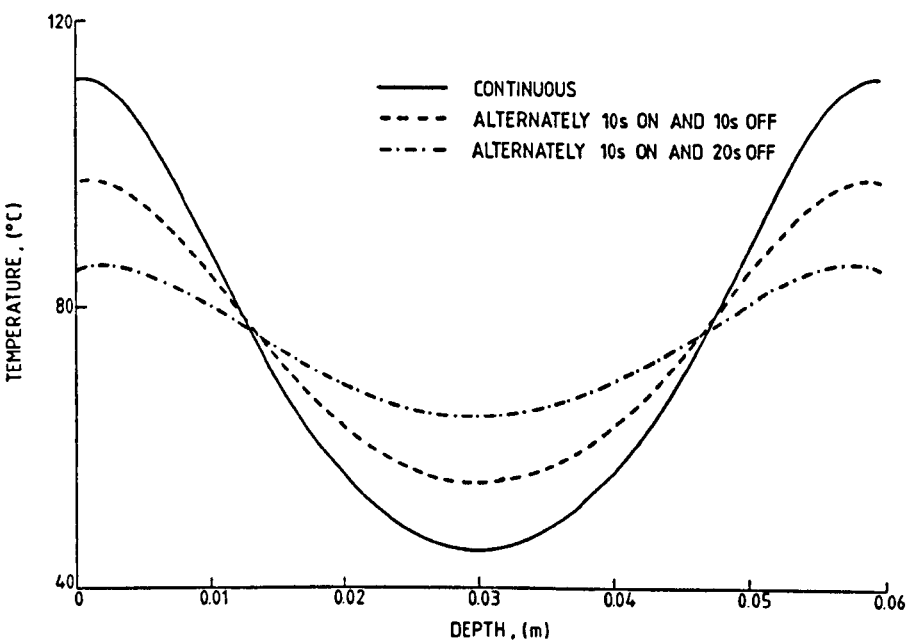

Fig.2.24 Comparison of the temperature profiles at the end of heating period for a base case slab when heated (a) continuously and (b) at different "on-off" duty cycles

Table 2.4

Comparison of heating period for intermittent heating of a base case slab for various duty-cycle

Duty cycle "on" period (s)	Duty cycle "off" period (s)	Total period required to achieve a mean bulk temperature of (75°C) min	s.d. from mean-bulk temperature
continuous	0	8.4	23.0
10	10	17.1	15.0
10	20	36.0	7.5

2.7.2 Multi-Layered Materials

Many products consist of components made of two or more different materials. Heating characteristics for such composite products, when irradiated normally, indicate differential heating effects due to the distinct attenuation coefficients of each layer (Fig.2.25). The concept of impedance mismatch between the product and the adjacent free space (which determines the field pattern within the material and in the free space), may be applied to composite systems with dissimilar phase properties. Reflections at internal boundaries also add to differential-heating effects depending upon the impedance mismatch of the layers. Nevertheless, the sequence of attenuation coefficients is the dominant factor influencing the power absorbed in a multi-layered product. The layer of relatively-high attenuation coefficient will absorb more power than its otherwise equivalent adjacent layer. This results in a peak temperature in that layer (see Fig.2.25). However, in this case, the attenuation coefficient of each layer is assumed to be constant during the heating period, whereas α may vary distinctly with temperature for each material. Also, the heating rate in different layers is equally affected by the values of their respective thermal diffusivity, $(k/\rho_d C_p)$ which is also temperature dependent. Therefore,

in developing a multi-layered product, the optimal (or an acceptable) combination of these effects is sought in order to achieve the required temperature distribution. For example, a temperature profile which indicates cold spots at the centre of the solid is undesirable when cooking food because the surface temperatures cannot be relied upon to provide a visual confirmation of 'doneness'. To eradicate the cold spot at or near the centre, the material with a low attenuation factor should (if practicable) be located at the surface (Fig. 2.24). Alternatively the density and/or specific heat-capacity of the material with a lower α may be decreased or the thickness of each layer adjusted so as to obtain a more even temperature profile (Figs 2.25 and 2.26). A classic example of this is in microwave doughnut proofing and frying, where changes in the base material led to a successful microwave heating system [Schiffman et al 1971 a,b]. Similarly with pre-packaged meals, different foods can be made into different shapes and sizes depending upon their dielectric properties so that the complete meal can be heated so that an almost uniform temperature is attained by the end of the cooking period. Finally the packaging (or food container) can be chosen to enhance or suppress the heating of a heterogeneous food product as desired [O'Meara, 1988; Buffler, 1992].

2.8 TEMPERATURE DEPENDENT MATERIAL PROPERTIES

In the aforementioned analyses, material properties were functions of space only and did not change with time (or temperature). However, in general, material properties vary with respect to temperature and also with respect to the moisture content and chemical composition in the case of biological materials. The variations in dielectric properties have a great influence on the power generated within the material, whereas the thermal properties affect the rate of heat transfer. For example, with direct resistance and induction heating, the power generated depends primarily upon how the material's resistivity and permeability change with temperature. The variation in resistivity with respect to temperature is quite significant (see Table 2.5).

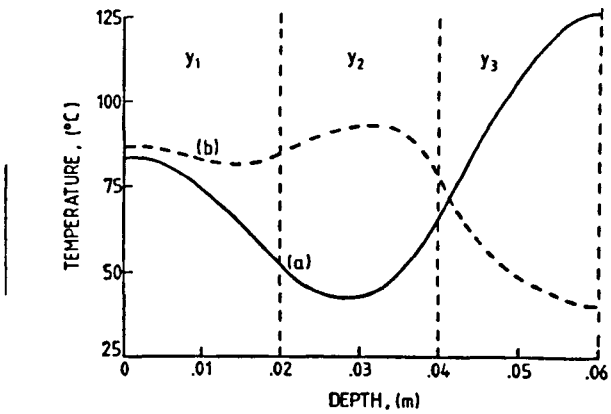

Fig.2.25 Temperature distribution at the end of heating period within a three-layered slab (mean temp. 75°C) each layer of thickness 0.02m; dielectric properties are such that:

(a) $\alpha_1 = 25m^{-1}$; $\alpha_2 = 5m^{-1}$; $\alpha_3 = 50m^{-1}$

(b) $\alpha_1 = 25m^{-1}$; $\alpha_2 = 50m^{-1}$; $\alpha_3 = 5m^{-1}$

(Other parameters same as base-case)

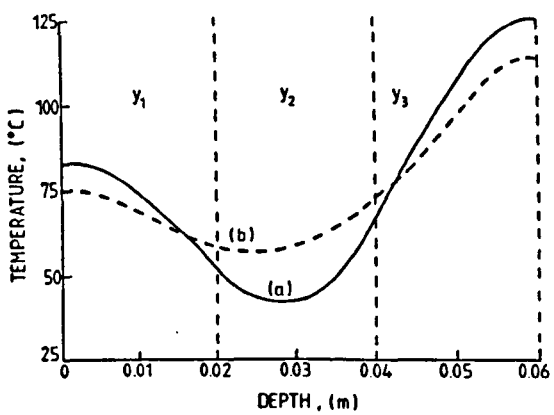

Fig.2.26 Temperature profile (a) for a slab in Fig.2.25 is compared with the temperature profile (b), which is achieved by reducing the $\rho_d C_p$ of the middle layer by 50% (other parameters same as in Fig.2.25)

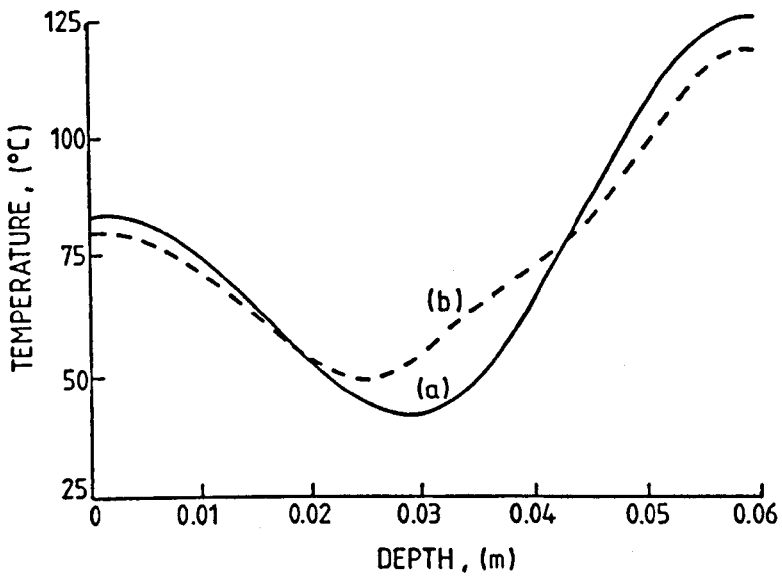

Fig.2.27 Temperature profile (a) for a slab in Fig.2.25 is compared with the temperature profile (b), which is achieved by changing the thickness of the layers to 0.03m, 0.01m and 0.02m repectively, (other parameters same as in Fig.2.25 a)

For a ferrous metal, heating to above the Curie temperature reduces the rate of change of resistivity with temperature and the permeability decreases to unity. Hence the heating periods required to increase the temperature of a material through say 100°C below and 100°C above the Curie point will be significantly different (see Table 2.6).

The practical importance of property variations was evaluated from the influence of the net effect of varying thermal and dielectric properties on the model's predictions. In this investigation, direct resistance heating of a steel rod and microwave heating of a potato slab was analysed (Table 2.6 and Fig. 2.28 & 2.29).

a) Steel rod

Above the Curie point the attenuation factor of a metal decreases: this reduces the temperature difference between the specimen's surface and centre. Therefore through-heating by induction becomes much more effective above the Curie point ($\approx$ 760°C for mild steel), although the power intensity falls sharply (Fig. 2.28). Thus a dual-frequency DRH system, or a supplementary-induction heating system for use above the Curie temperature, is desirable to ensure the efficiency and economic viability of a metal-heating process.

b) Potato slab

For many products there may not be a great difference between the predicted final temperature distributions when modelled with constant properties or temperature-dependent properties for a certain temperature range (Fig. 2.29a). But during thawing water within the material may exist in different phases and behave as layers of different materials. After the initial absorption of energy by the frozen specimen, the temperature rises, until it reaches 0°C where upon the attenuation factor is greatly increased. This in turn, greatly increases the rate of temperature rise near the surface (i.e. 'thermal runaway'). The surface temperature then begins to rise rapidly, because all the energy is absorbed near the surface the unfrozen layers, while the interior regions remains frozen. Thus the assumption of constant properties across the range, say -10°C to 5°C will result in large errors in the predictions of a numerical model (Fig.2.29b).

Table 2.5

Physical properties of mild steel (~ 0.23% carbon content) as a function of temperature (adapted from Davies and Simpson, 1979)

Temperature (^{o}C)	ρ (10^{6} Ωm)	$\rho_d C_p$ ($10^{-6} Jm^{-1}K^{-1}$)	k ($Wm^{-1}K^{-1}$)	α_t ($10^{6} m^{2}s^{-1}$)
20	0.160	3.65	52.0	14.44
100	0.220	3.85	51.0	13.25
200	0.290	4.10	49.0	11.95
300	0.380	4.40	46.0	10.45
400	0.480	4.77	43.0	9.01
500	0.610	5.19	39.3	7.57
600	0.755	5.66	35.5	6.27
700	0.922	6.66	31.5	4.72
800	1.095	6.73	26.0	3.80
900	1.135	6.94	26.5	4.46
1000	1.168	5.09	27.3	5.36
1100	1.195	5.10	28.5	5.58
1200	1.220	5.10	29.7	5.82

Curie point = 760°C

Table 2.6

Comparison of required heating periods for a mild steel rod (r = 10mm) during a DRH process ($E=8Vm^{-1}$) per 100°C temperature-rise for the range 0-1200°C (material properties as defined in Table 2.5)

Temperature range (°C)	Δ t (s)
0 - 100	1.2
100 - 200	1.6
200 - 300	2.5
300 - 400	3.1
400 - 500	4.8
500 - 600	6.0
600 - 700	8.8
700 - 800	11.5
800 - 900	12.8
900 - 1000	12.2
1000 - 1100	10.8
1100 - 1200	10.5

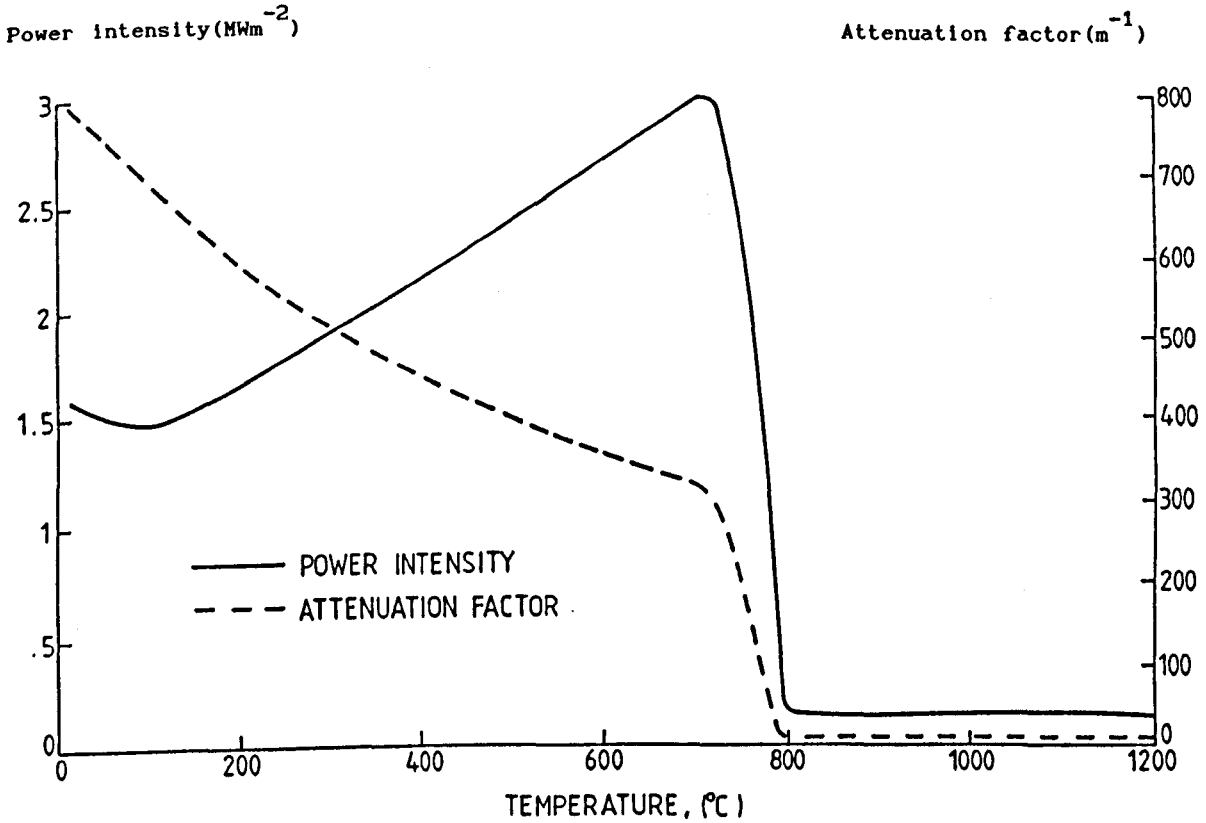

Fig.2.28 Variation of attenuation factor and power intensity with temperature for IH of mild steel bar (materials properties from Table 2.5), μ_r=500Hm^{-1}, H_{rms}=10^{5}Am^{-1}, f=50Hz

a)

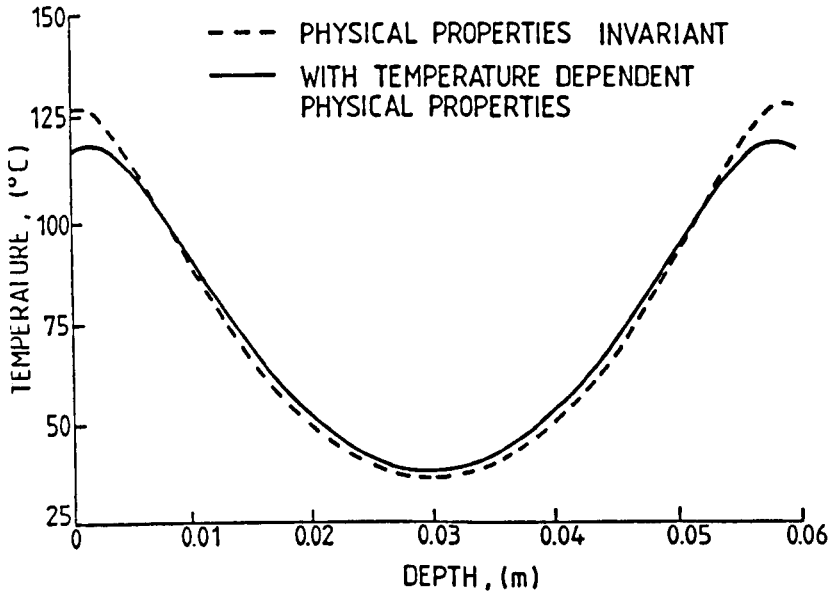

b)

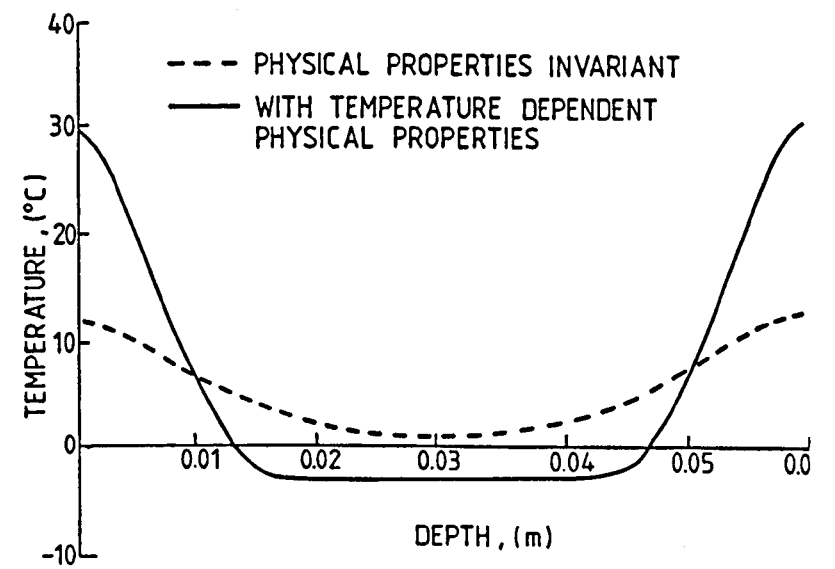

Fig.2.29 Temperature profiles for a potato slab assuming (i) constant (ii) temperature-dependent properties; when heated (a) from 20 to 75°C (b) from -10 to 5°C

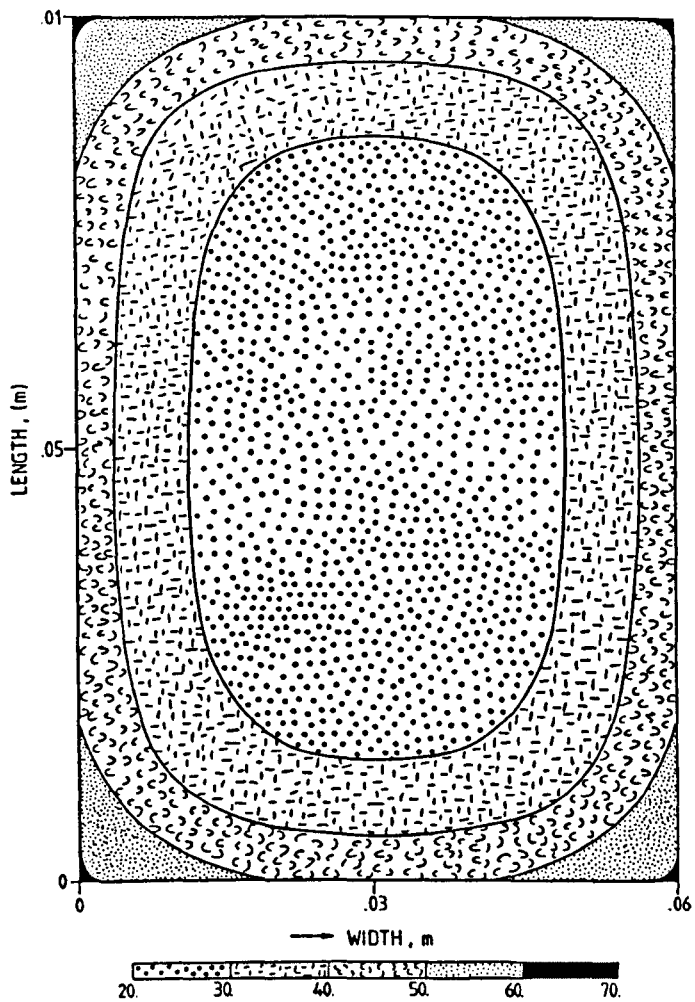

Fig.2.30 Two dimensional temperature distribution in a base case slab, heated from four sides for 120s.

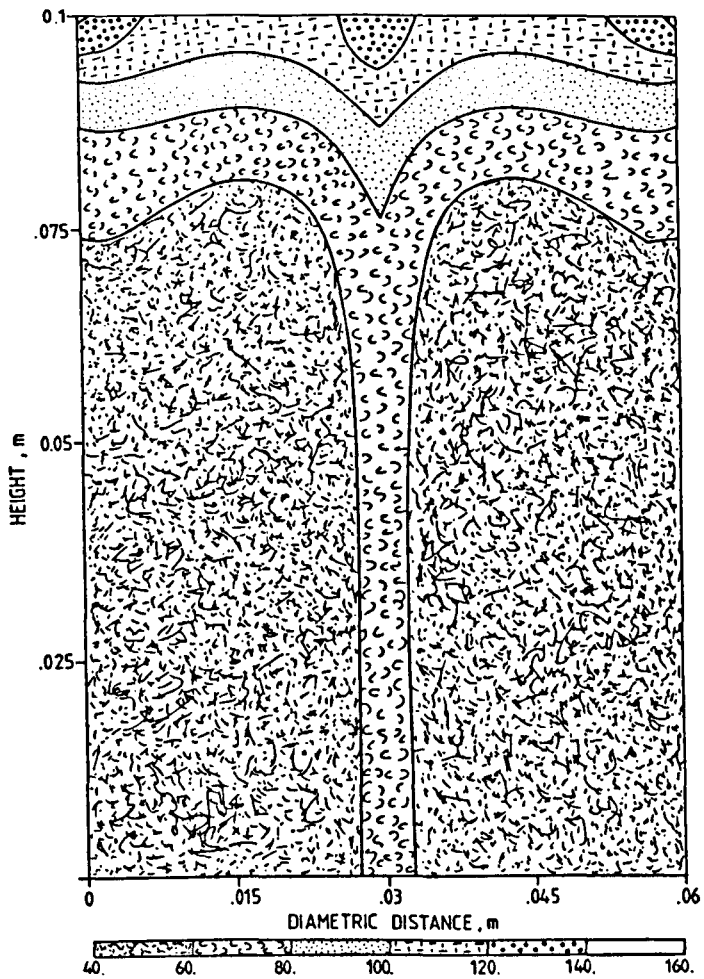

Fig.2.31 Two dimensional temperature distribution in a base case cylinder, heated radially and axially from the top for 120s.

2.9 Two-dimensional Simulations

The one dimensional model is sufficient to examine the heating characteristics for various processes and geometries e.g. DRH of long rods and microwave heating of spherical products. In practice, significant variations in temperature distribution occur over large flat surfaces (whether the product is of square, rectangular, circular or irregular cross-section) as well as the in-depth variations. Therefore, to achieve a better understanding of temperature distributions near the edges and corners of cylinders and slabs two and three dimensional analyses need to be undertaken. Two dimensional model was employed to illustrate the core heating effect for a slab and cylinder respectively for microwave heating (Figs. 2.30 and 2.31).

2.11 CONCLUSIONS

A general mathematical model has been developed to provide a means for understanding parametrically EM heating processes. The model is based on the use of the standard heat diffusion equation with a variable heat generation term which depends upon the type of process. The model is mathematically represented as a non-linear differential equation. The study illustrates the utility of a theoretical model for investigating the influence of a large number of parameters, most of which are experimentally difficult to obtain. A simple one dimensional model with all its simplifications provides a powerful educational tool for analysing the characteristically rapid depth-dependent EMH processes and is especially useful for comparisons with the conventionally studied heating processes where the heat generation term is constant.

The accuracy of the predictions by a mathematical model is restricted by the various assumptions made for simulating the actual physical process and boundary conditions. From this study, the extent to which various parameters may influence an EMH process has been assessed and thereby appropriate assumptions may be made to improve the accuracy of the predictions. For example, for short heating periods convection does not make significant difference in the mean-bulk temperature in a

dielectric heated by MW or RF. However, when heating metals by DRH or IH radiative losses must not be ignored. Thus, the assumptions concerning boundary conditions may be made depending upon their order of influence upon different types of EMH processes. Similarly, in a drying process, a reduction of moisture content will decrease the heating rate of a material. Therefore to achieve a good simulation of the process, allowance must be made for the moisture dependency of the properties.

Because the physical interactions which govern the heating of materials (ranging from metals to dielectrics) by EM techniques (from DC to 10^{12}Hz) are quite distinct, the underlying weakness of any thermal model is the assumption concerning the distribution of EM energy within the material. However, the conclusions made by employing the model are valid qualitatively and unlikely to change even for a more complex model for heat generation via EMH processes.

In the following chapters various assumptions made in the general model are discussed in detail, in the context of microwave heating of foods, and the model is modified accordingly.

CHAPTER 3

3. DIELECTRIC PROPERTIES OF FOODS

3.1 INTRODUCTION

Microwave energy has been used successfully to yield products with improved quality for a lower expenditure of energy for many commercial processes, as well as in the domestic sector. The increasing proliferation of computers is providing a favourable climate for developing mathematical models for solving many optimisation problems relating to food processes. With microwave heating the challenge is to optimize the product heating rates and achieve the desired temperature distribution within the product. An accurate description of heat transfer via the heat diffusion equation requires an appropriate solution method and accurate property values for the material under investigation. The accuracy with which these properties are known influences the accuracy of the thermal predictions from a mathematical model.

The dielectric property of general interest in microwave heating is the material's relative permittivity $\varepsilon_r^*(= \varepsilon'-j\varepsilon'')$, which determines the energy absorption by the material from the applied EM field (see Chapter 2). In principle, the computations of power absorption and reflection, attenuation factor and internal resonances depend upon the accurate permittivity data for the material.

A large amount of experimental data exist for the dielectric properties of various foods [Bengtsson & Risman, 1971; Tinga & Nelson, 1973; Kent, 1987]. Many of the measurements have been taken at a single temperature and as such need to be treated with caution when applied over wide temperature ranges in simulation models. For example, the substitution of such single-temperature values of dielectric properties into a mathematical model simulating a microwave heating process may result in inaccurate predictions of cross-sectional temperature-profiles (see

Chapter 2). Although presentations of data for several products are available in tabular as well as in graphical form to illustrate the various relationships between the property data and the frequency, moisture content and temperature [e.g. see Bengtsson & Risman , 1971; Jain & Voss, 1987; Nelson et al, 1991], it is desirable to be able to express dielectric properties in the form of equations.

Some discrepancies in the published values for the dielectric constant and loss factor for nominally similar foods exist partly due to the different measuring-techniques employed. Also the accuracy of measurements is often not stated; strictly each measurement should be repeated for every composition occurring in practice. The best that can be hoped for are data which approximate to the average (i) composition for the food and (ii) applied conditions. Thus, it is not surprising that many models do not account for the temperature and moisture dependencies of dielectric properties. As Mudgett [1990] stated, this is a fundamental weakness of the available predictive models for microwave heating.

Recently presented numerical models for microwave heating of certain materials have accounted for the temperature and moisture dependence of the dielectric properties by employing polynomial or exponential expressions to describe the associated experimental data [Jolly & Turner, 1990; Ayappa & Davis, 1991] . However, in general, simple predictive equations for inclusion in the microwave heating simulation models are desirable. Thus a systematic evaluation of the available experimental data is performed in order to:

a) propose predictive equations for the dielectric properties of individual food products at the commonly employed microwave frequencies; and

b) identify a relationship between the food type, temperature and dielectric properties, so as to propose equations for groups of similar types of foods (e.g. meats, vegetables and grains).

3.2 PHYSICAL BASIS OF DIELECTRIC LOSS

The presence of an applied electric field **E**, causes charge motion (conduction) or charge displacement (polarisations). The latter is of more importance in dielectric materials such as foods and arise due to the following mechanisms (Fig.3.1);

a) *Electronic polarisation:* the displacement of electrons around atomic nuclei which occurs within the optical region of the EM spectrum.

b) *Atomic polarisation:* the relative displacement of atomic nuclei due to unequal charge distribution in molecule formation occurring in the infra-red region.

c) *Orientational polarisation:* the displacement of polar molecules (e.g. water, proteins, NH_3) with spatially unbalanced charges, which tend to reorientate under the influence of a changing electric field which occurs in the *microwave region.*

d) *Interfacial polarisation:* the interaction between a field and the charge build up at interfaces of components in heterogeneous systems [deLoor, 1969] taking place at sub microwave frequencies.

The relative permittivity, ε_r^* $(=\varepsilon'-j\varepsilon'')$, is a manifestation of these polarisation phenomena and defined as a proportionality constant between the polarisation field **D**, and applied field **E** (see Appendix 1). The dielectric constant ε', and dielectric loss ε'', determine the material's ability to store and dissipate energy. Dielectric loss involves the total energy dissipative effects of all the elastic distortions, deformations and displacements which occur under stimulation from the field plus the restoration forces.

(a)

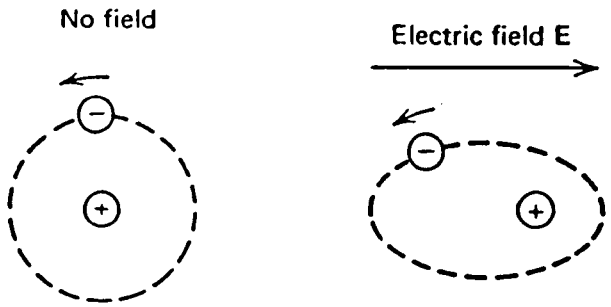

(b)

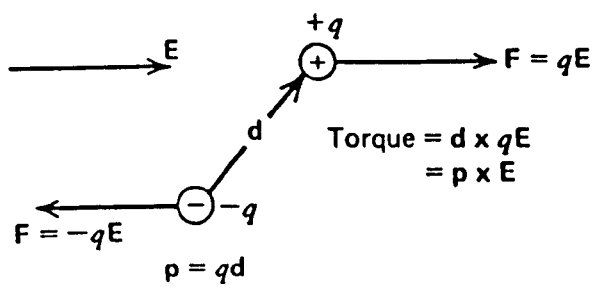

(c)

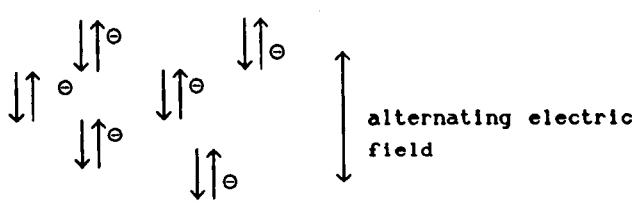

Fig.3.1 Electromagnetic interaction
(a) electronic (b) orientation & ionic
(c) interfacial polarisations

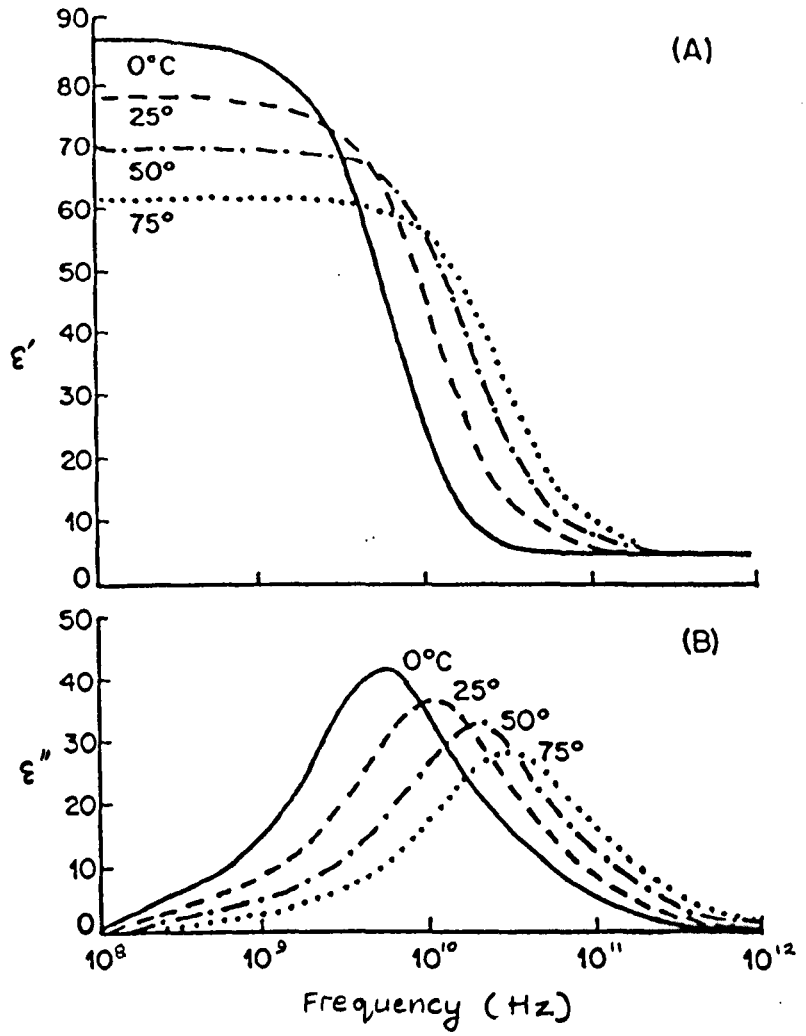

Fig.3.2 Variation of dielectric constant and dielectric loss of water with temperature and frequency [adapted from Mudgett, 1985]

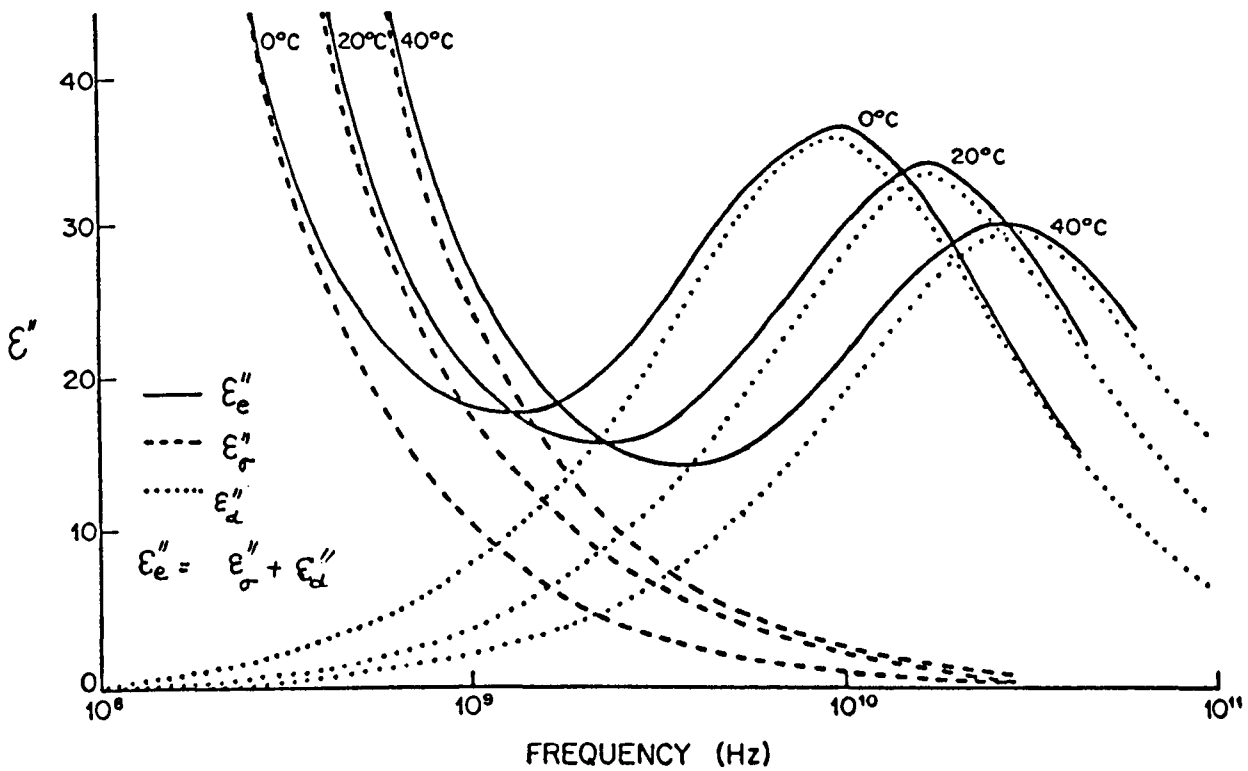

Fig.3.3 Variation of permittivity of ionic-aqueous solution with temperature and frequency [adapted from Mudgett, 1985]

The orientational polarisation is the most significant in microwave heating applications at frequencies above 1GHz. It is frequency and temperature dependent and so changes continuously during a heating process even at a certain applied frequency. The frequency dependence of the mechanism of dielectric loss in polar materials was expressed by [Debye, 1929]; (see Fig.3.2):

$$\varepsilon = \varepsilon_\infty + \frac{\varepsilon_s - \varepsilon_\infty}{(1 + j\omega\tau)} \qquad (3.1)$$

or separating real and imaginary parts we get;

$$\varepsilon' = \varepsilon_\infty + \frac{\varepsilon_s - \varepsilon_\infty}{1 + \omega^2 \tau^2} \qquad (3.2)$$

$$\varepsilon'' = \frac{(\varepsilon_s - \varepsilon_\infty)\,\omega\tau}{1 + \omega^2 \tau^2} \qquad (3.3)$$

Where ε_s and ε_∞ are the dielectric constant at d.c. and low frequencies (the static region) and at very high frequencies (i.e. the optic region) respectively, where $\varepsilon'' \to 0$. Between the static and optic regions is the region of dispersion or dipolar loss, in which the ε', decreases logarithmically with frequency from its maximum value ε_s to its minimum value ε_∞. Conversely ε'' increases with frequency from a negligible value to a maximum at the critical frequency ω_s and then again

decreases to a negligible value in the optic region (Fig 3.2). The relaxation time τ (= $1/\omega_s$) which is defined as the time required for the dipoles to revert to random orientations. ε_s is temperature dependent (see Fig. 3.2 & Table 3.1). The ε_∞ of the material is constant and related to its index of refraction (n) e.g. for water ε_∞ is 5 [von Hippel, 1954].

$$\varepsilon_\infty = n^2 \tag{3.4}$$

Unlike pure polar materials, real dielectrics such as foods, have many relaxation times or a distribution of τ. Cole (1941) modified the Debye equations by applying an empirical relaxation time distribution parameter, α, where $0 \leq \alpha \leq 1$.

$$\varepsilon = \varepsilon_\infty + \frac{\varepsilon_s - \varepsilon_\infty}{1 + (j \omega \tau)^{1-\alpha}} \tag{3.5}$$

Dissolved salts have further effects on the dielectric behaviour of pure water. Dissolved ions bind with water molecules and reduce "free water" content levels so depressing the material's dielectric constant, whereas the loss factor is elevated above the normal conditions due to increased ionic conductivity (Hasted et al;1948) as shown by the following "Hasted-Debye" equations;(see Fig.3.3)

$$\varepsilon' = \frac{\varepsilon_s - 2\bar{\delta}C - \varepsilon_\infty}{1 + (\omega \tau)^2} + \varepsilon_\infty \tag{3.6}$$

$$\varepsilon'' = \frac{(\varepsilon_s - 2\bar{\delta}C - \varepsilon_\infty)(\omega\tau)}{1 + (\omega\tau)^2} + \frac{\Lambda C}{1000\ \omega\ \varepsilon_\infty} \qquad (3.7)$$

Detailed discussions on dielectric theories for real dielectric materials are presented in many references [Bottcher,1952; von-Hippel,1954; Smyth 1955; Hill et al,1969; Meakins,1961; Hasted 1972; Jonscher, 1983].

Table 3.1

Experimental values of Debye model parameters for pure water (data from Collie et al, 1948)

Temprature (°C)	Static dielectric constant ε_s	Critical frequency f_s (GHz)
0	88.2	9.0
10	84.2	12.5
20	80.4	16.6
30	76.7	21.4
40	73.1	27.3
50	69.8	33.3
60	66.6	37.5
75	62.1	50.0

3.3. MEASURING METHODS

The measurement of dielectric properties requires specialized techniques and different methods are used for frequencies below and above 100Mhz. Several methods exist for measuring dielectric properties of foods. The classical method is the standing-wave wave guide. Others include; time domain spectroscopy, cavity perturbation techniques and the Roberts and von Hippel method. Each method has its merits and demerits. Detailed description of these methods is available in the literature [Chamberlain and Canary;1973; Metaxas and Meredith, 1983; Kent, 1990].

3.4 PREDICTIVE MODELS

3.4.1 Physiochemical model

Water content is the primary determinant of dielectric behaviour of foods, therefore the available predictive models are based on the dielectric behaviour of water or aqueous-ionic solutions. The foods are assumed to be two-phase systems with the aqueous or aqueous-ionic phase and modelled based upon aforementioned Debye or Hasted-Debye equations (3.2, 3.3 and 3.6, 3.7). The effects of soluble ash and protein contents in food can be related to ionic effects. Whereas the solid phase may be assumed similar to that of ice which is invariant with temperature and frequency [von Hippel, 1954]. The properties of each of the phases are combined by a linear relationship such as in the "distributive model" [Mudgett et al, 1977]

$$\varepsilon^*_m = \varepsilon^*_s V_s + \varepsilon^*_c (1-V_s) \qquad (3.8)$$

or by a non linear relationship (modified Fricke model), based on Maxwell's model [Mudgett, 1986]

$$\varepsilon^*_m = \frac{\varepsilon^*_c \left\{ \varepsilon^*_s (1 + X V_s) + \varepsilon^*_c (1 - V_s) X \right\}}{\left\{ \varepsilon^*_c (X + V_s) + \varepsilon^*_s (1 - V_s) \right\}} \qquad (3.9)$$

These models each require the estimation of the physical state and chemical composition of the food. They also require some other variable to be determined, e.g. the form factor, X, in Maxwell's model (which is difficult to define in structural terms for most food materials), and the equivalent conductivity in the Hasted-Debye model.

Predictive models for products rich in soluble sugars and starches such as bakery products are not available. It has been observed [Buck, 1965; Roebuck et al, 1972; Engelder and Buffler, 1991] that the dielectric loss in carbohydrate-water mixtures is higher than the loss of either pure component and the distributive model is unable to explain this synergistic effect.

3.4.2 Predictive Models based on experimental data

Some efforts have been devoted to the development of models for estimating dielectric properties for grain. Early models were based on dielectric mixture theory for two-phase mixtures of kernel and air [Kraszewski, 1978, 1989], multi phase theory [Ptitsyn et al, 1982] and polynomial regression [Nelson, 1978, 1983]. Based on linear relationships between the permittivity of grain and moisture content, temperature and bulk-density equations were developed for ε' and ε'' at various frequencies by applying multiple regression to the experimental data [Nelson, 1978, 1984, 1985, 1986, 1987]. Other models though not

particularly for food materials, such as those for a wide range of air-cellulose-water mixtures (e.g. for wood, paper, wool drying applications) are reported in the literature [Bottcher, 1952; Deloor, 1956; Tinga, 1969]. Some attempts have also been made to correlate the chemical composition of foods with their dielectric data [Van Dyke et al, 1969; Ohlsson et al, 1974]

Table 3.2.

Models for predicting the dielectric properties of various materials

Model	Material
Debye	Pure water
Hasted-Debye	Ionic solutions
Fricke and Distributive models	Non-interactive mixtures (solid-aqueous mixtures)
Maxwell-Debye model	Interactive mixtures (e.g. sugars and starch solutions)
Mixture equations and regression models	Granular and pulverised materials (grains, powders)

3.5 REVIEW OF EXPERIMENTAL DATA

A major difficulty in reviewing the data for dielectric constant and loss factor has been in extracting the relevant reliable information for the nominally-similar foods from the data, which are widely scattered in the literature. Many experiments on food products have been undertaken for various frequencies in the range 50 Hz to 10 GHz. Recent compilations of electrical properties for a wide range of foods have been provided by Kent [1987], who collated data for a frequency range from 100Hz to 10GHz. Much of this is at the frequencies 0.9, 1.0, 2.45, 2.8 and 3GHz within the 20 to 60°C temperature range.

Experimental data for many individual products such as bread dough, fruit pulp and honey are scattered in the literature [Tran and Stuchly, 1987; Kent, 1990; Zuercher et al , 1990; Puranik et al, 1991; Seaman and Seals, 1991; Kudra et al, 1992]. Generally in this investigation, data at the common microwave frequencies of 0.915 and 2.45GHz were considered. Data are available for temperatures as low as -40°C and also some at temperatures of up to 140°C, the latter being useful in modelling sterilization processes. For several materials, sufficient information is provided at various frequencies to permit the frequency dependence of the material to be assessed. However, it is difficult to compare the data found in the literature, because the proximate analyses of the specimen products are not always stated. Although food materials differ considerably in composition, examination of the available data leads to the identification of the following parameters which influence the dielectric properties of foods:

3.5.1 Moisture content

The bulk aqueous regions within a food sample are where microwave interactions (i.e. heating) in intermediate and high moisture-content foods occur. The dielectric loss can be governed by the losses of free and bound water present in the product. The relaxation of bound water occurs well below the microwave spectrum and thus its effects may be considered negligible in microwave food processing. However at lower frequencies (e.g. ≈915MHz) bound water contributes more to the loss factor. The dielectric constant and loss factor increases with moisture content [Bengtsson & Risman, 1971; Roebuck et al, 1972; Nelson, 1978; Nelson et al, 1991]. At low moisture contents (i.e. m ≤20%) $\frac{d\varepsilon'}{dm}$ and $\frac{d\varepsilon''}{dm}$ are small, increasing rapidly up to moisture contents of about 45% and thereafter increasing gradually.

3.5.2 Frequency

The value of ε'' for pure water increases with frequency at the microwave frequencies of interest in food processing (see Fig.3.2) But in general for food materials, ε'' tends to decrease with frequency (see Fig 3.4). Higher conduction losses at lower frequencies have more

pronounced effects upon the loss factor in foods with high salt-contents (e.g. processed ham and gravy). For many foods, the value of ε'' is approximately halved when the frequency is increased from 0.45GHz to 0.9GHz and again from 0.9 GHz to 2.8GHz [Ohlsson & Bengtsson, 1975].

3.5.3 Temperature

The nature of temperature dependence of ε' and ε'' is a function of the dielectric relaxations occurring in the material. Thus the rate of change of ε' and ε'' with respect to temperature depends on the frequency as well as upon the bound and free water-content and the ionic conductivity of the material. In general, the values of ε' and ε'' increase significantly with temperature as the material thaws, but as the temperature rises further they tend to show a gradual decrease (see Fig.3.4). However the low moisture materials with larger proportion of bound water possess a positive temperature coefficient and the conductive losses also have a positive temperature dependence, and thus exhibit increase in ε' and ε'' with temperature.

The dissolved salts in a product reduce the free water content and depress the dielectric constant and the dipolar loss, while the conductive losses are increased (Fig 3.3.). At the frequencies of interest in microwave food processing, dipole and conductive losses decrease and increase with temperature respectively. At 915MHz the loss factor has a positive temperature gradient due to the dominant conductive loss. But at 2450MHz due to the negative temperature gradient of the dominant dipolar loss, ε'' initially decreases and then increases, as conductive losses take over at higher temperatures (i.e. $> \approx 65^{\circ}C$). Thus, the total dielectric loss and its variation with respect to temperature depends upon the ionic activity of the product. Foods with added salts (e.g. cooked ham) show continuous increases in ε' and ε'' above $0^{\circ}C$ (see Fig. 3.5). The influence of salt content on $\frac{d\varepsilon'}{dT}$ and $\frac{d\varepsilon''}{dT}$ has been observed by many researchers [Parkash & Armstrong, 1970; Ohlsson & Bengtsson, 1975]. Table 3.3 summarises the temperature dependence of ε' and ε'' for various types of foods.

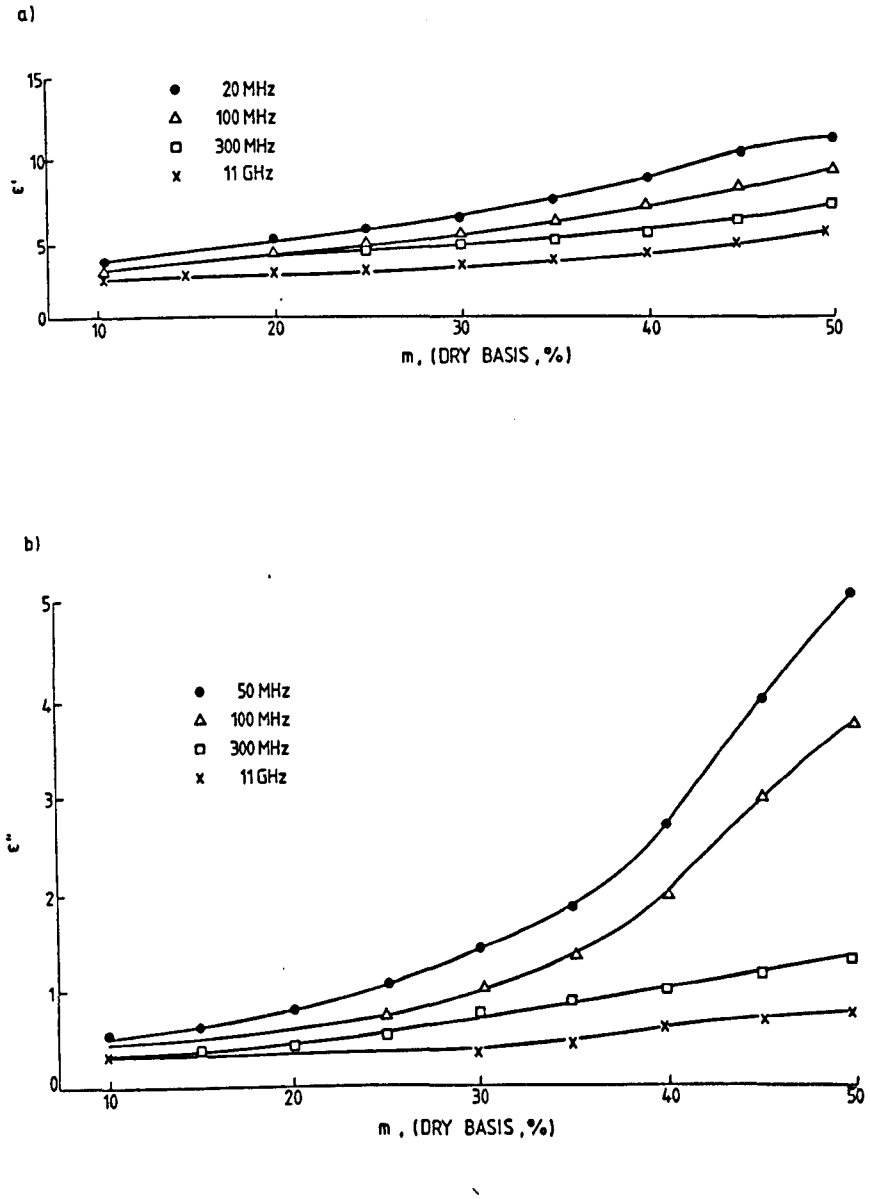

Fig.3.4 Variation of dielectric constant and dielectric loss with moisture content & frequency [data for corn Nelson, 1978]

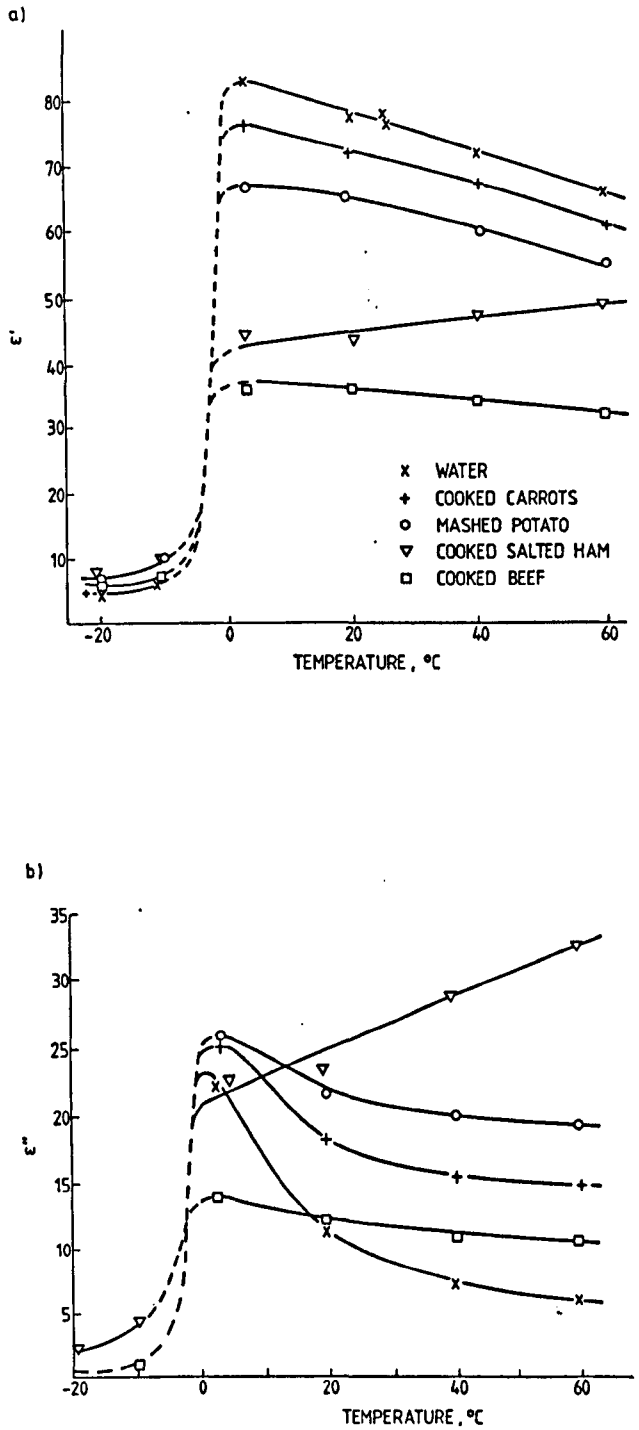

Fig.3.5 Variation of ε' and ε" of various foods with temperature [adapted from Bengtsson & Risman, 1971]

Table 3.3

Temperature variation of the dielectric properties of typical food-constituents

Food Constituent	Rate of change in dielectric activity
Moisture content	
a) Bound	$\frac{d\varepsilon'}{dT} > 0$, $\frac{d\varepsilon''}{dT} > 0$ for $0 \leq T \leq 65^{\circ}C$
b) Free	$\frac{d\varepsilon'}{dT} < 0$ for $0 \leq T \leq 140^{\circ}C$
	$\frac{d\varepsilon''}{dT} < 0$ for $0 \leq T \leq 65^{\circ}C$
	$\frac{d\varepsilon''}{dT} > 0$ for $65 \leq T \leq 140^{\circ}C$
Salt content	
a) Bound	$\frac{d\varepsilon'}{dT} \to 0$ $\frac{d\varepsilon''}{dT} \to 0$
b) Free	$\frac{d\varepsilon'}{dT} > 0$, $\frac{d\varepsilon''}{dT} > 0$ } $0 \leq T \leq 140^{\circ}C$
Fat content	$\frac{d\varepsilon'}{dT} \to 0$ $\frac{d\varepsilon''}{dT} \to 0$

3.5.4. Fat content

The absorption of microwave energy by fats, in the absence of moisture, is quite different from that due to free water and ionic activity. Although, the actual mechanism that ensues in such materials is not as yet well understood, the basis for the interactions is thought to result from the rotational modes of the molecules and is related to the permanent and induced dipole moments [Mudgett, 1990]. Van Dyke et al [1969] reported a decrease in ε'' with increasing fat-content in a reconstituted ground-beef sample, when the water content and protein to ash ratio were maintained at 45% and 21 to unity respectively. The rate of decrease was less noticeable between zero and 15% fat content and more pronounced between 15 and 30%. However, in the above-mentioned experimental setup, increase in fat content implies decreases in protein and ash, because protein to ash ratio was maintained constant. Therefore, the resultant lower ε'' must be partly due to the weaker ionic activity. Nevertheless, experimental data for some commercial fat spreads have been reported that showed a decrease in ε' and ε'' with an increased fat content (Table 3.4). The tendency for ε'' is to increase slightly with temperature, but the rate of change is too small to be of practical significance [Mukerjee, 1966; Pace et al, 1969]. The experimental data of Pace et al [1969] showed decreases in the dielectric constants of oils (at constant temperature) as the frequency increased, which is in accord with the Debye equations for water. From a practical view-point, there is little difference between an unsaturated vegetable oil and an animal fat.

3.5.5 Other Factors

a) Sugar content: Some data are available for sugars such as glucose and sucrose in solutions of various concentrations [Kent, 1987]. Because sugar molecules are relatively large and non-polar they do not dissociate on dissolving, and thereby inhibit orientational polarization. Thus, an increase in the sugar content of a food

decreases the dielectric constant, whereas the loss factor slightly increases due to the reduced free water relaxation frequency.

b) Density: The dielectric activity depends upon the amount of mass interacting with the EM fields. Thus the mass per unit volume (or ρ_d) has a great effect on the dielectric properties. This is particularly noticeable in particulate materials such as grains, flour, and dough. A rise in the bulk density of these materials serves to increase the values of ε' and ε''. Similarly, the orientation of muscle fibres/grains in meat products, with respect to the direction of the applied electric field, also affects these properties. The values of ε' and ε'' are higher when the applied field is along the grains rather than in a transverse direction [Bengtsson et al, 1963].

Table 3.4

Dielectric data for some commercial fat-spreads at 18°C, f=2.45GHz [Desai, 1991]

Product	Moisture content % vol	Salt content % vol	Fat content % vol	ε'	ε''
Cream	76.1	0.2	23.7	63	15
Gold Lowest	65.8	0.4	33.8	31	17
Philadelphia	61.5	0.3	38.2	35	17
Krona marg.	22.8	1.1	76.1	6	0.7
Anchor butter	14.3	2.3	83.4	5	0.8
Flora marg.	13.4	2.2	84.4	4	0.2

3.6 REGRESSION ANALYSIS

There are many methods for obtaining a functional relationship or a set of relationships between the dependent variable and the independent variable(s) (e.g. polynomial interpolation, Langrange form, divided-difference form, spline interpolation and least-squares approximation). However when the experimental data are likely to exhibit significant random errors, it is the least-squares method that is usually the most appropriate to employ. So the least-squares approximation was used in this investigation to obtain a set of predictive equations involving multivariable data (Appendix A.8).
The choice of independent variables was based upon their degrees of influence upon ε' and ε'' for a certain food or a class of foods. However in using multiple-regression analysis, suitable functions of of the independent variables for coupling with the parameters need to be determined. While there is a definite positive correlation between ε' and the moisture content, the relationship for ε'' is uncertain and influenced by the presence of salt. The same applies for the correlation between ε' (or ε'') and temperature. Also the supposedly-independent variables are not truly independent in the case of foods. For example, the fat contents of meats, and the free-salt concentrations in foods such as fruits and vegetables, vary with the moisture content. Similarly the bulk density of granular materials vary with the moisture content. It is usually assumed in regression analysis that the independent variables are known without error, but this is not always the case with foods. To try to overcome the incompleteness of the data available in the literature the following assumptions were made:-

a. if a composition variable (i.e. m, M or F) was not provided in the quoted reference, an appropriate value was assumed based on guidance from the literature [McCance & Widdowson, 1978; ASHRAE, 1985];

b. moisture, salt and fat contents are expressed as percentages of the total mass of the food product; and

c. the density for a granular material was assumed to be equal to bulk density of the mixture.

Also because some of the data were only readily available in graphical form (e.g. ε' and ε'' against temperature, frequency or moisture content), the numerical interpretation of data from the published curves may be subject to smoothing errors, but these are likely to be smaller than for the individual experimentally-measured data.

Multiple regression analysis was performed for each group of foods (e.g. meats, fats, fruits or vegetables) and also for each food within each group when enough experimental data were available. The quality of fit was assessed by the coefficient of determination (r^2) for each equation For convenience in using the equations, the number of parameters employed in each regression equation was minimised.

3.7 DISCUSSION

The equations obtained are presented in Table 3.5. On comparing predicted and measured values or selected foods (Table 3.6) the agreement was usually to within $\pm$15%. In some individual cases, the variations are as much as 31% for ε' and 35% for ε''. However, the discrepancies between the predicted and published data can be attributed partly to the assumptions, which had to be made concerning the compositions of some of the materials. Although few data sources offered information as to the possible errors in the measured value, variations of 5 to 20% for ε' and 10 to 30% for ε'' are found for nominally the same food material.

Other equations were tested, but only those with a coefficient of determination $r^2 \geq 0.70$ were selected to be representative of the general dielectric behaviour of the specified group of food materials. Multiple regression was also performed on all the data surveyed in an attempt to find a suitable general equation for all foods. However this was not feasible as the discrepancies for some materials exceeded $\pm$40%. This clearly indicates that the dielectric behaviours of different components in a food depend on both the macroscopic and microscopic structures of the system. The responses of different components in a system (e.g. salt or ash content, and carbohydrates) depend upon the manner in which they are bound to the other components in a food matrix. The particle geometry in a food mixture is also an important parameter [deLoor 1956]. Therefore for food mixtures, the prediction of dielectric properties from data for the individual components is difficult.

Including a parameter to account for the frequency variations caused greater variations in ε'' values from observed values for most foods (e.g. see eq.15). This is because the frequency response of the dielectric loss depends on (i) the variation in relaxation times of different components in a food and (ii) the increase in the conduction losses at lower frequencies. However, in practice, only a few discrete frequencies are allocated for heating purposes and so one is usually concerned with the properties at these particular frequencies. Some products (e.g. bread-dough, eggs, flour and milk-powders) within the examined groups are not included in the presented list because there were not enough published data to formulate predictive equations.

The combined effect of the variations of ε' and ε'' during a transient heating process, is important with respect to predicting the power absorbed within a material and thereby the cross-sectional temperature distributions. In Table 3.7, values for the attenuation factors obtained from predictive equations for some materials are compared with the values calculated from the literature data.

3.8 CONCLUSIONS

The presented equations in Table 3.5 provide reasonably accurate dielectric property data for a wide variety of food materials. When the experimental data are inadequate, or in order to avoid developing temperature or moisture-dependent equations for particular foods, the presented equations for ε' and ε'' may be utilised by incorporating them within a microwave-heating simulation model. As more experimental data become available, the correlations can be improved. Nevertheless the present variations between predicted and measured values lie generally within the limits of anticipated experimental uncertainties.

Table 3.5

Predictive equations for the dielectric constant and loss factor for various types of foods

Food Type	Limits for the following variables					r^2	Eq.no
	f,GHz	T,°C	m,%	M,%	F,%		
CEREAL GRAINS ($600 \leq \rho_d \leq 850 kgm^{-3}$)							
$\varepsilon' = 1.82+0.0621m-0.0253f$	0.9-10	10-30	3-30	-	-	0.81	3.8
$\varepsilon' = 1.72+0.066m-0.0254f+0.0003\rho_d$	0.9-10	10-30	3-30	-	-	0.91	3.9
$\varepsilon' = 1.71+0.0701m$	2-3	10-30	3-30	-	-	0.87	3.10
$\varepsilon'' = 0.12+0.00519m$	2-3	10-30	3-30	-	-	0.78	3.11
$\varepsilon' = 1.788+0.0488m$	≈10	10-30	3-30	-	-	0.82	3.12
$\varepsilon'' = 0.052+0.0149m$	≈10	10-30	3-30	-	-	0.80	3.13
FATTY/LOW-MOISTURE CONTENT FOODS							
$\varepsilon' = 2.63-0.0015T+0.162m$	1-3	0-100	0-30	0-5	70-100	0.98	3.14
$\varepsilon'' = 0.177-.00021T+0.0235m$	1-3	0-100	0-30	0-5	70-100	0.77	3.15
FRUITS/VEGETABLES							
$\varepsilon' = 4.3+0.033T+0.006m$	0.9-3	-30-0	20-60	-	-	0.91	3.16
$\varepsilon'' = 0.34+0.0051T+0.001m$	0.9-3	-30-0	20-60	-	-	0.91	3.17
$\varepsilon' = 2.14-0.104T+0.808m$	≈2.45	0-70	50-90	-	-	0.98	3.18
$\varepsilon'' = 3.09-0.0638T+0.213m$	≈2.45	0-70	50-90	-	-	0.90	3.19
$\varepsilon' = -12.8-0.103T+0.788m+5.49f$	0.9-3	0-70	50-90	-	-	0.82	3.20
$\varepsilon'' = 10.1+0.008T+0.221m-3.53f$	0.9-3	0-70	50-90	-	-	0.76	3.21

continued.....

MEAT PRODUCTS							
a. General							
$\varepsilon' = -52-0.03T+1.2m+(4.5+0.07T)M$	2-3	0-70	60-80	0-6	0-20	0.72	3.22
$\varepsilon'' = -22-0.013T+0.48m+(4+0.05T)M$	2-3	0-70	60-80	0-6	0-20	0.73	3.23
$\varepsilon' = 23.6+0.0767T-0.231m$	2-3	-30-0	60-80	0-6	0-20	0.76	3.24
$\varepsilon' = 29.3+0.076T-0.3m-0.11F$	2-3	-30-0	60-80	0-6	0-20	0.79	3.25
$\varepsilon'' = 9.8+0.028T-0.0117m$	2-3	-30-0	60-80	0-6	0-20	0.70	3.26
b. Pork							
$\varepsilon' = -70-0.1T+1.7m+(1.5+0.02T)M$	2-3	0-70	60-80	0-6	0-20	0.89	3.27
$\varepsilon'' = -18-0.084T+0.5m+(3.3+0.05T)M$	2-3	0-70	60-80	0-6	0-20	0.79	3.28
c. Raw Beef							
$\varepsilon' = -37.1-0.145T+1.2m$	2-3	0-70	60-80	0-3	0-20	0.71	3.29
$\varepsilon'' = -12.7+0.082T+0.405m$	2-3	0-70	60-80	0-3	0-20	0.70	3.30
d. Cooked Beef							
$\varepsilon' = -88.6-0.04T+1.89m$	2-3	0-70	60-80	0-3	0-20	0.75	3.31
$\varepsilon'' = -10.2-0.033T+0.325m+0.31F$	2-3	0-70	60-80	0-3	0-20	0.75	3.32
e. Fish							
$\varepsilon' = 48.2-0.075T+0.0001T^2$	≈2.45	0-70	≈70	-	-	0.78	3.33
$\varepsilon'' = 15.1-0.05T-0.0003T^2$	≈2.45	0-70	≈70	-	-	0.73	3.34
$\varepsilon'' = -41.1-0.075T+1.16m$	≈2.45	0-70	60-80	-	-	0.79	3.35
$\varepsilon'' = -108-0.05T+1.6m$	≈2.45	0-70	60-80	-	-	0.70	3.36
f. Poultry							
$\varepsilon' = -87.3-0.051T+1.91m+(2+0.02T)M$	2-3	0-70	60-80	0-5	≈10	0.9	3.37
$\varepsilon'' = -82.6+0.029T+1.42m+2.01M$	2-3	0-70	60-80	0-5	≈10	0.8	3.38

Table 3.6

Comparison with published data

Material	Temp. °C	Predicted value ε′	Predicted value ε″	Published value ε′	Published value ε″	Error % ε′	Error % ε″	Eq. no.
Rice (m=12%,f=11GHz)								
i) 696kg/m^3		2.45	0.25	2.38[a]	0.26[a]	3	4	3.9, 3.13
ii) 811kg/m^3		2.49	0.25	2.7[a]	0.35[a]	7	25	
Corn (m=10% f=10GHZ)	24	2.3	0.21	2.1[b]	0.2[b]	10	5	3.12, 3.13
Butter (m=22% f=3GHz	0	4.4	0.36	4.05[c]	0.39[c]	9	8	3.14, 3.15
Peas (m=78% f=2.8GHz	-20	4.16	0.31	4.1[d]	0.29[d]	2	7	3.16, 3.17,
	-10	4.46	0.4	4.46	0.45	0	11	
	20	61.9	17.5	63.2	15.8	2	11	3.20, 3.21
	60	55.6	15.0	53.0	12.1	5	24	
Beef (m=76% f≈2.8GHz	-20	4.9	0.58	4.6[d]	0.5[d]	7	16	3.25, 3.26
	40	46.9	14.4	45.2[e]	12.5[e]	4	15	
	60	44.1	12.8	44.4	12.0	1	7	3.22, 3.23
Chicken f=2.45GHz	-40	3.7	0.14	3.5[f]	0.15[f]	6	7	3.25, 3.26
	-20	4.8	0.69	4.5	0.51	7	35	
Fish f≈2.8GHz	60	43.7	12.2	45.0[e]	11.94[e]	3	2	3.35, 3.36

References:

a: You & Nelson, 1988
b: Nelson, 1978
c: Metaxas & Meredith, 1983
d: Bengtsson & Risman, 1971
e: Ohlsson & Bengtsson, 1975
f: Mudgett et al, 1979

Table 3.7

Attenuation factor calculated from literature data compared with those derived from the predicted data (ref. Table 3.6)

Material	Temp. °C	Predicted α, m^{-1}	Literature α, m^{-1}	Discrepancy %
Rice	-	18.4	19.4	5
		18.3	24.5	25
Corn	24	14.4	14.5	1
Butter	0	4.4	5.0	12
Peas	-20	3.9	3.7	5
	-10	4.9	5.2	6
	20	65.7	59.8	9
	60	58.5	55.5	5
Beef	-20	6.7	6.0	12
	40	60.9	54.1	13
	60	56.3	52.4	7
Chicken	-40	1.9	2.0	5
	-20	8.0	6.2	29
Fish	60	54.8	52.7	4

CHAPTER 4

4. THERMOPHYSICAL PROPERTIES OF FOODS

4.1 INTRODUCTION

The thermophysical properties of a food determine how it is heated after it begins to absorb energy from the applied electromagnetic field. The skin depth of most foods at ≈3GHz lie in the range 10-100mm. This means that for typical food samples heat diffusion plays an important role in ensuring that material reaches desirable temperatures (Chapter 2). The influence of the material's thermophysical properties may be as important in a given microwave heating process as in a conventional heating process.

The thermophysical properties of interest are: bulk density, ρ_d, specific heat capacity, C_p, thermal conductivity, k, and thermal diffusivity, ($\alpha_T = k/\rho_d C_p$). Thermal diffusivity is the key for predicting the time-temperature profiles, while the thermal conductivity is sufficient for determining the steady-state heating characteristics. Mathematical modelling of food process operations requires the use of predictive equations for estimating these properties in order to accommodate any variations with respect to the process conditions. Unlike dielectric properties, many predictive equations for C_p, k and α_T of foods have been reported by several researchers [Miles, et al 1983; Vegenas et al, 1990).

In this chapter the availability of experimental data and predictive equations for thermophysical properties of foods are reviewed. It was noted however that the validation of some predictive equations is based on a limited comparison between actual and computed properties for a number of food products. Therefore, available predictive equations are compared with the experimental data for the groups of food products selected in the same manner as for dielectric properties in the previous Chapter. The likely variations in these properties during thermal processes and their influence on the model predictions is discussed.

4.2 REVIEW

4.2.1 Measuring Methods

Experimental procedures for evaluating thermal properties involve measuring the time-temperature profiles at the known point (usually the centre) of an object of a well-defined shape (e.g. a sphere, a semi-infinite slab or cylinder) which is heated/cooled at a constant rate. The measured temperature and predicted temperature obtained by solving the heat transfer equation are matched to evaluate thermal properties. Several models exist for computing thermal properties from the experimental data. For example, non-linear regression may be used to estimate both k and α_T using data obtained from the heat-source method [Narayana and Krishnamurthi, 1981]; heat conduction taken data over a long period can be analysed using the regular regime methods [Rizvi et al, 1980; Peterson and Adams, 1983]; or using analytical solutions of the heat-equation available in the form of time-temperature charts [Scheinder 1963] to compute α_T.

Usually it is practically difficult to achieve the assumed boundary conditions in an experimental setup. Therefore different errors may arise during the data acquisition procedures. Possible errors and the methods that have been used to minimize these errors are discussed below:

a) The heating rate is not constant- Hayakawa and Bakal [1973] used time-dependent surface temperature.

b) Boundary conditions may not be satisfied when the effect of surface heat transfer is to be taken into account; Hayakawa and Bakal [1973] used a method where surface temperature need not be monitored.

c) The dimensions of the sample may not conform to the assumption of semi-infinite medium. In some cases a single piece of the product is unable to approximate a semi-infinite body, and different pieces joined together to create a single product introduces an error due to the contact resistance between the pieces [Narayana and Krishnamurthy, 1981].

d) Inaccurate positioning of the thermocouples; this is one of the major causes of error in the measurements . Hayakawa and Bakal [1973] found that an error of ±1mm in the positioning of the thermocouples caused a ±27% error in the property value.

e) The inaccuracy due to thermal conduction effects of the thermocouples wires can be reduced by using thin wires. Larkin and Steffe [1987] applied an evaluated correction factor for the measured α_T to compensate for these errors.

f) Thermocouple response time increases as the difference between the initial temperature and surface temperature increases. A good contact between the heater and the sample ensures maximum heat transfer and reduces this error.

g) The temperature dependence of the property value causes some error. Therefore, the temperature measurements should be made over a narrow range. A line heat source can be employed to apply quite a small temperature increase (≈1°C) [Martens, 1980].

h) Almost all the calculation methods assume pure heat-transfer conditions. Whereas in setting up an experiment much care is required to minimize the mass transfer effects. Narayana and Murthy [1981] proposed a mathematical model which accounts for combined heat and mass transfer effects. This was simulated in a simple experimental set up. The theoretical and experimental thermal histories were matched through a non-linear regression method for determining the thermal properties.

4.2.2. Experimental Data

Some large compilations of thermal property data are available in the literature [Polley, 1980; Kent et al, 1984; ASHRAE, 1985; Rao and Rizvi, 1986; Jowitt et al, 1987]. Although the difficulty of measuring thermal properties can be ranked in ascending order ρ_d, α_T, C_p and k, the associated research effort has been focused on k and C_p. Very few

data are available for thermal diffusivity. Experimental data for formulated and engineered foods are scarce.

Unfortunately, the existing literature data also show a great deal of scatter. There are variations in the experimental data reported by different investigators for similar products due to the varying composition and structure of food products. However, the composition of the food material, the accuracy of the measuring method and the temperature at which the measurement was made is not always reported. Most foods are complex materials, varying in composition and structure both within and among a similar product category. Every slight change in food composition influences the thermophysical property value.

However, the temperature and moisture content affect the thermal properties of a material more than any other factor. Water is a major constituent of many foods (e.g. up to 95% for some vegetables). Therefore moisture content significantly influences all thermal properties of food materials. The influence of the variation in the solid fraction (fat, proteins, carbohydrates) is very small. It is evident that the thermal properties of basically all foods suitable for microwave heating lie in a narrow range and thus heat similarly (see Table 4.1).

4.3 PREDICTIVE EQUATIONS

The data on thermal properties is by no means comprehensive and data for many food products are needed. Also in a modelling exercise or in a feasibility study concerning a new product, measuring these properties is an expensive task. By recognising the influence of food constituents, particularly the moisture content, efforts have been made to correlate the experimental data with the composition of the food. As a result, several empirical models derived by curve-fitting the experimental data are available in the literature [Riedel, 1969; Sweat, 1974, 1975; Singh and Heldman, 1984; ASHRAE, 1985; Vagenas et al, 1990]. However, only a few equations exist which apply to a whole category of foods, most are specific to the product being studied.

Table 4.1

Thermal properties of some foods of interest for microwave product developers (adapted from ASHRAE, 1985)

Food	Temp. °C	Moisture content m, %	Thermal conductivity k, $Wm^{-1}K^{-1}$	Sp.heat capacity C_p, $kJkg^{-1}K^{-1}$	Thermal diffusivity α_T, mm^2s^{-1}
Apple	0-30	85	0.56	3.78	0.14
Potatoes	0-70	78	0.54	3.7	0.13
Codfish	5	81	0.56	3.68	0.12
Beef	40-65	71	0.48	3.43	0.13
Ham	40-65	64	0.41	3.33	0.14
Chicken	≈30	74	0.51	3.53	0.14
Water	0	100	0.57	4.19	0.16

4.4. A COMPARISON OF THE AVAILABLE EQUATIONS

The property data predicted from the available equations were compared with the published experimental data for different food products. The data were grouped into three categories; general, vegetables and fruits, and meat products. Published compilations (references in **4.2.2**) were used for the data acquisition. The original sources were referred to when obtaining the information regarding the experimental errors, measuring temperature and product composition. The data were carefully selected to avoid random errors disguising the real trends. A total of 431 data points were selected. Appendix 9 gives a list of the equations considered. The equations which performed well for the whole group of data are presented in Table 4.2.

4.4.1 Specific heat capacity, C_p

Water content is the most important variable for predicting the C_p of any food. The value increases linearly with the water content. The constant and parameter for water content are also very similar in these equations. Reidel's equation (4.3) is quite accurate for a range of products and moisture contents, i.e. from 6% for nuts to 94% for lettuce (Fig 4.1).

The specific heat capacity for many foods is nearly independent of temperature above freezing, because the C_p for water varies only 1% over the temperature range 0-100°C. However for meat products with high fat contents the error in the predicted value increases for temperatures between 20°C to 50°C. This is because the fat components in meat change state at different temperatures and the energy required for a unit change in temperature is highly variable. For similar reasons the data for egg yolk should not be extrapolated into the temperature range 0°C to 20°C.

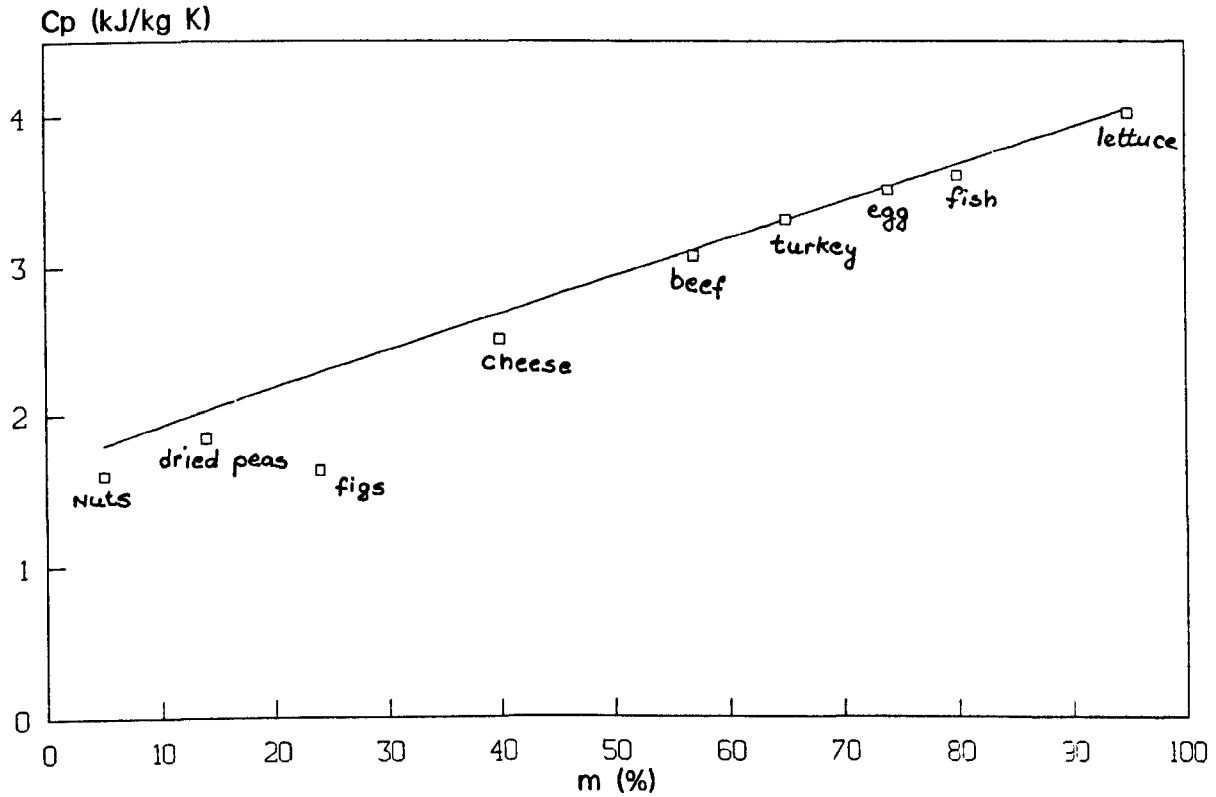

Fig.4.1 Cp of various foods in the temperature range; meats=0-20°C; egg=20-40°C; other=4-30°C [ASHRAE,1985] and Reidel's correlation (eq.4.3)

Table 4.2

Comparison between experimental and predictive data for a selection of different foods

Equation	Standard deviation of estimate (s.d)	Eq.no.
A. FRESH FOODS (General) (n=298)		
a) C_p (kJ $kg^{-1}K^{-1}$)	(kJ kg^{-1} K^{-1})	
0.0335m + 0.84 ($T>0^oC$)	0.09[a]	(4.1)
0.0126m + 0.84 ($T<0^oC$)	0.1[a]	(4.2)
0.0251m + 1.675	0.03[b]	(4.3)
0.0272m + 1.4654	0.02[c]	(4.4)
b) k, ($Wm^{-1}K^{-1}$) (n=431)	($Wm^{-1}K^{-1}$)	
0.0.00493m + 0.0148 (n=88, m>60%)	0.04[d]	(4.5)
$0.0045m + 0.0005T_K$	0.05[e]	(4.6)
c) α_T, (mm^2s^{-1})	(mm^2s^{-1})	
$0.05763m + 0.000288T_K$	0.015[e]	(4.7)
$0.088 + (\alpha_{TW} - 0.088)m$	0.016[f]	(4.8)

continued.....

B. Vegetables and Fruits (n=102)		
a) C_p (kJ $kg^{-1}K^{-1}$)	(kJ kg^{-1} K^{-1})	
0.0295m + 1.288 (m>25%)	0.065[g]	(4.9)
b) k, ($Wm^{-1}K^{-1}$) (n=231)	($Wm^{-1}K^{-1}$)	
0.00566m + 0.057	0.02[g]	(4.10)
C. Meats		
b) k, ($Wm^{-1}K^{-1}$) (n=129)	($Wm^{-1}K^{-1}$)	
0.0052m + 0.08 ($0^{\circ}C<T<60^{\circ}C$)	0.02[h]	(4.11)

References:

a. Seibel [1892]
b. Reidel [1956]
c. Lamb [1976]
d. Sweat [1974]
e. Marten [1980]
f. Reidel [1969]
g. Vegenas et al [1990]
h. Sweat [1975]

4.4.2 Thermal conductivity, k

Besides water content, thermal conductivity depends upon other factors such as the structure (amorphous crystalline, dielectric, liquid, solid), and composition (impurities, mixtures) of the material and the structural orientation in fibrous materials (such as meat) with respect to the heat flow. Therefore two types of relationships are found in the literature; (i) purely empirical derived by curve-fitting the data for various products and (ii) based on physical models (such as Maxwell's model and its various adaptations), which assume the food to be a mixture composed of different phases. Nonetheless the parameters used must still be found by curve-fitting to ensure good agreement with the data.

Pham [1990] compared the empirical equation of Sweat [1975] and seven mixture models found in the literature for predicting the thermal conductivities of various meats. He reported that Sweat's equation (4.11) was reasonably accurate for predicting thermal conductivity data for meats with low fat contents.

Many of these equations (see Appendix 9) also use temperature as a variable. However the value for water changes by 15% over the range 0-100°C, which is below the uncertainty reported by some researchers. The variation may also be assumed to lie within the experimental errors in complex foods and therefore the temperature dependence may be ignored for preliminary investigations.

4.4.3 Thermal diffusivity, α_T

Thermal diffusivity may be calculated (i) indirectly from the predicted values for C_p, k and ρ_d of the product or (ii) directly using functions based on composition and temperature. Both will achieve a similar accuracy provided that the best combination of equations are used in the indirect calculations [Martens, 1980]. However, only two general correlations for α_T are found in the literature. First, Reidel's correlation [1969] which can be used for a wide range of foods of m ≥

40%) and provides good agreement with the experimental data for a variety of meats [Dickerson and Read, 1975]. Second, Martens [1980] included temperature as an independent variable in his equation (based on 246 data points for various foods). He obtained better agreement with experimental data (standard error of the estimate was $0.014mm^2s^{-1}$) than the Reidel's equation which resulted in slightly higher error ($0.017mm^2s^{-1}$) for the same set of data. (a typical α_T value for foods $\approx 0.15mm^2s^{-1}$).

4.5 MASS DIFFUSIVITY, D_v

During cooking mass transfer accompanies the process of heat transfer. A typical example is the expression of water from meat when the fibres start shrinking at $\approx 50^{\circ}C$. Similarly in a drying process, moisture is driven out of the material via the surface by diffusion. However no generalised theory exists to explain these mechanisms. The application of the simplified mass diffusion model (i.e. Fick's law which is analogus to Fourier's law) requires a value for the diffusion constant or mass diffusivity. Unfortunately experimental data is practically non-existent for the concentrated fluids found in many food operations. However some experimental data and predictive models applicable to the product/process studied are available [Saravacos, 1986; Marousis et al, 1991]

4.6 FROZEN FOODS

The properties of foods in the freezing range are important in microwave food processing as tempering and thawing represent the most successful applications of microwave energy. The prepackaged meals heated in a domestic microwave oven also largely belong to the frozen-food category. The experimental data for thermal and dielectric properties is very scarce in the freezing zone. Rapid changes of phase and the possibility of sub cooling make values in the 0 to $-10^{\circ}C$ more difficult to measure and less reliable than those recorded at other temperatures.

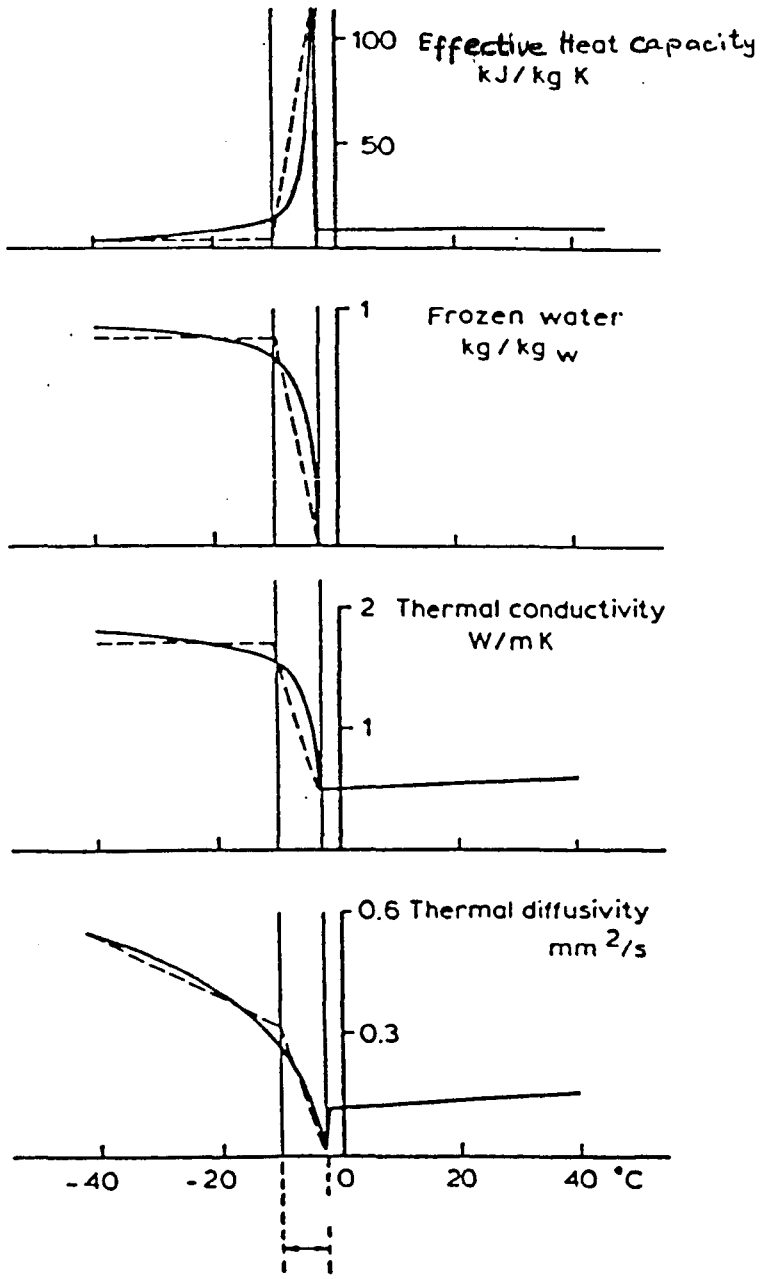

Fig.4.2 Variation of thermophysical properties of foods with temperature

The food properties change dramatically when the phase change occurs in the -10 to 0°C range (Fig. 4.2), and the change has a significant effect on the heating characteristics of a product. Therefore the knowledge of the initial freezing temperature and suitable assumptions concerning the amount of water frozen at a certain temperature below 0°C for a food product are essential for obtaining accurate predictions from a mathematical model.

However, the effect of moisture content on food properties is also significant for frozen foods. For the same reason the properties of frozen foods depend upon the amount of unfrozen water present. Most foods have different initial freezing temperatures and complete freezing takes place over a wide temperature range. Conversely, predictive models usually assume that all the water is frozen to ice and the property of a food is calculated based on the property value of ice, e.g. Siebel's formula for C_p [ASHRAE, 1985]. The error in the prediction depends on the assumption for the ice-to-water ratio at a certain temperature in the the freezing zone for a product. The effect of latent heat is also significant in the prediction of dielectric properties. However, for high moisture content foods the errors caused are small, because the initial freezing starts at 0°C for such foods. Whereas, in some foods with low moisture contents and with high fat contents very little water will be frozen at -20°C. Thus a greater error may occur if a 100% frozen assumption is made.

4.7 CONCLUSION

The water content and temperature are the most important variables in the prediction of thermal properties. The influence of the solid fraction (proteins, carbohydrates, fats) has been considered in few correlations, but is very small. For example, values for k and α_T decrease as the sugar content of a food increases. This can be accommodated as the relative decrease in the moisture content of a product of high sugar/fat content. Thus equations based on moisture content can be employed for predicting thermal properties. The accuracy of the predictions may be increased by taking the effect of other

constituents in to account. However, it may be difficult to assess the correct proportions of each constituent in a food product. However, when data are lacking, simple equations can provide data adequate for many practical purposes. Equations (4.6) and (4.7) were found to provide temperature dependent data for k and α_T respectively for foods of a wide range of moisture contents. During a cooking processes structural and chemical changes tend to vary the property values, e.g. in meat products, juices are expressed and the change in heat transfer rates depend upon whether the expressed juices remain in the sample and contribute to heat transfer or drain away, in which case the overall k and α_T of the sample decrease. Similarly dough products (such as bread and cakes) undergo changes in their structure and volume and hence in property value. Therefore a property value emanating from the literature should be viewed as an estimate for that type of material. Ideally, actual data for a certain material/process would be measured experimentally, but for practical purposes simple equations based on water content are recommended for generating property data for numerical thermal models. Temperature dependence may be incorporated to improve the accuracy of the model as dictated by its application.

CHAPTER 5

5. MICROWAVE HEATING OF FOODS

5.1 INTRODUCTION

The assumptions concerning the distribution and absorption of EM energy within the material have the greatest influence upon the predictions of a thermal model. The model developed in Chapter 2 may be applied to obtain useful indicators for the microwave heating of foods, where it can be assumed that the power varies exponentially with distance in to the sample (i.e. Lambert's Law). At 2.45GHz the wavelength is ≈12cm in air and is of the same order dimensionally to those of both common microwave ovens (25cm-50cm) and food products (e.g. 2-20cm) generally heated in ovens. Thus, strictly the wave like nature of microwaves should be considered. and the internal reflections at the material boundaries should be taken into account. However, Lambert's law (which is strictly valid only for semi-infinite geometries) has been widely used to predict temperature profiles for microwave heating of foods [Ohlsson and Bengtsson, 1971; Krul et al, 1978; Taoukis et al, 1987]. To apply Lambert's law one needs to know the value of power at the surface, which depends not only on the available power at the source, but the sample's volume and dielectric properties. Therefore the absorbed power has been estimated by calorimetric measurements [Nykvist and Decareau, 1976, Swami et al, 1982; Tong and Lund, 1989].

The wave like nature of microwaves (i.e. reflection, transmission and absorption) exhibits strong oscillatory behaviour in the domain of propagation. Because the propagation of microwaves through a material of finite thickness may consist of large backward components as a result of internal reflections at the material boundaries, it is desirable to simulate such effects in order to obtain the correct value of power absorption in the medium. To a large extent, this appears to have been ignored in the thermal/food engineering sector.

Ayappa et al [1990] compared the power distributions obtained by using Lambert's law with those found from solving Maxwell's equations (where the backward components due to internal reflection were taken into account) for several food products. A linear least-squares fit to the data was obtained. This yielded the criterion for defining the minimum sample thickness, L_{crit} for which Lambert's law is a good approximation.

$$L \geq L_{crit} = (2.7\ \alpha^{-1} - 0.08) \qquad (5.1)$$

(where α is in cm^{-1})

This is ≈2.5 times the material's skin depth, δ or ≈5.0 times the penetration depth, D_p. L_{crit} is similar to the criteria employed when analysing thin slabs for DRH and IH (see Appendices 4 and 5). It follows that the assumption of semi infinite geometry is not valid for many foods heated in a microwave oven (see Table 5.1). Following the same argument Fu and Metaxas [1992] proposed a new definition for power penetration depth applicable to samples of finite thickness, which is based on the power absorption instead of the power decay within the material.

Table 5.1

Skin depth of some common foods materials (≈3GHz)

(based on data adapted from Kent, 1987)

Food	Skin depth, δ mm	L_{crit} mm
Ice	20×10^3	54×10^3
Bacon fat	476	1300
Butter	182	500
Water	26	71
Beef	21	58
Carrot	20	55
Potato	19	52
Pork	13	36
Ham	11	30

Mathematical modelling of power absorption in objects exposed to microwave radiation has been performed extensively in the biomedical and electrical engineering sector. Maxwell's equations have been solved by various numerical techniques: (i) finite difference [Lau and Sheppard, 1986; Dennis et al, 1988], (ii) finite element [de Pourcq, 1984, Jia and Jolly, 1992], (iii) transmission line matrix [Hoefwer, 1985] and (iv) methods of moments [Zhu and Han-kui, 1988; Yang, 1989]. However, in the microwave heating models developed in the food engineering domain, the power absorbed is usually modelled by calorimetric measurements and Lambert's law [Taoukis et al, 1987, Komolprasert and Ofoli, 1989; Datta and Liu, 1992]. Although one study concerning the modelling of foods heated in a domestic microwave oven calculated the electric field by the transmission line matrix method [Desai, 1991], the material properties were assumed to be constant and heat transfers at the surface were neglected. Another model for heating by microwaves has recently been reported [Barratt, 1993], which employs the finite volume and finite difference formulation to compute the electric field and power density in a sample and is used in conjunction with a commercially available heat transfer software package to obtain the corresponding temperature evolution in the sample .

Another common feature in many of the studies is the assumption of constant material properties, which may result in unreal predictions for many processes. This undermines the precision obtained from any of the sophisticated numerical models. Some studies applicable to general microwave heating have included temperature-dependent dielectric properties and constant thermal properties [DeWagter, 1984; Jolly and Turner, 1990]. Ayappa et al [1991] studied the microwave heating of multi-layered slabs with temperature dependent material properties by the finite-element method.

The effects of food geometry and position in an EM field may easily be obtained from the studies available in the literature which are related to microwave heating in general, but the effects of dielectric properties on the heating characteristics of food materials are not reported widely [Lorenson, 1990]. The limited publication of recent

developments in the thermal modelling of microwave processes involving foods, may be due to their potential commercial value.

Solving Maxwell's equations in a multi mode cavity in the presence of food sample, which may be of any arbitrary shape while taking any wave related phenomena (i.e. scattering, diffraction and interference) into consideration, is itself a major research topic. The complete simulation of the oven environment is time-intensive and requires an advanced computer hardware facility (e.g. the Cray, Convex or SGI power series) [Yang, 1989; Lorenson, 1990]. Full specifications of the excitation source may be impossible due to the theoretical complexity of practically useful stirrer systems. Only a few three dimensional calculations of power distribution in lossy dielectrics for simplified conditions have been reported, due to the complexity of the multi mode resonant cavity (e.g. a simple short-circuited rectangular wave guide [de Pourcq, 1983, 1984], a multi mode rectangular cavity [Jia and Jolly, 1992]).

The relative importance of the various phenomena resulting in the power density pattern cannot easily be deduced for a qualitative analysis by using numerical methods for calculations of "completely" specified problems [Risman et al, 1987]. Therefore, time and effort spent in such expensive analyses may not be justified at all times. On the other hand, the simple assumption of exponential decay for foods heated in microwave ovens is theoretically valid only for a limited range of problems. Another alternative is to study a series of systems selected for enhancement of phenomena such as large heating surfaces, edge-heating and internal resonance effects in order to obtain the practical insight of how foods are heated. Relatively simple but suitable assumptions for the microwave-excitations may be made.

The modelling of heat transfers in foods is reasonably well appreciated by thermal and food engineers, but the distribution of EM field is less well understood. The personnel involved in electrical engineering are reluctant to integrate in to the food industry. Much of the published research is also from the electrical engineering point of view.

Therefore in this chapter the modelling of electric field distributions in a food sample is discussed in detail, because it is the electric field intensity which causes the food to heat. The various assumptions concerning the electromagnetic field are modified to simulate the microwave heating of foods in a microwave oven. The developed mathematical model is employed to calculate the power absorbed in a sample which can be input as a source term (P_v) in the heat diffusion equation (Chapter 2, eq. (2.35). The influence of various parameters (e.g. the food formulation and the container on the heating characteristics of a certain type of food) may be undertaken.

5.2 THEORETICAL BACKGROUND

5.2.1 Plane Waves and Multi-mode Cavity

The domestic microwave oven is a common example of a multi mode cavity, i.e.a closed rectangular metal box with a suitable means of coupling power from the magnetron (see Fig. 5.1). The dimensions of the cavity should ideally be several wavelengths long in at least two dimensions [Metaxas and Meredith, 1983]. However a cavity with dimensions 2-3 times the wavelength in each directions is used for domestic ovens. The multiple reflections in three directions result in a large number of resonant modes (or standing waves) depending upon the size of a cavity (width, w; height, h; depth, d) which are characterise by integer indices l, m, and n in the x, y and z coordinates of a cavity respectively (Fig.5.2). There may be different cavity resonance modes namely;

a Transverse Electric (TE) or Perpendicular polarisation:
The electric field vector is the sum of the components transverse or perpendicular to the direction of propagation (Fig.5.4a).

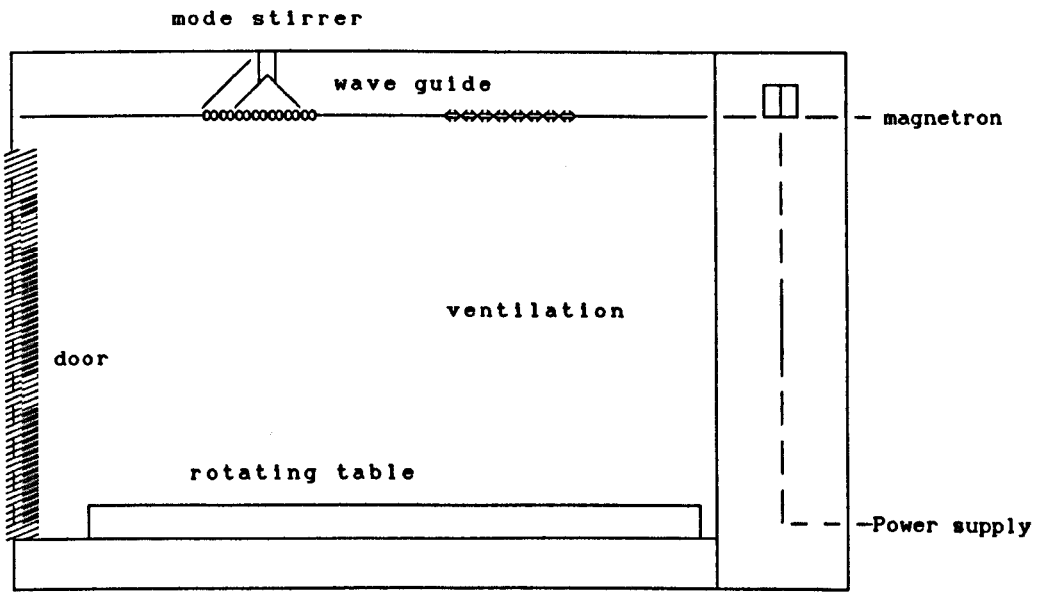

Fig. 5.1 Components of microwave oven

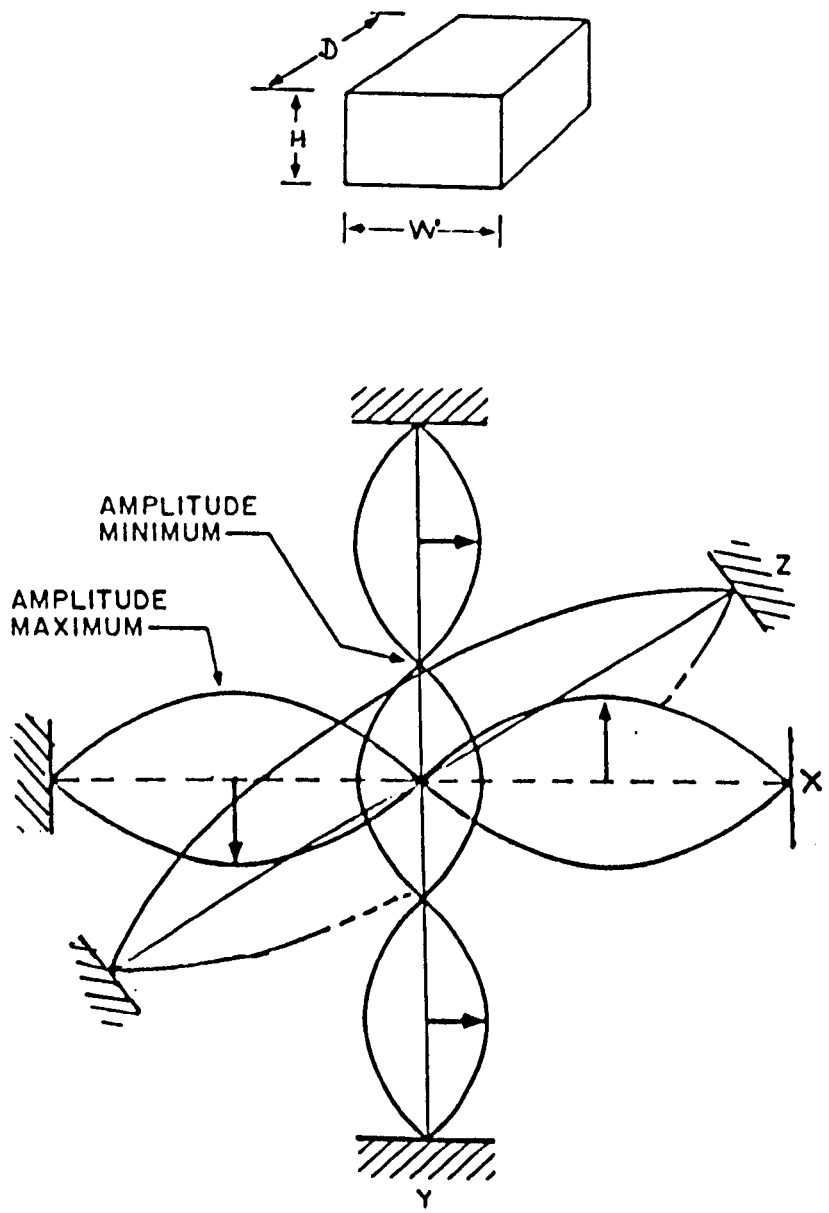

Fig 5.2 Cavity standing waves: modes in the x, y and z directions

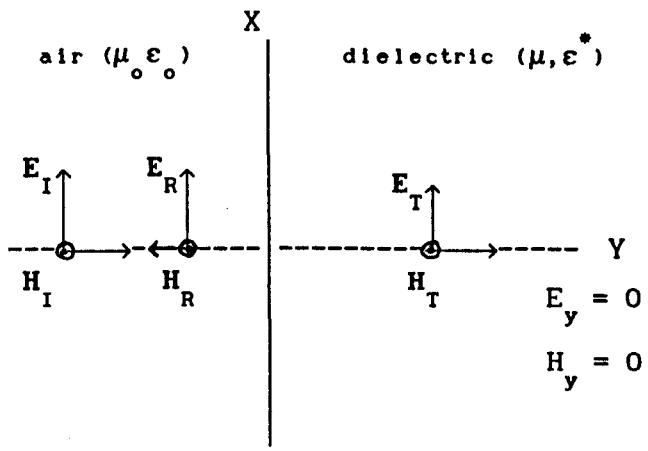

Fig. 5.3 Reflection and Transmission at normal incidence transverses Electromagnetic field (TEM)

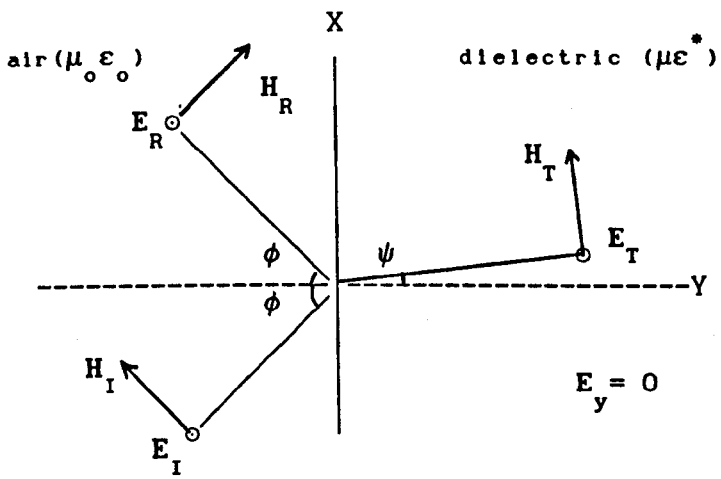

Fig.5.4a Perpendicular polarisation: (TE)

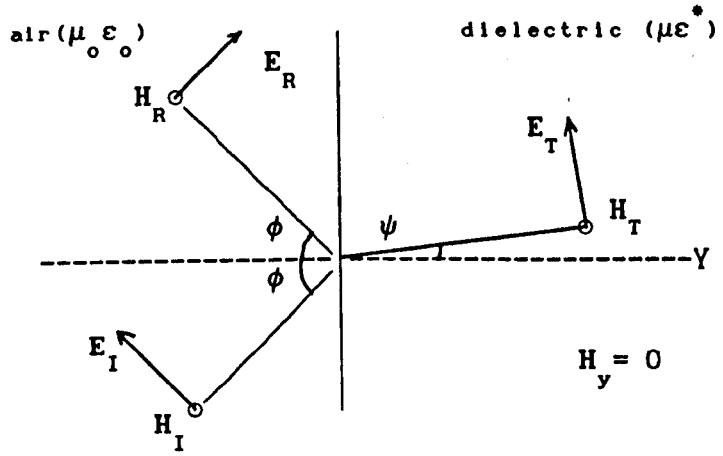

Fig.5.4b Parallel polarisation: (TM)

b) Transverse Magnetic (TM) or Parallel polarisation:
The electric field vector is the sum of the components parallel to the direction of propagation (see Fig.5.4b).

The EM field in a cavity satisfy the wave equation (2.4) i.e.

$$\nabla^2 \mathbf{E} + \gamma_o^2 \mathbf{E} = 0$$

The general solution of (2.4) in rectangular coordinates provides the well known relationship for the resonant frequencies (or propagation constant) and the cavity dimensions as follows;

$$\gamma_o^2 = \left(\frac{\pi l}{w} \right)^2 + \left(\frac{\pi m}{h} \right)^2 + \left(\frac{\pi n}{d} \right)^2 \qquad (5.2)$$

where, $\gamma_o = j\omega(\mu_o \varepsilon_o)^{1/2}$

Thus the number of modes supported in a rectangular geometry, regardless of whether TE or TM modes are sought is represented by the equation (5.2). By considering the boundary conditions for the two polarisations the different modes in a given cavity can be counted. The TE wave function satisfies the Dirichlet condition on those parts of the boundary surface where the TM wave function holds the Newmann condition and vice versa i.e.

for TE; $H_y = 0$ at $y = 0, h$ (5.3a)

$\nabla H_y . \mathbf{n} = 0$ at $x = 0, w$ and $z = 0, d$ (5.3b)

for TM; $E_y = 0$ at $x = 0, w$ and $z = 0, d$ (5.3c)

$\nabla E_y . \mathbf{n} = 0$ at $y = 0, h$ (5.3d)

Table 5.2

Number of modes for a microwave oven

(w x h x d : 330x227x335)mm, 2.4≤f≤2.5GHz

Mode Index number			Type of	Resonant frequency
l	m	n	mode	f, (GHz)
1	3	3	TE/TM	2.436
2	0	5	TM	2.414
2	2	4	TE/TM	2.402
3	3	0	TE	2.404
3	3	1	TE/TM	2.446
4	2	2	TE/TM	2.420
5	0	2	TM	2.441
5	1	1	TE/TM	2.410

If any one of the mode numbers (l, m, or n) is zero, then the corresponding wave function can only satisfy one set of boundary conditions and the solution is either the TE or the TM mode. Whereas if none of the mode numbers are zero, then mode number represents TE or TM mode (Table 5.2). If two or three mode numbers are zeros, it leads to the trivial solutions where all the eigenfunctions vanish and mode does not exist.

A larger cavity would support a greater number of modes and so provide a more uniform field distribution, but the manufacturing of such large ovens is not economically feasible and typical microwave ovens do not have modes with l, m, or n greater than 7 [Buffler, 1992]. Therefore other means such as turn-tables and mode stirrers are employed to remove the inequalities of field distributions and so toimprove the uniformity of heating.

Ideally, in order to calculate the field distribution, modes for the loaded oven should be known. These are different from those found by equation (5.2), which represents the modes in an empty cavity, whereas, the mode patterns in the cavity change in the presence of a load depending upon the material's shape, size and dielectric properties [Lorenson, 1990]. However, the influence of a load on resonance frequencies can be calculated approximately. Sayed et al [1984] reported that typical TE resonant frequencies would drop by at least 5%, when a typical load is introduced into a cavity. While TM resonant frequencies drop more than TE frequencies. Oven designers try to design MW cavities with uniform electric field distributions which are less sensitive to load variations (and hence achieve uniform temperature distribution in the foods heated in the MW oven). However, large temperatures variations have been found in the identical products heated in different MW ovens [Burfoot & Foster, 1989]. This poses a real problem for food manufacturers who have to design products for ovens with large variations (discussed in detail in Chapter 6)

5.2.2 Power Density patterns in Food loads

A well stirred multi-mode cavity can be assumed as an approximately isotropic source of randomly polarised plane waves. Typical modes in the oven cavity and their influence on foods can be studied by plane wave interpretation of wave guide modes [Risman, 1992a]. Oblique incidence of a plane wave can be considered by applying geometric optics. At large angles of incidence an almost perpendicular propagation is achieved in typical food samples, e.g. for $\varepsilon' = 50$ and $\phi = 85^{\circ}$, propagation inside the material will be at $\psi = 8^{\circ}$ (Snell's law, Chapter 2). The assumption of plane waves is applicable to many practical situations for microwave heating of foods (e.g. heating by a plane wave applicator, heating small samples in a microwave oven when the electric field at the surface may be assumed to be uniform). However, although oven designers try to achieve a uniform field distribution (through stirrers, turn-tables and multi-port feed systems etc.) in the oven cavity, the electric field intensity at the surface

of larger samples is not uniform. Therefore, the field intensity in the horizontal plane (xz) may have to be considered. This has been undertaken for loads extending to four walls of the cavity by analysing it as a dielectric filled wave guide [Zhu and Hankui, 1988; Paolini, 1989, Risman, 1992a].

Experimental results for heating rectangular loads in an oven showed that, in horizontal plane there is approximate symmetry in two axes in the heating/power density patterns. The turn-table smears the power density patterns at the surface of the load to some extent, but hot or cold spots at the surface may still exist depending upon the horizontal propagation pattern (as determined by the propagation constants γ_x and γ_z). The typical distance between the maxima for the power density profile is half the free space wave length (≈6cm at 2.45GHz). The other two most general localised heating effects in foods heated in a microwave ovens, edge heating and core heating, are functions of the food sample's geometry and dielectric properties.

Edge heating effects are commonly found in large slab like loads (rectangular and flat cylindrical types load; Figs.5.5 & 5.6). Even in the ovens with turn-tables this effect is significant, particularly if the material has a high permittivity. Edge heating effects change slightly when the location of the load is altered in the oven. This occurs due to the concentration of the electric field at the corners by diffraction. Internal standing waves occur depending upon the geometry of the food corner and produce overheated regions which vary in size due to the corner angle and the dielectric properties of the material [Risman, 1993]. The electric field component parallel to the edge causes the edge to over heat. However, some ovens are designed to have smaller horizontal electric field components (or with dominant TM modes). Therefore, edge heating of slab like loads is less in these ovens than typical ovens. For a typical oven plane waves incident upon a load from all directions may be assumed to represent the effects of microwave oven cavity modes.

Fig.5.5 A practical illustration of edge-heating in rectangular slab loads heated in MW ovens

Fig.5.6 A practical illustration of edge-heating in flat cylindrical loads heated in MW ovens

Usually ovens have microwave feeding near (on a side wall) ceiling or on the ceiling. Therefore, the load is not heated equally from above and below. The foods with low ε^* (e.g. frozen foods) experience greater underheating. As it was practically observed (see. Chapter 6) the overheating extends typically 10-15mm inwards from the edges and around the periphery of the load. Therefore it may be assumed that electric field intensity at the edges is about 4 times higher than that existing in the centre region of the irradiated surface. This assumption is consistent with the application of the exact theory in a typical microwave oven [Risman, 1992b].

Internal focussing effects are common in quasi-spherical and cylindrical shaped foods; they cause hot spots in the core (see Chapter 2). The power distribution can be computed by assuming the plane waves scattered by the load. Two polarisations can be considered separately, TE when the E-vector is perpendicular to the cylinder axes and TM when E-vector is parallel to the cylinder axes. The analyses for TE and TM polarisations for infinite cylinders have been performed for loads with dielectric properties of typical foods [Risman and Ohlsson, 1991]. They found out that the power coupling efficiency in the TE field is less than the TM field for cylinders of radius up to 100mm, but on further increase in the radius the power distribution for TE approaches that for the TM case.

5.3 MATHEMATICAL ANALYSIS

The primary excitation of the microwave oven cavity is through a wave guide opening with the magnetron antenna transition into the wave guide being so far away that no significant evanescent fields from the magnetron coupling remain at the port. Mode stirrers are claimed to balance the relative coupling of excitation of the resonances so that these modes are excited in turn [Risman, 1991]. Thus for a typical microwave oven with a mode stirrer, sequential TE and TM excitations should be expected. However, when $|E_x|$ or $|E_z| \gg |E_y|$ the wave pattern approaches TEM mode. Therefore the analysis for a TEM case can be

employed to obtain the power distribution in a typical food load heated in a typical microwave oven.

5.3.1 Power Distribution

By considering the wave equation for the electric field vector (ref. Chapter 2). The radiation boundary condition at a hypothetical boundary surrounding the sample is assumed.

$$\nabla^2 \mathbf{E} + \gamma^2 \mathbf{E} = 0$$

which in the expanded form is

$$\frac{\partial^2 \mathbf{E}}{\partial x^2} + \frac{\partial^2 \mathbf{E}}{\partial y^2} + \frac{\partial^2 \mathbf{E}}{\partial z^2} + \gamma^2 \mathbf{E} = 0$$

For a plane wave propagating in the y-direction (Fig.5.7);

$$\frac{\partial^2 \mathbf{E}}{\partial y^2} + \gamma^2 \mathbf{E} = 0 \qquad (5.4)$$

where, $\gamma^2 = \gamma_o^2 \varepsilon_r^*$ (in a dielectric) and ε_r^* is space and time (or temperature) dependent i.e. $\{\varepsilon'(y,T)-\varepsilon''(y,T)\}$.

For oblique incidence, the propagation constants are the vector sum of the propagation constants for the incident and transmitted waves (as per Snell's law, see Fig. 5.8).

$$\left.\begin{aligned} \gamma_I^2 &= \gamma_x^2 + \gamma_y^2 \qquad (\ \gamma_x = \gamma_o \sin\phi,\ \gamma_y = \gamma_o \cos\phi\ ) \\ \gamma_T^2 &= \gamma_x^2 + \gamma_y^2 \qquad (\ \gamma_x = \gamma \sin\psi,\ \gamma_y = \gamma \cos\psi\ ) \end{aligned}\right\} \quad (5.5)$$

The power absorbed in a dielectric was calculated from equation (2.13) by substituting for the electric field and integrating over the considered volume:

$$P(y) = \frac{\omega\, \varepsilon_o\, E_o^2}{2\,\Delta y} \int_V \varepsilon''(y)\, E(y)\, E^*(y)\, dv \quad (5.6)$$

5.3.2 Temperature Distribution

To obtain the transient temperature distribution in a material heated by microwaves, the heat diffusion equation (2.35) with the source term, P_v, was solved simultaneously with equation (5.4) to obtain the electric field distribution. The resulting power absorbed is calculated via equation (5.6).

The solution of the boundary value problem (5.4) is complex. So real and imaginary components for the electric field and propagation factor are separated and solved simultaneously using the Gauss-elimination method. The derivatives were discretised using the finite-difference method (Appendix 10).

5.3.3 Boundary Conditions for Microwave radiation

The non-uniform distribution of ε^* (due to differences in temperature and composition within a material) was considered by dividing the length of the considered material into n layers of thickness Δy (Fig.5.7). Each layer may have a different permittivity and thus different reflection and transmission coefficients. The continuity of tangential components of the electric and magnetic fields provides the necessary boundary conditions at the interfaces at the surface and between adjacent layers.

The surface exposed to radiation:

$$\frac{\partial E}{\partial y} = \gamma_o (E - 2E_o) e^{-\gamma L} \quad \text{for } y = L \qquad (5.7)$$

If the material is exposed to radiation from the other side:

$$\frac{\partial E}{\partial y} = \gamma_o (2E_o - E) e^{-\gamma L} \quad \text{for } y = -L \qquad (5.8)$$

In the case of the reflective boundary (e.g. the metal sides of an oven or food container):

$$E = 0 \qquad (5.9)$$

The continuity conditions for electric and magnetic field vectors at the interface are:

$$\left.\begin{aligned} n \times (E_i - E_{i+1}) &= 0 \\ n \times (H_i - H_{i+1}) &= 0 \end{aligned}\right\} \quad \begin{aligned} &\text{at } y = y_2 \ldots\ldots y_n \\ &\text{and } i = 1 \ldots . n-1 \end{aligned} \qquad (5.10)$$

which gives the following:

$$\left.\begin{aligned} E_i &= E_{i+1} \\ \frac{\partial E_i}{\partial y} &= \frac{\partial E_{i+1}}{\partial y} \end{aligned}\right\} \quad \begin{aligned} &\text{at } y = y_2 \ldots\ldots y_n \\ &\text{and } i = 1 \ldots . n-1 \end{aligned} \qquad (5.11)$$

Similarly, variations in the xz-plane consist of cosinusoidal or sinusoidal functions with periodicity depending upon the horizontal propagation constants. The solutions satisfy the natural boundary conditions and the interface continuity of tangential field components as for vertical modes. Thus the power absorption due to the incident wave from the (x) direction was obtained by employing the same procedure. The total power absorbed was:

$$P \text{ (total)} = P(x) + P(y) \qquad (5.12)$$

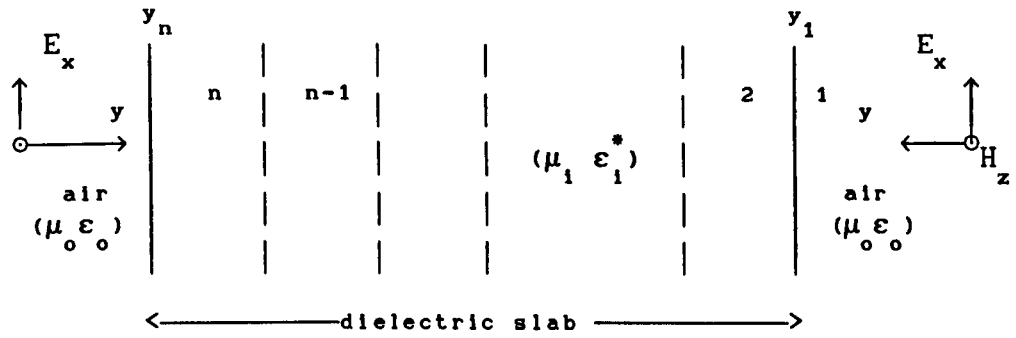

a. Exposed to radiation from both sides

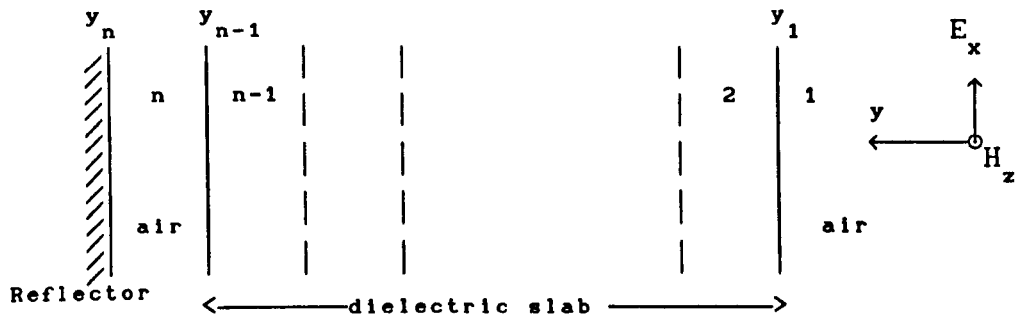

b. Exposed to radiation from one side and metal end at certain distance, such that; $T_n = -R_n$

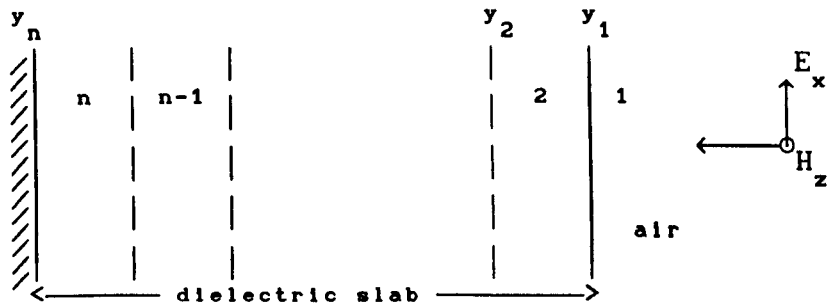

c. As above in b. but metal backing at the other end such that; $E_n = 0$

Fig.5.7 Heating of composite slab by plane waves at normal incidence (i.e. TEM mode), (i = 1,n)

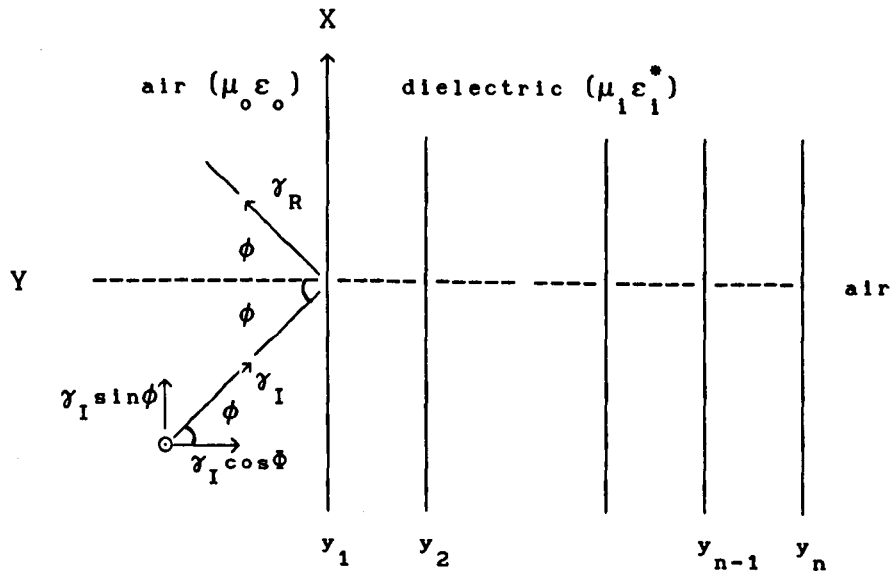

Fig.5.8 Heating of composite slab at oblique incidence any of the boundary conditions as in Fig.5.7 may apply

5.4 PARAMETRIC ANALYSIS

The effects of various parameters (i.e. size, dielectric properties and temperature) on the absorbed power by a material were investigated by employing the presented model. The transient temperature profiles for various foods subjected to microwave heating were also obtained in few cases. To evaluate the effect of temperature on the absorbed power during a heating process, the variation in material properties with temperature was incorporated in the model. This functional variation was based on the assumptions discussed in Chapters 3 and 4, otherwise mean values of material properties were chosen above $0^{\circ}C$. The assumed frequency was 2.45GHz. Other parameters (e.g.ambient temperature, heat transfer coefficient) were identical to those applying to the base-case slab in Chapter 2 (Table 2.2).

5.4.1. Thickness and Dielectric properties

To investigate the effect of thickness for slab like loads and dielectric properties upon power deposition, a free space slab of varying thickness was considered. Two food materials representing typical materials with high ($\alpha \approx 52 m^{-1}$) and low attenuation factors ($\alpha \approx 5 m^{-1}$) respectively were selected.

The standing wave pattern is independent of the amplitude of the electric field and it is a characteristic of the medium through which the wave propagates i.e. the material's dielectric properties and boundary conditions. Therefore, the power density profiles are normalised against the maximum value of P_v within the material.

The reflections at the surfaces set up a standing wave pattern, depending upon the attenuation of wave within the material. The ratio of maximum to minimum electric field intensity (i.e. VSWR) is $(\varepsilon_r)^{1/2}$, thus the ratio of maximum to minimum power density is ε_r. The distance between the maxima of power density profiles is half the wave length in the material (i.e. $\approx$0.089m for the material with $\alpha \approx 52 m^{-1}$ and $\alpha \approx 0.031$m

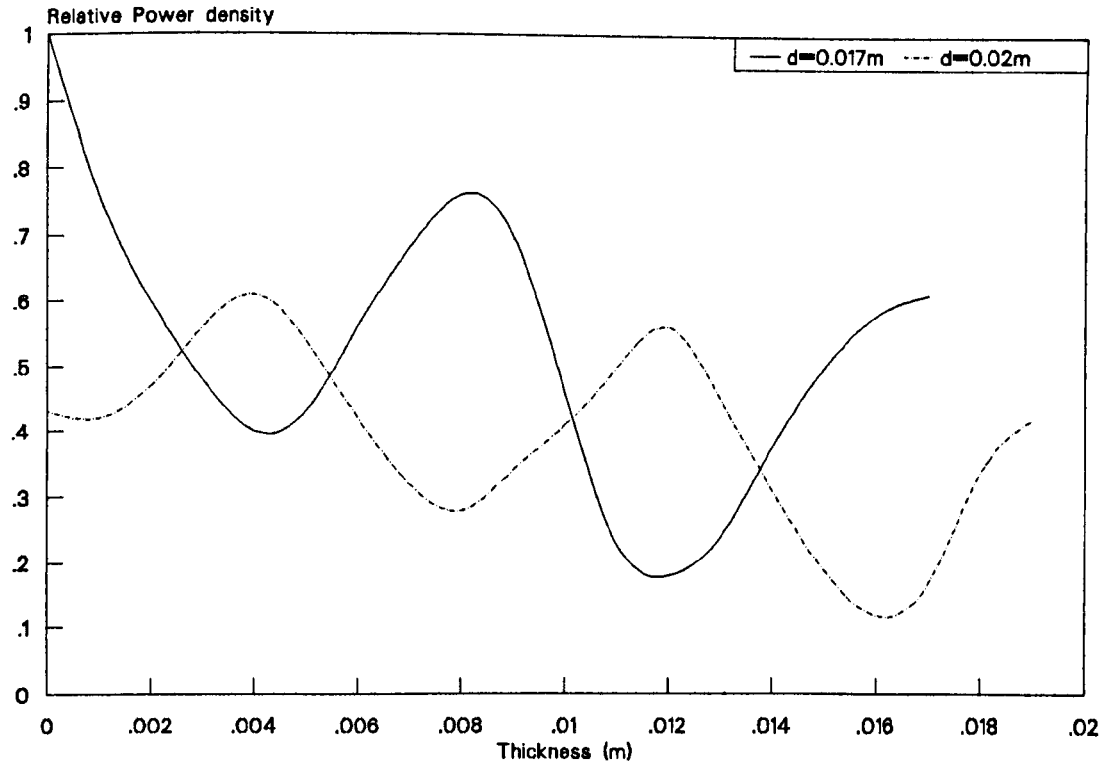

Fig.5.9a Variation in power density profiles for 2 slabs of thicknesses; 0.017m, 0.02m, (α=52m^{-1}), pofiles are normalised to the max. power density i.e. for d=0.017m

2

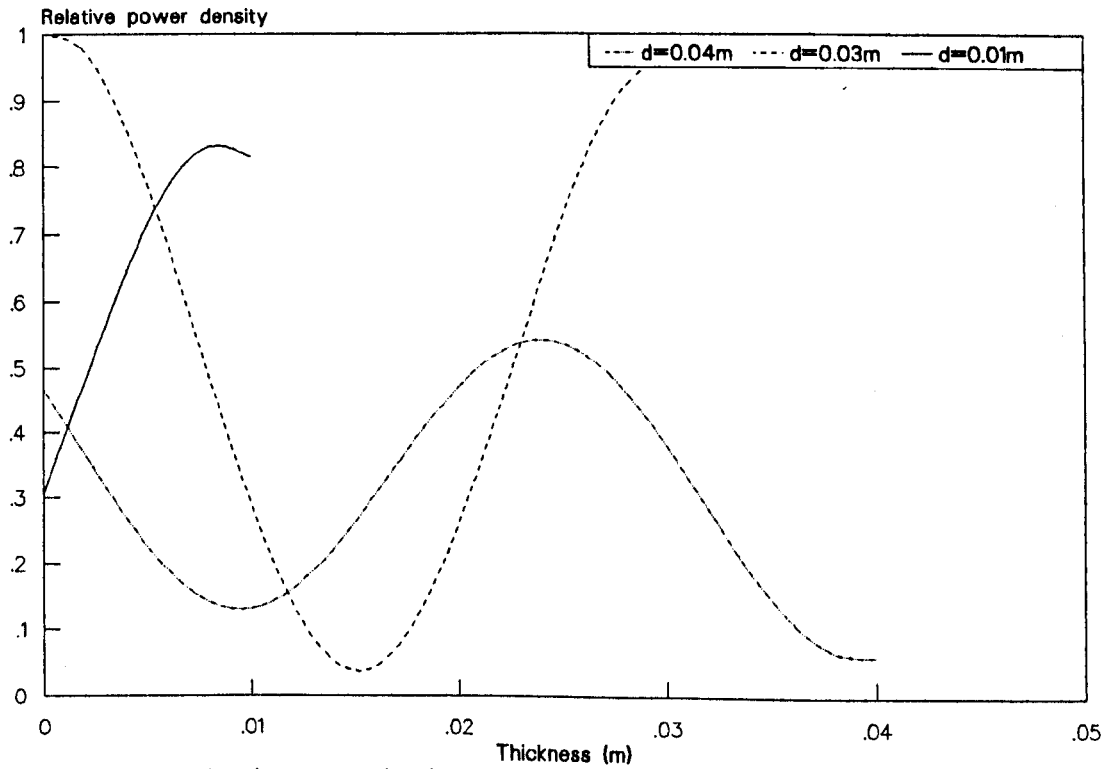

Fig5.9b Variation in power density profiles for 3 slabs of thicknesses:0.04m 00.03m, 0.01m (α=5m^{-1}). profiles are normalised to the max. power density i.e. for thickness 0.03m

3

for the material with $\alpha \approx 5m^{-1}$-Fig.5.9a,b). Therefore, when the thickness of the material is an integer number of half wavelength in the material, the mode pattern results in maximum absorption (i.e. a higher VSWR), whereas other thicknesses result in a weaker standing wave. For example, thicknesses of about 0.017m and 0.03m result in the maximum power absorption for high and low loss materials respectively (i.e. for $\alpha \approx 52m^{-1}$ and $\approx 5m^{-1}$).

5.4.2 Metallic shielding

Analyses were undertaken for slabs of thickness 0.1m irradiated from one side with a metal shield on the other side to represent a metal container. Different dielectric properties representing typical food materials heated in microwave ovens were used (Fig.5.10).

Three food materials i.e. butter, potato and ham of 0.1m thickness were considered. The material with the lowest attenuation factor (i.e. butter with $\alpha \approx 5m^{-1}$) exhibits standing waves within the material. For the potato and ham (with $\alpha \approx 52m^{-1}$ and $\approx 78m^{-1}$ respectively), the maximum P_v is at the surface due to the standing waves at the surface, which means that most of the power is absorbed near the surface. There are no propagating modes within potato and ham samples and the power attenuates exponentially within. Also because there is no internal reflection, thus the metal backing has no effect. It can also be concluded that Lambert's law may be applied for calculating the distribution of power within materials of similar dielectric properties and sample sizes

Fig.5.11 and 5.12 provide a comparison for butter and potato slabs of thickness 0.1m, for the power distribution obtained by assuming exponential decay with that by considering the reflections at the rear boundaries. The power intensity at the surface is obtained by solving the field equations in both cases. It is obvious that for a low loss material (Fig.5.11), the errors incurred in making the assumption of exponential decay may be large. Whereas, for $\alpha \approx 52m^{-1}$the difference

between the two profiles is hardly visible. However, with a change in the thickness of the material, the mode pattern would change. Figs.5.13 and 5.14 represents profiles for both materials for slab thicknesses; 0.1m, 0.05m and 0.025m. The mode pattern starts to become apparent for $\alpha \approx 52m^{-1}$ as the thicknesses decreases to 0.05m and for a thinner slab (0.025m) the effect is clear.

Mode patterns for a 0.025m thick slab load of $\alpha=52m^{-1}$ (characteristic impedance $\approx 55\Omega$) were compared for normal incidence and for oblique incidence ($\phi=60^{\circ}$) in Fig.5.15. The reflection at the surface increases for the oblique incidence (see Chapter 2), thus power density amplitude at the surface also decreases. There is a shift in the mode pattern and the power absorbed is reduced as compared with perpendicular incidence.

5.4.3 Effect of Temperature on the Power absorption

During heating, the power absorbed in a material may change significantly. The temperature dependence of the material properties expressed as functions of temperature (depending upon the material selected) were included in this analysis (Table 5.3). Figure 5.16 shows the change in the mode pattern for a frozen material with ε^{*} (= 4-j0.4) when exposed to microwave radiation for 10 minutes. When the material thaws, the ratio of maximum to minimum changes and also a phase change in the EM field occurs. After 2 minutes of heating, when the material is still frozen, the maxima is at the surface due to higher wave impedance. The resonance peaks are high, because of the low attenuation and the corresponding temperature profile is uniform within the material. Once the material has passed through the transition the mode pattern changes and the power density amplitude decreases (impedance mismatch) after 4 minutes. However as the attenuation increases, temperature run-away effects are also apparent, because more and more power is absorbed near the surface. The power density profiles become stable as the material thaws. These mode patterns indicate that the dielectric properties do not vary significantly for this material in the considered temperature range (i.e. $0^{\circ}C<T<35^{\circ}C$) at 2.45GHz.

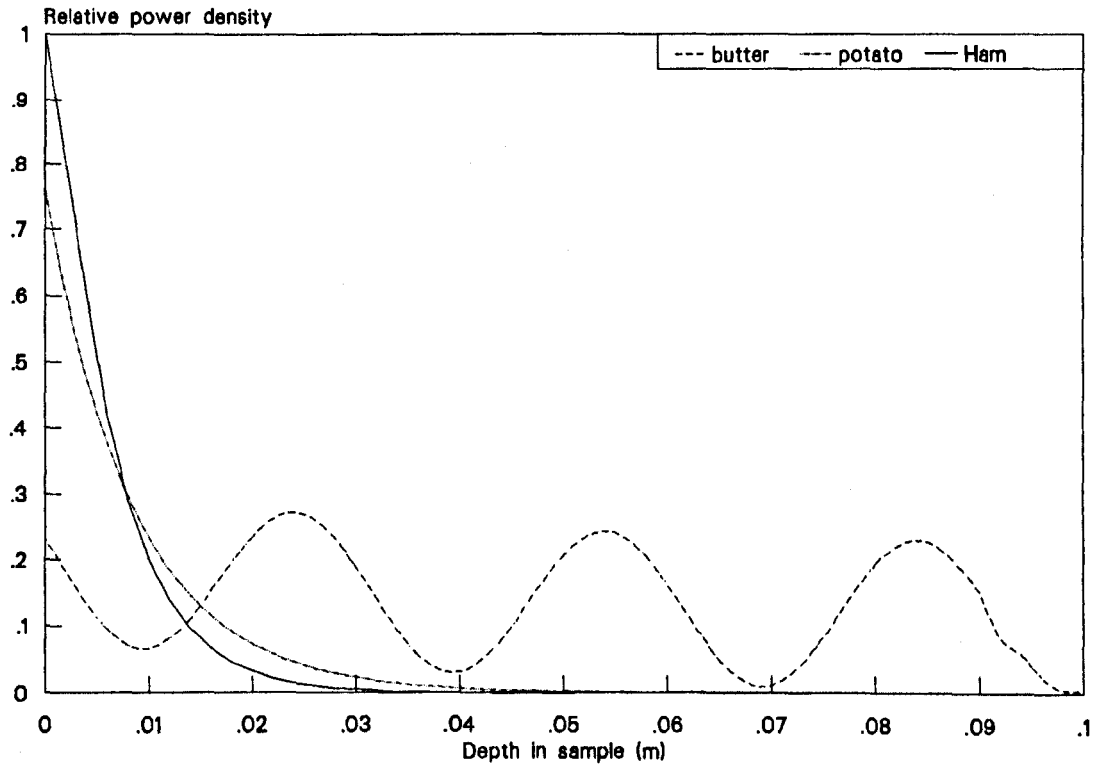

Fig.5.10 Comparison of power density profiles in 0.1m thick slabs of; butter(α=5m^{-1}); potato(α=52m^{-1}); Ham(α=78m^{-1})

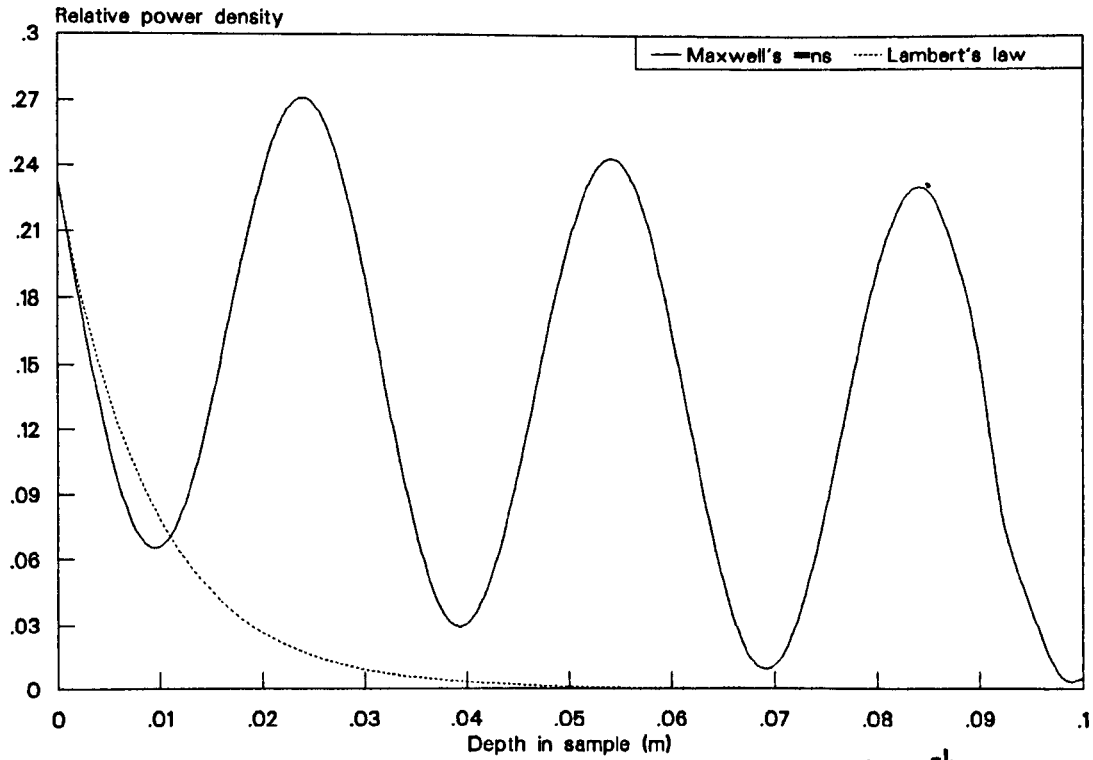

Fig.5.11 Comparison of power density profiles for 0.1m thick slab (α=5m^{-1}) calculated by Lambert's law and solving Maxwell's eqns (same as in Fig.5.10)

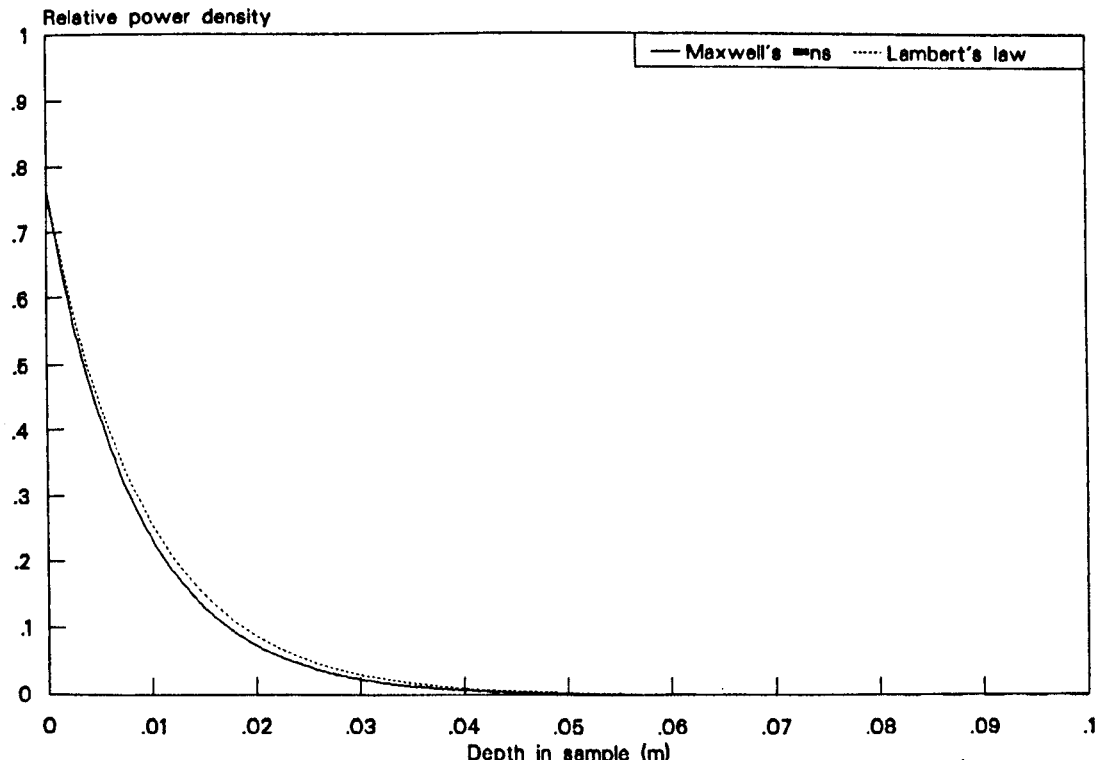

Fig.5.12 Comparison of power density profiles for 0.1m thick slab (α=52m^{-1}) calculated by Lambert's law and solving Maxwell's eqns (same as in Fig.5.10)

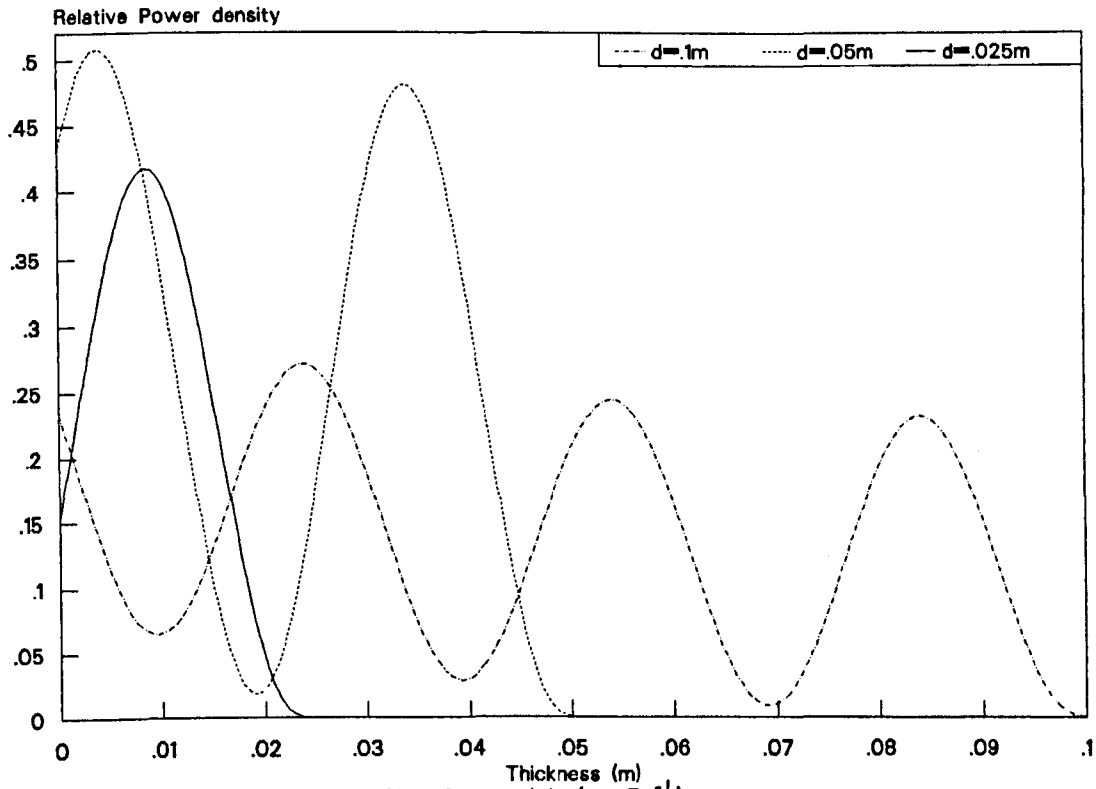

Fig.5.13 Power density profiles for a slab ($\alpha \simeq 5m^{-1}$) of thicknesses: 0.1m, 0.05m, 0.025m

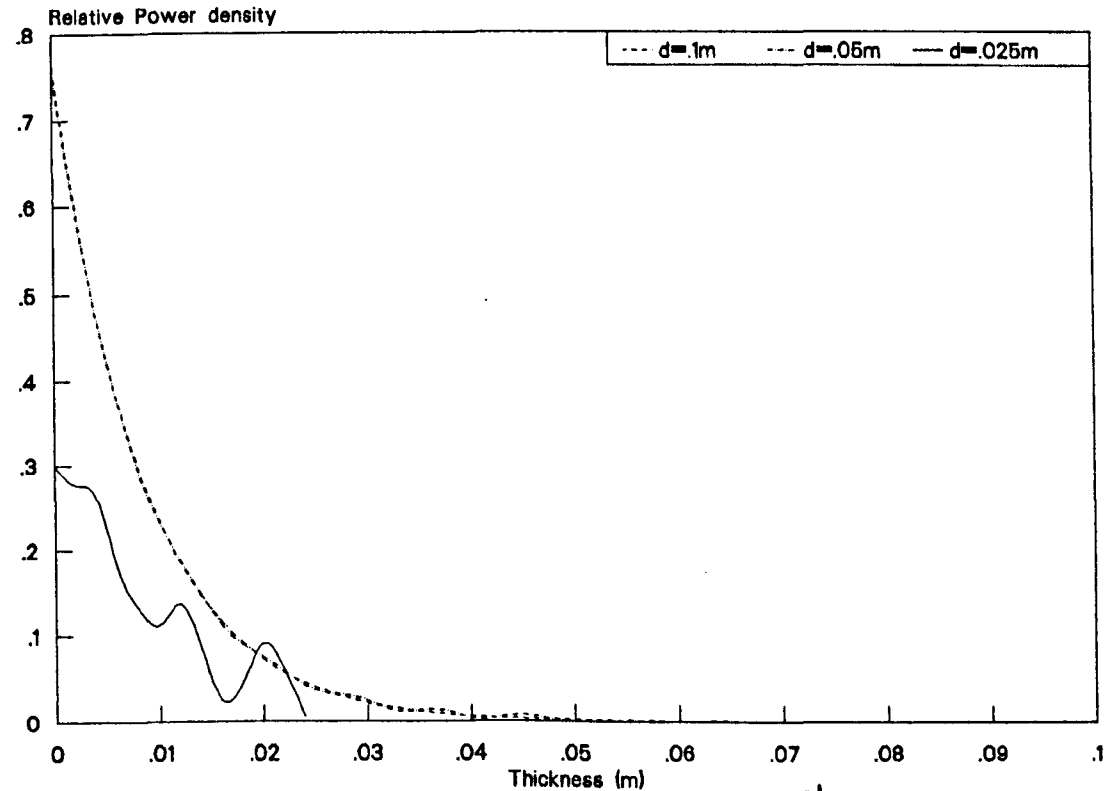

Fig.5.14 Variation in power density profiles for a slab ($\alpha \simeq 52m^{-1}$) of thicknesses: 0.1m, 0.05m, 0.025m

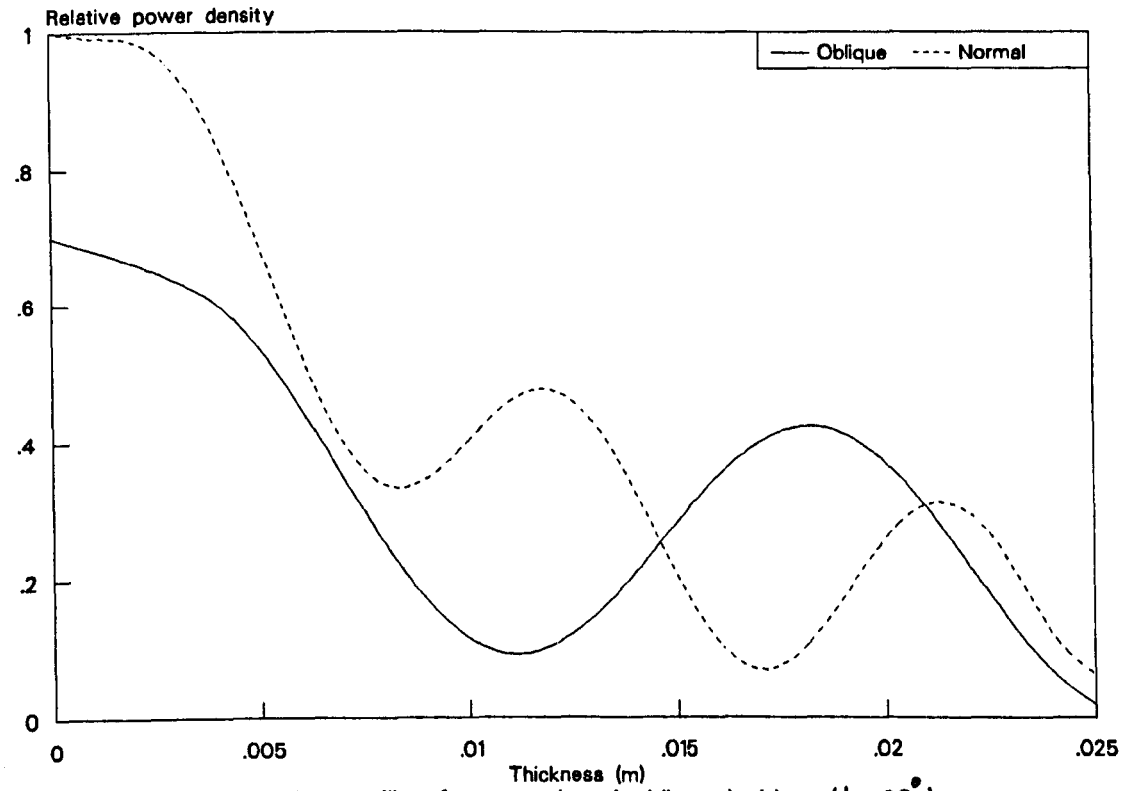

Fig.5.15 Power density profiles for normal and oblique incident ($\phi \simeq 60^{\circ}$) for perpendicular polarisation ($\alpha \simeq 52 m^{-1}$)

5.4.4. Temperature Distribution

The wave length, λ (at 2.45GHz) in low loss food materials is comparable with the size of typical food loads. In the frozen state, for the material ($\varepsilon^*=4 - j0.4$), the distance between resonance peaks of power density appear large (i.e. $\frac{\lambda}{2}\approx 0.03$m) (see Fig.5.16). Although, the temperature profile follows the profile of the power density profile, the peaks are less significant in the temperature distribution due to the effects of thermal conduction within the material (Figs.5.16 and 5.17).

The large penetration depth in the frozen state results in the uniform distribution of power absorption and thus even temperature distribution within the depth of the material is achieved(i.e. after 2 minutes)-Fig.5.17. Thermal conductivity is also large in the frozen regions. Absorption of latent heat also restricts the temperature variations. In the thawed region attenuation factor increases rapidly and thermal conductivity decreases. Owing to the governing effects of the dielectric properties, the temperature in the thawed regions increases rapidly (e.g. thermal runaway effects apparent in Fig.5.17).

Many foods consist of a fluid phase, which on heating becomes mobile and combined mechanisms of conduction and convection take place, then serve to enhance the rate of heat transfer. For materials with large attenuation factors ($\approx 50\ m^{-1}$) the distance between the power peaks is less, which means power is absorbed more uniformly. However, the absorption may dominate (depending upon the thickness of material in the direction of propagation) (Fig.5.14) and in which case there will be no further propagation of modes. Hence, power is absorbed near the surface and again the interior of the material is heated by heat transfer mechanisms.

Table 5.3

Material properties data for Figs.5.16 and 5.17

Parameter	$T \leq 0^{\circ}C$	$T > 0^{\circ}C$
k	(0.65-0.0008T)	0.225+0.0005(T+273)
α_T	$\{(0.36-0.002T)\times10^{-6}\}$	$\{0.046+0.0003(T+273)\times10^{-6}\}$
ε'	(4.4+0.03T)	(6.2-0.0015T)
ε''	(0.44+0.0051T)	(0.69-0.0002T)

Table 5.4

Material properties data for Figs.5.18 and 5.19

Material	Parameter			
	k	α_T	ε'	ε''
Beef	0.45	0.15×10^{-6}	44.2	11.3
Pastry	0.4	0.2×10^{-6}	4.0	0.4
Hydrogel	0.47	0.15×10^{-6}	(62.7-0.0104T)	(19-0.064T)

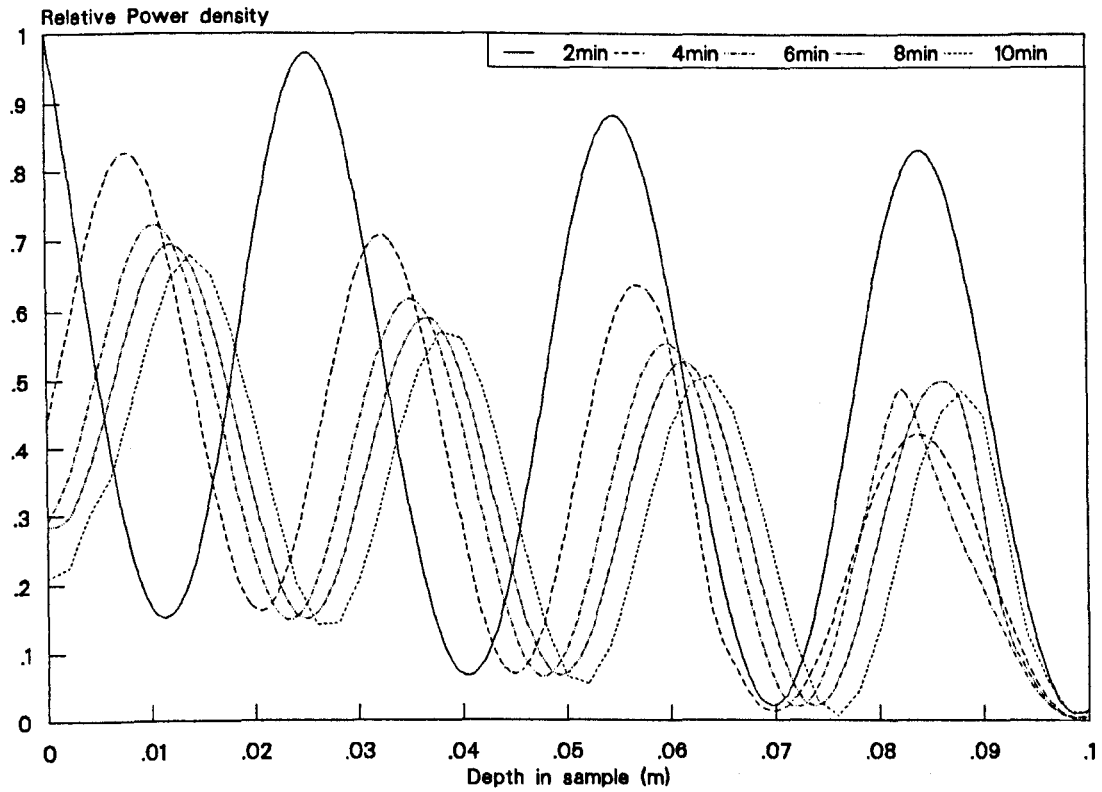

Fig.5.16 Power density profiles at 2min interval for a slab heated from -5°C, E_o=3000V/m

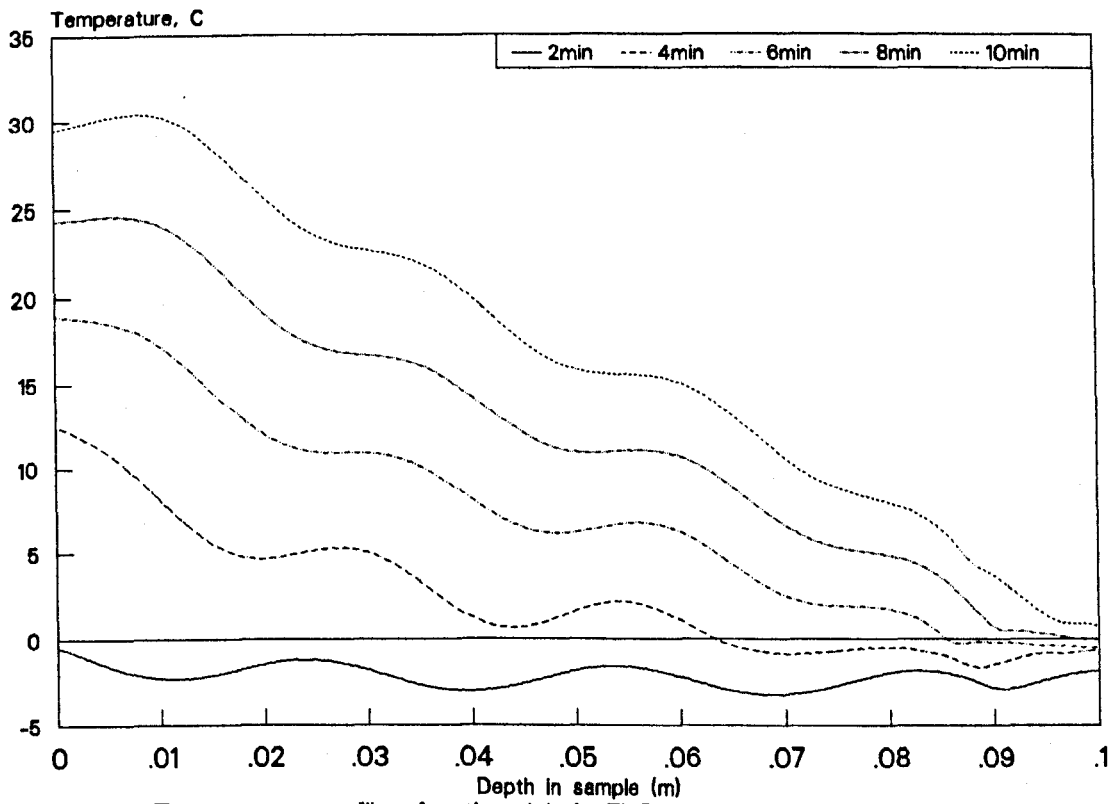

Fig.5.17 Temperature profiles for the slab in Fig5.16

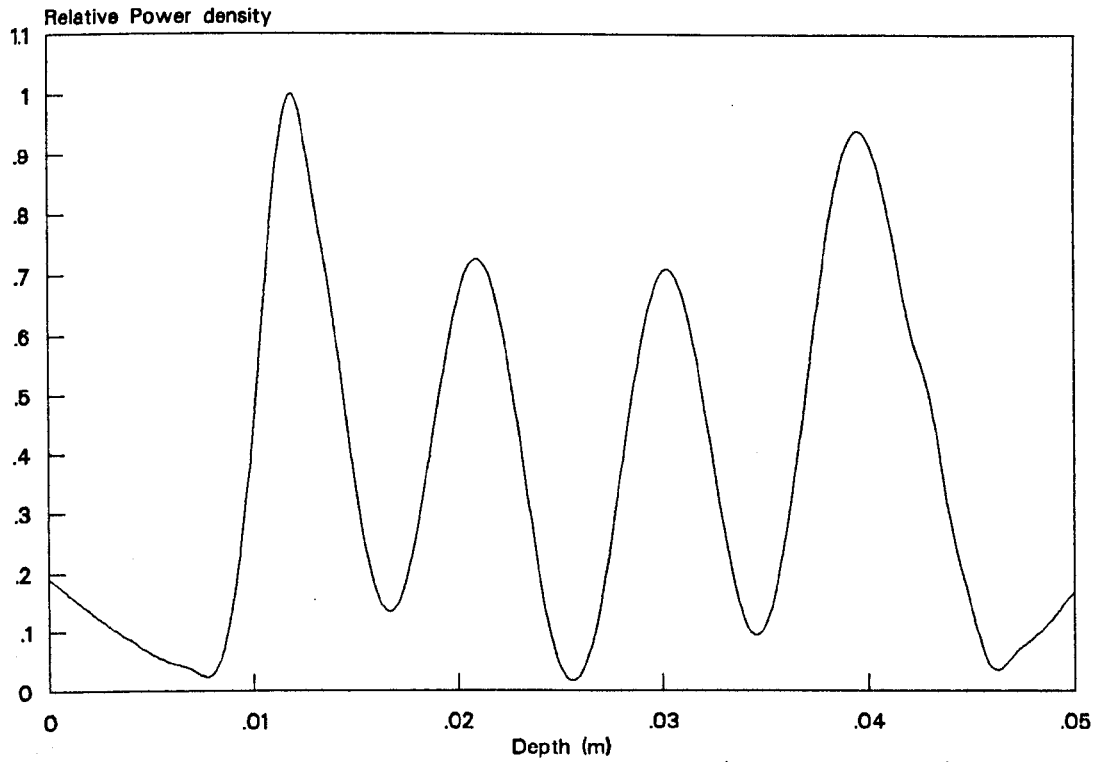

Fig.5.18a Power density profile in a three layered slab (pastry,beef,pastry) 0.01m, 0.035, and 0.005m thick respectively
E_o = 3000V/m

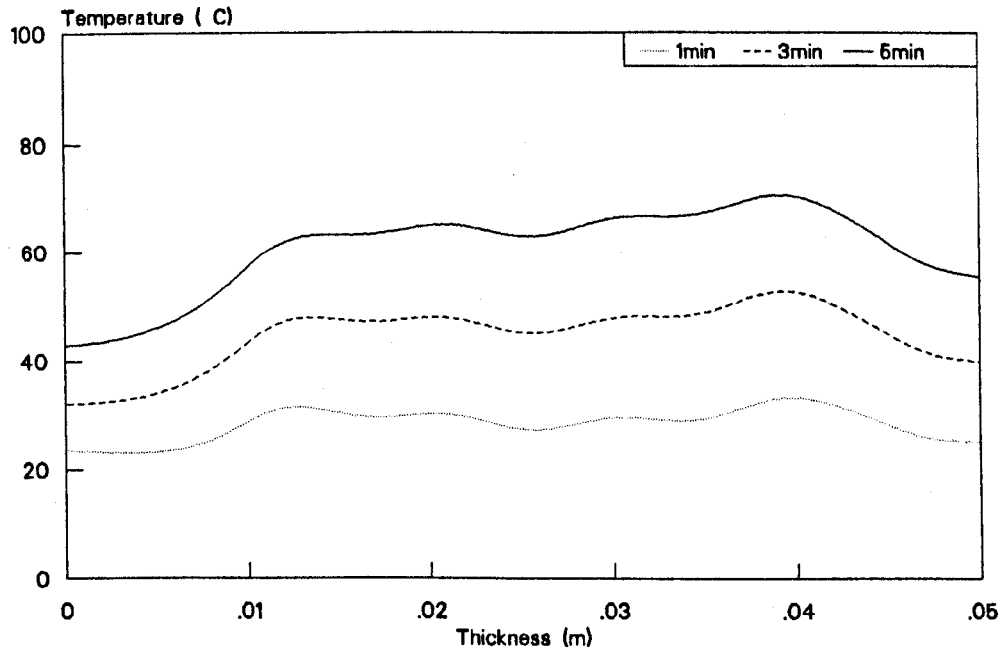

Fig5.18b Transient temperature profiles for the slab in Fig.5.18a

5.4.5 Multi-layered Material

Different materials have distinct properties and the temperature dependence of each depends upon the composition. When such materials are heated with microwaves their coupling efficiencies are different and therefore they heat at different rates. This is observed when composite food materials (e.g. pizza, doughnuts, lasagne) are heated in microwave ovens. Fig. 5.18a,b shows the heating of a three layered slab representing a 0.03m layer of meat-in-gravy sandwiched between two layers of pastry of thickness, 0.015 and 0.005m respectively. The slab is irradiated from both sides. The microwaves penetrate through the layer of pastry without being significantly absorbed ($\varepsilon^* = 4-j0.4$).Meat has a comparatively high attenuation factor ($\varepsilon^* = 44.1-j11.3$), and so power is absorbed in the middle layer. However, as the thickness of the layer is comparable with the skin depth (see Table 5.1), the reflections at the intermediate boundaries set up standing waves within this layer. The resonant peaks are 0.008m apart (i.e. half wave-length in the material) as illustrated in Fig.5.18a. The same effect is apparent in the temperature distribution, but as before the peaks are not so prominent in the temperature distribution due to thermal conduction effects (Fig. 5.18b).

5.5 COMPARISON WITH EXPERIMENTAL MEASUREMENTS

The model predictions for a two dimensional slab were qualitatively compared with experimental measurements.

5.5.1 Experimental details

The experimental set up consisted of a test load of a model material (hydrogel*, m= 75%) in a rectangular plastic container, heated in a domestic MW oven. The test loads were kept at a temperature of ≈4°C, which was the initial temperature used in the numerical calculations. The temperatures measurements were taken immediately after heating by thermocouples, which were compared with the model predictions.

(*Hydrogels have been shown to be valid thermal-load models and are therefore acceptable as a justification of the theoretical model. Details of the sample preparation and the temperature measurement are also described; see Chapter 6).

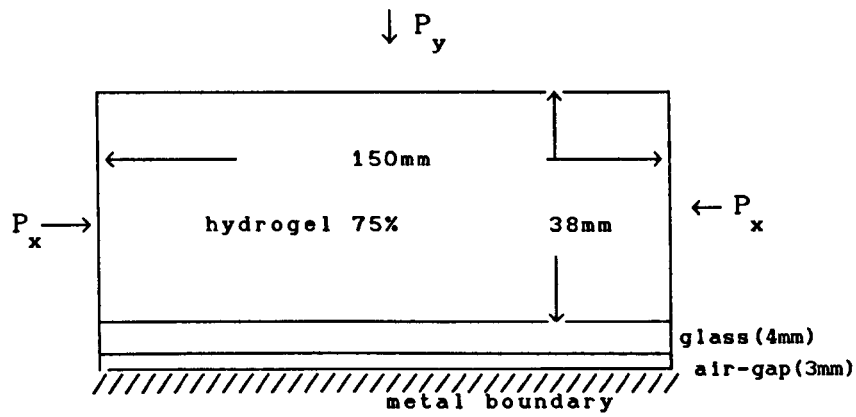

Fig.5.19 Schematic diagram of slab

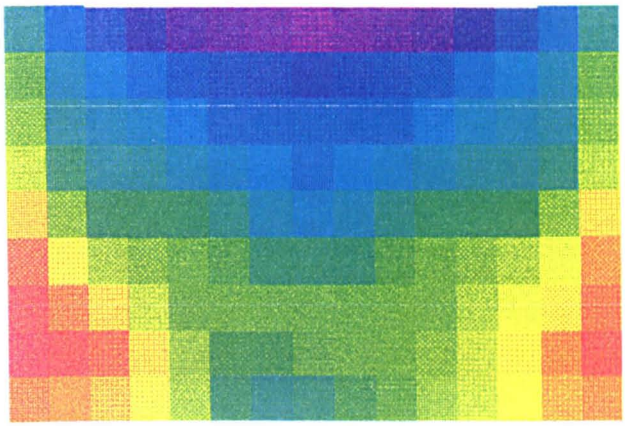

(a)

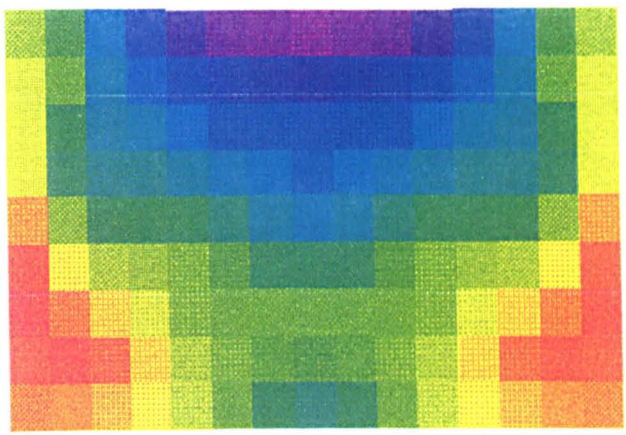

(b)

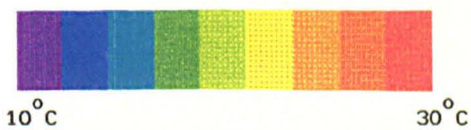

Fig.5.20a Comparison of measured temperature distribution (a) with numerical simulation in (b) after 120s

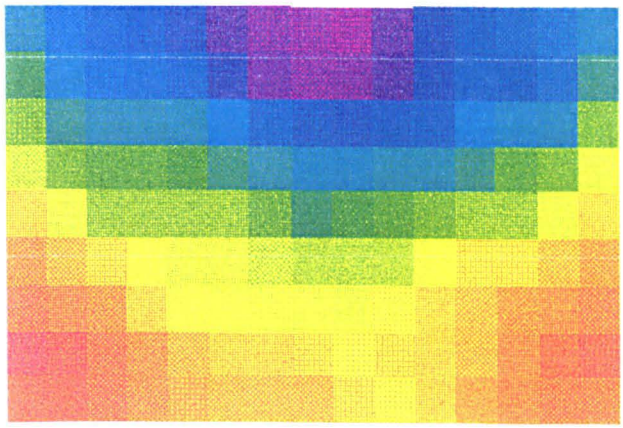

(a)

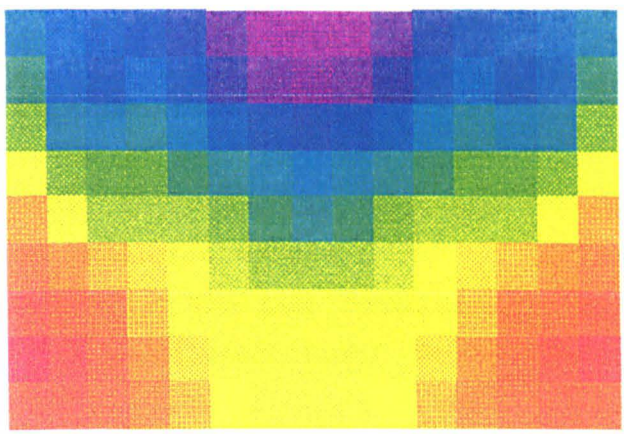

(b)

Fig.5.20b Comparison of measured temperature distribution (a) with numerical simulation in (b) after 240s

5.5.2 Numerical simulations

For numerical investigations a composite slab, irradiated from the top and two sides was considered to represent the load (Fig.5.19). The material of the container was relatively transparent to microwaves compared with the test-load (75% hydrogel), material properties of which were estimated (Table 5.4) based on predictive correlations (Chapter 3). The influence of the container was ignored in the simulations. Convective heat losses were considered to occur only at the top surface. However, to avoid excessive losses the heating time was kept short.

The strength of the incident electric field depends on the output power of the magnetron. Because of the difficulties in measuring the absolute field distributions, it was assumed to be based upon the declared power of the MW oven used (850W).

5.5.3 Results and Comparison

Figs. 5.20a,b shows that qualitatively, the temperature distributions in the test-load predicted by model are in good agreement with those obtained experimentally. The main features of the experimental results are apparent in the model predictions. Due to the internal reflections, temperatures near the base of the slab were higher than near the top surface. Temperatures at the surface are lowest due to the surface losses. Hot spots near the edges (around the periphery of the slab) were also evident. There was a slight asymmetry in the experimental results, which is due to the non uniformity of field distribution in the oven. The discrepancy between the experimental and numerical simulations increased with the heating time (Fig5.20b) due to various factors. The differences may be attributed to the following:

a) Uncertainties associated with the experimental setup and in the measurement procedure.
b) The assumption of the plane waves (TEM) in the numerical

simulations, whereas the field distribution in a cavity depends on all the existing modes in three dimensions.

c) Approximations used in the calculations for material properties and for the thermal boundary conditions.

d) Numerical errors inherent in the finite-difference method and computer round-off errors also contribute to the differences between the model and experimental results.

5.6. CONCLUSIONS

The model presented aids the understanding of the power distributions achieved in foods of various compositions subjected to microwaves. It augments the predictions of the general purpose model (which is only valid for limited cases). In particular, the wave like nature of microwaves was considered in this model (i.e. reflection and transmission at the interfaces between the material's surface and air and between the adjacent layers of different permittivities). Thereby, the accuracy of the temperature predictions is increased.

Generally, in microwave ovens due to mode-stirrers and rotating tables there is approximate symmetry in the power distribution achieved in the horizontal plane (and hence in the temperature distribution) (Fig.5.5 & 5.6). However, a number of factors (cavity dimensions, location of the waveguide, material of the cavity walls) cause asymmetry in the power distribution in ovens (and loads), and no two ovens have similar power distribution patterns. The presented one-dimensional model is adequate for evaluating the effect of various parameters (material properties, boundary conditions, incidence angle) on the power distribution and thus the temperature distribution in a material. The presented two-dimensional model provided qualitatively accurate temperature profiles for the slab like loads heated in microwave ovens.

CHAPTER 6

6. FOOD MODELS

6.1 INTRODUCTION

The optimization of any food processing operation requires a thorough understanding of the food's structure and behaviour throughout the process. In practice, a heating process leads to irreversible changes in the food, i.e. in its texture and its chemical composition. The performance of any food-heating equipment is assessed by these changes in order to achieve a product of desired culinary quality. During development, experiments employing actual foods are the conventional option, but this may be expensive particularly when protein-rich foods (e.g. meat) are used as foodstuffs can only be used once. Furthermore, reproducibility is often poor with real foods.

Cooking efficiency and performance are the important test parameters for microwave ovens. Therefore, the testing of MW ovens involves employing methods which replicate as closely as feasible the actual functions expected of the oven during its useful life. However, real foods are inherently variable in their initial composition and morphology (e.g. the amount and distribution of fat in meats, particle size and moisture content in granular systems). Similarly although numerical modelling provides a useful insight into the fundamentals of a new food product during the design stage, experiments are essential to obtain actual quantitative as well as qualitative data. Ideally, the two procedures should compliment one another in a design exercise.

To measure the output power of a MW oven, water loads have been widely employed so far. Gelatin, egg-white, mince, mashed-potatoes etc. are used to obtain the power distribution in the oven, to identify the "hot" and "cold" regions in a cavity and to determine the performance of the oven.

In this chapter, replacement synthetic materials which have similar heating characteristics to those of food materials and which may be used as test loads to provide the required performance parameters for an oven were investigated. Experiments were conducted to compare the heating characteristics of a synthetic material with the heating characteristics of various food materials. The primary aim was to assess the suitability of hydrophilic materials as a food simulator, which may be used as a test material for assessing microwave ovens and hence assist in the process of improving their performance. The most important requirement is that the test-results should correlate with the results obtained when the appliance is used for its intended purpose. At present the accepted test methods employ procedures involving different food materials. The use of a simulator test-material which can be prepared easily to a certain specification would therefore result in one less variable in the test methods. Food simulators can also provide information relating to real food heating behaviour during a microwave process which would result in a better quality product judged by consumer appeal.

Synthetic food models may become suitable for heating experiments, and for providing standard test-loads for testing microwave ovens, because;

i) they can be prepared in a definite prescribed manner; and
ii) they can be kept for long periods and so the allowing use of a batch testing system is feasible.

In addition to these attributes, this study also aimed to find a suitable replacement material which can be *re-used*.

6.2. PREVIEW

6.2.1. Performance Standards

There are three main aspects of microwave oven tests:

a. Output power measurement
b. Microwave energy distribution
c. Heating/cooking performance of foods

The following section summarises the recommended methods of testing and measuring the performance and output power of MW ovens by IEC705(1988) and BS 3999 (Part 15 & Technical committee LEL/94/8)

a) Measuring Output Power

Power output measurements are made by heating a known volume of water for a given period of time. Variations in the methods involve load in one container or in a array of containers The calculation is straightforward: the power output in watts is

$$P = \frac{V \rho C_p (\Delta T)}{t} \qquad (6.1)$$

BS 3999 and IEC 705 recommend slightly different procedures. The BS 3999 method requires four measurements using loads of:

1. 275 cc $\pm$1%
2. 500 cc $\pm$1%
3. 1000 cc $\pm$1%
4. 2000 cc $\pm$1%

of distilled water (containing 1% of NaCl by weight) at an initial temperature of 20$\pm$5° C. The duration of the test is until the mean temperature of the load has risen by $\approx$5°C. The average power output of the oven is determined by calculating the simple average of the tests using the four loads. Cylindrical glass containers of 85-110mm inner diameter are used for the tests. For the 2000cc load, two containers of 110mm diameter (each filled with 1000cc of water) are used. The containers are positioned side-to-side in the middle of the oven-shelf.

The IEC method uses a load of 1000±5g of potable water initially at 10±2°C. This is heated for a period t, until a mean temperature rise of about 10°C is achieved. A cylindrical borosilicate glass container (outer diameter approximately 190mm and maximum thickness 3mm) is used.

Both of these methods, as well as the American Standards did not take account of the thermal mass of the container. Japanese Industrial Standards recommended the use of 2000cc of water and utilise a procedure which eliminates the thermal mass of container. The latter obviously gives rise to a higher value for the output power of any given MW oven.

b & c) Microwave Energy Distribution and Cooking Performance for Foods

IEC 705 describes test procedures using single or multiple beaker water loads to obtain heating uniformity data. To complement these there are test-procedures involving real foods (e.g. mince, egg custard, cake) which evaluate cooking performance in terms of three factors: speed, cooking results and convenience. Several methods have been reported for measuring the energy distribution in a MW oven; these employ foods (e.g. egg-white), non-food materials (e.g. asbestos paper or silica gel) [Ohlsson, 1981] and purpose-built transducers [Kashiwa et al 1991].

6.2.2. Output Power

A series of tests was performed to determine the effects of factors such as the load size, material's properties, the shape of the container and the initial temperature on the output power of a microwave oven. The test oven was connected to a stabilised 240V power supply. The standard test condition was to heat a 500cc water load in a pyrex beaker of size 750cc initially at 20±2°C, through 5°C (as per BS 3999). This small ΔT was chosen to reduce the significance of heat losses. All times were measured using a stopwatch. The water was stirred after the heating period and the average temperature was noted. Each test was repeated three times and the average of the final temperature measurements was used in calculations.

Each variable was changed to identify its effect on the measured power (see Table 6.1). The lower the initial temperature of the load, the higher the measured output power (Table 6.1). This demonstrates the decreasing absorption of microwave energy as temperature rises (due to a decrease in dielectric loss of water at high temperatures (Chapter 3.). The containers for evaluating the shape effects were chosen from those commonly available as one litre size containers. These seemed appropriate for determining the power that a food would couple if placed in these containers. The influence of the shape of a container and the volume of a test load on the measured output power of the oven is clear (see Table 6.1). A water load placed in a rectangular container coupled less power than when it occupies a cylindrical one, due to the wasted power in edge-heating of rectangular loads (see Chapter 5). The measured output power is different for the loads in the containers of different materials due to the different thermal properties of the container materials.

Similar measurements were taken using vegetable oil ($\alpha \approx 2m^{-1}$) and the power coupling characteristics compared with those obtained by using water loads($\alpha \approx 40m^{-1}$)-see Fig.6.1a. The variation in coupling coefficients (kv) with the load volume and dielectric properties of the material is illustrated in Fig.6.1b. These curves are oven-specific due to variations in foods and ovens, which is why Mudgett [1990] suggested that such calibration curves for ovens should be supplied in the operating manuals. Thus, the individual oven's food-size coupling characteristics become more important than its maximum output power. These discrepancies in the declared power of the oven and the power coupled by a load pose difficulties for food manufacturers, when designing standard heating instructions for microwavable food products as well as for the user who experiments with different recipes. The standards are continuously under development to seek further improvements in performance criteria for each category of microwave ovens, through participation of appropriate international standard organisations [Andrews, 1992].

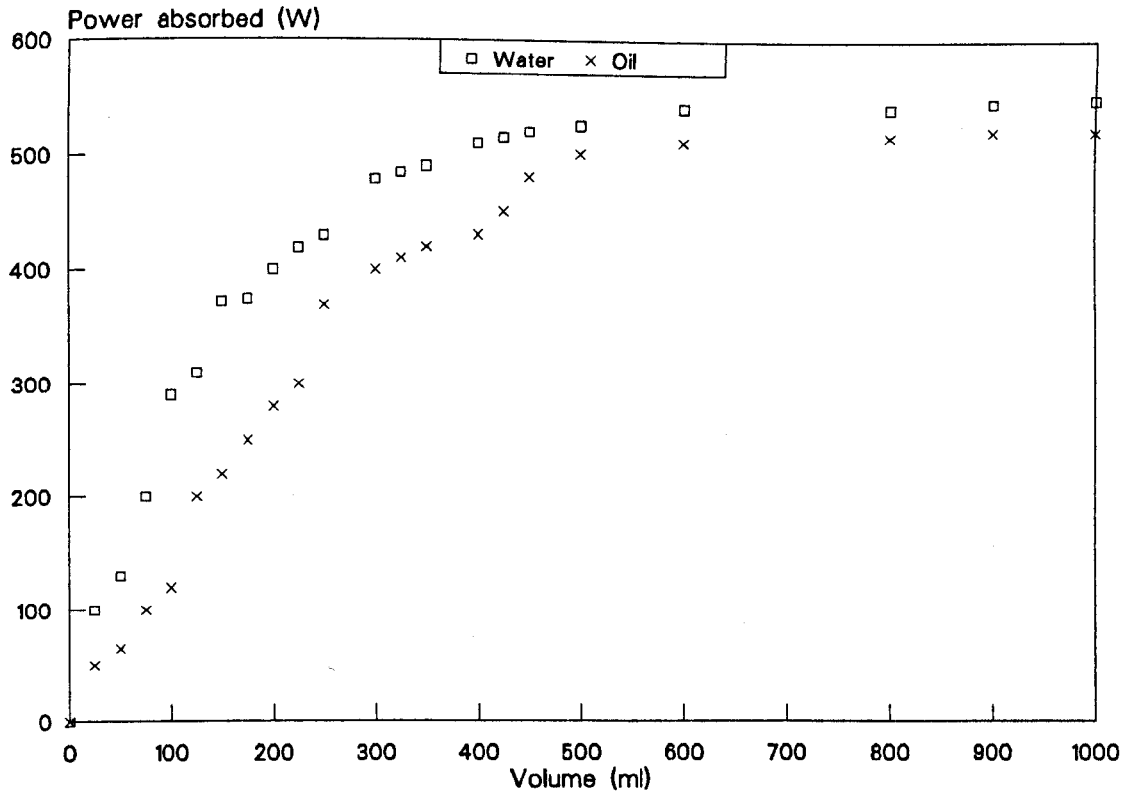

Fig.6.1a Variation of power absorbed by a load with the volume of load and dielectric properties of the material (for a 500W domestic oven)

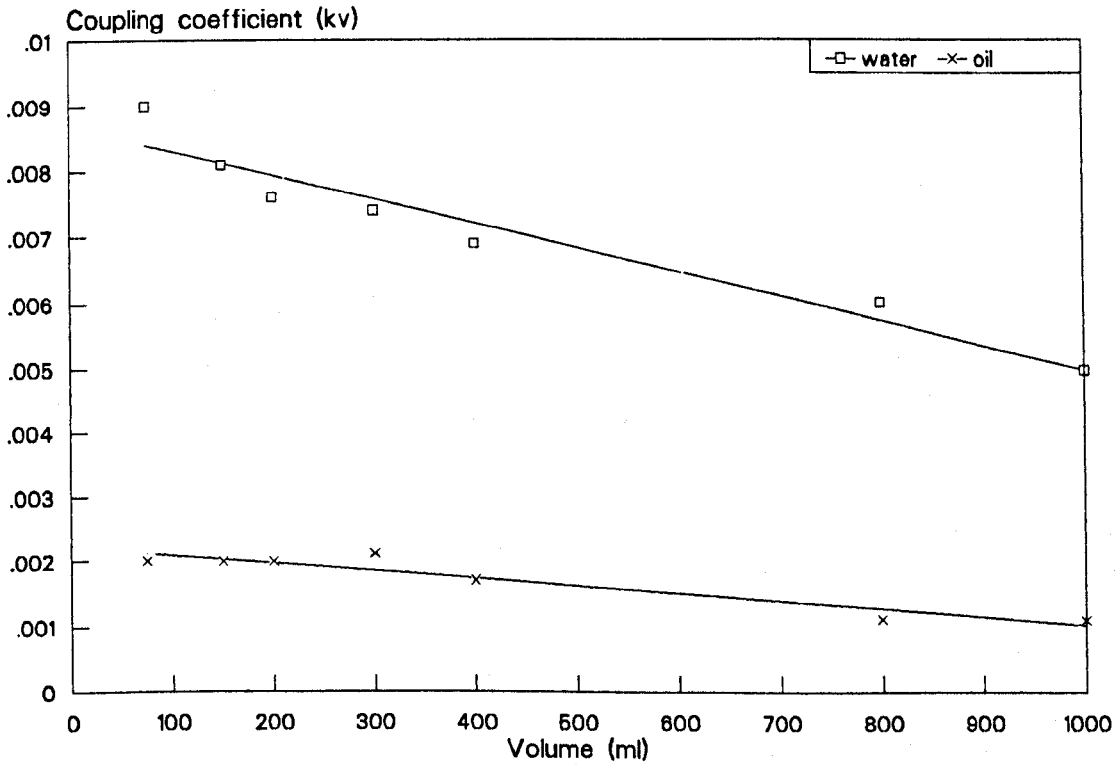

Fig.6.1b Variation of coupling coefficient (kv) with dielectric proerties and load volume for oven in Fig.6.1a
water (α=40m^{-1}); oil (α=2m^{-1})

Table 6.1

Output power of test MW oven (declared power; 500W) measured using a 500ml water load (T_i=20+2°C) in a pyrex beaker unless stated otherwise

Test Variable	Measured power (Watts)
(A) Initial temperature of load °C	
5	509
10	491
15	489
20	483
(B) Volume of water load ml	
100	343
150	373
200	416
500	483
1000	527
(C) Type of the container	
i) Cylindrical (pyrex)	484
ii) Cylindrical (plastic)	500
iii) Rectangular (plastic)	478
(D) Preheat period (due to magnetron heating)	
i) none	483
ii) 5min	469
(E) IEC method	530

6.2.3 Practical Complexities

It is difficult to standardise oven test-methods due to the wide variations in food properties and in the geometry/size of food containers and oven cavities. However, a new voluntary labelling scheme for ovens and food packs, developed by MAFF in partnership with oven and food manufacturers, has been introduced in 1992. New ovens sold after September 1992 are rated for output power according to the test procedure given in the international standard IEC 705. The associated new labelling scheme also describes the power delivered by an oven to a small food load in terms of a letter descriptor ranging from "A" to "E" (Table 6.2). Precooked ready meals also carry the required heating/cooking times depending upon a similar categorization. The introduction of a smaller test load (350g) measurement allows the food manufacturer and oven user to more accurately define the heating time. The values of output power as per new labelling scheme for different ovens are listed in a guide-booklet by MAFF [1992].

However, a recent survey by the Consumers' Association [1993] reports that even this new labelling scheme does not provide sufficient information concerning the required heating times for various loads to a typical oven user. The delivered power during actual use of the appliance is also affected by the line voltage variations and the length of cooking time due to changes in the output of magnetron.

An example of the new labelling scheme for output power, letter D *is the "heating category" as per Table 6.2*

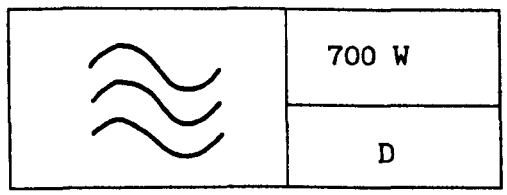

Table 6.2

Heating Category	Power output for a 350g water load (W)
A	500-560
B	561-620
C	621-680
D	681-740
E	741-800

6.2.4. Synthetic Food models

Bentonite-water dispersions have been used as food models in catering energy research, largely in order to reduce the costs of testing with real foods. Energy consumptions for processing frozen protein-rich foods (steaks, sausages, patties) in infra-red ovens [Unklesaby et al, 1980] and in forced-convection electric ovens [Unklesaby et al, 1981] were measured using bentonite. Energy consumptions during these simulations were similar to those for real foods. In another study [Yamano et al,1975] the thermal diffusivity of a 40% dispersion of bentonite was found to be similar to the published values for meat and fish. Different properties can be achieved by adding water into the bentonite clay or vice versa. When water is added to bentonite, a dough-like consistency is achieved, but when bentonite is added to water, it breaks up and settles, and the mixture has completely different properties.

Badary Narayana and Krishna Murthy [1976, 1978] used food models consisting of agar, sugar, soluble starch and water to study the effect of moisture, sugar and starch content on the thermal properties of food products. Various studies have been reported using food models for the estimation of thermal and dielectric properties. For example, Larkin et al [1987] used Kelset (commercially available gum containing sodium-calcium alginate) for measuring thermal diffusivity of foods and

Mudgett et al [1974] predicted the dielectric behaviour of non-fat milk by using aqueous ionic solutions of various inorganic salts. The food models based on agar gels have been used to simulate microwave heating [Swami et al, 1982]. Other materials such as a "phantom model" consisting of a water based mixture of polyethylene powder and a binding agent [Guy et al 1968] and polyacrylamide gels [Andreuccetti et al, 1988] have been used to simulate human tissue in diathermy applications. Ohlsson and Bengtsson [1971] found good agreement in microwave heating characteristics for beef and the simulated meat material introduced by Guy et al [1968]. Ohlsson and Risman [1978] later used this material with some modifications to simulate the temperature distribution in spherical and cylindrical food samples. Brugioni [1991] found reasonably good agreement between the heating characteristics of various hydrophilic materials (i.e. bentonite, polyacrylamide and hydrogels) with selected food materials heated in a conventional electric oven.

6.3 MATERIALS AND METHODS

6.3.1. Characterisation of Real Food Behaviour

A wide range of food materials are heated/cooked by microwave ovens. IEC705 recommends tests for assessing heating/cooking uniformity with the standard recipes for egg-custard, cake and meat-loaf. Mashed potatoes have also been used by several researchers to test the uniformity and reproducibility of MW ovens as well as the heating of ready meals [Burfoot and Foster, 1989]. However, for this study, foods are classified coarsely on the basis of following main properties

a) moisture content: e.g. foods with m>60% are classified as high moisture content and foods with m<40% as low moisture content.
b) homogeneity: a distinction is made with respect to texture/structure, (e.g.sponge cakes and mashed potatoes are considered as quasi-homogeneous and fruit cake and apple pie as heterogeneous foods).

There are other characteristics which may be employed to differentiate food products. For instance, foods with a continuous phase (e.g. apple sauce, milk) and others which are discontinuous (e.g. mince, rice) while some foods may also be characterised by significant volumetric changes during cooking (e.g. meat, cake, bread). Open-cell type structures offer path-ways for vapour movement (i.e. a high vapour permeability or connectivity) and dry quickly (e.g. sponge cake and leavened bread), whereas dense connected-cell type structures inhibit vapour movement (e.g. fruit cake and rye bread).

For the purpose of the present investigation, the choice was made based on the materials recommended in IEC705

i) High moisture content (m >70%) and homogeneous: most vegetables and fruits represent this class of foods; the materials selected were mashed apple and grated carrots.

ii) Low moisture content (m <40%) and homogeneous: the selected material was cake as IEC705 proposes this for evaluating the heating (baking) uniformity of a thick expanding food.

iii) High moisture (m >60%) discontinuous: the material selected was minced beef; IEC705 also proposes minced beef for evaluating the cooking uniformity of a brick shaped food.

6.3.2 Characterisation of Hydrogel Material

In this study hydrophilic polymeric gels, also known as hydrogels (see Fig. 6.2 & Appendix 11) originally designed in the manufacturing of soft contact lenses are proposed as food models. The material is clear and brittle in a dry state, but it has a property of absorbing water to a degree which can be accurately determined during the production of the polymer (water uptake). Thus hydrogels can be manufactured to

provide specific moisture contents which are similar to those for the aforementioned foods. Each hydrophilic material is able to absorb a given quantity of water by weight at a given temperature. The water held in the hydrophilic polymer is present as bound and free water (However here "bound and free" water do not have same meaning as these terms have for ionic solutions in Chap 3. Also the influence of "bound and free" water in hydrophilic systems on dielectric properties is not yet known)

a) bound water, which is the water absorbed by water-attracting centres within the polymer. This readily penetrates at the early stage of the hydration and consequently is the most difficult to remove. It represents about 40% of the equilibrium water content.

b) free water, which is the unattached water content that occupies the free spaces around the polymer molecules. It easily enters or moves out of the hydrated material. This is a part of the equilibrium water content which takes part in osmotic reactions.

The ratio of free-to-bound water in a fully hydrated hydrophilic material is related to the water content at full hydration [Highgate, 1989]. The proportion of free water rises as the equilibrium water content is increased (see Fig 6.3). If the hydrophilic polymer is granular then in the hydrated test sample, some water may be trapped in the spaces between the particles (Fig. 6.4) which may be referred to as "loose water" and is difficult to estimate. If there is loose water present, the sample is not perfectly reproducible. The porosity of a sample, and therefore the amount of loose water varies, although the amount of water that a hydrogel material is able to absorb is clearly defined at a given temperature and decreases with temperature (approximately 1% per $10^{o}C$). Therefore, particle size can be controlled if necessary to more accurately reproduce the properties of the material.

To determine which food each hydrogel material may simulate it was necessary to draw a reference line depending upon the heating characteristics of the tested foods. The primary criterion was the

moisture content due to the lack of thermal and dielectric property data for hydrogel materials. However, the hydrogel material's properties may be calculated approximately from the properties of water, depending on the material's water content and the solid matrix. The water losses due to heating were also taken into consideration, because of the form in which water may exist within the material. The ratio of free to bound water determines the quantity of water removed. Therefore even if the water content is similar for a food and a hydrophilic material, the water loss may be different. The amount of free and bound water also affects the dielectric properties and thereby the absorbed power (Chapter 3).

Preliminary tests were undertaken with hydrophilic materials and selected food materials to identify any similarities in their heating characteristics. Once the similarity between a food and a hydrogel material was known, a decision was made with respect to the latter's suitability as a food simulator. If considered to be a good candidate, the IEC test procedure was followed and the results compared with those obtained from the real foods.

6.4 EXPERIMENTAL PROGRAMME

6.4.1 Preparation of the Sample

a) Apple/carrot

The cooking apples were peeled, cut into pieces and then mashed for 3 minutes in a food mixer with a flat-blade attached. The carrots were peeled and grated using a food mixer with a grating blade attached. Five ≈900g portions of each material were produced so that the tests could be repeated five times. The microwavable plastic trays (190mm x 130mm x 50mm) were filled with sample material to a depth of 30±2mm and levelled using a perspex template. For each test the weight of the tray before and after filling was noted. The trays were covered with cling film and left for a minimum of 6 hours in the refrigerator at about 4°C.

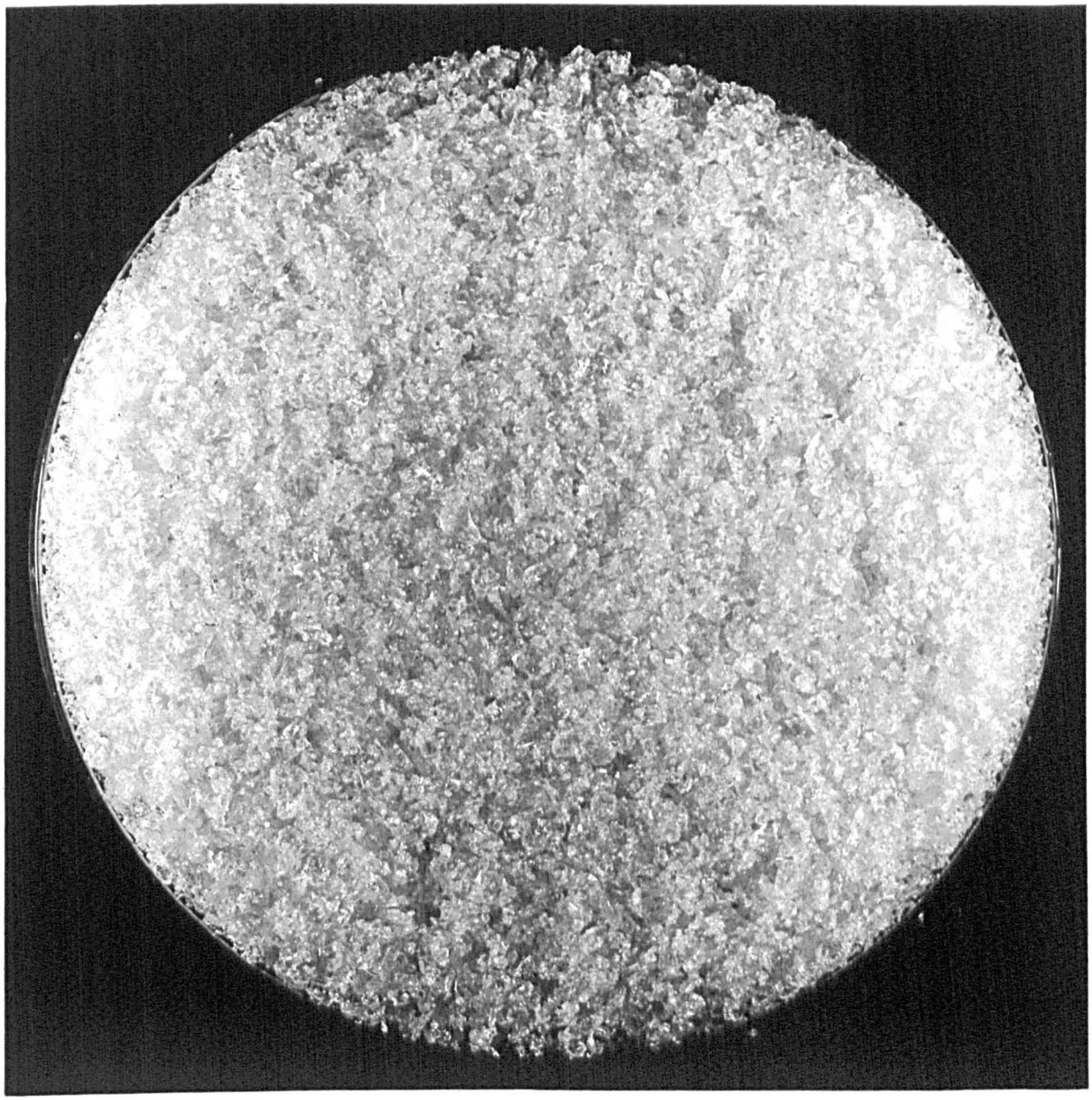

Fig.6.2 Hydrophillic polymeric material (m = 70%)

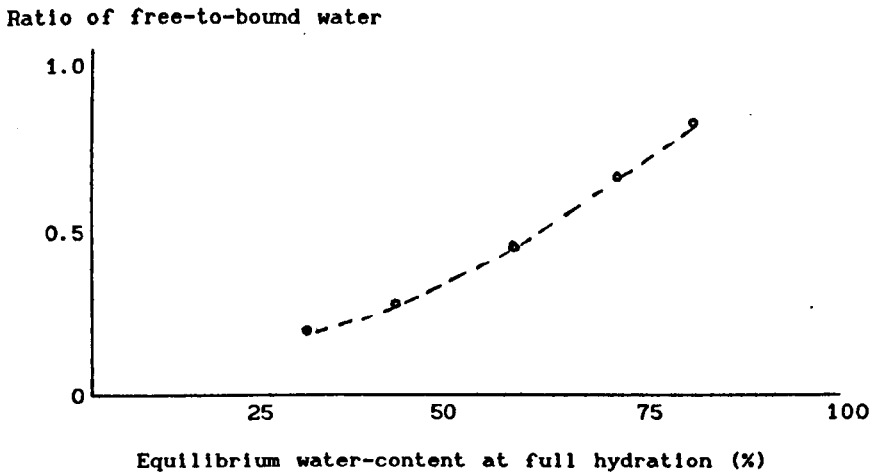

Fig.6.3 Free-to-bound water characteristic of a hydrophilic polymeric structure [Highgate et al,1989]

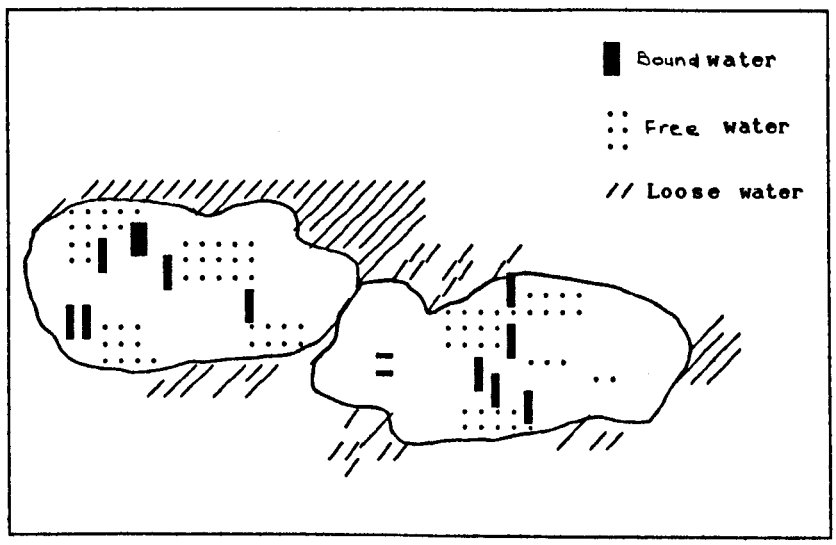

Fig.6.4 Water containment in a hydrophilic structure

b) Minced Beef

Frozen minced lean beef (fat content ≈ 15%), the type readily available from superstores, was used for the tests. The material was defrosted at room temperature and then the above procedure was followed to prepare five samples.

c) Cake

The cake batter was prepared to the recipe given in IEC705. The mixture was poured in the trays which were lined with grease proof paper, to a depth of 28±2mm. The initial temperature of the mix was 20±2°C. The standing time for the mixture prior to cooking was ≈10minutes.

d) Hydrophilic Material

Hydrophilic materials of 40% and 75% of equilibrium water uptake (hereafter referred to as water content; m) were chosen. To obtain a relationship, if any, between the particle size and rate of heating and moisture loss, the 75% hydrogel was sieved to separate the material into particle sizes of 0.1-1mm and 1-2mm. The exact amount of water required to fully hydrate the type of polymer under test was poured over the dry sample and mixed thoroughly. The wet sample was stored in a tightly closed polyethylene container which was placed in a refrigerator (≈4°C) overnight to allow the water to fully penetrate in to the material. The hydrated material was mixed again, poured into similar plastic trays and placed under the same conditions as the samples of real food. The initial temperature and the heating period for the 40% hydrogel were adjusted to those applying for the cake. Before cooking, the hydrophilic materials were wet, soft, spongy and transparent (see Fig. 6.2).

6.4.2 Test Oven

One of the common brand domestic microwave ovens (IEC power 850W E) was used for the tests. The oven was a typical multi-mode design operating at 2450MHz, with a metallic interior and a glass turntable. The cavity dimensions were; 330mm x 227mm x 335mm (W x H x D).

6.4.3 Temperature Measurement

Few techniques are available for measuring food temperatures during microwave heating. Fibre-optic thermometry is one solution for real-time measurements. Infra-red imaging is another method which provides surface-only measurements. In the microwave oven, the top surface of a product cannot be easily viewed perpendicularly by the scanner. This can make the viewing angle unacceptably acute and limits thermal measurements until after heating and removal from the oven. The technique has been modified recently to permit continuous temperature measurement in a MW cavity [Goedeken et al, 1991]. These systems are expensive (e.g. in 1993, a single-channel fibre-optic systems cost around £6000 while infra-red imaging systems cost from £15,000-£80,000. Specially designed thermocouples may be employed for continuous temperature monitoring by inserting them in to the cavity [van de Voort et al, 1987; Taoukis et al, 1987].

Alternatively, a "hedgehog" arrangement of thermocouples (see Fig.6.5) may be used to obtain the temperature measurements at the desired locations in the sample immediately after a given heating period. This should provide reasonably accurate information regarding the temperature distribution in a food-sample provided that the measurements are carried out quickly so as to minimise the effects of heat loss and thermal conduction. Thermocouples were used to assess the heating rates and the mean temperature of the material and this intermittent monitoring method was found to produce results similar to those obtained by a continuous method [Kudra et al; 1993]. However, usually a certain standing-period, to even out the temperature distribution, is recommended for heating ready-meals in a MW oven. Therefore, thermocouples at several locations can be used as a cheap means for obtaining the temperature history in a sample heated in a MW oven. The lower cost also encourage their use at more locations within the sample.

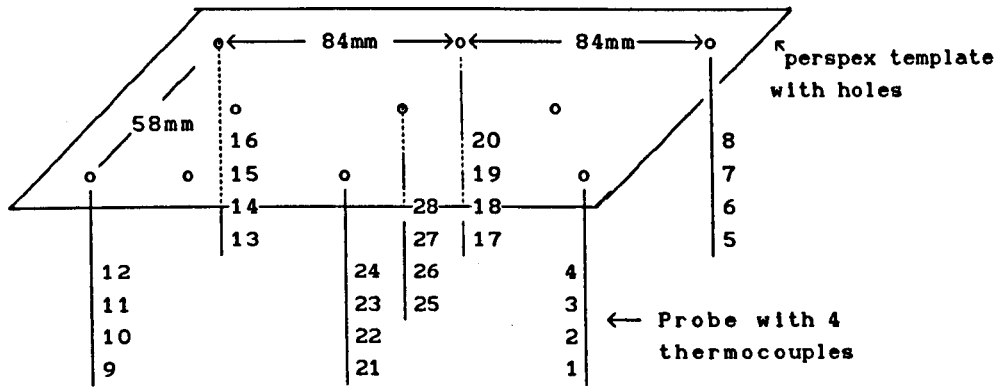

Fig.6.5a Labelling scheme for thermocouples

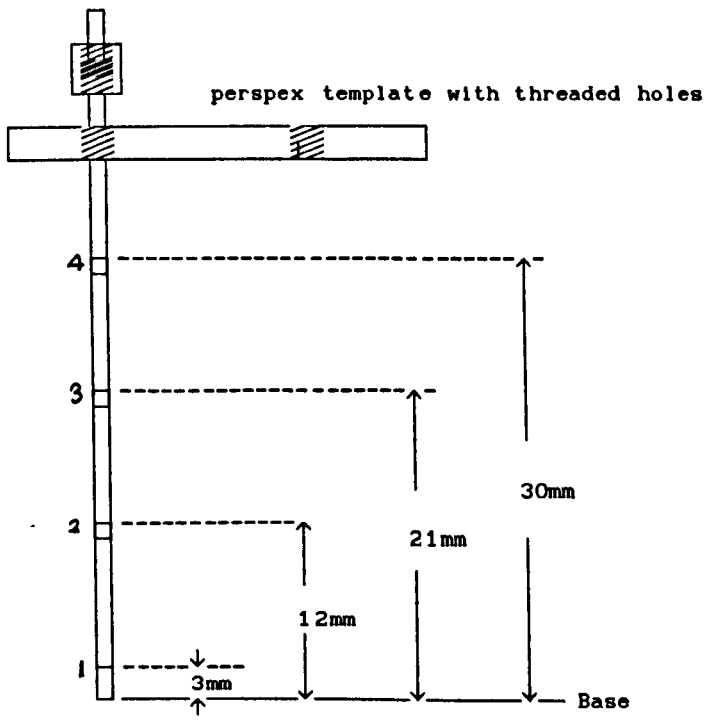

Fig.6.5b Arrangement of thermocouples on a probe

In this investigation, seven probes consisting of four (type T) thermocouples specifically designed for this purpose were used. The probes could be located as desired by a Perspex template sheet with appropriately positioned holes (see Fig 6.5a,b). The height of the probes could be adjusted by means of small screws to achieve the required thermocouples positions. Thermocouples were connected to a computer controlled data logging system [Biodata, 1992] and temperatures were recorded at 5s intervals commencing ≈10s after completion of the heating period. The 10s period prior to measurement was needed for removing the tray from the oven and inserting the probes. The maximum temperature recorded at each location within the sample was used to produce graphical output of the measured temperatures. Transient temperature profiles at the centre and at the corners were also produced. The thermocouples were calibrated by comparing them with precision mercury-in-glass thermometer, at the boiling and the melting points of water. The error never exceeded 0.5°C. However, it was noted that the agreement when measuring the melting point of ice was more accurate than for the boiling state of water.

6.4.4. Other Measurements

The accuracy of using thermocouples to determine the post-irradiation temperature distribution was calculated. A sample of hydrogel (m=75%, 0.1-1mm particle size) was prepared and heated in a microwave oven for 10 minutes. The temperatures in the centre and corners were measured as ≈70°C and ≈94°C respectively. Another sample similar to the previous sample was placed in a water bath operating at ≈94°C to heat it to an equilibrium temperature. Then it was removed from the water bath and its temperature was measured using the thermocouple array. The measured temperatures were compared with the equilibrium temperature to determine the errors incurred when using the thermocouples. It should also be remembered that in practice there is usually a time delay of at least 2-3min between heating and consumption of a food item. Thus the temperature distribution in a food sample after the actual heating period has more significance from the user's view point.

Each time the test load was weighed just prior to heating and weighed again after removal from the oven. The trays were filled to the predetermined level, so that the initial volume (and thereby the apparent density) of the sample could be calculated. The height after heating was noted and the final volume was calculated by assuming that the top surface remained flat. This was a valid assumption except for cake and mince, which underwent significant expansion and shrinkage respectively. In this case the final volume was measured by the seed displacement method [McWilliams, 1989]. A container somewhat larger than the sample was used to measure the rape seeds required to fill the container level with and without the sample. Other subjective assessments such as shape, colour and dryness of crust were also made.

6.4.5 Heating Procedure

The oven was connected to a stabilised voltage supply (input voltage; 240±2V). The initial temperature of the sample was recorded and the tray was placed at the geometric centre of the turntable, the longer side of the tray being maintained parallel to the length of the oven. The oven was operated at its highest power setting for about 10 minutes (depending upon the material tested) to produce a temperature of ≥70°C at the geometric centre of the sample. The transient temperature profile during the heating period was assessed on an intermittent basis. This was done by heating the sample for 20s, followed by inserting thermocouples into the sample for 5s and repeating the sequence in order to obtain the heating response curve over a certain period. The heating time was measured using a stop-watch. The ambient temperature in the vicinity of the oven was also recorded, which was constant to 20±2°C throughout. Immediately after heating, the temperature probes were inserted into the tray for taking the final temperature measurements.

After each test, the probes and the perspex template were rinsed with water. The interior of the oven was also cleaned to remove any condensation and the door was left open so that the temperature of the

oven cavity could fall rapidly to that of the ambient temperature. After a 30 min delay, as specified by IEC705, the next test was undertaken. This procedure was adopted to eliminate any changes in performance that could otherwise be caused by large variations in the temperatures of the oven compartment and the magnetron. The preliminary tests with each material were repeated five times to assess reproducibility.

6.4.6 Performance Tests

Similar procedures to those above were followed when preparing the test samples (i.e. with respect to temperature measurements and the rest period between successive tests). However, the cooking process was not interrupted for recording the incremental temperatures. Only the final temperature distribution was recorded after the cooking period at 10s interval. These tests were repeated three times with each material. The following cooking performance tests were chosen (according with IEC705), in order to evaluate the cooking uniformity of:

a) a cylindrical, thick, expanding food, i.e. cake;
b) a thick brick-shaped food, i.e. minced beef; and
c) defrosting a thick food item, i.e. minced beef.

The test conditions for real foods (i.e. size and shape of test load, cooking time and power level) were adjusted according to the instructions in IEC705 in conjunction with the MW oven manufacturer's recommendations for achieving adequate results with similar materials. The following changes were made:

a) Cake and Hydrogel (m ≈40%)

The cylindrical microwavable plastic container of inner diameter (200±2mm), height (55±2mm) was used. The container was filled with cake batter to 25±2mm. The height of the hydrogel material was adjusted to achieve similar mass. The Cooking time was 8 minutes at full power plus a standing period of 5 minutes.

b) Beef Mince and Hydrogel (m ≈75%)

A similar test sample as before was adopted for these tests except the sample was cooked covered with a lid, in order to simulate normal practice. The heating period adopted for this test was 12 minutes at full power plus a standing period of 3 minutes. The same procedure was followed for the hydrogel material.

c) Sample for Defrosting Performance (minced beef and hydrogel; m 75%)

A plastic container (180mm x 90mm x 40mm) was lined with plastic film, and then packed with minced beef which was compacted using a flat template to eliminate air pockets and to level the top surface. The sample was left in a freezer (≈ -18°C) for at least 18 hours. Just before each test, a sample was removed from the freezer and turned onto a flat plate. The frozen block was defrosted using the defrost-feature provided by the oven manufacturer. Similar test loads of hydrogel were prepared and the same defrosting instructions were followed.

6.5 RESULTS AND DISCUSSION

It is very difficult to simulate the qualitative and quantitative aspects of the cooking of food materials by employing synthetic non-biological food models. However, there are some macro factors (such as heating rate, cross sectional and surface temperature distribution, the location of hot and cold spots, energy consumption, moisture loss and change in volume) which can be evaluated and compared. Such factors were obtained from the preliminary tests, and used to establish a relationship between the hydrogel material and real food materials. Several other aspects (e.g. expansion, shrinkage, the existence of a crust, drying, appearance and texture) were also recorded for comparison purposes.

6.5.1 Accuracy of Employing the Post-Heating Method

Clearly, the temperature recorded by employing thermocouples after the heating period is different to the actual temperature of the material at the end of heating, due to thermal conduction and surface heat losses during the measuring period. But the rate of cooling is small in the coolest region, where the local temperature rises due to conduction from the hotter regions. The mean difference between the measured and the control temperature (94°C) was ≈4.2°C but the maximum difference was at the surface (≈6°C), where local temperatures fell during the measuring period. The temperature at the geometric centre of the sample showed good agreement with the control temperature (i.e. a difference of ≈2.3°C). However, in actual tests the temperature profile after the heating period would not be uniform (as occurred in the sample heated to a uniform temperature) and therefore the redistribution of heat in the real case involves (i) surface heat loss and (ii) heat conduction along the temperature gradient. Nonetheless the comparison did give some measure of errors incurred in the post irradiation technique.

Errors (e.g. associated with the accurate positioning of thermocouples and response time), which are common to other temperature sensing systems may have occurred. Such errors are worse when large temperature gradients exist within the material, but for these tests the maximum temperatures were restricted to ≤100°C. The temperatures observed for the hydrogels and food materials were primarily for assessing the heating uniformity of the microwave oven, thus inherent error in the measuring technique (≈4°C) was considered acceptable.

6.5.2 Cooking Apples (m ≈ 75%)

The ten minute heating period resulted in a complete change of texture. The discontinuous phase of mashed apples was changed into continuous homogeneous apple sauce. During heating the material started boiling near the edges, splashed out of the container and developed a thick sauce like consistency. (see Fig 6.6). There was hardly any shrinkage noticeable around the edges, but the material did settle down by about 2mm (i.e. a volume reduction of about 3%, see Table 6.4).

Table 6.3 Water losses during cooking (cooking apple)

Test no.	Initial mass (g)	Final mass (g)	Moisture loss (g)	(%)	Rate of loss ($g\ min^{-1}$)
1	788.3	755.2	33.1	4.2	3.3
2	790.0	756.8	33.2	4.2	3.3
3	789.0	758.0	31.0	3.9	3.1
4	788.5	756.8	31.7	4.0	3.2
5	790.6	759.7	30.9	3.9	3.1
Mean	789.3	757.3	32.0	4.0	3.2
s.d.	0.9	1.0	0.1	0.1	0.1

Table 6.4 Average change in apparent density (cooking apple)

Initial Volume $10^{-4}.m^3$	Final Volume $10^{-4}.m^3$	Initial Density kgm^{-3}	Final Density kgm^{-3}	Volume Change %
8.64	8.38	912.9	903.7	-3.0

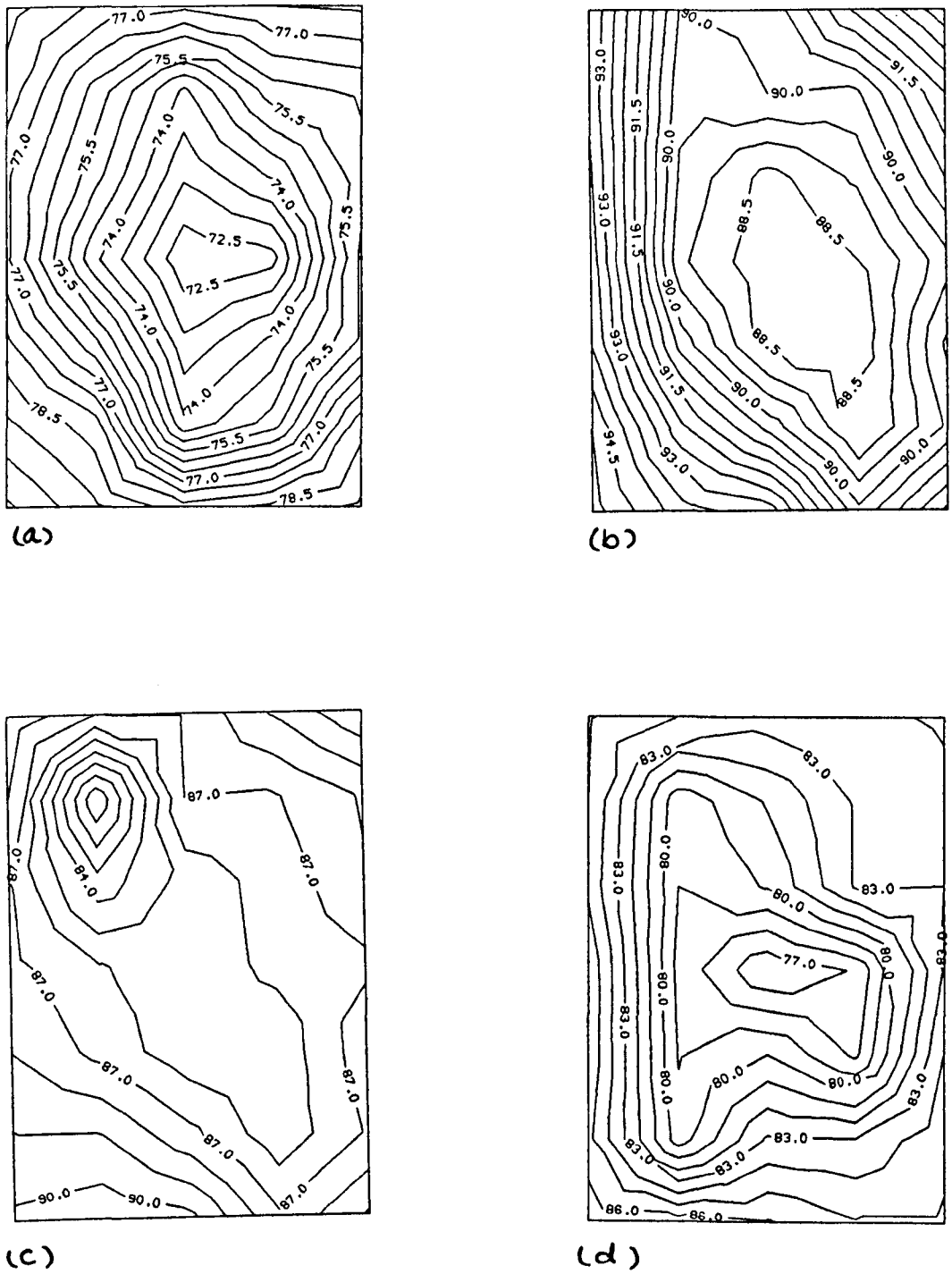

Fig.6.6 Temperature profiles for apples after heating at plane (a) 30mm; (b) 21mm; (c) 12mm; (d) 3mm from base

6.5.3 Carrots (m ≈ 87%)

After heating, the grated carrots were almost cooked. The colour was paler and the texture softer than that of the raw material. The temperatures around the edges were higher than the centre (see Fig. 6.7). The material shrank slightly near the edges, settling by 1-2mm (see Table 6.6)

Table 6.5 Moisture losses during cooking (carrots)

Test no.	Initial mass (g)	Final mass (g)	Moisture loss (g)	(%)	Rate of loss (g min^{-1})
1	650.1	612.2	37.9	5.8	3.8
2	650.5	611.9	38.6	5.9	3.9
3	650.6	609.1	41.5	6.3	4.1
4	651.2	610.7	40.5	6.2	4.0
5	648.3	607.3	41.0	6.3	4.1
Mean	649.7	609.8	39.9	6.1	4.0
s.d.	1.1	0.6	1.3	0.2	0.1

Table 6.6 Average Change in apparent density (carrots)

Initial Volume $10^{-4}.m^3$	Final Volume $10^{-4}.m^3$	Initial Density kgm^{-3}	Final Density kgm^{-3}	Volume Change ± %
8.65	8.3	751.6	746.4	-4.0

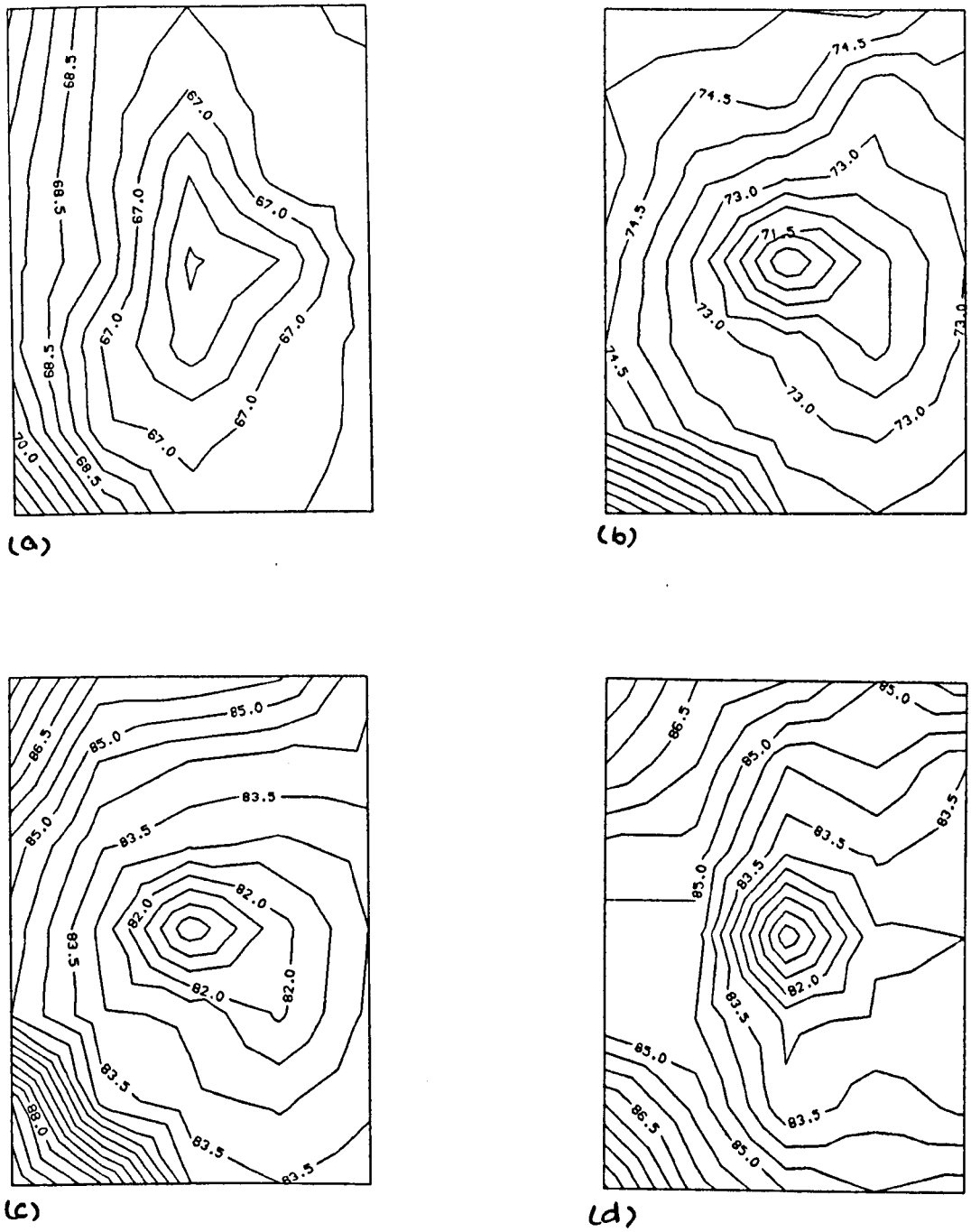

Fig.6.7 Temperature profiles for carrots after heating at plane (a) 30mm; (b) 21mm; (c) 12mm; (d) 3mm from base

6.5.4 Minced Beef

The cooked meat shrank mainly at the top around the edges of the container by 5-8mm. This represented the energy absorbed near the corners and around the edges, which is typical of such slab like loads. Fluids were expressed from the meat and resided at the base of the container upon completion of the test. About 20% of the material remained uncooked; this occupied the middle portion of the load, while the regions near the corners were over-cooked. Therefore the cooking period and power level to be used in the cooking performance tests were also determined by these trials. The preferred reference cooking period for a load of about 700gm was to heat the sample covered for 12 minutes at a power level of 850W.

Table 6.7 Moisture losses during cooking (mince)

Test no.	Initial mass (g)	Final mass (g)	Moisture loss (g)	(%)	Rate of loss (g min^{-1})
1	700.8	594.7	106.1	15.1	10.6
2	700.0	600.9	99.2	14.1	9.9
3	698.0	591.1	106.9	15.3	10.6
4	701.7	599.7	102.0	14.5	10.2
5	703.1	601.3	101.8	14.4	10.2
Mean	700.7	597.5	103.2	14.7	10.3
s.d.	1.7	4.0	2.9	.5	.3

Table 6.8 Average Change in apparent density (mince)

Initial Volume $10^{-4}.m^3$	Final Volume $10^{-4}.m^3$	Initial Density kgm^{-3}	Final Density kgm^{-3}	Volume Change ± %
8.65	7.58	810.0	788.3	-12.4

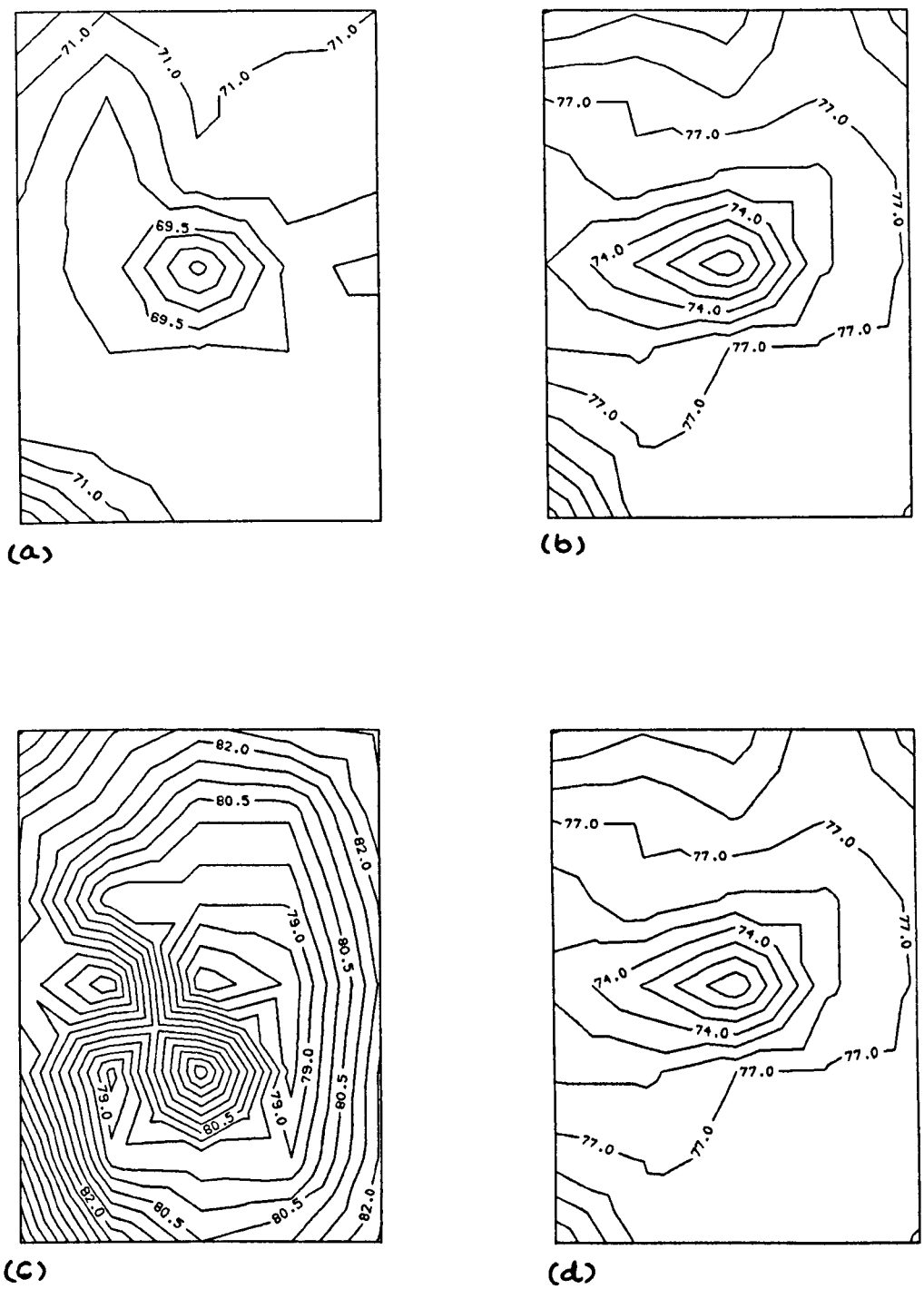

Fig.6.8 Temperature profiles for minced beef after heating at plane (a) 30mm; (b) 21mm; (c) 12mm; (d) 3mm from base

6.5.5 Cake

Cakes undergo remarkable changes during baking. The protein causes coagulation while starch is gelatinising and these reactions are responsible for permanent structural changes. In addition, moisture losses take place and the heat generates carbon dioxide to cause considerable expansion. After three trials the reference heating period to achieve an acceptable cooked product was found to be 8 minutes at a power level corresponding to 600W plus a standing period of 5 minutes. Because the temperature measurements were taken on an intermittent basis to obtain the heating rate of the sample, this caused interruption in the baking process. The end products achieved in the first two tests were of poor quality; the surfaces being flat and soggy. Therefore, the heating process was not interrupted for temperature measurements during the remaining three tests and two additional tests were performed. The results of these five tests were used to calculate moisture loss and the final temperature distribution.

Table 6.9 Moisture losses during cooking (cake)

Test no.	Initial mass (g)	Final mass (g)	Moisture loss (g)	(%)	Rate of loss (g_{min}^{-1})
1	549.7	509.4	40.3	7.3	6.7
2	548.5	508.5	40.0	7.3	6.6
3	547.0	507.5	39.5	7.2	6.6
4	550.1	510.2	39.9	7.2	6.7
5	549.0	509.9	39.1	7.1	6.5
Mean	548.9	509.1	39.8	7.2	6.6
s.d.	1.1	1.0	0.4	0.1	0.1

Table 6.10 Average Change in apparent density (cake)

Initial Volume $10^{-4}.m^3$	Final Volume $10^{-4}.m^3$	Initial Density kgm^{-3}	Final Density kgm^{-3}	Volume Change ±%
6.9	8.9	795.5	571.3	28.9

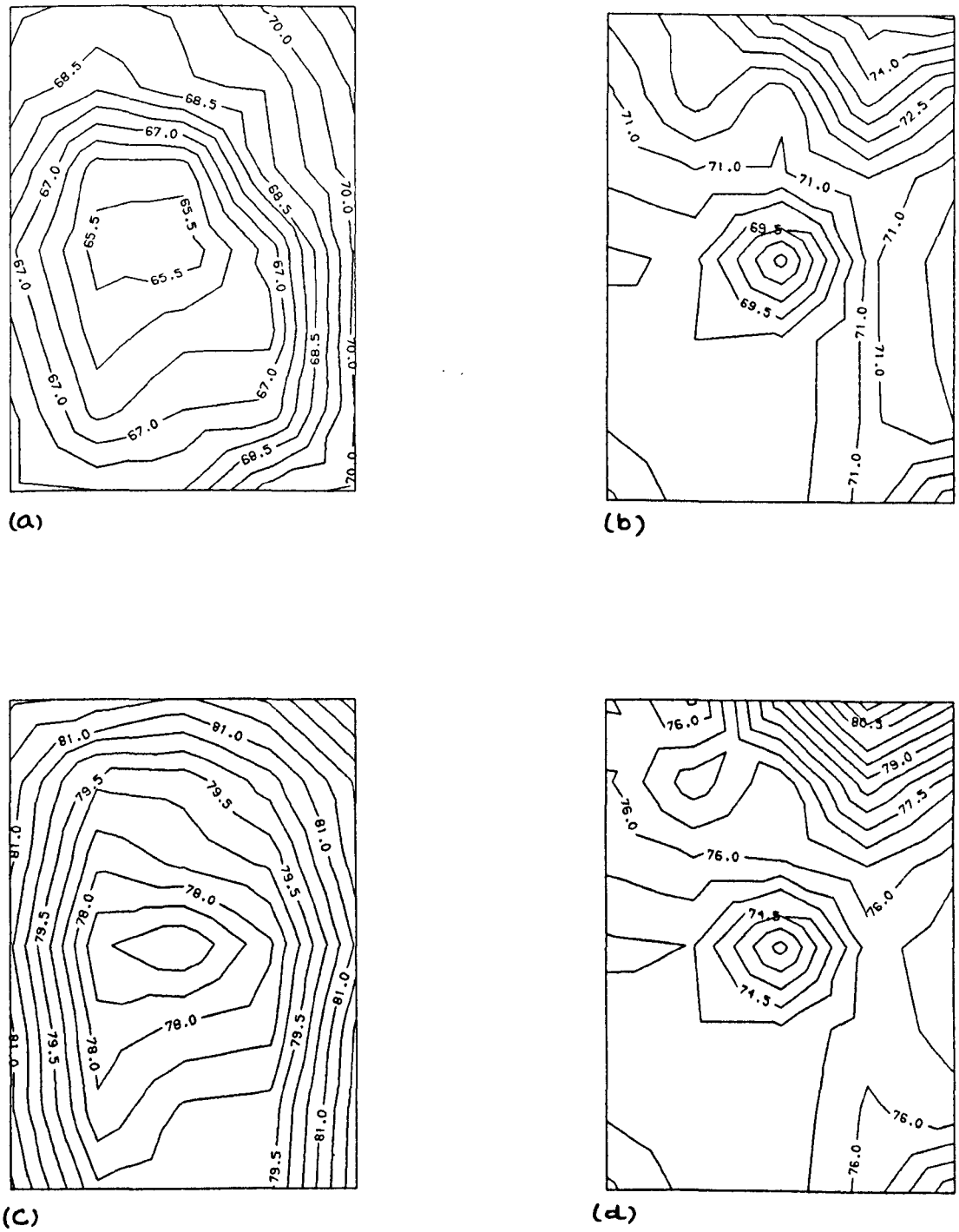

Fig.6.9 Temperature profiles for cake after heating at plane (a) 30mm; (b) 21mm; (c) 12mm; (d) 3mm from base

6.5.6 Hydrophilic Material (m = 75%)

Hydrogel mixtures with particle size of 0.1-1mm looked very much like apple sauce in texture and consistency, whereas the larger particle size (1-2mm) mixture looked like a very wet slurry. The free water molecules which occupy the spaces around the polymer molecules are relatively easy to remove, and so these moved through porous pathways upon heating. The rate of moisture removal by evaporation was not high enough to cope with the former phenomenon. Therefore after the heating period, the material appeared to be flooded with a clear water layer near the base of the container. Surprisingly, there was not much difference in the moisture loss for the materials with different particle sizes (see Tables 6.11 and 6.13), despite the increased porosity for larger particle sizes. This may be due to the very short heating period and the two rates may start diverging after a certain period. The effect of porosity on moisture loss should be investigated further in a convection oven where cooking times for foods are longer than those for microwave ovens.

Table 6.11

Moisture losses during cooking hydrogel; 75% (0.1-1mm)

Test no.	Initial mass (g)	Final mass (g)	Moisture loss (g)	(%)	Rate of loss (g min^{-1})
1	933.1	906.5	26.6	2.8	2.7
2	930.0	903.7	26.3	2.8	2.6
3	932.7	907.4	25.3	2.7	2.5
4	930.5	905.0	25.5	2.7	2.5
5	930.9	904.8	26.1	2.8	2.6
Mean	931.4	905.5	25.9	2.8	2.6
s.d	1.2	1.3	0.5	0.05	0.05

Table 6.12 Mean change in apparent density for hydrogel; 75% (0.1-1mm)

Initial Volume $10^{-4}.m^3$	Final Volume $10^{-4}.m^3$	Initial Density kgm^{-3}	Final Density kgm^{-3}	Volume Change ±%
8.65	8.4	1076.8	1077.9	-2.8

Table 6.13 Moisture losses during cooking hydrogel; 75% (1-2mm)

Test no.	Initial mass (g)	Final mass (g)	Moisture loss (g)	(%)	Rate of loss ($g\ min^{-1}$)
1	776.0	748.6	27.4	3.5	2.7
2	777.9	748.2	29.7	3.8	2.9
3	778.4	748.8	29.6	3.8	2.9
4	776.8	747.3	29.5	3.8	2.9
5	778.6	750.4	28.2	3.7	2.8
Mean	777.5	748.6	28.9	3.7	2.9
s.d.	1.2	1.0	0.9	0.1	0.1

Table 6.14 Mean Change in apparent density

Initial Volume $10^{-4}.m^3$	Final Volume $10^{-4}.m^3$	Initial Density kgm^{-3}	Final Density kgm^{-3}	Volume Change %
8.65	8.5	898.7	891.2	-1.7

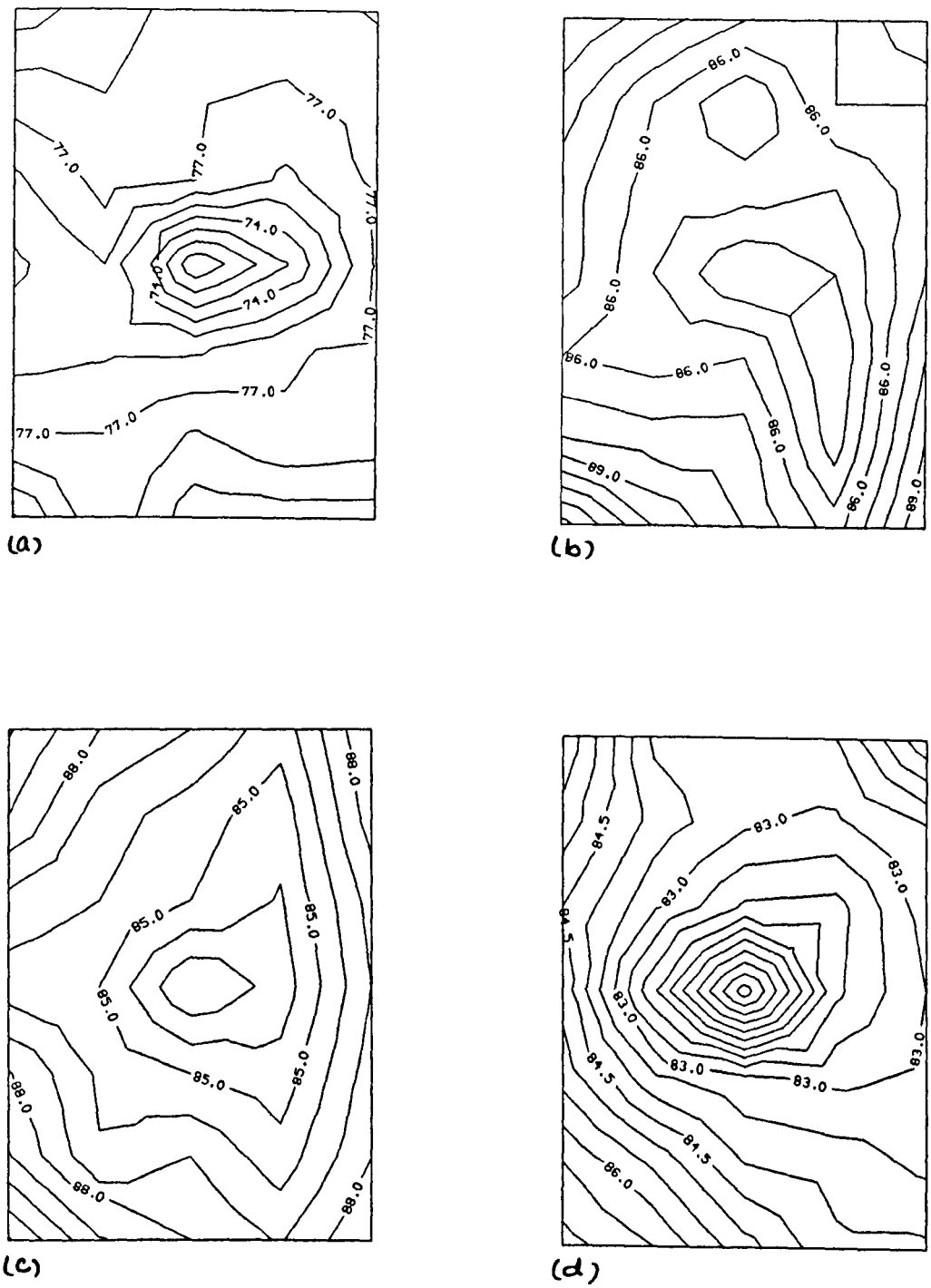

Fig.6.10 Temperature profiles for hydrogel (m=75%; 0.1-1mm) after heating at plane; (a) 30mm; (b) 21mm; (c) 12mm; (d) 3mm from base

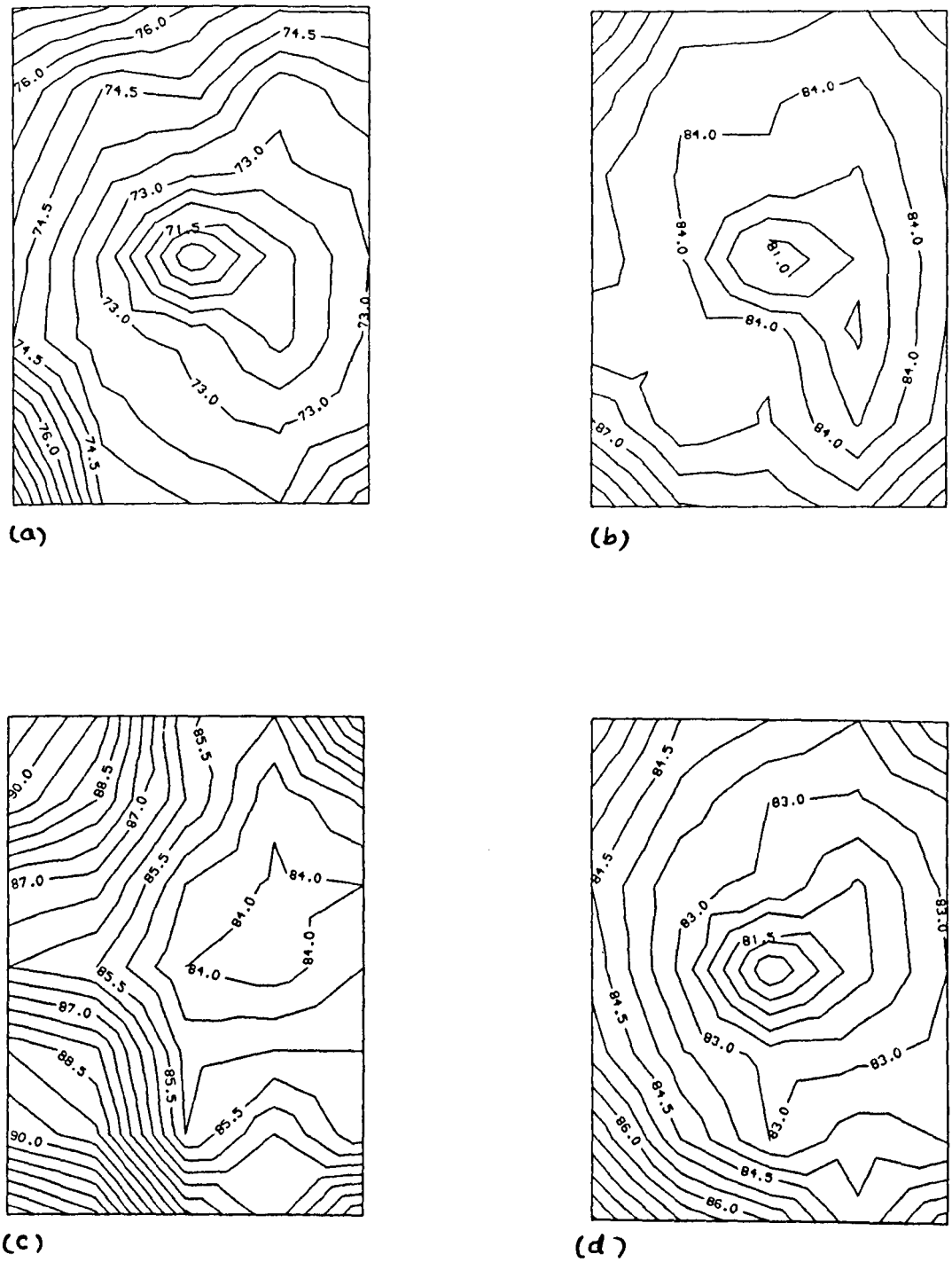

Fig.6.11 Temperature profiles for hydrogel (m=75%; 1-2mm) after heating at plane; (a) 30mm; (b) 21mm; (c) 12mm; (d) 3mm from base

6.5.7 Hydrophilic Material (m = 40%)

The hydrogel with a moisture content of 40% was considered as a feasible simulator for food materials of similar water content (e.g. cake batter, bread/pizza dough), although its appearance was very different to these materials. On hydration the hydrogel was spongy and rubber like. Also, unlike food materials, no significant change took place in its volume on heating. The material dried around the periphery of the container which was due to the relatively high absorption of energy of in this region. Also, the top surface was drier than the inner layers which became somewhat sticky due to partial drying.

Table 6.15 Moisture losses during cooking hydrogel (40%)

Test no.	Initial mass (g)	Final mass (g)	Moisture loss (g)	(%)	Rate of loss (g min^{-1})
1	550.1	491.8	58.3	10.6	5.8
2	551.5	495.8	55.7	10.1	5.6
3	552.1	492.5	59.6	10.8	5.9
4	553.1	494.5	58.6	10.6	5.8
5	552.8	494.8	58.0	10.5	5.8
Mean	552.0	493.8	58.0	10.5	5.8
s.d.	1.0	1.5	1.3	0.1	0.1

Table 6.16 Average change in apparent density

Initial Volume $10^{-4}.m^3$	Final Volume $10^{-4}.m^3$	Initial Density kgm^{-3}	Final Density kgm^{-3}	Volume Change %
8.65	8.65	638.1	570.9	0.0

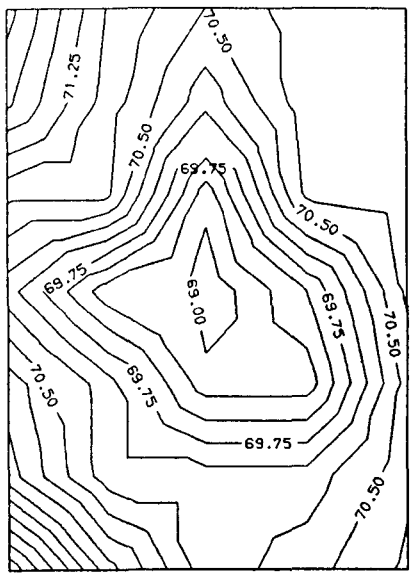

(a)

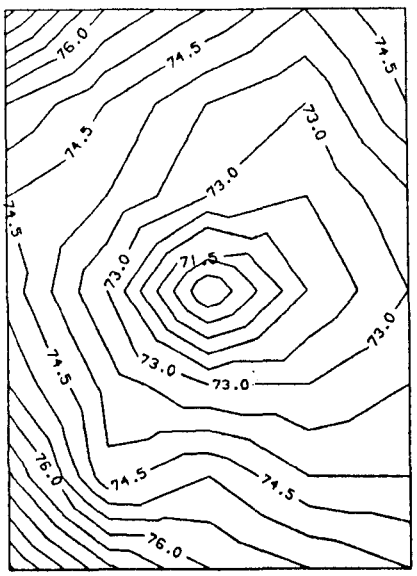

(b)

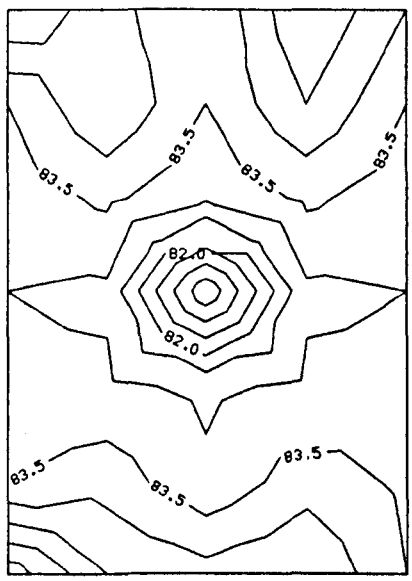

(c)

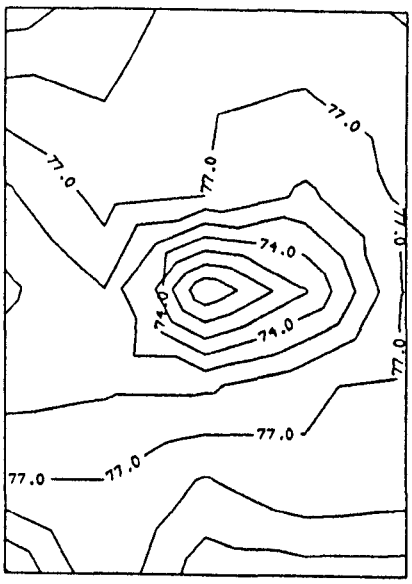

(d)

Fig.6.12 Temperature profiles for hydrogel (m=40%) after heating at plane; (a) 30mm; (b) 21mm; (c) 12mm; (d) 3mm from base

6.6 COMPARISON WITH REAL FOODS

6.6.1 Preliminary tests

There exist numerous potential parameters which should be compared between a real food and a prospective simulator in order to establish a criterion for defining a good food model. Moisture content can be a major property-determinant for a food. Therefore the primary comparison criterion was considered to be moisture content. Table 6.17 compares the thermal properties of selected food materials and the supposedly similar hydrogel materials. However many chemical and structural changes which take place in biological materials during heating are absent in a non-biological material such as hydrogel. Thus the number of parameters which can be evaluated and compared is restricted.

Hydrophilic materials and foods, each showed the typical characteristics of slab-like loads heated by microwaves (Fig.6.6-6.12). The temperature was lowest at the centre of each horizontal plane.The lowest temperature distribution was in the plane near the surface for all cases, which was due to the surface losses and typical of such loads heated in MW oven. No clear distinction and equivalence between foods and simulator could be made for the maximum temperature distribution among horizontal planes. In general the maximum temperatures were located either at level 2 or 3 (i.e. ≈12mm or 21mm from the base; see Fig.6.5b). This ambiguity could have been due to the effects of conduction in the post-irradiation period. However, for cakes the maximum temperature was invariably located at level 2.

The maximum difference between the centre temperature and corner temperature was ≈11°C. There was a difference among the temperatures of the four corners, the maximum difference being ≈5°C. The position of the samples in the oven was reversed to confirm the resulting temperatures in each certain corner. This highlighted the non uniform heating of homogeneous products achieved by a microwave oven due to the uneven field distribution in the cavity.

Although the initial moisture content for selected plant food materials were higher (i.e.16% higher for carrots), the moisture losses were lower for the hydrogel materials when compared with carrots and apples (Table 6.18). This may be due to the different free to bound water ratios for the real foods and the hydrogel. The apparent density before and after heating was higher for the hydrogel than that of the real foods.

The rate of heating and temperature distribution for the hydrogel material and carrots showed good agreement (Fig. 6.14). When compared with cooking apples the average temperature achieved at the end of heating period by the hydrogel was slightly lower (Fig.6.14). This is due to the initial higher heating rate ($\frac{\partial T}{\partial t}$), due to the low apparent density of mashed apples (Table 6.18), which after reaching about 78°C, decreased due to the increased rate of evaporative losses. The temperature in the centre seemed to rise due to conduction.

The 75% hydrogel material (0.1-1mm) was also compared with lean minced beef which has a similar water content (see Fig. 6.15 and Table 6.18). The moisture loss of the mince was much higher than the hydrogel, this may be again due to the difference in the ratio of bound and free water in the two materials. However, the associated water movement in the hydrogel was similar to that occurring in meats. On heating, meat looses its water-binding capacity. When meat reaches temperatures between about 74 and 80°C (the "well done" stage) bound water is converted to free water very rapidly [McWilliams, 1989], thus resulting in the higher rate of moisture loss. The other major difference was that the mince underwent a marked shrinkage while virtually no change was noticed in the hydrogel material. Shrinkage is due to the fibrous nature of meat which begins to shrink at about 55°C and continues to do so until about 80°C [McWilliams, 1989]. The heating rate is similar for both materials, although as the meat started being cooked the rate of heating decreased due to several endothermic chemical reactions (i.e. the melting of fats and denaturation of proteins). Whereas in the hydrogel only drying takes place.

Table 6.17 Typical property values at ~20°C for food materials [adapted from ASHRAE, 1985; Incropera, 1990] and for hydrogels calculated from empirical formulae.

Property / Material	Moisture content %	Specific heat capacity kJ $kg^{-1}K^{-1}$	Thermal conductivity W $m^{-1}K^{-1}$
Food			
Apple	75	3.60	0.48
Carrot	87	3.88	0.50
Beef mince	70	3.5	0.42
Cake batter	40	2.55	0.22
Hydrogel	75	3.50*	0.47+
	40	2.5*	0.30+

* Lamb [1976]
\+ Marten [1980]

Apart from the initial moisture content for the cake batter (≈40%), no other parameter was simulated by the 40% hydrogel material. The density was higher initially for the cake mix, and it remained higher than the hydrogel, even though the cakes expanded significantly. Initially the rate of heating was higher for the hydrogel, due to its lower density (Fig. 6.16). After about 5 minutes the heating rate decreased for both materials and became approximately equal for different reasons. Some permanent changes in proteins (coagulation) and carbohydrates (gelatinisation) took place during the baking process which involved endothermic reactions. The evaporative losses resulted in extra drying at the surface and near the edges of the hydrogel.

Table 6.18 Comparison between real food and simulator

Parameter	Real Food	Simulator
a.	*Carrot*	*Hydrogel (1-2mm)*
Moisture content (%)	≈ 87	75
Moisture loss (%)	6.1	3.7
Apparent density (kgm^{-3})		
i) Initial	751.6	898.7
i) Final	746.4	891.2
Volume change (%)	-4.0	-1.7
Mean temp. rise (°C)	80.4	82.1
b.	*Apple*	*Hydrogel(0.1-1mm)*
Moisture content (%)	≈75	75
Moisture loss (%)	4.0	2.8
Apparent density (kgm^{-3})		
i) Initial	912.9	1076.8
ii) Final	903.7	1077.9
Volume change (%)	-3.0	-2.8
Mean temp. rise (°C)	85.2	84.1
c.	*Mince*	*Hydrogel(1-2mm)*
Moisture content (%)	≈74.5	75
Moisture loss (%)	10.0	3.7
Apparent density (kgm^{-3})		
i) Initial	810.0	898.7
ii) Final	788.3	891.2
Volume change (%)	-12.4	-1.7
Mean temp. rise (°C)	81.1	82.1
d.	*Cake*	*Hydrogel*
Moisture content (%)	≈40	40.0
Moisture loss (%)	7.2	10.7
Apparent density (kgm^{-3})		
i) Initial	795.1	638.1
ii) Final	571.2	570.9
Volume change (%)	28.9	0.0
Mean temp. rise (°C)	79.4	82.8

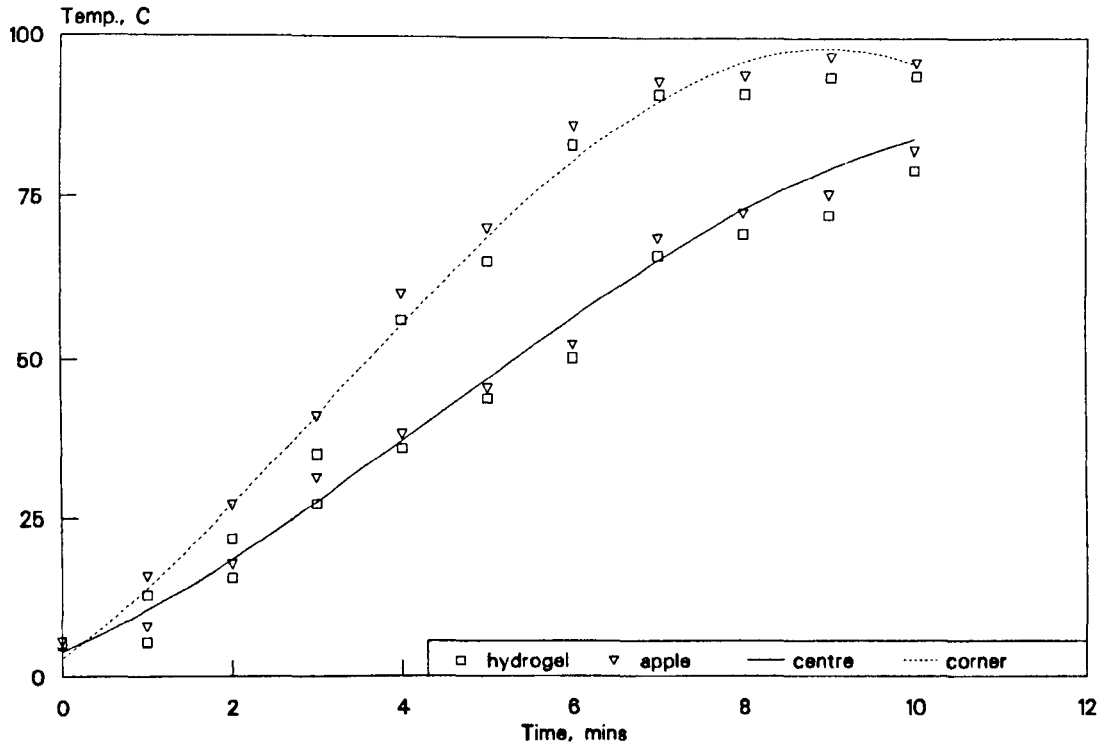

Fig.6.13 Heating rates for hydrogel (75%) and apples

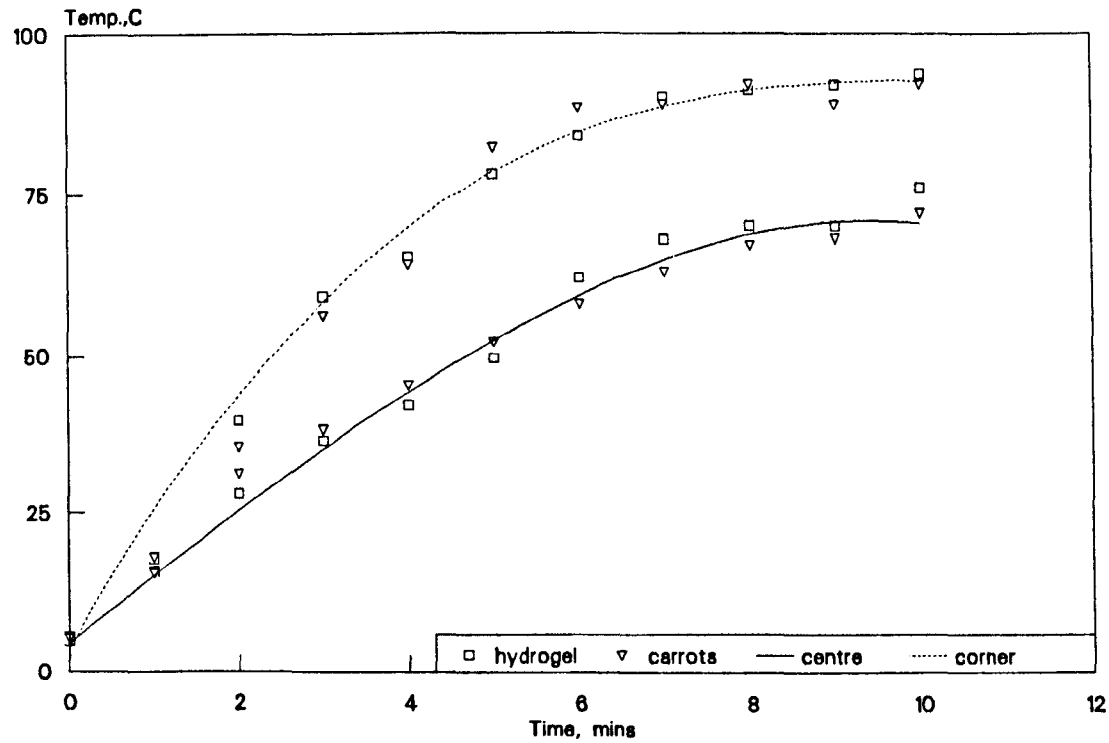

Fig.6.14 Heating rates for hydrogel (75%) and carrots

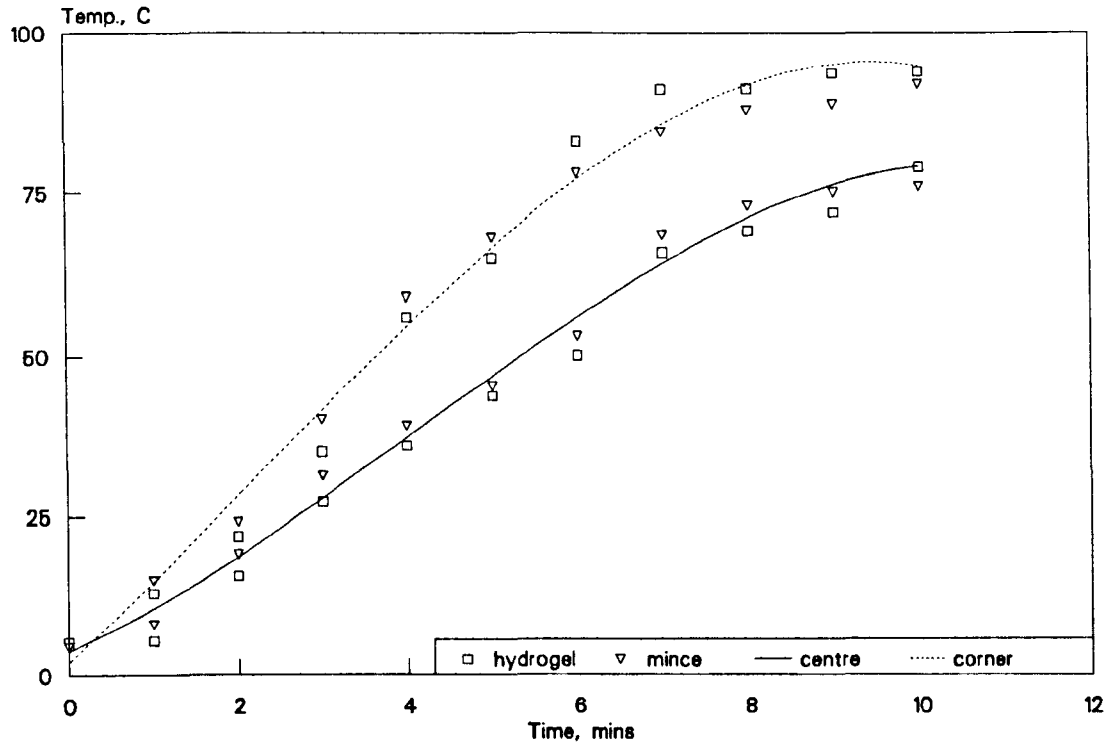

Fig.6.15 Heating rates for hydrogel (75%) and mince

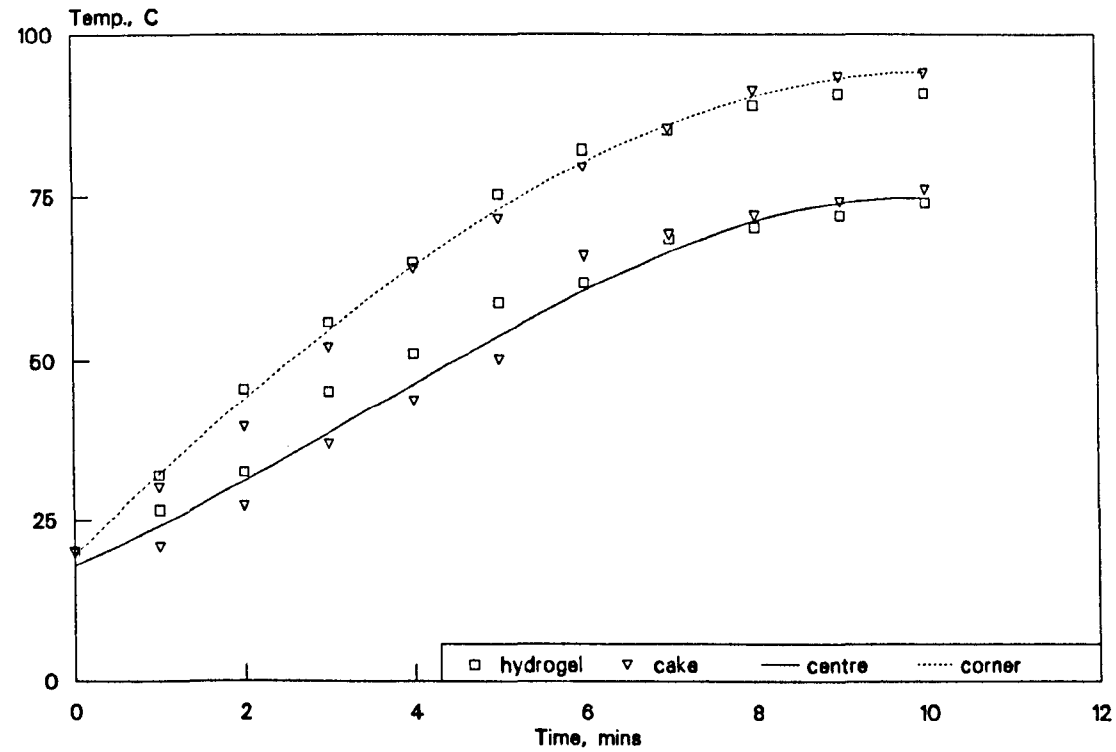

Fig.6.16 Heating rates for hydrogel (40%) and cake

6.6.2 Performance Tests Evaluation

a) Cooking performance

IEC 705 proposes three factors which may be employed to define the performance of an oven (i.e. speed, cooking results, and convenience). Although, the hydrogel was unable to simulate qualitative characteristics of complex foods, comparisons could be made on the basis of the heating rate and cross sectional temperature distribution. The subjective concept of "undercooked" or "overcooked" cannot be easily applied to the hydrogels. The same applies to the evaluation of cooking speed and convenience. The convenience of cooking involves the number of procedures required during a cooking operation to achieve the desired results; these may include manual stirring, separation or removal of parts of the load to avoid over-cooking or burning. Efforts were made to assign some measures to the qualitative attributes of heating real foods, which may be employed to assess the hydrogel materials.

The surface temperature was lower in all cases (i.e. for the real foods as well as in the hydrophilic materials) due to convective and evaporative losses. The load was positioned in the centre of the oven for these tests. However, it was found that small changes in the sample's position, that may commonly happen during the actual use of the appliance did not influence the results noticeably. To define the uniformity of cooking, minimum and maximum temperatures values were recorded at the end of heating period for the 28 measured locations and from these, the mean bulk temperature was calculated. The difference is expressed as percentage of the mean bulk temperature. The highest and lowest recorded temperature and the standard deviation of the temperatures for the three replicates are also given (see Tables 6.19 and 6.20).

TABLE 6.19

Uniformity of cooking of cake and hydrogel (m ~40%) for the three tests; mean temperature and maximum difference between the lowest and highest temperature measured at 28 locations.

Test	Temperature, °C		
	mean	max. difference. % of mean	standard deviation
a) Cake	88.6	7.8	4.7
b) Hydrogel	92.5	6.7	2.6

TABLE 6.20

Uniformity of cooking of mince and hydrogel (m ~75%) for the three tests; mean temperature and maximum difference between the lowest and highest temperature measured at 28 locations.

Test	Temperature, °C		
	mean	max. difference % of mean	standard deviation
a) Mince	89.8	5.6	2.9
b) Hydrogel	94.4	5.1	2.5

The hydrophilic materials exhibited slightly more uniform heating when compared with the cake and minced beef. During cooking several permanent changes take place in cake and meat at different temperatures. When any part reaches these specific temperatures, the local heating rate decreases. Also due to structural changes, the rate of heat transfer within the sample varies and usually results in an increased temperature differential, whereas in the hydrophilic materials the temperature continues to rise until it reaches the boiling temperature of water (≈100°C) (i.e. the maximum temperature reached in this case). Loose water movement in the sample helps to achieve a more uniform temperature distribution. If minimum and maximum temperatures are to be representative of the degree of "doneness" of a food material, it is still very difficult to assign numerical values to describe the cooking of hydrogels. For example, in practice a food material even with a high moisture content (e.g. potato) may partly burn due to a rise in the local temperature to a certain value, while no similar degradation is associated with hydrophilic materials which keep on drying if heated for a longer period.

The cooked mince and cake were sliced and examined for the degree of doneness and dehydrated areas and temperatures values were assigned to these qualitative measures so that similar measures could be applied to the hydrogels. However, as seen in the preliminary tests no equivalence was found between cake and hydrogel. The score sheet is devised for hydrogels simulating minced beef for the cooking performance tests (Table 6.21).

b) Defrosting Performance

It was difficult to locate the thermocouples after the defrosting tests, because the frozen slabs of hydrogel and mince collapsed on defrosting. The material was separated into frozen and defrosted parts and the criteria stated in IEC 705 were used to assess the defrosting performance of both materials. Both materials behaved in a similar way. (see Table 6.22).

Table 6.21

Proposed Score sheet to assess the cooking performance of microwave ovens using hydrogel for simulating foods

Date		
Oven	Rated Power	Total Score .....
Hydrogel 75% (≈minced beef)	Perfect score = 100	
Penalties;		
for each 4° temperature difference	= 5	
for each temp. < 70°C (≈ undercooked)	= 10	
for each temp. > 95°C (≈ overcooked)	= 10	

Table 6.22

Uniformity of defrosting for hydrogel and mince: the minimum, the maximum and the mean temperature (along with standard deviation (s.d.) for 5 tests)

Merit	Hydrogel		Mince	
Temperature °C		s.d.		s.d.
a) minimum	-1.7	0.4	-1.0	0.3
b) maximum	34.1	2.1	35.3	2.8
c) mean	12.0	1.3	10.1	1.1
	(% of total mass)			
T ≤ 2°C	14.2		13.8	
2°C< T ≤ 12°C	47.6		48.2	
12°C-max T	38.2		38.0	

6.7 EMPLOYING HYDROPHILIC MATERIALS AS TEST MATERIALS

75% hydrophilic material was used to assess the uniformity of heating, or differences in temperature, achieved in a similar product by different microwave ovens. Two ovens (A) and (B) with respective IEC output powers 850W and 530W and were used. Oven (A) was the same as that used previously. The cavity size of oven (B) was: 195mm; 295mm; 272; (w; h; d). It was also of multi mode design with a rotating glass shelf. The sample size used was 400g which represents an average food load based on various ready-meals currently available. Similar procedures for sample preparation and temperature measurements as described above were followed. The test samples were kept (i) at ≈4°C to simulate chilled products and (ii) at room temperature to simulate the shelf-stable products. The heating times were also adjusted to provide an energy input of approximately 300kJ for case (i) and 180kJ for case (ii) respectively, based on the recommended heating times for the commercially available food products. Each test was repeated three times.

TABLE 6.23

Output power and power consumption of the ovens used

	Maximum power consumption (W)	IEC rated output power (W)	Heating times Min'sec	Energy kJ
(A)	1400	850	5'53	300
			3'32	180
(B)	1150	530	9'26	300
			5'40	180

The data were adequate to assess the uniformity of heating achieved in the tested ovens. The test load was homogeneous but real products are generally multi layered or heterogeneous, and so the temperature differences found in real situations may be larger. Nonetheless, the uniformity and reproducibility of heating by different ovens is one of the great concerns. The tests employing hydrophilic materials were able to assess such differences.

Tests showed that at both energy levels, oven (B) produced more uniform temperature distribution, although its cavity size was smaller (Fig.6.17a,b and Fig.6.18a,b). This may be due to the longer period required to input the same amount of energy, allowing more time for thermal conduction within the samples (see Chapter 2). Also the higher temperature was near the base for 92% of the profiles for oven B. Thus it could be concluded that the energy in oven (B) was concentrated near the floor of the cavity. The lowest temperature was located always at the centre of load for both ovens which is typical of slab like geometries. The highest temperature was located at ≈12mm from the base and invariably in the rear-left corner for oven (A). The maximum differences between the temperatures of the corners were ≈28°C for oven (A) and 22°C for oven (B). This clearly shows that some ovens fail to achieve uniform heating in loads of average size, despite having turn-tables.

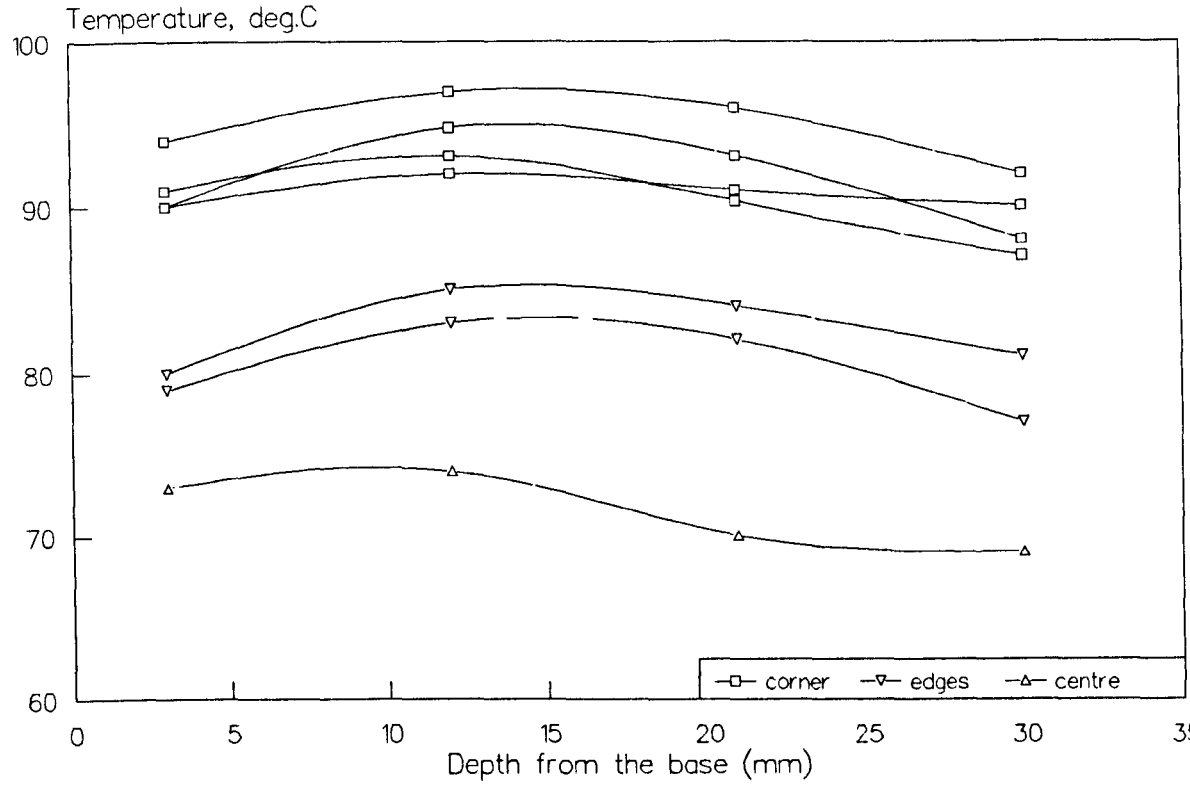

Fig.6.17a Temperature distribution in the test load for oven A, energy = 300kJ

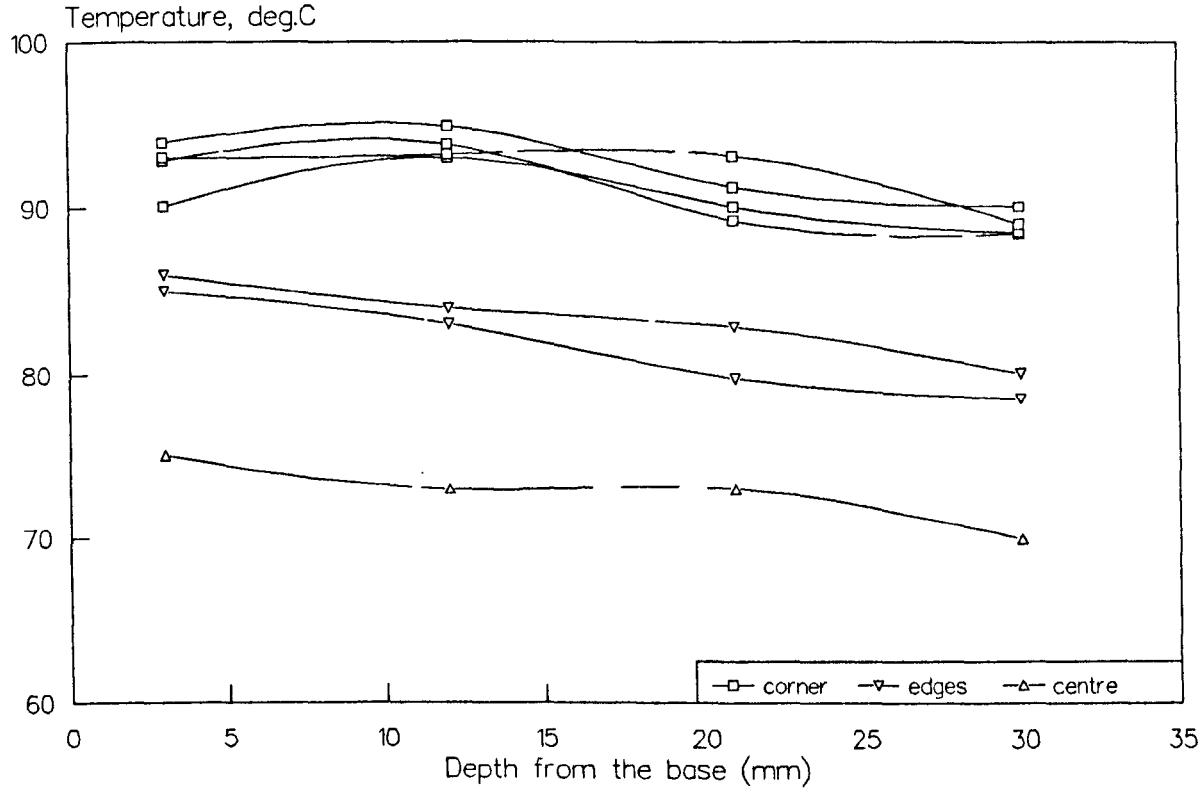

Fig.6.17b Temperature distribution in the test load for oven B, energy = 300kJ

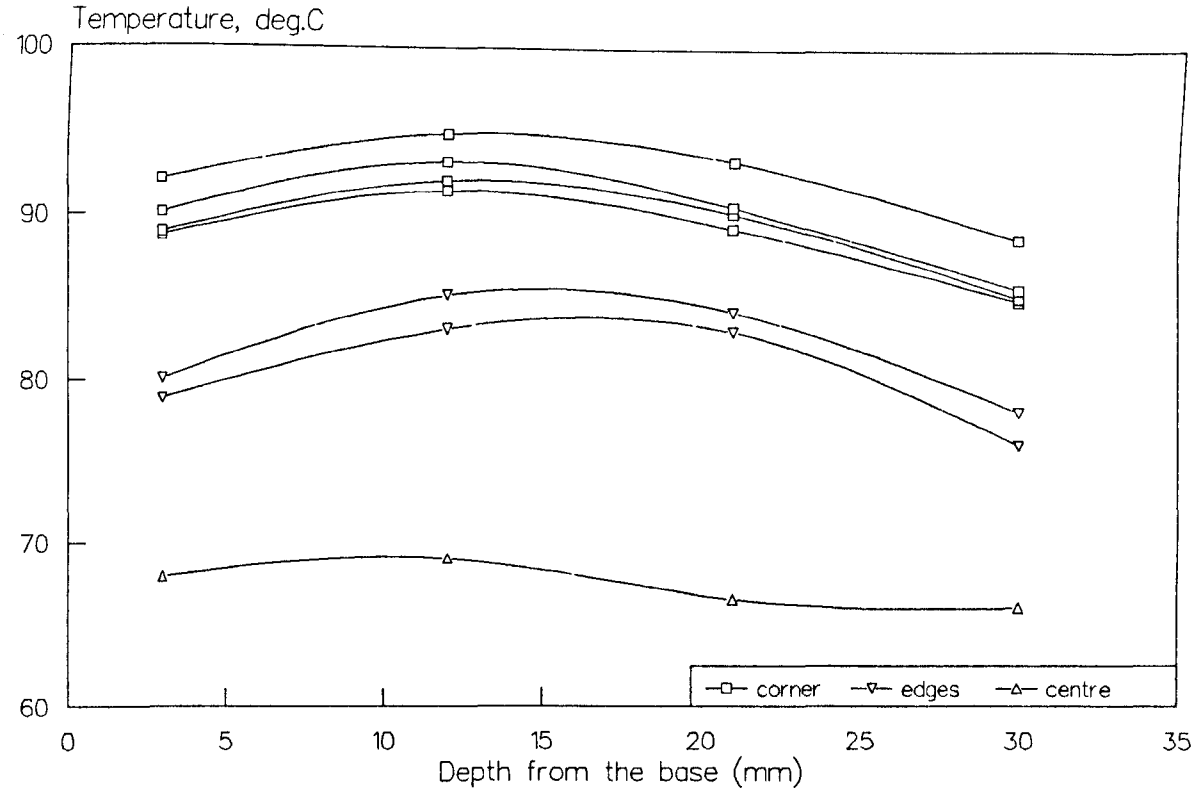

Fig.6.18a Temperature distribution in the test load for oven A, energy = 180kJ

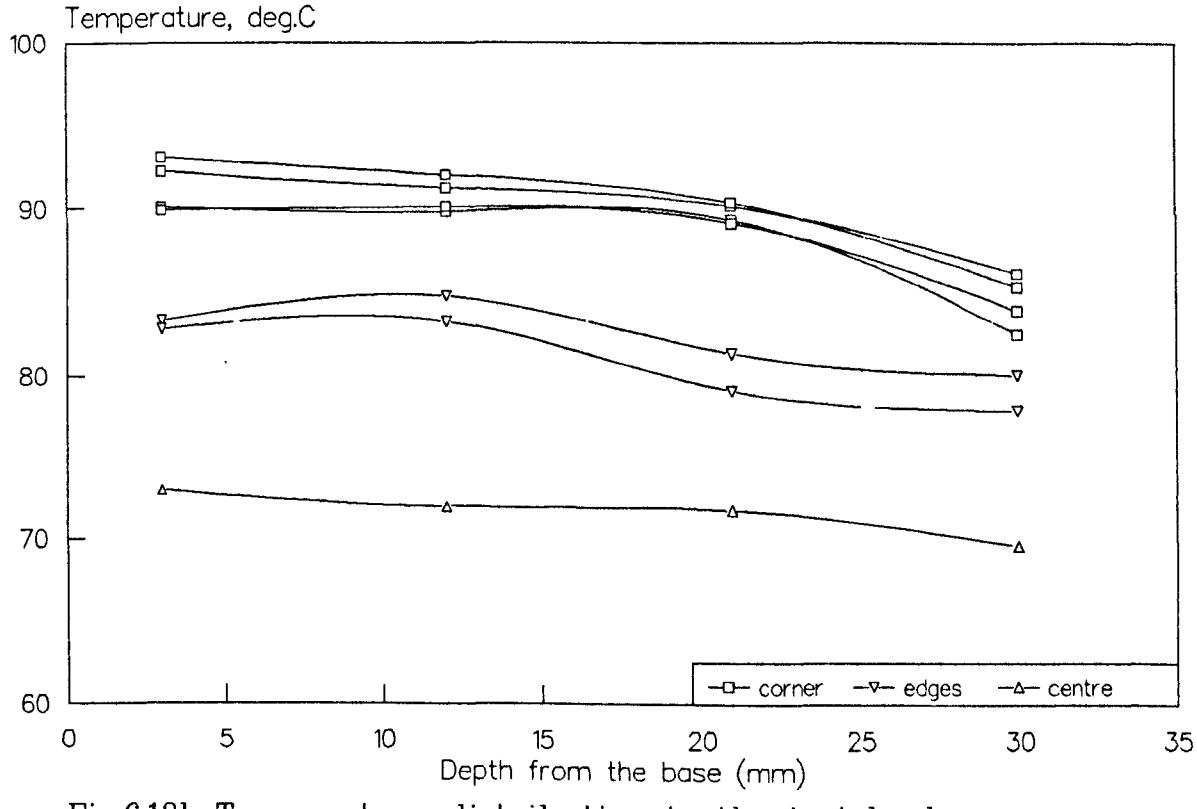

Fig.6.18b Temperature distribution in the test load for oven B, energy = 180kJ

6.8 REUSABILITY OF HYDROPHILIC MATERIAL

It was found that hydrophilic materials did not undergo great physical and chemical changes on heating and the material could be reclaimed by drying the used material. Therefore these materials can be reused. The properties of the material remain unchanged if it is dried at temperatures of less than 150°C. Ideally a vacuum oven should be used, but a forced convection oven in conjunction with a microwave oven was used to dry the material in this investigation. The product was left for 36 to 48 hours in the convection oven at 60°C to ensure that all the water was evaporated. Because the bound water is difficult to remove, any moisture left was removed by drying in the microwave oven until no further change in mass took place. There was some change in colour due to oxidation which occurred during drying (see Fig.6.19) and the dried material tended to form into lumps. These lumps were ground and sieved to obtain the mix of material of the same particle size each time. This is an important factor to ensure the reproduction of material of similar heating characteristics.

To assess the reusability characteristics of hydrogel materials as food models, the 75% moisture content material was used ten times and 40% moisture material fifteen times over a total period of six months. There were no apparent differences in the moisture loss and heating characteristics of the reused materials (see Tables 6.24-6.25). The individual measured temperatures could be reproduced to within 6°C for replicated tests for every use which indicated the degree of reproducibility and the reusability of the material. Maximum temperature differences of up to 10°C were observed in few cases due to the reasons discussed earlier in section **6.5.1**

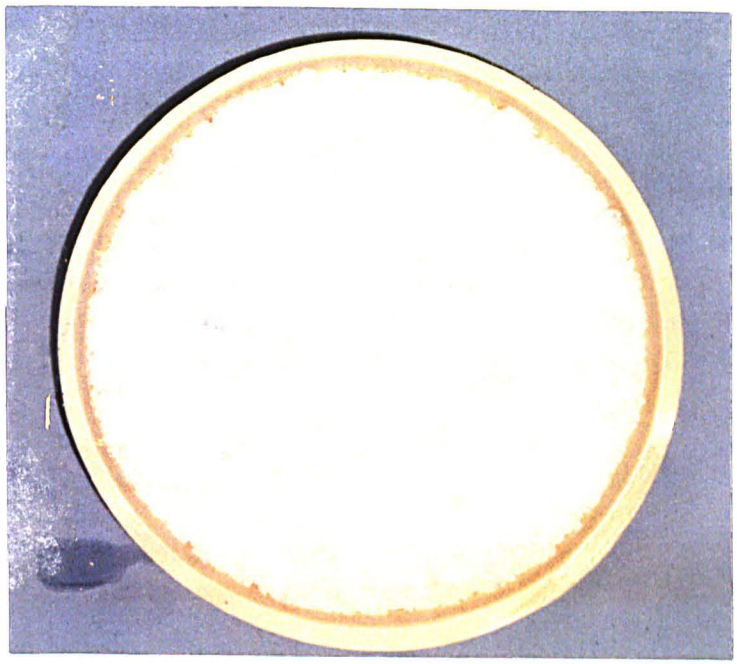

a. Fresh

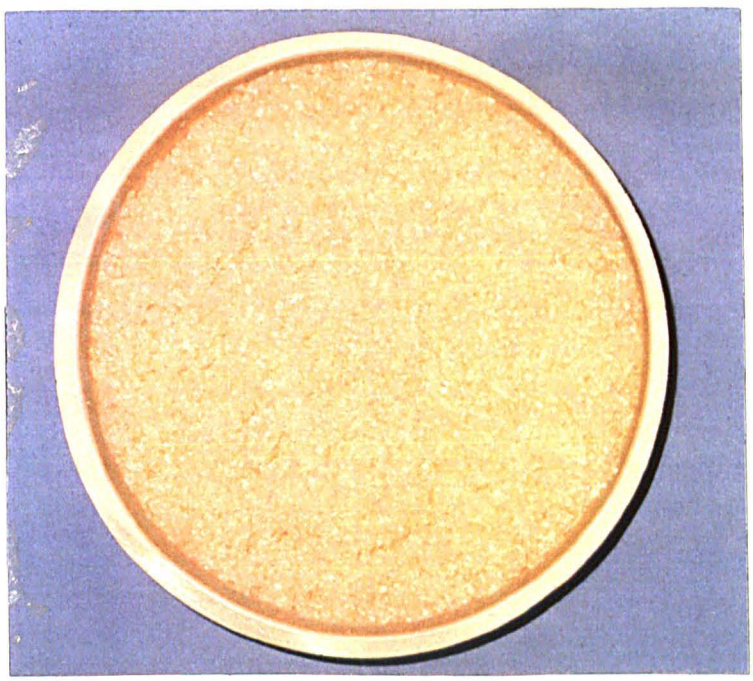

b. After ten uses

Fig.6.19 Apparent difference in fresh and used hydrogel (m=75% , 1-2mm)

Table 6.24

Moisture losses for each successive use of hydrogel (m=75%,0.1-1mm)

(each test no. represents the mean of three tests)

Test no.	Initial mass (g)	Moisture loss as % of initial mass	Rate of moisture loss ($gmin^{-1}$)
1	500.1	2.9	2.6
2	505.7	3.1	2.3
3	510.9	2.8	2.4
4	499.6	2.8	2.3
5	489.0	3.1	2.9
6	523.0	3.5	3.1
7	524.9	3.3	2.9
8	496.5	2.8	2.5
9	500.0	2.9	2.8
10	491.0	3.1	2.6

Table 6.25

Moisture losses for each successive use of hydrogel (m=40%)

(each test no. represents the mean of three tests)

Test no.	Initial mass (g)	Moisture loss as % of initial mass	Rate of moisture loss ($gmin^{-1}$)
1	555.1	11.3	5.9
2	500.1	10.8	5.5
3	551.0	12.5	6.1
4	504.6	11.3	5.8
5	499.9	10.6	5.5
6	500.1	10.8	5.5
7	499.1	9.9	5.4
8	493.3	8.9	5.0
9	491.1	10.9	5.6
10	490.2	10.7	5.7
11	450.1	11.7	6.0
12	450.7	12.8	6.3
13	445.7	11.2	5.8
14	450.2	10.5	5.5
15	430.0	10.2	5.0

(Note:Variations in initial mass are due to the loss of granules during handling so there was less material for the later tests)

6.9 CONCLUSIONS

Based on simple criteria of initial moisture content and moisture loss after a chosen heating period in a microwave oven, the considered hydrophilic polymeric materials were compared with selected food materials (carrots, apples, mince and cake). As expected, the results indicated that hydrogels could not simulate expansion, shrinkage or change in texture of the various foods. Even minced beef and 75% hydrogel which had similar initial moisture content exhibited different moisture losses when heated under similar conditions. This may be due to the fact that each material had different ratios of free to bound water. Unfortunately, free to bound water content ratios for food materials were not found in the literature, so it is difficult to select a food with a free-to-bound water content ratio similar to that of the hydrogel.

75% hydrophilic materials exhibited a typical characteristic close to that of cooking minced beef which is not available in any other model material. Free water in the material was driven out of the polymer structure and formed a layer of water. In meats water is also expressed at temperatures when the fibres start shrinking. However virtually no shrinking occurred within the hydrophilic materials.

The temperature distribution and rate of heating were simulated reasonably well for the tested hydrogel material and foods. This showed that the hydrogel and the simulated food material had effectively similar thermal and dielectric properties. A linear relationship existed between the maximum temperature difference and the lowest temperature within a product. The differences between the temperature distributions were generally within the same error band for the simulator and the food material. Present results show that hydrogels may be used for evaluating uniformity of heating in microwave ovens for foods of varied moisture content, size and shape (e.g. slab, cylindrical). Their use for assessing the cooking performance of foods such as cakes is somewhat restricted, although some criteria (in terms of temperature values) were assigned to equate with the doneness of

meat products. The defrosting performance can be effectively evaluated by using hydrogels instead of real foods (e.g. minced beef).

Another important aspect of the hydrophilic material is its reusability as a food model. This study showed that it can be used with good reproducibility for at least 40 times. Apart from the change in the appearance of the hydrogel no change in the heating characteristics of the material was noticed. Therefore the use of hydrogels as test loads in place of real foods is economically justified even at its present price, which is more than some foods. Its price is expected to fall as new methods to manufacture the material are found.

This was the first attempt to determine the feasibility of using hydrogel materials as food models for testing the heating performances of microwave ovens. The present results established the potential similarities of hydrogels and various food. Further use of the material is recommended at least to assess the heating uniformity of microwave ovens for different food products. Similar tests should be repeated using a number of ovens to ensure the reproducibility of similar characteristics of these materials achieved with a single oven. More research needs to be done to establish further equivalence between the heating behaviour of various foods and hydrogels. Appropriate procedures employing hydrogels for testing performance of microwave ovens which effectively relate to the actual use of the appliance may then be determined.

CHAPTER 7

7. CONCLUSIONS AND RECOMMENDATIONS

7.1 CONCLUSIONS

As a result of the investigations reported in this thesis, the following concluding remarks are made.

7.1.1 A general mathematical model developed for thermal analyses of electromagnetic heating processes is a useful tool for establishing the influence of a large number of describing parameters (material properties, process frequency, ambient conditions) on the practical heating characteristics. The model may be employed as a design tool in the development of a product/process and may thereby serve as a means for reducing the amount of experimentation required. Also by employing such a model there are educational benefits to be gained with respect to understanding the thermal effects of EMH techniques.

7.1.2 Uncertainties in the values of the heating parameters (i.e. the material's properties, assumed boundary conditions) can undermine the precision obtained from any numerical model. The effects of temperature induced property variations for a particular process/material were assessed with the model in order to determine suitable assumptions. The temperature dependence of the dielectric properties of foods must be considered for thawing processes and for heating products with high salt contents. Similarly, it is not desirable to underestimate temperature values when modelling for the food quality (e.g. flavour, thiamine degradation) or to overestimate temperature values when predicting for microbial lethalities. Thus temperature dependent properties should be included in the numerical model as dictated by the considered process.

7.1.3 Correlations based on food composition and temperature for determining the dielectric properties of a wide range of foods were

developed. Using these, the dielectric properties of various foods can be predicted to ±15% accuracy. Furthermore the predictive equations can be incorporated easily in a numerical model in order to encourage consideration of the functional variations of these properties with temperature and moisture content.

7.1.4 Several available correlations for thermal properties of foods were compared with the experimental data for different food materials. Correlations for the temperature dependent k and α_T [Martens,1980] were found to be valid for a wide range of products. The average discrepancy between the predicted and experimental data for k and α_T was only about 10%.

7.1.5 The accuracy of predicting the spatial power distribution within a material influences the accuracy of the thermal model's predictions. For microwave heating of foods, the assumption of exponential decay of power may be used to describe the spatial variation of power absorption. However, the oscillatory nature of EM waves can only be considered by solving Maxwell's equations to obtain the power distribution. Thus, the general model was modified, such that the power generation was based on the solutions of Maxwell's equations, in order to improve the representations of the physical mechanisms of MW heating of foods. The solutions were found via finite-difference discretisation of the wave equation. The model was employed to assess the influence of food properties, product size and the boundary conditions on the predicted temperature distributions. A qualitative comparison between the numerical and experimental results indicated good agreement. Thus the theoretical basis of the model is sound and it can be used to obtain the necessary relationships between different parameters and heating characteristics for heating of various foods.

7.1.6 Hydrophilic materials of different water uptake were found to adequately simulate the heating characteristics of different food materials of similar moisture contents. For example, the rate of heating and temperature distribution within a sample of 75% hydrogel showed good agreement with that of the mashed apple, carrots and minced

beef (≈75%), while the 40% hydrogel exhibited a similar thermal behaviour to that of cake. These hydrogels are recommended as test materials for assessing the heating uniformity of MW ovens for different foods. The material is reproducible in properties and can be *reused* without any change in its heating characteristics.

7.2 SUGGESTIONS FOR FURTHER WORK

7.2.1 Mathematical model

Parametric analyses and correlations for material properties form a framework for developing assumptions and generating property data for a numerical model applicable to a certain EMH process. The presented models could be enhanced as a software package by incorporating graphical processors to allow the graphical display of the geometry of the sample and results on the screen or as a hard copy. In this study, derivatives of the heat and wave equations were discretised using the general finite-difference method and then solved by the Gauss-elimination technique. If a software package were to be developed, alternative mathematical formulation and solution methods depending upon the available computer memory space should be tried to improve the speed and accuracy of the calculations.

At this stage only heat transfers were considered. However, the model for MWH of foods should be extended to simulate simultaneous moisture transfer characteristics occurring during microwave heating (e.g. drying). The model may be used in conjunction with another model for predicting bacterial counts and the cooking losses of food constituents (vitamins, riboflavin, thiamine etc.), and hence as a design tool for efficient microwave sterilisation and pasteurisation processes.

7.2.2 Dielectric Properties

The predictive equations were based on the available experimental data. As more data become available, the equations can be improved to include more materials or to extend the range for temperature and other variables.

7.2.3 Food Simulators

Considering the novelty of the suggested use of hydrophilic materials as a test material for testing MW ovens, a series of test programmes should be developed in order to improve the general understanding of the heating characteristics of these materials. In the present work it has been established that these materials can be used to assess the heating uniformity of MW ovens for foods products of different moisture contents. However, more tests should be carried out using several ovens so that testing procedures for assessing output power and cooking performance of MW ovens, which effectively relate to the actual use of the appliance, may be defined.

Taking advantage of the experience gained in the present course of work, other parameters that may be considered in any future investigations are as follow:

(i) Measurements of the thermal and dielectric properties of hydrogel materials in the temperature ranges applicable to thawing, cooking and sterilisation processes.

(ii) Use of partly hydrated samples (to simulate 100% bound water and 0% free water).

(iii) Multi-layered foods should be simulated by using layers of hydrophilic of different moisture contents.

(iv) The influence of water permeability and vapour permeability due to the porosity of the hydrophilic materials, should be assessed in convection ovens.

(iii) Other hydrogels with different moisture contents should also be investigated. Selection criterion should be based on other parameters in addition to moisture content (e.g. porosity, texture and structure) in order to improve the capability of a model(s).

7.2.4 Experimental programme

Finally, there is scope for making improvements in the experimental set up. In this study a domestic MW oven was used, which simulates a real situation but lacks adequate control for achieving desired changes in different heating parameters e.g. input power, convection. Properly designed laboratory MW systems would provide better control of experimental conditions to quantify the effects of various parameters on the heating characteristics and to compare the predictions of a numerical model. To corroborate the presented experimental data, studies employing optical fibre thermometry should be undertaken. Real-time temperature measurements can thus be made and results may be obtained at intermediate stages of a continuous heating process.

7.3 Post-script

A final quick literature survey was undertaken while this thesis was being written (1994). An analytical solution for the 1-d heat equation with the heat generation term based on Lambert's law for studying MWH of solids was published recently [Dolande and Datta, 1993]. Relative roles of diffusion, heat generation and convection on heating characteristics were discussed and similar heating characteristics for semi-infinite slabs to those presented in this study (Chapter 2) were obtained but analytically. Zeng and Faghri [1994] undertook a combined experimental and numerical study of microwave thawing in a domestic oven of a food model material. The material used was (Tylose), a 23 percent solid methyl-cellulose gel and it was reported that its thermal properties were similar to those of lean beef.

New applications for microwave energy such as rice-bran stabilisation [Tao et al, 1993] and pest control for potatoes [Clopitts et al,1993] and numerical modelling of simple and complex systems of heating, drying, sterilisation, hazard sensing etc. need dielectric data for more materials and wider temperature ranges. Data for a few more substances have been reported recently [Kraszewski and Nelson, 1993].

However, concerns regarding the inconsistency of experimental dielectric data are still being made. As Risman [1993] pointed out, availability of modern measurement hardware and associated computer software do not mean that absolute data are obtained and the digital resolution of a computer algorithm is neither the same as measurement precision nor accuracy. He suggested that the data for reference substances (pure water, aqueous-ionic solutions) representing the typical dielectrics (biological materials and foods) over large temperature and frequency ranges should be made available.

Despite the optimistic views expressed in the recent literature [Decareau, 1992, 1993], a decline in the growth prospects for shelf stable MW prepared foods was reported. The sale of such products dropped by 15% during 1993 [Freidman, 1994]. Lack of understanding of the varying interactions between microwaves and foods of different geometries and dielectric properties, and the safety issues related to the microwave oven and associated food products, are the primary causes of slow and reluctant acceptance of MW products/processes. Although some commercial software packages for high frequency dielectric heating applications have been reported [Weimer, 1992; Stefens and Dommelen, 1993], government departments in the UK and USA [MAFF, 1992; USDA 1990; FMI 1991] provide some consumer orientated data. However, information in the non-electrical engineering sector is still scarce.

REFERENCES

Andreuccetti D., Bini M., Ignesti A., Olmi R., Rubino N., and Vanni R., 1988. Use of polyacrylamide as a tissue-equivalent material in the microwave range. IEEE Trans. BME-35(4), 275-277.

Andrews G., 1992. Microwaves Reviewed An appraisal of the present situation. Modus, 10(1), 15-17.

ASHRAE Fundamentals, 1985. Chapter 31, American Society of Heating and Air Conditioning Engineers, Atlanta, USA.

Ayappa K.G., Davis H.T., Crapiste G., Davis E.A., and Gordan J., 1991. Microwave Heating: an evaluation of power formulations, Chemi. Eng. Sci., 46(4), 1005-1016.

Ayappa K.G., Davis H.T., Davis E.A., and Gordan J., 1991. Analysis of microwave heating of materials with temperature-dependent properties, AIChE Journal, 37(3), 313-322.

Barrat L., 1993, Experimental validation of a computer simulation of microwave heating, Proceedings Conference on Modeling for food safety, IMA and IFST, April 14-16, Belfast.

Bengtsson N.E., Melin J., Remi K. and Sonderlind S., 1963. Measurements of the dielectric properties of frozen and defrosted fish. J. Sc. Food Agri. 14, 592-604.

Bengtsson N.E. and Risman P.O., 1971. Dielectric properties of foods at 3GHz. as determined by a cavity perturbation technique II. Measurements on food materials, J. Microwave Power, 6(2), 107-123.

Bengtsson N.E. and Lycke E. 1969. Experiments with a heat camera for recording temperatures in foods during microwave heating, J. Micr. Power, 5(1), 47-52.

Bottcher C.J.F. 1952. Theory of electric polarisation, Elsevier Publishing Co., New York.

Bowman R.C., 1970. Thermal conductivity of cooked foods. M.Sc. thesis, Leeds University.

Bows J. and Joshi K., 1992. Infrared imaging feels the heat in microwave ovens. Physics World, August, 21-22.

Brugioni M., 1991. Simulating food-heating processes with re-usable hydrophilic materials. MSc. thesis, CIT, Cranfield.

Buffler C.R., 1992. Microwave cooking and processing: Engineering fundamentals for the food scientist. Chap.2, AVI book, pub. Van Nostrand Reinhold, New York.

Buck D.E., 1965. The dielectric spectra of ethanol-water mixtures in the microwave region. PhD.thesis, Massachusetts Institute of

Technology, Cambridge, Massachusetts..

Burfoot D and Foster A.M., 1989. Microwave reheating of ready meals. AFRC Institute of Food Research, Bristol, IFR-B Memorandum No. 59.

Carnahan B., Luther H.A. and Wilkes J.O., 1969. Applied Numerical Methods. Pub. Wiley, New York.

Chamberlain I. and Chantry G.W. 1973. High frequency dielectric measurements IPC Ltd., New York.

Charm S., 1963. The fundamentals of food engineering, AVI Publ.Co., Westport, Connecticut.

Checcucci A., Benelli G., and Duminuco M., 1983. Reliability of microwave heating of homoderivative thawing, J. Microwave Power, 18(2), 163-168.

Choi Y. and Okos M., 1986. Thermal Properties of liquid foods -review, in Physical and Chemical Properties of foods, ed. Okos M., pub.American Society of Agricultural engineers, St. Joseph Michigen, 35-57

Collie C.H., Hasted J.B. and Ritson D.M. 1948. The dielectric properties of water and heavy water. Proc. Royal Soc. of London, 60, 145-160.

Cross, A. D, Jones, P. L. and Lawton, J., 1982. Simultaneous energy and mass transfers in RF fields, Trans. Chem.E, part I, 60, 67-74.

Davies J., and Simpson P.,1979. Induction-Heating Handbook, McGraw-Hill, London.

Datta A.K. and Liu J., 1992. Thermal time distributions for microwave and conventional heating of food. Trans. IChemE, part C, 70, 83-90.

De Alwis A.A.P. and Fryer P.J., 1990. A finite element analysis of heat generation and transfer during ohmic heating of food, Chemical Engineering Science, 45(6) 1547-1559.

Debye P., 1929. Polar Molecules, Chemical Catalogue, New York.

Decareau R.V., 1977. The Litten microwave-cooking products story, Microwave Energy Appl. Newsletter, 3, 3-10.

Decareau R.V., 1992. Microwave foods: new product development. Food and Nutrition press, Inc., Trumball, Connecticut.

Decareau R.V., 1993. Looking ahead: editorial, J.Microwave power and Electromagnetic Energy, 28(3), 121-122.

deLoor G.P., 1968. Dielectric properties of heterogenous mixtures containing water. J.Microwave Power, 3(2), 67-78.

Dennis M.S., David T.B., and Gandhi O.P., 1987. Use of finite difference time domain method in calculating EM absorption in human

tissues. IEEE transactions on Biomedical Engineering, BME-34(2), 148-157.

de Pourcq M., 1984. New power density calculation method by three dimensional finite elements. IEE proceedings Part H, 131(6), 411-419.

Desai R., 1991. Transmission line modelling of heating in a domestic oven, PhD thesis, University of Nottingham.

Dewagter C., 1984. Computer simulation predicting temperature distributions generated by microwave absorption in multilayered media, J.Microwave Power, 19(2), 97-105.

Dolande J and Datta A, 1993. Temperature profiles in microwave heating of solids: A systematic study, J.Microwave power and Electromagnetic Energy, 28(2), 58-67.

Engelder D. and Buffler C., 1991. Measuring Dielectric properties of food products at microwave frequencies. Microwave World, 12(2), 6-15.

FMI 1991, Food safety and the microwave, Food Marketing institute, Washington DC.

Foster K.R., Kritikos H.N. and Schwan H.P., 1978. Effects of surface cooling and blood flow on the microwave heating of tissue, IEEE Transactions, BME-25, 313-316.

Frachette R.J., and Zahradnik J.W., 1968. Thermal properties of macintosh apple, Transactions, ASAE, 21, 23-25.

Fricke H.,1955. The complex conductivity of a suspension of stratified particles of spherical or cylindrical form. J. Phys. Chem., 59, 168-172.

Friedman, M., 1994. Microwavable products. Prepared Foods, January, 59.

Frohlich H., 1958. Theory of dielectrics. Oxford University Press, London.

Gaffeny J.J., Baird C.D. and Eshleman W.D., 1980. Review and analysis of the transient method for determining thermal diffusivity of fruits and vegetables. ASHRAE Trans. 86(2), 261-270.

Goedeken D.L., Tong C.H. and Lentz R.R., 1991. Design and calibration of a continuous temperature measurement systems in a microwave cavity by infrared imaging, J. Food processing and Preservation, 15, 331-337.

Guy A.W, Lehmann J.F., Mcdougall J.A., 1968. Studies on therapeutic heating by electromagnetic energy Proceedings ASME, 26-45.

Hasted J.B., Ritson D.M. and Collie C.H., 1948. Dielectric properties of ionic solutions, Parts 1 and 2. J.Chem. Phys., 16, 1-21.

Hasted, J.B., 1972. A Comprehensive Treatise, in Water ed.by Franks F. vol 1, 255-305, Plenum Press, New York.

Hayakawa K. and Bakal A., 1973. New computational procedure for determining apparent thermal diffusivity of a solid body approximated with an infinite slab, J. Food Science, 38, 623-629.

Highgate D.J., Knight C., and Probert S.D., 1989. Anomalous 'freezing' of water in hydrophilic polymeric structures. Applied Energy, 34, 243-259.

Hill N., Vaughn W.E., Price A.H. and Davies M., 1969. Dielectric properties and Molecular Behaviour, pub. van Nostrand, New York.

Hoefer W.J.R., 1985. The TLM method: theory and applications, IEEE transactions on microwave theory and techniques, MTT-33(10), 882-893.

Jain R.C. and Voss W.A.S., 1987. Dielectric properties of raw and cooked chicken and eggs at 3GHz, 23-140°C, J.Microwave power and Electromagnetic Energy, 22(4), 221-227.

Jia X. and Jolly P., 1992. Simulation of microwave field and power distribution in a cavity by a 3-d finite element method. J. Microwave power and Electromagnetic Energy, 27(1), 11-22.

Johnson C.C., Durney C.H. and Massoudi H., 1975. Long-wavelength electromagnetic power absorption in prolate spheroidal models of man and animals, IEEE Transactions, MTT-23(9), 739-747.

Jolly P.G., 1989. Microwave heating of materials with spatially varying properties, 1st Australian Microwave Symposium, Wollongong.

Jolly P. and Turner I., 1990. Non-Linear field solutions of one dimensional microwave heating. J. Microwave power and Electromagnetic Energy, 25(1), 3-15.

Jonscher A.K., 1983. Dielectric Relaxation in solids. Chelsea Dielectrics, London.

Jowitt R., 1987. Physical Properties of Foods -1, pub. Applied Science, London.

Kashiwa T., Naya H. and Fukai I., 1991, A new transducer for thermography to observe the electric field distributions in a microwave oven. Microwave and Optical Technology Letters, 4(2), 81-83.

Kent M., Christiansen K., van Haneghem I.A., Holtz E., Morley M.J., Nesvabo P. and Poulsen K.P., 1984. Cost 90 collaborative measurements of thermal properties of foods. J.Food Engineering, 3, 117-150.

Kent M., 1987. Electric and Dielectric Properties of Food Materials. Science and Technology Publishers, London.

Kent M., 1990. Measurements of dielectric properties of herring flesh using transmission time domain spectroscopy. International J. Food Sci. and Tech., 25, 26-38

Kopelman I. 1966. Transient heat transfer and thermal properties in

food systems, PhD.Thesis, Michigun State Univ. East Lausung, Michigan.

Komolprasert V. and Ofoli R.V., 1989. Mathematical modelling of microwave heating by the method of dimensional analysis. J.Food Processing and Preservation, 13, 87-106.

Kraszewki A., 1978. A model of the dielectric properties of wheat at 9.4Ghz. J.Microwave Power, 13, 293-296.

Kritikos H.W. and Schwan H.P., 1975. The distribution of heating potential inside lossy spheres, IEEE Transactions,.BME-22, 457-463.

Kruhl L., Attema E.P.W. and de Haan C.D., 1978. Modelling microwave heating processes, Proc. IMPI Conf. Ottawa, 77-79.

Kudra T., Raghvan V., Akeyl C., Bosisio R., van de Voort F, 1992, Electromagnetic properties of milk and its constituents at 2.45 GHz. J. Microwave power and Electromagnetic Energy, 27(4), 199-204.

Kudra T., Raghvan V., van de Voort, F., 1993, Microwave heating characteristics of rutile. J. App. Physics, 73(9), 4534-4540.

Larkin J.W. and Stefee J.F., 1987. Experimental errors associated with the estimation of thermal diffusivity from thermal process data. J.Food Sc., 52(2), 419-424,428.

Lau R.W.M., Sheppard R.J., 1986. The modelling of biological systems in three dimensions using the TDFD method, Phys. Med. Biol., 31(11), 1247-1256.

Lorenson C., 1990. The why's and how's of mathematical modelling for microwave heating, Microwave world, 11(1), 14-22.

Lozano J.E., Martin J., Rotstein E., 1979. Thermal conductivity of apples as a function of moisture content, J.Food Sc., 44, 11-13.

Marousis S.N., Karathanos V.N. and Saravacos G.D., 1991. Effect of physical structure of starch materials on water diffusivity, J.Food Processing and Preservation, 15, 183-191.

Martens T., 1980. Mathematical model of heat processing in flat containers, PhD thesis, University of Leuven, Belgium.

Maxwell C.J., 1904. A treatise on Electricity and Magnetism. Oxford University Press (Clarendon), London and New York.

McCance R.A. and Widdowson E.M., 1978. The composition of foods. Medical Research Council Special Report Series, revised by Paul A.A. and Southgate D.A.T., HMSO, London.

McWilliams M., 1989. Foods: Experimental perspectives. pub. Macmillan, New York.

Metaxas A.C., 1987. Heating with electromagnetic fields - a unified approach, Teaching monograph-4, pub. The Electricity Council, London.

Metaxas A.C. and Meredith R.J., 1983. Industrial microwave heating. pub. IEE Power Engineering Series.

Meakins R.J., 1961. Mechanisms of dielectric absorption in solids, Prog. Dielectrics, 3, 151-160.

Miles C.A., 1982. Heat transfer at the air/meat interface, Memorandum 53, Agricultural Research Council, Meat Research Institute, Bristol.

Miles C.A., Vanbeek G. and Veerkamp C.H., 1983. Calculation of thermophysical properties of foods in "Physical properties of Foods", ed. R.Jowitt et al., Applied Science Publishers, London.

Morita T.and Singh R.P., 1979. Physical and Thermal properties of short grain rough rice. Trans. ASAE, 22(3), 630-638.

Mudgett R.E., 1974. A physical chemical basis for prediction of dielectric properties of foods at ultra-high and microwave frequencies. PhD. thesis Massachusetts Institute of Technology, Cambridge, MA.

Mudgett R.E., Smith A.C., Wang D.I.C. and Goldblith S.A., 1974. Prediction of dielectric properties of non-fat milk at frequencies and temperatures of interest microwave processing. J. Food Sci. 39(1), 632-635.

Mudgett R.E., Goldblith S.A., Wang D.I.C. and Westphal W.B., 1977. Prediction of dielectric properties in solid foods of high moisture-content at ultra-high and microwave frequencies, J. Food Processing and Preservation, 1, 119-151.

Mudgett R.E., Goldblith S.A., Wang D.I.C. and Westphal W.B., 1979. Dielectric properties of frozen meats. J. Microwave Power, 14(4), 209-216.

Mudgett R.E., 1985. Modelling microwave-heating characteristics in "Microwaves in the food processing industry" ed. Decareau R.V., Academic Press, New York, 38-56.

Mudgett R.E., 1986. Microwave properties and heating characteristics of foods, Food Technology, 40, 86-98.

Mudgett R.E.,1990. Development in Microwave Food Processing in Biotechnology and Food Process Engineering, pub. Marcel and Dekker, Inc.New York.

Mukerjee R.N., 1966. Dielectric properties of some vegetable oils. Indian J. Tech., 4, 345-346.

Narayana K.B. and Krishnamurthi M.V., 1981. Heat and mass transfer characteristics and the evaluation of thermal properties of moist food materials. Trans.ASAE, 24, 789-793.

Nelson S.O. and Stetson L.E., 1975. 250Hz to 12GHz dielectric properties of grain and seed, Trans. ASAE, 18, 714-718.

Nelson S.O. and Stetson L.E., 1976. Frequency and moisture dependence of the dielectric properties of hard red winter wheat. J.Agri. Engng.Res., 21, 181-192.

Nelson S.O., 1978. Frequency and moisture dependence of the dielectric properties of high moisture corn, J. Microwave Power 13(2), 213-218.

Nelson S.O., 1980a. Frequency and moisture dependence of the dielectric properties of chopped pecans. ASAE paper (80-3051) ASAE St. Joseph MI, USA.

Nelson S.O., 1980b. Microwave dielectric properties of fresh fruits and vegetables. Trans. ASAE, 16(2), 384-400.

Nelson S.O., 1984. Moisture, frequency and density dependence of the dielectric constant of shelled, yellow-dent field corn. Trans. ASAE 27(5) 1573-1578,1585.

Nelson S.O., 1985. Constant of hard red winter wheat. Trans. ASAE 28(1), 234-238.

Nelson S.O., Prakash A. and Lawrence K., 1991. Moisture and Temperature dependence of the permittivities of some hydrocolloids at 2.45 GHz. J Microwave Power and Electromagnetic Energy, 26(3), 178-185.

Nelson S. 1991. Dielectric properties of agricultural products-Measurements and applications. IEEE Trans. on Electrical Insulation 25(5), 845-869.

Newborough M. and Probert S.D., 1990. Electromagnetic Heating - An inter disciplinary activity, IEE Proceedings, part A, 137(5), 280-286.

Nykvist W.E., and Decareau R.V., 1976. Microwave meat roasting. J. Microwave power, 11, 3-8.

Ofoli R.V. and Komolprasert V., 1988. On the thermal modelling of foods in electromagnetic fields, J. Food Process & Preserv, 12, 219-241.

Ohlsson T, 1981. Methods of measuring temperature distribution in microwave ovens, Microwave World, 2(2), 14-16.

Ohlsson T., 1988. Dielectric properties and microwave processing. Paper presented at the NATO Conference Food Properties and Computer-aided Engineering of Food Processing Systems. Porto 17-21,October.

Ohlsson T. and Bengtsson N.E., 1971. Microwave heating profiles in food, Microwave Energy, Appl. Newsletter, 4(6), 1-8.

Ohlsson T, Bengtsson N.E. and Risman P.O., 1974. Dielectric properties of foods at 3Ghz. as determined by a cavity perturbation technique. J. Microwave Power, 9(2), 129-145.

Ohlsson T. and Bengtsson N.E., 1975. Dielectric Food data for microwaves sterilization. J.Microwave Power, 10(1), 93-108.

Ohlsson T and Risman P.O., 1978. Temperature distribution of microwave heating-spheres and cylinders. J.Microwave Power, 13(4), 303-310.

Olver A.D., 1992. Microwave and Optical Transmission, Wiley & Sons Ltd. London.

O'Meara J.P., 1988. Using Science for consumer products: an ISMI-CAS connection, Microwave World, 9, 9-11.

O'Meara J.P., 1989. Variable Microwave power:a dilemma for the microwave-oven user, Microwave world, 10, 2-15.

Osepchuk J.M., 1984. A history of microwave-heating applications, IEE Trans. MTT-32(9), 1200-1233.

Pace W.E., Westphall W.B. and Goldblith S.A., 1969. Dielectric properties of commercial cooking oils. J. Food Sci., 33, 30-36.

Parkash S and Armstrong J.G., 1970. Measurement of dielectric constant of butter, Dairy Ind., 35(10), 688-689.

Parker R.E. and Stout B.A. 1967. Thermal properties of tart cherries. Trans. ASAE, 10(4), 489-495.

Patankar S.V., 1980. Numerical Heat Transfer and Fluid Flow. Hemisphere Publishing Corporation, London.

Peterson W.R. and Adams J.P.,1983. Water velocity effect on heat penetration parameters during institutional size retort pouch processing, J.Food Sci., 48, 457-460.

Perkin R.M., 1979. Prospectus of drying with rf and mw electromagnetic fields, J. Separation Process Technology 1(2), 14-24.

Pham Q.T., 1990. Prediction of thermal conductivity of meats and other animal products from composition data, in Engineering and Food Vol. 1-Physical Properties and Process Control, pub. Spiese Schibert, 410-423.

Platts J., 1991. in Microwave ovens ed. by Platts J., IEE state of the art digest 4, Peregrinus Ltd.,Oxford, 1-3.

Pomeranz Y. and Meloan C.E., 1987. Food Analysis: Theory and Practice, 2nd ed. Van Reinhold Nostrand Co., New York.

Ptitsyn S.D., Sekanov Y.P., and Batalin M.Y., 1982. Modelling the dielectric properties of grain. Mekhanizatsiya i Elektrifikatsiya Sel'skogo Khozyaistva, 12, 47-49.

Puranik S., Kumbharkhane A. and Mehrotra S., 1991. Dielectric mixture of honey-water mixtures between 10MHz-10GHz using time domain technique. J. Microwave power and Electromagnetic Energy, 26(4), 196-201.

Rao M.A. and Rizvi S.S., 1986. Engineering Properties of Foods, Marcel

Dekker Inc., New York.

Reidel L.,1969. Measurements of thermal diffusivity of foodstuffs rich in water, Kaltetechnic-Klimatisierung, 21(11), 315-316.

Risman P.O. and Ohlsson T., 1991. 2450 MHz microwave heating distributions in food material slab and cylinders. Mikrowellen & HF magazin, 17(3), 184-187.

Risman P.O., 1991. The role of TM_z cavity modes in MW ovens. SIKs Services-Serie, Nr.856. SIK GOTEBORG, Sweden.

Risman P.O., 1992a. Different types of microwave oven cavity modes and their interaction with food loads. Paper presented at 27th IMPI Symposium, August.

Risman P.O., 1992b. Metal in microwave oven. Microwave world, 13(1), 28-35.

Risman P.O., 1993. Private Communication.

Risman P.O., 1993. Dielectric data and measurements. J Microwave power and Electromagnetic Energy. 28(1), 1-2.

Roebuck B.D., Goldblith S.A. and Westphal W.B., 1972. Dielectric properties of carbohydrate mixtures at microwave frequencies. J Food Sci. 73, 199-204.

Rzepecka M. and Pereira R.R., 1974. Permittivity of some dairy products at 2450MHz. J. Microwave Power 9(4), 277-280.

Saravacos G.D., 1986. Mass transfer properties of foods. In Engineering properties of foods. ed. M.A.Rao and S.S.Rizvi, Marcel and Dekker, New York, 89-132.

Sayed El-Deek M. and Morsy M.N., 1984. Use of transmission-line-matrix method in determining the resonant frequencies of loaded microwave ovens. J. Microwave power, 19(1), 65-71.

Seaman R., and Seals J., 1991. Fruit pulp and skin dielectric properties for 150MHz-6400MHz, J. Microwave Power and Electromagnetic Energy, 26(2), 72-81.

Schneider P.J., 1963. Temperature response charts, John Wiely & Sons, Inc. New York.

Schiffmann R.F., 1986. Parameters in microwavable product development, Food Technology, 40(6), 93-98.

Schiffman R.F., Stein E.W. and Kaufmann H.B., Jr., 1971a. The microwave proofing of yeast raised doughnuts, Baker's Digest, 1, 55-61.

Schiffman R.F., Stein E.W. and Kaufmann H.B. Jr., 1971b. Dough-proofing method, U.S. Patent, 3,630,755.

Singh R.P., 1982. Thermal diffusivity in food processing. Food Technol. 36, 87-91.

Singh R.P. and Heldman D.R., 1984. Introduction to food engineering. Academic press, London.

Smyth C.P., 1955. Dielectric Behaviour and Structure, McGraw-Hill Book co., New York.

Stefens P and van Dommelen D., 1993. C.A.D software package for high frequency dielectric applications. J Microwave power and Electromagnetic energy, 28(1), 3-10.

Stuchly S.S , 1970. Dielectric properties of some granular solids containing water. J. Microwave Power, 5(2), 62-69.

Swami S., Mudgett R.E. and Keenan M.C., 1982. Temperature profiles in simulated high moisture foods. Paper presented at 17th Symp.Int. Microwave Power Inst., San Diego, California.

Sweat V.E. 1974. Experimental values of thermal conductivity of selected fruits and vegetables. J.Food Sc., 39, 1080-1084.

Sweat V.E. 1975. Modelling of thermal conductivity of meats. Trans. ASAE, (18), 564-568.

Taukis P., Davis E.A., Davis H.T., Gordan J., Talmon Y., 1987. Mathematical modelling of microwave thawing by the modified isotherm method. J. Food Sci. 52, 455-460.

The Times, 1990. Poisoning risk in home microwave oven used by caterers, Monday, Dec. 24, 9.

Tinga W., 1969. Multiphase dielectric theory applied to cellulose mixtures. PhD thesis, University of Alberta, Edmonton, Canada.

Tinga W., and Nelson S.O., 1973. Dielectric properties of materials for microwave processing, J. Microwave Power, 5(2), 62-68.

To E.C.H., Mudgett R.E., Wang D.I.C., Goldbltih, S.A. and Decareau, R.V., 1974. Dielectric properties of food materials. J. Microwave Power 9(4), 303-316.

Trans V.N. and Stuchly S.S., 1987. Dielectric properties of beef, beef-liver chicken and salmon at frequencies from 100-2500MHz. J.Microwave Power and Electromagnetic Energy, 22(1), 29-33.

Unklesbay N., Unklesbay K., Henderson J.B., 1980. Simulation of Energy used by infra red equipment with bentonite models of menu-items. J. Food Protection, 43(10):789-794.

Unklesbay N., Unklesbay K., Buergler D., and Stringer W., 1981. Bentonite water dispersion simulate food service energy consumption of sausage patties. J. Food Sci. 46, 1808-1812.

Vagenas G.K., Drouzas A.E., Kouris D.M. and Saravacos G.D., 1990. Predictive equations for thermophysical properties of plant foods, In Engineering and Food Vol.1-Physical Properties and process control. Pub. Spiese Schibert, 399-407.

Vanbeek H., 1976, Eigenschappen van voedingswaren Vademencum Koeltechniek, pub. P.C., Noordervliet, BV Zeist.

van de Voort F.R., Laureanno M., Smith J.R., 1987. Can. Inst. Food Sc. Technol. J, 20, 279-290.

van Dyke D., Wang D.I.C. and Goldsmith S.A., 1969. Dielectric loss factor of re-constituted ground beef: the effect of chemical composition. Food Technol., 23, 944-946.

von Hippel, A., 1954. Dielectrics and waves. John Wiley and sons, Inc. N.York.

Wadsworth J.I. and Spadaro H., 1969. Transient temperature distribution in whole sweet potato during immersion heating- 1.Thermal diffusivity of sweet potato. Food Technology, 23(2), 85-90.

Wang D.C.I. and Goldblith S.A., 1976. Dielectric properties of foods, Tech. Rep. TR 76-27-FEL. US Army Natick Development center, Natick, Massachusetts.

Walker C.M.B., Huizings, A.H., Voss, W.A.G. and Tinga, W.R., 1976. A system for controlled microwave heating of small samples, J. Microwave Power, II(1), 29-32.

Weimer J., 1992. An engineering work station for microwave food product development. Proceedings 27th Microwave power symposium, August 2-5, Washington D.C. 49-57.

Which?, Microwave Ovens. May-1991.

Which?, Microwave Ovens. March-1993.

Witsenburg E.C., 1949. Heating by high frequency fields: Induction Heating, Philips Tech. Rev., 11(6), 165-175.

Yamano Y., Ejiri K., EndoT., and Senda M., 1975. Heat processing into flexible packages with food simulated materials. Japanese J. Food Sci. Technol. 22, 199-203.

Yang S., 1989. Numerical and experimental studies of microwave heating patterns in lossy dielectric materials. PhD thesis, The University of Texas at Austin.

Zeng X, Faghri A., 1994. Experimental and numerical study of microwave thawing heat transfer for food materials. Trans ASME, J.Heat Transfer, 116, 446-445.

Zhu-Shou-zheng and Chan Han-kui, 1988. Power distribution analysis in rectangular microwave heating application with stratified load. J.

Microwave Power and Electromagnetic energy, 23(3), 139-143.

Zuercher J., Hoppie L., Lade R., Srinivasan S., and Misra D., 1990. Measurement of the complex permittivity of bread dough by an open-ended coaxial line method at ultra high frequencies, J.Microwave power and Electromagnetic energy, 25(3), 161-167.

APPENDIX 1

NATURE OF DIELECTRIC LOSS

An electric field **E**, induces a displacement field **D** in a dielectric which is proportional to the electric field;

$$D = \varepsilon_o \varepsilon_r E \qquad (A1.1)$$

Where ε_o is the permittivity of free space and ε_r is the relative permittivity of the material. To demonstrate the complex nature of ε_r, consider a sinusoidal a.c. electric field, $E = E_o e^{j\omega t}$, which can also be written as;

$$E = E_o \cos \omega t \qquad (A1.2)$$

Subsequently, **D** will also vary periodically but be displaced from E by a phase angle, ϕ;

$$\begin{aligned} D &= D_o \cos(\omega t - \phi) \\ &= D_o \cos \phi \cos \omega t + D_o \sin \omega t \sin \phi \\ &= D_1 \cos \omega t + D_2 \sin \omega t \end{aligned} \qquad (A1.3)$$

Because **D** is proportional to **E** and the ratio **D/ E** is usually frequency dependent, two frequency-dependent constants, $\varepsilon'(\omega)$ and $\varepsilon''(\omega)$ are required for interpretation;

$$\begin{aligned} D_1 &= \varepsilon_o \varepsilon' E_o \\ D_2 &= \varepsilon_o \varepsilon'' E_o \end{aligned} \qquad (A1.4)$$

Comparing the real and imaginary parts for **E**, it is deduced;

$$\begin{aligned} D &= E\,(\varepsilon' - j\varepsilon'')\varepsilon_o \\ &= \varepsilon_r^* \varepsilon_o E \end{aligned} \qquad (A1.5)$$

where, $\varepsilon_r^* = (\varepsilon' - j\varepsilon'')$. Now the total current density in a dielectric material due to the sinusoidal electric field (A1.2) is;

$$J = \sigma E + \frac{dD}{dt} \qquad (A1.6)$$

It is assumed that ε^* is real (i.e. $\varepsilon^* = \varepsilon' - j\,0$) and contributes to the stored energy and the losses are only due to conduction.

$$J = \sigma E + j\omega \varepsilon_o \varepsilon' E \qquad (A1.7)$$

Rearranging equation (A1.7)

$$J = j\omega\varepsilon_o(\varepsilon' - j\sigma/\omega\varepsilon_o)E \qquad \text{(A1.8a)}$$

Let $(\varepsilon' - j\sigma/\omega\varepsilon_o) = \varepsilon^*_{cond}$ because it only has conductive losses and

$$\varepsilon^*_{cond} = \varepsilon' - j\varepsilon''_{cond}$$

$$= j\omega\varepsilon_o(\varepsilon' - j\varepsilon''_{cond}) \qquad \text{(A1.8b)}$$

In free space where $\sigma = 0$, (7) becomes

$$= j\omega\varepsilon_o\varepsilon' E \qquad \text{(A1.9)}$$

Now ε^*_{cond} can be considered as an effective dielectric constant where conduction losses dominate (represented by the imaginary part) whereas the real part describes the amount of stored energy. By analogy any other form of losses (e.g.dipolar), can only be included into the imaginary part of the complex dielectric constant.

APPENDIX 2

Derivation of the modified wave equation for EM heating techniques

Considering the four Maxwell's equations;

$$\nabla \cdot E = 0; \qquad \nabla \times E = \frac{-\mu \, \partial H}{\partial t} \; ; \qquad \nabla \cdot H = 0; \qquad \nabla \times H = J + \frac{\partial D}{\partial t}$$

Ampere's Law;

$$\nabla \times H = \sigma E + \frac{\varepsilon \, \partial E}{\partial t} \qquad \text{(using } D = \varepsilon E \text{)} \qquad \text{(A2.1)}$$

which expresses the current-density flow in terms of a conductive and a displacement component. To develop the general solution for all types of material, take the curl of $\nabla \times E$ to obtain the following expression:

$$\nabla \times \nabla \times E = -\mu \frac{\partial}{\partial t} (\nabla \times H) \qquad \text{(A2.2)}$$

Substituting (A2.1) into (A2.2) yields:

$$\nabla \times \nabla \times E = -\sigma\mu \left(\frac{\partial E}{\partial t} \right) - \varepsilon\mu \left(\frac{\partial^2 E}{\partial t^2} \right) \qquad \text{(A2.3)}$$

Using the vector identity;

$$\nabla \times \nabla \times E = \nabla (\nabla \cdot E) - \nabla^2 E$$

For time-harmonic fields, $E = E \, e^{j\omega t}$, then (A2.2) yields;

$$-\nabla^2 E = -\mu \left[\varepsilon - \frac{\sigma \, j}{\omega} \right] \frac{\partial^2 E}{\partial t^2} \qquad \text{(A2.4)}$$

or:

$$= \mu \, \varepsilon_o \, K \frac{\partial^2 E}{\partial t^2} \qquad \text{(A2.5)}$$

where $K = (\varepsilon' - j\varepsilon''_e)$

Using the relationship between $\partial E/\partial t$ and $\partial^2 E/\partial t^2$, the equivalent form of the diffusion equation is:

$$\nabla^2 \mathbf{E} = j\omega\varepsilon_o K \frac{\partial \mathbf{E}}{\partial t} \qquad \text{(A2.6)}$$

Finally, because $\partial \mathbf{E}/\partial t = j\omega \mathbf{E}$, (A2.6) becomes:

$$= -\omega^2 \mu\varepsilon_o K\mathbf{E} \qquad \text{(A2.7)}$$

Similar equations for the other fields quantities **H** and **J** can be written. However, only one equation need to be solved as the other field quantities are related to one another via Maxwell's equations.

APPENDIX 3

Power generated in a dielectric

From Maxwell's current law:

$$\nabla \times H = \sigma E + j\omega\varepsilon_o \varepsilon E \qquad \text{(A3.1)}$$

Substituting $\varepsilon = \varepsilon' - j\varepsilon''$ into eqn. (A3.1), and grouping conductive and displacement losses together;

$$\nabla \times H = (\sigma + j\omega\varepsilon_o \varepsilon' + \omega\varepsilon_o \varepsilon'') E$$

$$= (\varepsilon_e'' + j\varepsilon')\omega\varepsilon_o E \qquad \text{where} \quad \varepsilon_e'' = (\varepsilon'' + \frac{\sigma}{\omega\varepsilon_o})$$

Now;

$$(\nabla \times H^*).E = \omega\, \varepsilon_o \varepsilon_e'' E.E^* - j\omega\varepsilon_o \varepsilon' E.E^*$$

$$= (\varepsilon_e'' - j\varepsilon')\, \omega\varepsilon_o E.E^* \qquad \text{(A3.2)}$$

Using Maxwell's law for $(\nabla \times E)$ and finding the dot product with H^* gives:

$$(\nabla \times E).H^* = -j\omega\mu_o \mu\, H.H^* \qquad \text{(A3.3)}$$

Subtracting (A3.2) from (A3.3) yields:

$$(\nabla \times E)^*.E - (\nabla \times^* H).E = -j\omega\mu_o \mu\, H^*.H + j\omega\varepsilon_o \varepsilon' E^*.E - \omega\varepsilon_o \varepsilon_e''\, E^*.E$$

(A3.4)

Integrating (A3.4) over a volume and using the divergence theorem, we get;

$$\int_v \nabla(E \times H^*)dV = \int_s (E \times H^*)dS'$$

$$= -j\omega \int_v (\mu_o \mu\, H.H^* - \varepsilon_o \varepsilon' E.E^*)dV - \int_v \omega\, \varepsilon_o \varepsilon_e''\, E.E^*\, dV$$

(A3.5)

Now the average power for a sinusoidally-varying EM field is half the real component of (A3.5), i.e.

$$P_v = \frac{1}{2} \omega \varepsilon_o \varepsilon''_e \int_v (\mathbf{E}.\mathbf{E}^*) \, dV \qquad \text{(A3.6)}$$

RELATIONSHIP BETWEEN POWER AND IMPEDANCE

Poynting vector, $\mathbf{S} = \mathbf{E} \times \mathbf{H}$ can be derived for a linear polarised plane wave, which has one electric field component E_z and one magnetic field component H_x, the complex poynting vector has only one component in the y direction (Fig.2.2 & 2.3), which is the direction of wave travel

$$\mathbf{S} = S_y = E_z \times H_x \qquad \text{(A3.7)}$$

Now substituting for E and H in the form of sinusoidal equations as (Chapter 2, eq2.8)

$$S_y = \frac{E_o^2}{\eta} \sin^2(\omega t - \beta y) \qquad \text{(A3.8)}$$

As described before the real part of S_y gives the power intensity in the plane transverse to the direction of propagation.

APPENDIX 4

Exact solution for the power generation in a thin slab for a DRH process

An exact one-dimensional solution for DRH is developed for the power generated in a wide rectangular slab of thickness 2b (see Fig. A4.1). The wave equation for J is;

$$\frac{\partial^2 J}{\partial y} = \gamma^2 J_x \qquad \text{(A4.1)}$$

where for metals, $\gamma^2 = j\omega\mu\sigma$ and the general solution is of the form;

$$J_x = A\, e^{y\gamma} + B\, e^{-y\gamma} \qquad \text{(A4.2)}$$

Boundary conditions; J_x is equal for $y = \pm b$, this gives

$$J_x = J_o \cosh(\gamma y) \qquad \text{(A4.3)}$$

At surface, $J_s = J_o \cosh(\gamma b)$ (A4.4)

The expression for the ratio of the current densities is;

$$\frac{J_x}{J_s} = \frac{\cosh \gamma y}{\cosh \gamma b} = \frac{\cosh (1+j)\alpha y}{\cosh (1+j)\alpha b} \qquad \text{(A4.5)}$$

Power intensity at the surface;

$$P_s = \frac{1}{2\sigma} \int_{-b}^{+b} |J_x|^2 \, dy \qquad \text{(A4.6)}$$

Substituting for J_x from (A4.5) and expanding cosh terms.

$$P_s = \frac{J_s^2}{2\sigma} \int_{-b}^{+b} \frac{\cosh 2\alpha y + \cos 2\alpha y}{\cosh 2\alpha b + \cos \alpha b} \qquad \text{(A4.7)}$$

$$= \frac{J_s^2}{2\alpha\sigma} \left[\frac{\sinh 2\alpha y + \sin 2\alpha y}{\cosh 2\alpha b + \cos 2\alpha b} \right]_{-b}^{+b} \qquad \text{(A4.8)}$$

$$= \frac{J_s^2}{2\alpha\sigma} \left[\frac{\sinh 2\alpha b + \sin 2\alpha b}{\cosh 2\alpha b + \cos 2\alpha b} \right] \qquad \text{(A4.9)}$$

for large αb (i.e. thickness of the slab, $2b \gg \delta$) the square bracket $\rightarrow \tanh \infty \cong 1$, so P_s tends to twice the value for the semi-infinite slab. Therefore, the slab can be analysed as two semi-infinite slabs.

Exact solution for the power generation in a thin slab for an IH process

An exact one-dimensional solution for IH is developed for the power generated in a wide rectangular slab of thickness 2b (see Fig. A5.1). The current density is due to the induced axial magnetic field;

$$\frac{\partial^2 H_x}{\partial y^2} = \gamma^2 H_x \qquad \text{(A5.1)}$$

The solution may be derived as for DRH i.e.

$$\frac{H_x}{H_s} = \frac{\cosh (1+j)\alpha y}{\cosh (1+j)\alpha b} \qquad \text{(A5.2)}$$

where H_s is the magnetic field strength at y=±b J_z may be expressed as;

$$J_z = H_s \alpha (1+j) \frac{\sinh (1+j)\alpha y}{\cosh (1+j)\alpha b} \qquad \text{(A5.3)}$$

Power intensity;

$$P_s = \int_{-b}^{+b} \frac{|J_z|^2}{2\sigma} dy \text{(A4.14)}$$

Substituting $|J_z|$ from (A5.3) and integrating we get;

$$P_s = \frac{\alpha H_s^2}{\sigma} \left[\frac{\sinh 2\alpha b - \sin 2\alpha b}{\cosh 2\alpha b + \cos 2\alpha b} \right] \qquad \text{(A5.4)}$$

Following the similar argument as in Appendix A.4, where slab is thick as compared to the skin depth (i.e. $2b \gg \delta$) $|J_s| \rightarrow (\sqrt{2})\alpha H_s$. The slab can be considered as two independent half slabs each behaving like semi-infinite slabs. This is correct to 1% accuracy for $2b > 5.3\delta$.

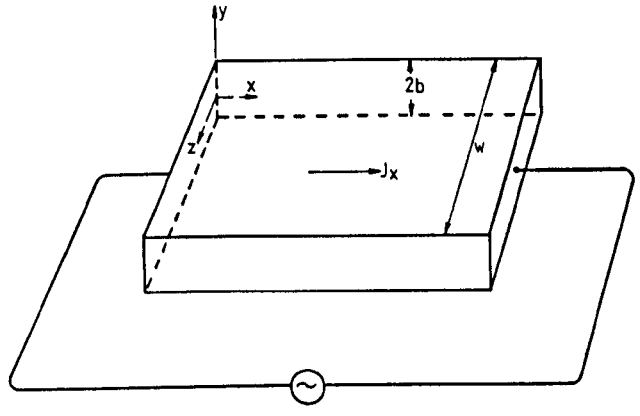

Fig.A4.1 Heating of slab of thickness 2b, by DRH

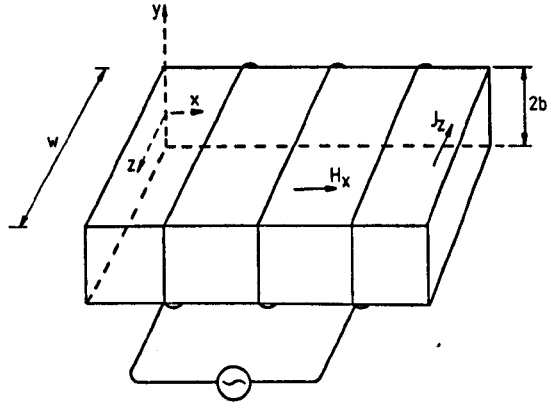

Fig.A5.1 Heating of rectangular slab of thickness 2b, by IH

APPENDIX 6

Formulation of the numerical method

For the one-dimensional problem, a portion of grid points is shown in Fig.A6.1, we seek to solve the following equation;

$$\frac{\partial T}{\partial t} = \frac{\partial}{\partial y}\left(\alpha_T(T)\frac{\partial T}{\partial y}\right) + \frac{P_v\,\alpha_T(T)}{k} \qquad (A6.1)$$

A general finite difference descretisation of the above heat equation in cartesian coordinates for an interior node is as follows:

A. Constant material properties

$$\frac{\Delta y}{\Delta t}\,(T_i^1 - T_i^0) = \theta\left[\frac{\alpha_{T1}\,(T_{i-1}^1 - T_i^1)}{\Delta y} - \frac{\alpha_{T2}\,(T_i^1 - T_{i+1}^1)}{\Delta y}\right] + \left(\frac{P_v\,\alpha_T}{k}\right)_i \Delta y$$

$$+(1-\theta)\left[\frac{\alpha_{T1}\,(T_{i-1}^0 - T_i^0)}{\Delta y} - \frac{\alpha_{T2}\,(T_i^0 - T_{i+1}^0)}{\Delta y}\right] \qquad (A6.2)$$

By rearranging (A6.2) to bring terms related to the volumetric rate of heat generation and all known temperatures at a current time (^{0}) to the R.H.S., the L.H.S. terms contain unknown temperature at the time (^{1})Δt as follows

$$-\theta\left(\frac{\alpha_{T11}}{\Delta y}\right) T_{i-1}^1 + \left\{\frac{\Delta y}{\Delta t} + \theta\left(\frac{\alpha_{T11}}{\Delta y} + \frac{\alpha_{T12}}{\Delta y}\right)\right\} T_i^1 - \theta\left(\frac{\alpha_{T11}}{\Delta y}\right) T_{i+1}^1$$

(A6.3a)

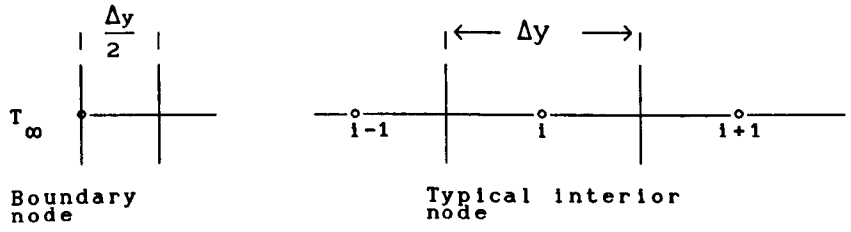

Fig.A6.1 Control volume for the internal and boundary nodes

while the R.H.S is:

$$(1-\theta)\left(\frac{\alpha_{T11}}{\Delta y}\right)T^{0}_{i-1} + \left\{\frac{\Delta y}{\Delta t} - (1-\theta)\left(\frac{\alpha_{T11}}{\Delta y} + \frac{\alpha_{T12}}{\Delta y}\right)\right\} T^{0}_{i} + (1-\theta)\left(\frac{\alpha_{T12}}{\Delta y}\right) T^{0}_{i+1}$$

$$+ \left(\frac{P_v\, \alpha_T}{k}\right)_i \Delta y \qquad \text{(A6.3b)}$$

Similarly for the surface node:

$$-\theta\left(\frac{h_c \alpha_{T11}}{k_i}\right)T^{1}_{\infty} + \left\{\frac{\Delta y}{2\Delta t} + \theta\left(\frac{h_c\, \alpha_{T11}}{k} + \frac{\alpha_{T11}}{\Delta y}\right)\right\} T^{1}_{i} - \theta\left(\frac{\alpha_{T11}}{\Delta y}\right) T^{1}_{i+1} =$$

$$(1-\theta)\left(\frac{h_c \alpha_{T11}}{k_i}\right)T^{0}_{\infty} + \left\{\frac{\Delta y}{2\Delta t} - (1-\theta)\left(\frac{h_c\, \alpha_{T11}}{k_i} + \frac{\alpha_{T11}}{\Delta y}\right)\right\} T^{0}_{i} +$$

$$(1-\theta)\left(\frac{\alpha_{T11}}{\Delta y}\right)T^{0}_{i+1} + \left(\frac{P_v\, \alpha_T}{k}\right)_i \Delta y \qquad \text{(A6.4)}$$

To handle the abrupt changes in thermal conductivity in a composite material, k, the interface conductivity was taken as the harmonic mean of the conductivities of the two adjacent nodes,[Patankar,1980] (Fig.A6.1)

$$k_{i,i-1} = \frac{2\,k_i k_{i-1}}{k_i + k_{i-1}} \qquad \text{and} \qquad k_{i,i+1} = \frac{2\,k_i k_{i+1}}{k_i + k_{i+1}} \qquad \text{(A6.5)}$$

B. Temperature dependent properties

Because of the temperature dependence of the thermal diffusivity, the partial differential equation (A6.1) becomes non-linear. For a α_T as a function of temperature;

$$\alpha_T(T) = a + bT + cT^2 \qquad \text{(A6.6)}$$

Equation (A6.1) becomes;

$$\frac{\partial T}{\partial t} = \alpha_T(T)\,\frac{\partial^2 T}{\partial y^2} + \frac{\partial T}{\partial y}\left\{ b\,\frac{\partial T}{\partial y} + c\,\frac{\partial T^2}{\partial y} \right\} + \frac{P_v\,\alpha_T(T)}{k} \qquad \text{(A6.7)}$$

The temperature dependent material properties were evaluated for the known temperature at the current time. Similarly, the power due to EM fieldis updated at each time step depending upon the dielectric properties at the known temperatures.

C. The 1-d equations for cylindrical and spherical geometries are as follows;

$$\frac{\partial T}{\partial t} = \frac{1}{r}\,\frac{\partial}{\partial r}\left(r\,\alpha_T(T)\frac{\partial T}{\partial r} \right) + \frac{P_v\,\alpha_T(T)}{k} \qquad \text{(A6.8)}$$

$$\frac{\partial T}{\partial t} = \frac{1}{r}\,\frac{\partial}{\partial r}\left(r\,\alpha_T(T)\frac{\partial T}{\partial r} \right) + \frac{P_v\,\alpha_T(T)}{k} \qquad \text{(A6.9)}$$

The discretization of equations (A6.8) and (A6.9) is the same as for cartesian coordinates ($\partial/\partial y$) is replaced by ($\partial/\partial r$) and there is an additional term for the first derivative ($\frac{1}{r}\frac{\partial r}{\partial r}$). For a 1-d sphere the additional term is ($\frac{2}{r}\frac{\partial T}{\partial r}$). However, at the axis of symmetry (i.e. when r=0, $\partial T/\partial r=0$), the term ($\frac{1}{r}\frac{\partial T}{\partial r}$) becomes indeterminate (= $\frac{0}{0}$). L'Hopital's rule was applied at r=0;

$$\frac{1}{r}\frac{\partial T}{\partial r} \rightarrow \frac{\partial^2 T}{\partial r^2} \quad \text{as } r \rightarrow 0$$

The discretized equations were represented in a matrix form to obtain the tridiagonal coefficient matrix [A]. (TDMA).

$$[A]\ [T^1] = [C] \qquad (A6.4)$$

where numerical values for the coefficients of matrix [C] are determined from the nodal temperatures at t=0.

$$\begin{vmatrix} b_1 + c_1 & & & & \\ a_2 + b_2 + c_2 & & & & \\ - & - & - & & \\ & a_i + b_i + c_i & & & \\ & & - & - & - \\ & & & a_n + b_n & \end{vmatrix} \begin{vmatrix} T_1 \\ T_2 \\ - \\ - \\ - \\ T_n \end{vmatrix} = 0$$

A direct solution method (Gauss-elimination) was used to solve the simultaneous equations at each time step. Unlike general matrix methods the TDMA requires computer storage and time proportional only to number of nodes. The code developed compresses the matrix so that only non-zero coefficients are stored, other coefficients being implicitly zero. The weighting factor θ can be chosen from 0 to 1. In the present calculations θ was taken 0.5 (Crank Nicolson). The numerically estimated temperatures distribution was smoothed by applying the quadratic least squares technique for each five successive nodes at each time increment. This ensured numerically stable solutions for a different values of the physical parameters used.

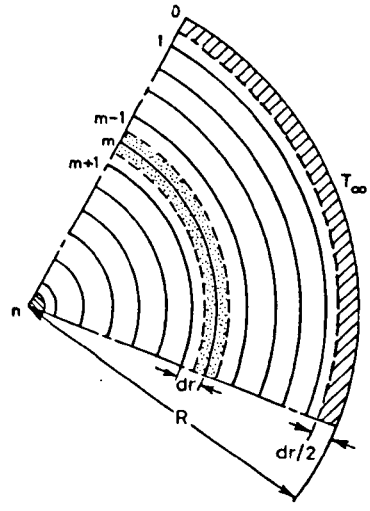

Fig A 6.2 Interior and boundary nodes for a sphere

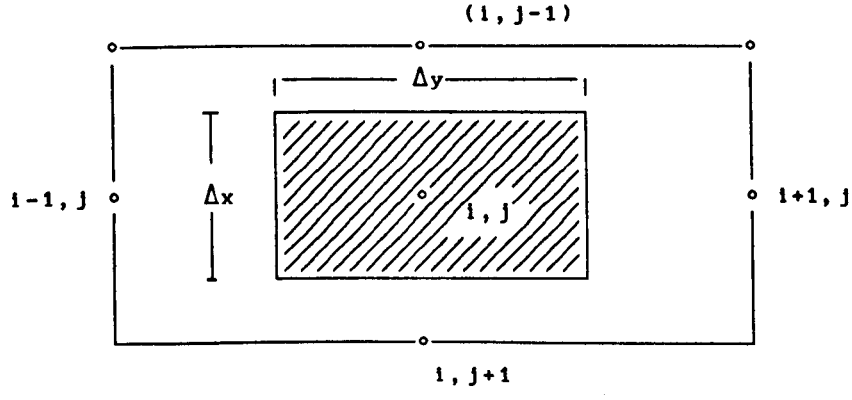

Fig. A7.1 Control volume for an interior node for a 2-d slab

APPENDIX 7

A portion of a two-dimensional grid is shown in Fig.A7.1. The spatial index j is used for the x-direction. For 2-d solutions the alternating direction implicit method (ADI) was used. The method represents one of the second order spatial derivatives fully implicitly and the other fully explicitly [Carnahan et al, 1969]. Similar equations as for 1-d was used for derivatives (i.e. explicit and implicit discretisation was obtained by substituting θ = 0 and 1 respectively). The time step was split into two parts. In the first half of the time step one of the spatial derivatives (in the y-direction) are expressed explicitly and in the x-direction implicitly. The direction was reversed in the next time step.

In the first step:

$$\frac{1}{\Delta t}\left(T^{1/2}_{i,j} - T^{0}_{i,j}\right) = \frac{\alpha_{T(i,j)}}{2\Delta y^2}\left[\left(T^{0}_{i-1,j} - T^{0}_{i,j}\right) - \left(T^{0}_{i,j} - T^{0}_{i+1,j}\right)\right] + \left(\frac{P_v \alpha_T}{k}\right)_{i,j}$$

$$\frac{\alpha_{T(i,j)}}{2\Delta x^2}\left[\left(T^{1/2}_{i,j-1} - T^{1/2}_{i,j}\right) - \left(T^{1/2}_{i,j} - T^{1/2}_{i,j+1}\right)\right] \qquad \text{(A7.1)}$$

In the second step

$$\frac{1}{\Delta t}\left(T^{1}_{i,j} - T^{1/2}_{i,j}\right) = \frac{\alpha_{T(i,j)}}{2\Delta y^2}\left[\left(T^{1}_{i-1,j} - T^{1}_{i,j}\right) - \left(T^{1}_{i,j} - T^{1}_{i,j+1}\right)\right] + \left(\frac{P_v \alpha_T}{k}\right)_{i,j}$$

$$\frac{\alpha_{T(i,j)}}{2\Delta x^2}\left[\left(T^{1/2}_{i,j-1} - T^{1/2}_{i,j}\right) - \left(T^{1/2}_{i,j} - T^{1/2}_{i,j+1}\right)\right] \qquad \text{(A7.2)}$$

The only unknown temperatures in (A7.1) are at nodes i,j; i,j-1; i,j+1 for the first time step and at i,j; i-1,j; and i+1,j for the second time step. Similarly, the discretised equations for boundary conditions were obtained. In each case, a tridiagonal matrix was formed which was solved as the one dimensional case. The method is consistent after two time steps have been completed. The same space increment was used in the x and y direction. However, the algorithm allows for different Δx and Δy.

APPENDIX 8

Least-Squares Approximation

a. Discrete data

Let $P_m(x)$ be a polynomial of order m ($m \leq n$) that approximates to the function y(x). Let $e_i = p(x_i) - y_i$ be the error between the predicted value p(x) of the equation x_i and the measured value y_i at x_i. The criterion used to find a suitable function $p(x)_n$ is the weighted least squares approximation which is to minimise $\sum_{i=1} w_i e_i^2$, where the weights w_i (i=1,2,.....n) are given positive numbers. The inclusion of weights permits varying degrees of importance to be attached to different data points. However, if equal importance is to be given to all the data points then we can set $w_i = 1$ (i=1,2,....n). Other assumptions about the data are (i) all observations of y have the same (though unknown) variance, otherwise the weighted least-squares should be used; (ii) there are no errors in the x-values; and (iii) the distribution of the errors is normal or nearly normal.

For illustration purposes, let the approximating equation be a straight line (m = 1) $p_1(x) = a_0 + a_1 x$ then;

$$E(a_0, a_1) = \sum w_i [y_i - p_1(x_i)]^2 \qquad \text{(A8.1)}$$

Forming the minimising equations by differentiating the above equation for E with respect to a_0 and a_1 respectively, we obtain

$$\frac{\partial E}{\partial a_0} = -2 \sum w_i [y_i - (a_0 + a_1 x_i)] = 0 \qquad \text{(A8.2)}$$

$$\frac{\partial E}{\partial a_1} = -2 \sum w_i [y_i - (a_0 + a_1 x_i)] x_i = 0 \qquad \text{(A8.3)}$$

These equations can be rearranged to give the following set of linear algebraic equations $\mathbf{Aa} = \mathbf{b}$, where $\mathbf{a}$ is the vector of the unknowns a_j's. Vector $\mathbf{b}$ and the square matrix A are given by the following;

$$A = \begin{bmatrix} \Sigma w_i & \Sigma w_i x_i \\ \Sigma w_i x_i & \Sigma w_i x_i^2 \end{bmatrix} \qquad \mathbf{b} = \begin{bmatrix} \Sigma w_i y_i \\ \Sigma w_i y_i x_i \end{bmatrix}$$

These equations were solved using the Gauss-Elimination method. The polynomial p(x) can also be exponential or any other type that the data may suggest.

b) Statistics of the estimators
In order to provide some measure of the uncertainty in the fitted values the coefficient of determination r^2 was used;

$$r^2 = \frac{\sum (\bar{y}_{xi} - \bar{y})^2}{\sum (y_i - \bar{y})^2} \qquad \text{(A8.4)}$$

c) Multivariable Data.

The general equation with K number of independent variables,

$$\underline{x}_k = [\underline{x}_1 , \underline{x}_2 , ..., \underline{x}_{n(k)}] \text{ , for } k = 1 \text{ to } K,$$

where n(k) depends on the value of k, has the form;

$$Y_j = \alpha_0 + \sum_{k=1}^{K} \alpha_k p_{mk} (x_k) \qquad \text{(A8.5)}$$

The functions p_{mk} are known, constant free functions of the independent variables x_i. The method of approximating coefficients, α_k is the same as for the one variable case.

APPENDIX 9

Other empirical equations for thermal properties compared with the selected data:

Equation	Reference
a) Specific heat, C_p, ($kJkg^{-1}K^{-1}$)	
1. $0.0418m+0.0209F+0.012S$	Charm, 1963
2. $0.042m+0.019(p+F)+.0122c$	Vanbeek, 1976
3. $0.042m+0.0155p+0.0168F+0.008A+0.014c$	Singh & Heldman 1984
b) Thermal conductivity, k, ($Wm^{-1}k^{-1}$)	
4. $0.0057m+0.0801$ (cooked vegetables & meats)	Bowman,1970
5. $0.283-.0256.e^{-0.0206m}$ (apple)	Lozano, 1979
c) Mixture Models for thermal conductivity k of the mixture is;	
6. $k_c V_c + (1-V_c)k_s$	Martens, 1980
7. $\left\{\frac{1-[1-a(k_s/k_c)b}{1+(a-1)b}\right\}k_c$	Maxwell,1904

(where $a = 3k_c/(2k_c+k_s)$, $b = V_s/(V_c+V_s)$)

8. $k_c \frac{1-V_c^2}{1-V_c^2(1-V)}$ (isotropic two-phase system) — Kopelman,1966

9. $k_c(1-V_c^2(1-k_s/k_c)$ (anisotropic parallel) — Kopelman, 1966

10. $k_c\{1-V_c(1-k_s/k_c)\}$ (layers parallel) — Kopelman, 1966

APPENDIX 10

MATHEMATICAL MODEL FOR MICROWAVE HEATING OF FOODS

Maxwell's equation (A1.7) in the full differential form is as follows

$$\frac{\partial^2 \mathbf{E}}{\partial x^2} + \frac{\partial^2 \mathbf{E}}{\partial y^2} + \frac{\partial^2 \mathbf{E}}{\partial z^2} + \gamma^2 (E_x \mathbf{x} + E_y \mathbf{y} + E_z \mathbf{z}) = 0 \qquad \text{(A10.1)}$$

Applying the restriction that $\partial/\partial y = \partial/\partial x = 0$ and $E_y = 0$, for plane wave propagating in the y-direction we get

$$\frac{\partial^2 E_x}{\partial y^2} + \gamma^2 E_x = 0 \qquad \text{(A10.2a)}$$

$$\frac{\partial^2 E_z}{\partial y^2} + \gamma^2 E_z = 0 \qquad \text{(A10.2b)}$$

The solution for the E-field distribution in an arbitrary direction is given (subscripts are therefore omitted). The composite slab of length 2L in the direction of propagation is divided into n-layers of Δy (Fig. A10.1). Each layer may have different dielectric properties which may also be temperature dependent. Real and imaginary components of the E-field and propagtion factor are separated and equated to provide the following

$$\frac{d^2 u(y)}{d y^2} + \mathrm{Re}[\gamma^2]\, u(y) + \mathrm{Im}[\gamma^2]\, v(y) = 0 \qquad \text{(A10.3)}$$

$$\frac{d^2 v(y)}{d y^2} + \mathrm{Re}[\gamma^2]\, v(y) - \mathrm{Im}[\gamma^2]\, u(y) = 0 \qquad \text{(A10.4)}$$

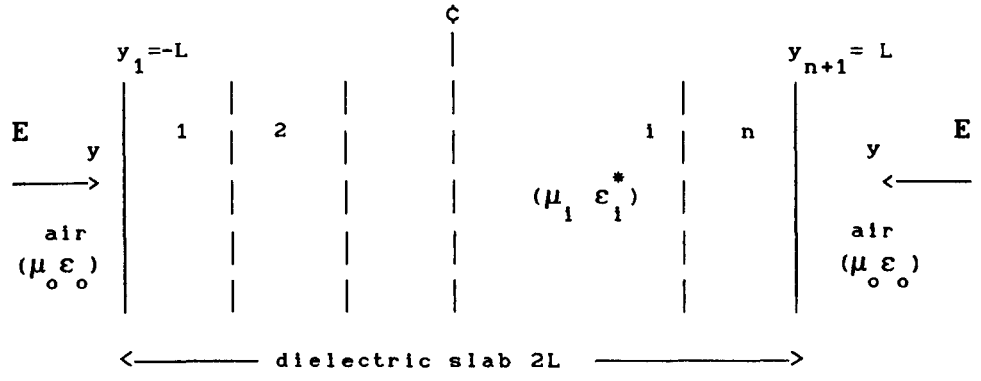

a. Slab exposed to radiation from both sides

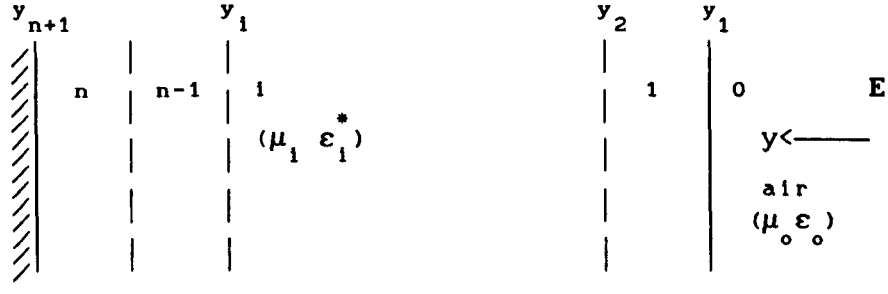

b. Reflective boundary at one end, i.e. $E_{n+1} = 0$

Fig.A10.1 Heating of slab by plane waves

where, u(y) and v(y), the real and imaginary comopnents of normalised electric field, e(y).

$$e(y) = \frac{E}{E_o} \quad , \qquad y = \frac{y_i + L}{2L} \tag{A10.5}$$

and real and imaginary parts of γ respectively are

$$\text{Re } [\gamma^2] = 4L^2 \gamma_o^2 \varepsilon'(T) \tag{A10.6a}$$

$$\text{Im } [\gamma^2] = 4L^2 \gamma_o^2 \varepsilon''(T) \tag{A10.6b}$$

The boundary conditions were also separated into real and imaginary components (for radiating boundaries)

At y = 0

$$\frac{d\,u(y)}{d\,y} - 2\,\gamma_o L\, v(y) = 4\gamma_o\, L \sin(\gamma_o\, L) \tag{A10.7a}$$

$$\frac{d\,v(y)}{d\,y} + 2\,\gamma_o L\, u(y) = 4\gamma_o\, L \cos(\gamma_o\, L) \tag{A10.7b}$$

and at y = 1

$$\frac{d\,u(y)}{d\,y} + 2\,\gamma_o L\, v(y) = -4\gamma_o\, L \sin(\gamma_o\, L) \tag{A10.8a}$$

$$\frac{d\,v(y)}{d\,y} - 2\,\gamma_o L\, u(y) = -4\gamma_o\, L \cos(\gamma_o\, L) \tag{A10.8b}$$

For a reflective boundary

$$\left.\begin{aligned} u(y) &= 0 \\ v(y) &= 0 \end{aligned}\right\} \quad \text{at } y = 1 \text{ (or 0)} \qquad \text{(A10.8)}$$

The differential equations discretised by finite-difference method are as follows

For interior nodes ($2 \le i \le n$)

$$u_{i-1} - 2u_i + u_{i+1} + s_i u_i + t_i v_i = 0 \qquad \text{(A10.9a)}$$

$$v_{i-1} - 2v_i + v_{i+1} + s_i v_i - t_i u_i = 0 \qquad \text{(A10.9b)}$$

Boundary nodes ($i=1, n+1$) (radiating boundary)

$$-u_i + u_{i-1} + c_i v_i = 0 \qquad \text{(A10.10a)}$$

$$-v_i + v_{i-1} - c_i u_i = 0 \qquad \text{(A10.10b)}$$

Thus we get (n+1) equations for real and (n+1) equations for imaginary components of the E-field vector, to be solved simultaneously.

$$\left.\begin{aligned} A\,\underline{u} + B\,\underline{v} &= \underline{r1} \\ -B\,\underline{u} + A\,\underline{v} &= \underline{r2} \end{aligned}\right\} \qquad \text{(A10.11)}$$

or in matrix notation

$$\begin{pmatrix} (A) & (B) \\ (-B) & (A) \end{pmatrix} \begin{pmatrix} (\underline{u}) \\ (\underline{v}) \end{pmatrix} = \begin{pmatrix} (\underline{r1}) \\ (\underline{r2}) \end{pmatrix}$$

where A and B are (n+1)x(n+1) matrices and $\underline{u}$, $\underline{v}$, $\underline{r1}$ and $\underline{r2}$ are (n+1) column vectors.

a) Radiation from both sides

$$A = \begin{pmatrix} -1 & 1 & & & \\ 1 & (s_2-2) & 1 & & \\ & & & & \\ & & 1 & (s_n-2) & 1 \\ & & & 1 & -1 \end{pmatrix} \quad \text{and} \quad B = \begin{pmatrix} c_1 & 0 & 0 & & \\ 0 & t_2 & 0 & & \\ & & & & \\ & & & t_n & 0 \\ & & & 0 & c_{n+1} \end{pmatrix}$$

$$\underline{u} = \begin{pmatrix} u_1 \\ - \\ - \\ \\ u_{n+1} \end{pmatrix}, \quad \underline{v} = \begin{pmatrix} v_1 \\ - \\ - \\ \\ v_{n+1} \end{pmatrix}, \quad \underline{r1} = \begin{pmatrix} 0 \\ 0 \\ 0 \\ 0 \end{pmatrix} \quad \text{and} \quad \underline{r2} = \begin{pmatrix} -2\gamma_o e \\ 0 \\ 0 \\ -2\gamma_o e \end{pmatrix}$$

b. Reflecting boundary

$$A = \begin{pmatrix} -1 & 1 & & & \\ 1 & (s_2-2) & 1 & & \\ & & & & \\ & & & & 1 \\ & & & 1 & (s_n-2) \end{pmatrix} \quad \text{and} \quad B = \begin{pmatrix} c_1 & 0 & 0 & & \\ 0 & t_2 & 0 & & \\ & & & & \\ & & & & 0 \\ & & & 0 & t_n \end{pmatrix}$$

$$\underline{u} = \begin{pmatrix} u_1 \\ - \\ - \\ \\ u_n \end{pmatrix}, \quad \underline{v} = \begin{pmatrix} v_1 \\ - \\ - \\ \\ v_n \end{pmatrix}, \quad \underline{r1} = \begin{pmatrix} 0 \\ 0 \\ 0 \\ 0 \end{pmatrix} \quad \text{and} \quad \underline{r2} = \begin{pmatrix} -2\gamma_o e \\ 0 \\ 0 \\ 0 \end{pmatrix}$$

where, $s_i = \gamma_o^2 \, \varepsilon'(T,y_i) \, \Delta y^2$

$t_i = \gamma_o^2 \, \varepsilon''(T,y_i) \, \Delta y^2$

$c_1 = c_{n+1} = \gamma_o \Delta y$

The resulting tridiagonal matrix was solved for real (u) and imaginary (v) components of E-field at each point using Gauss-elimination method.

The power absorbed in the ith layer was obtained by substituting for the electric field and integrating from the adjacent nodal points (e.g. y_i to y_{i+1})

$$P_{av} = \frac{\omega \varepsilon_o E_o^2}{2\Delta y} \int_{y_i}^{y_{i+1}} \varepsilon''(y) \left\{ u^2(y) + v^2(y) \right\} dy \qquad \text{(A10.12)}$$

$$P_{av} = \frac{\omega \varepsilon_o E_o^2}{2\Delta y} \left[\varepsilon''_i \left\{ u_i^2 + v_i^2 \right\} + \varepsilon''_{i+1} \left\{ u_{i+1}^2 + v_{i+1}^2 \right\} \right] \qquad \text{(A10.13)}$$

The heat generation term P_v at the i^{th} node was obtained by averaging the power dissipated in the adjacent layers

$$P_v = \frac{1}{2} \left(P_{av\,i} + P_{av\,i+1} \right) \qquad \text{(A10.14)}$$

To obtain the distribution of E-field component in either dimension the similar procedure was employed, and the power absorbed

$$P_v = P_v(x) + P_v(y) \qquad \text{(A10.13)}$$

Temperature distribution: P_v thus obtained was substituted in the heat diffusion equation and the temperature distribution was obtained by solving the equations as described in Apendices 6 and 7.

$$\nabla (k(T) \nabla T) + P_v = \rho_d C_p \frac{\partial T}{\partial t} \qquad \text{(2.34)}$$

Equations (A10.2) were solved to obtain the heat source term for (2.34) and the resulting temperature evoultion in a material due to microwave heating is obtained. Thus the heat equation is coupled to the wave equation via heat generation term.

APPENDIX 11

Hydrophilic Materials

Hydrophilic polymeric materials were discovered in the early 1960'sat the Institute of Macro Molecular Research in Czechoslovakia and subsequently have been developed for use as soft contact lenses. These may be produced by bulk polymerisation. Hydrophilic material may be classified according to the polar bond existing

a) Polyhydroxyethylmethacrylate (HEMA)
The water attracting centres results mainly from the electro-negativity of the oxygen.

b) N-vinyl, 2, pyrrolidone
The water attracting centres are due to the polarity of carbon-nitrogen bond.

c) Combination of pyrrolidone and hydroxyethyl functions
The co-monomers gather the properties of both previous groups.

In the presents tests 40% hydrogel belongs to *(a)* and 75% belongs to *(b)*. For details see Highgate [1989].

```
      program mwheat
c program calculates the temperature distribution across a
c dielectric slab irradiated with microwave radiation from both
c sides
c ***************************************************************
c *              Variables                                      *
c * Constants                                                   *
c * omega   = angular frequency                                 *
c * rmu     = magnetic permeability                             *
c * epsilon = permittivity of free space                        *
c * pnot    = input power (Wm^-2)
c *  w1     = on time (s)
c *  w2     = duty cycle (s)
c *  hc     = heat transfer coefficient (W m^-2K^-1)
c * Tini  = Initial temperature (°C)
c *  Tamb   = ambient temperature (°C)
c *  cond   = thermal conductivity (Wm^-1K^-1)
c *  diff   = thermal diffusivity (m^2s^-1)
c *       h = length (m)
c *       w = width (m)
c      d = depth (m)
c *
c *Parameters
c *nx = number of nodes in x-direction, n2x = 2(nx)+1
c *ny = number of nodes in y-direction, n2y = 2(ny)+1
c
      dimension a1(ny,ny), a2(ny,ny),cre(ny,ny),cie(ny)
     &          ,a(n2y,n2y),b(n2y), sj(ny), tj(ny), pav(ny)
c
     dimension T(ny), cond(ny), diff(ny)
c    dimension t(ny,nx), cond(ny,nx), diff(ny,nx)
     &
c delt  set value for machine zero
c     delta    = 1e-9
      n1       = n2y
      pi       = 3.1416
      rmu      = 4*pi*1e-7
      epsilon  = 8.854*1e-12
        omega    = 2*pi*2.45*1e9
C C OUTPUT FILES
     OPEN (10,FILE='output.dat',STATUS='old')
     open (12,file='graph.csv',status='old')
     open (13,file='new.dat',status='old')
c
c INPUT DATA
c datslab contains geometrical data and calculates nodal volume and
c area
c
      CALL DATmat (n,dy,Ar,VOL,TVOL,1,1m,n)
        WRITE (10,420)
        WRITE (10,412)
c
c material properties; conductivity, dielectric constant, dielectric
loss factor (or predictive equation constants & parameter) convective c
coefficient from data file
        OPEN(1,FILE='PROP.DAT',STATUS='OLD')
        READ(1,*) pnot,tamb,tini,timstop
```

```
          read(1,*) hc, w1, w2
          read(1,*) cre11, cre12, cre13, cre14 (1 layer)
          read(1,*) cie11, cie12, cie13, cie14
          read(1,*) cond11, cond12, diff11, diff12
c          read(1,*)   cre21,    cre22,    cre23,    cre24(2nd    layer)
c
       read(1,*) cie21, cie22, cie23, cie24
     read(1,*) cond21,  cond22,  diff21,  diff22
     read(1,*) cre31, cre32, cre33, cre34 (3rd layer)
     read(1,*) cie31, cie32, cie33, cie34
     read(1,*) cond31, cond32, diff31, diff32
 c
          CLOSE (1)
 c         print *, 'data read'
 c
 c centre point, 1/4  and 3/4 point:or can be adjusted to obtain temp. c
 at material boundaries
          np1 = n+1
          nm1 = n-1
          n2  = n*2
          mr  = 1
          mn  = n2+mr
          nb2 = int(np1/2)
          ix  = int((np1/4)+1)
          iy  = int((np1/2)+1)
            iz  = int((3*np1/4)+1)
 c c time-step set at tstep sec and kT is printing parameter.
 c initial temp. at nodes
      DO  5 I=1,Np1
          t(i) = TINI
5      CONTINUE
       itime = int(time)
       write (10,510) itime,t(1),t(ix),t(iy),t(iz),t(np1)
 c
          c1    = omega*(rmu*epsilon)**.5 *dy
          c2    = rmu*epsilon*(omega*dy)**2
          enot  = (pnot * 377 * 2)**.5
          edz   = 2*enot
          edzc1 = edz*c1
        wepsln = omega*epsilon
 c
200        KLAST = 1e6
          TIME  = 0
 c biot number
 c conductivity and diffusivity can be input as constant values or put
 c variables ans constant from predictive equations for each layer
          lm1=l-1
    do i=1,lm1
          if (tini .le. 0) then
            cond(i) = cond11+t(i)*cond12
            diff(i) = diff11+t(i)*diff12
          else
                diff(i)  = diff13+t(i)*diff14                    cond(i) =
 cond13+t(i)*cond14
          endif
 c             bio    = hc*dz/cond(1)
 c             biota = bio*tamb
```

```
 c set fourier number or tstep
 c           fo(i)= diff*tstep/dy**2
c           tstep = .35*dy**2/diff
    continue
 c for other layers
       lp1=l+1
         lmm1 =lm-1 do i=lp1, lmm1
         if (tini .le. 0) then
           cond(i) = cond21+t(i)*cond22
           diff(i) = diff21+t(i)*diff22
         else
                diff(i)  = diff23+t(i)*diff24                    cond(i) =
 cond23+t(i)*cond24
         endif
 c            bio   = hc*dz/cond(1)
 c            biota = bio*tamb
 c set fourier number or tstep
 c           fo(i)= diff*tstep/dy**2
          tstep = .35*dy**2/diff
    continue
c
         lmp1 =lm+1 do i=lmp1, n
         if (tini .le. 0) then
           cond(i) = cond31+t(i)*cond32
           diff(i) = diff31+t(i)*diff32
         else
                diff(i)  = diff33+t(i)*diff34                    cond(i) =
 cond33+t(i)*cond34
         endif
 c            bio   = hc*dz/cond(1)
 c            biota = bio*tamb
 c set fourier number or tstep
 c           fo(i)= diff*tstep/dy**2
          tstep = .35*dy**2/diff
   continuec common nodes
 cond(1) = (2*(cond(lm1)*cond(lp1))/(cond(lm1)+cond(lp1)
 cond(lm)=(2*(cond(lmm1)*cond(lmp1))/(cond(lmm1)+cond(lmp1)
 diff(1)=(diff(lm1)+diff(lp1))/2
 diff(lm)= (diff(lmm1)+diff(lmp1))/2
 c
 c Start the time loop
      kflag1 = int((w1+1e-3)/tstep)
      kflag2 = int((w2+1e-3)/tstep)
      print *, 'transient begins'
     DO 100  K=1,KLAST
         TIME  = TSTEP*FLOAT(k)
         itime = int(time)
      mw = 0
     if(mod(k-1,kflag2) .lt.kflag1) mw = 1
     if (mw .eq. 0) goto 129
 c
 cCalculation of electric-field (y-direction)
c  1-layer
      do 10 i=1,lm1
       if (t(i) .lt. 0) then
         cre(i) = cre11 + cre12 * t(i)
         cie(i) = cie11 + cre12 * t(i)
```

```
        else
          cre(i) = cre13 + cre14 * t(i)
          cie(i) = cie13 + cie14 * t(i)
        endif
  c
  c      'dielectric constant updated'
  c calculation of multiplying variables
               sj(i) = c2*cre(i)
               tj(i) = c2*cie(i)
  10       continue
c 2-layer
      do 20 i=lp1,lmm1          if (t(i) .lt. 0) then
          cre(i) = cre21 + cre22 * t(i)
          cie(i) = cie21 + cre22 * t(i)
        else
          cre(i) = cre23 + cre24 * t(i)
          cie(i) = cie23 + cie24 * t(i)
        endif
  c      'dielectric constant updated'
  c calculation of multiplying variables
               sj(i) = c2*cre(i)
               tj(i) = c2*cie(i)
  20       continuec 3-layer
      do 30 i=lmp1,n          if (t(i) .lt. 0) then
          cre(i) = cre31 + cre32 * t(i)
          cie(i) = cie31 + cre32 * t(i)
        else
          cre(i) = cre33 + cre34 * t(i)
          cie(i) = cie33 + cie34 * t(i)
        endif
c      'dielectric constant updated'
c calculation of multiplying variables
               sj(i) = c2*cre(i)
               tj(i) = c2*cie(i)
  30       continue
  c interface nodes
     cre(l)  =(cre(lm1)+cre(lp1))/2
     cie(l)=(cie(lm1)+cie(lp1))/2
     cre(lm)= (cre(lmm1)+cr2(lmp1))/2   cie(lm)=(cie(lmm1)+cie(lmp1))/2
       print *, 'matrix a1'
  cc  set matrix a1
        do  i = 1,n
        do  j = 1,n
         a1(i,j) = 0
         a2(i,j) = 0
      continue
c
        a1(1,1)   = -1
        a1(1,2)   = 1
        a1(2,1)   = 1
        a1(2,2)   = sj(2)-2
        a1(2,3)   = 1
        a1(n,nm1) = 1
c depends on the boundary condition
         a1(n,n)   = sj(n)-2
  c       a1(n,n)   = -1
c set
```

```
      do 50 i=3,nm1
        a1(i,i-1) = 1
        a1(i,i)   = sj(i)-2
        a1(i,i+1) = 1
 50     continue
 cc set matrix a2
c          print *, 'matrix a2'
        a2(1,1) = c1
     do 60 i = 2,n
        a2(i,i) = tj(i)
 c        a2(i,i) = c1
 60     continue
 c r.h.s vector
      do 70 i=1,n
        b(i)   = 0
        b(i+n) = 0
        do 70 j=1,n
          a(i,j)     =  a1(i,j)
          a(n+i,j)   = -a2(i,j)
          a(i,n+j)   =  a2(i,j)
          a(n+i,n+j) =  a1(i,j)
 70     continue
        b(n+1) = -edzc1
c       b(n,n) =  edzc1
 c
       do 80 i=1,n2
            a(i,n2+1) = b(i)
  80     continue
 c
 c      do 81 i =1,n2
 c            write (10,*) (a(i,j), j=1,n2), b(i)
 c 81   continue
c
 c       print *, 'solving '
     call gauss(n1,n2,mr,mn,a,delt)
 c       print * , 'solution          A               B'
 c       write(13,*)'Solution         A               B'
 c       do 90 i=1,n
 c        print * , a(i,n2+1),a(i+n,n2+1)
 c
 c 90    continue
 c      print *, ' power calculation'
 c power absorbed per nodal volume W/m^3
 c
       do 113 i=1,n
       pav(i)  = wepsln/4*(cie(i)*(a(i,n2+1)**2 + a(i+n,n2+1)**2) +
    &           cie(i+1)*(a(i+1,n2+1)**2  + a(i+1+n,n2+1)**2))
113    continue
 c **
 c HEAT-TRANSFER CALCULATIONS
 129        print *, 'heat transfer '
 c  do i=1,ny
 c  do j=1,nx
 c ld for alternating direction: 1=y, 2=x
 c  do ld=1,2
    if (ld .eq.1) then
       do 618 i=1,np1
```

```
            bio      = hc*dy/cond(1)
            biota    = bio*tamb
            fo(i)    = diff*tstep/dy**2
          endif
           if (fo(i) .gt. .35) goto 99
  618     continue
  c calculating temp. rise after time-step and next tstep
  call setmat1 (cond, diff, tstep, tamb, dy, h1,hn, n, pav, ar,
  +            vol, t, a,b)
 call tridia (a,b,t,n)
c if (ld.eq.2) then
c call setmat2(cond, diff, tstep, tamb, dx, n, pav, ar,
c  vol, t, a,b)
c call tridia
c mean bulk temperature
           tblk = 0
    do i=1,n
c   do j=1,nx
c    tblk=tblk+t(i,j)
            tblk = tblk + t(i)
    continue
           tmb = tblk/n
c           tmb = tblk/ny*nx
         print *, tmb
c
c  if (itime .ge. timstp) goto 75
c  if (itime .ge. tstop ) goto 75
  if (itime .ge jlast) goto 75
    write (10, 510) itime, t(1), t(ix), t(iy), t(iz) , t(n)
      write(13,*) 'time',',', itime
      write (13,*) 'node  ,  power absorbed '
       do 531  i=1,np1
          xi = dy*(i-1)
      write(12,*) xi,',',t(i)
      write(13,*)  xi, ',', pav(i)
 531   continue
        ENDIF
  100 continue
     continue
     continue
  c
  75 write (10,510) itime, t(1), t(ix), t(iy), t(iz) , t(n)
  c rise in mean bulk temperature
    tdiff = tmb - tini
  c process time in min
       ptime = time/60
  c
         write(12,*) 'time',',',itime
      do 533  i=1,n
  c   do 534j=1,m
            write(13,*) a(i,n2+1),a(i+n,n2+1)
          xi = dz*(i-1)
  c    write(12,*) xi, yi, (t(i,j))
      write(12,*) xi,',',t(i)
  c 534 continue
   533   continue
   c
```

```
 c rise in mean bulk temp.
         TDIFF =  TMB - TINI
 c process time
         PTIME = TIME/(60)
         write (10,512) tmb
         WRITE (10,515) TDIFF
         WRITE (10,520) PTIME
 76        write(10,*) ' analysis is completed'
 c
         tpabs = 0
       do 83 i=1,n
        tpabs = tpabs + pav(i)
 83     continue
 c          tpabs = tpabs*dy
         pabs = tpabs*ar
       write (13,*) 'power absorbed W/m^2 & W ' , tpabs, pabs
       pref = pnot/enot**2 *((a(1,n2+1)-enot)**2 + a(1+n,n2+1)**2)
       pnot1 = pref + tpabs
 c        er1  =  (pnot-pnot1)*100/pnot
 c       write(13,*)'az,n,d,delt,enot,rmu,epsilon,omega,c1,c2'
 c        write(13,*) enot,rmu,epsilon,omega
          STOP
 c
 c400   FORMAT(  'STEADY-STATE TEMP. DISTRIBUTION FOR SLAB')
 410   FORMAT(///'TRANSIENT ANALYSIS FOR 1-d SLAB'///)
 412   FORMAT(///'=====================================================
    +=========')
 420   FORMAT(      ' TIME        T(1)       T(2)       T(3)       T(4)
    +     T(5)')
 499   FORMAT(////'WARNING-PROCESS INCOMPLETE'//)
 999   FORMAT(////'WARNING-INSTABILITY DUE TO TIME-STEP'////)
 501   format(i4,3x,5f10.2)
 510   FORMAT (i6, 3X, 5F10.2)
 512   FORMAT(/'  Mean bulk temp. =',F10.2, '  Deg.C')
 515   FORMAT(/'  Temp.rise       =',F10.2, '   Deg.C')
520   FORMAT (//' Process time   =',F10.2, '   min'//)

   subroutine setmat(cond,diff,tstep,tamb,dy,h1,hn,n,paw,
  +       t,a1,b)
c
      dimension pav(nx),t(nx),a1(nx,3),b(nx),a1(nx,3)
         nm1 = n-1
  c f=0.5 for crank-nicolson)
  c for 2-d put f=1 for y-direction at ld=1and f=0 for x=direction to
  c obtain setmat1
  cfor ld=2 put f=0 for y-direction and f=1 for x=direction to obtain
  csetmat2
         f   = 0.5
         fm1 = 1-f
  c
  c  l.h.s matrix
  c surface node (1)
         a1(1,1)  = -f*h1*diff(1)/cond(1)
         a1(1,2) = f*( h1*diff(1)/cond(1) + diff(1)/dy) + dy/(2*tstep)
         a1(1,3)  = -f*diff(1)/dy
  c inner nodes
      do 50 i=2,nm1
```

```
          al(i,1)  = -f*diff(i)/dy
          al(i,3)  = al(i,1)
          al(i,2)  = 2*al(i,1) + dy/(2*tstep)
  50    continue
  c surface node (n)
c
     al(n,1)  = al(1,3)
     al(n,2)  = f*(hn*diff(n)/cond(n) + diff(n)/dy) + dy/(tstep*2)
     al(n,3)  = -f*h1*diff(n)/cond(n)
  c r.h.s. matrix
  c surface node (1)
     a1(1,1)  = -fm1*hn*diff(1)/cond(n)
     a1(1,2)  = -fm1*(h1*diff(1)/cond(n) + diff(1)/dy) + dy/(tstep*2)
     a1(1,3)  =  fm1*diff(1)/dy
  c inner nodes
      do 55  i=2,nm1
     a1(i,1)  = fm1*diff(i)/dy
     a1(i,2)  = -2*a1(i,1) + dy/tstep
     a1(i,3)  = a1(i,1)
  55    continue
  c surface node (n)
     a1(n,1)  = al(1,3)
     a1(n,2)  = -fm1*(hn*diff(n)/cond(n)+diff(n)/dy) + dy/(tstep*2)
     a1(n,3)  = 0
  c multiply r.h.s matrix with old temp.vector and add source vector
  c inner nodes
      do 60 i=2,nm1
     b(i) = a1(i,1)*t(i-1)+a1(i,2)*t(i)+a1(i,3)*t(i+1) +
 +          pav(i)*diff(i)/cond(i)
  60    continue
  c surface node
     b(1) = a1(1,2)*t(1)+a1(1,3)*t(2) + (pav(1)+
 +  h1*tamb)*diff(1)/cond(1)
         b(n) = a1(n,1)*t(n-1)+a1(n,2)*t(n) +
  +             (pav(n)+hn*tamb)*diff(n)/cond(n)
  c
  c
      return
      end

  c subroutine tridia (a,b,c,n)
  c this subroutine solves the system of tridiagonal equations
      do 89 i=2,n
         delt   = a(i,1)/a(i-1,2)
         a(i,2) =a(i,2) -a(i-1,3)*delt
         b(i)   = b(i) -b(i-1)* delt
  89   continue
  c back substitution
         c(n) = b(n)/a(n,2)
  c         print*, c(n)
       do 55 i=2, n
          j=n-i+1
         c(j)= (b(j)-a(j,3)*c(j+1)/a(j,2)
      print *, c(j)
  55    continue
     return
     end
```

```
      SUBROUTINE GAUSS(n1,N,M,MN,A,DELT)
C  *  FUNCTION: this subroutine computes the solutions for m  *
C   *            systwms with n equations and n unknowns using *
C  *            gaussian elimination                          *
C  *       :                                                  *
C  *                        call GAUSS(n,m,a,delt)            *
C  *  PARAMETERS:                                             *
C  *            :                                            *
C  *           n=number of equations and unknowns            *
C  *           m=number of systems r.h.s vectors)            *
C  *           nm=m+n                                        *
C  *           a=n by m+n array of coefficients augmented with*
C  *           each r.h.s vector                             *
C  *         delt = machine zero tolerance                   *
C  *       OUTPUT:                                           *
C  *         a(1,n+j),...,a(n,n+j)                           *
C  *             =solution of the j-th system (j=1,...,m)    *
C  ***************************************************************
      dimension a(n1,mn)
      if n..gt.1) then
      DO 1 k=1,n-1
      u=abs(a(k,k))
      kk=k+1
      in=k
C        *** search for index-in of maximum pivot value ***
c           print *, 'working'
            DO 2 i=kk,n
               IF(abs(a(i,k)).gt.u) then
                  u=abs(a(i,k))
                  in=i
               end if
    2       contiune
            if(k.ne.in) then
C        *** interchange rows-k and index-in ***
c            print *, 'changing'
             DO 3 j=k,m+n
                  x=a(k,j)
                  a(k,j)=a(in,j)
                  a(in,j)=x
    3          continue
            enf if
C        *** check if pivot too small ***
            if(u.lt.delt then
               write(*,4)
    4          format (2x'the matrix is singular gaussian'
     1                ' elimination cannot be performed.')
               return
            endif
C        *** FORWARD ELIMINATION STEP ***
               DO 5 1=kk,n
               DO 5 J=kk,m+n
                  a(i,j)=a(i,j)-a(i,k)*a(k,j)/a(k,k)
    5          CONTINUE
    1     CONTINUE
          if(abs(a(n,n)).lt.delt) then
             WRITE(*,4)
```

```
         return
       endifF
C     *** back substitution ***
       DO 6 k=1,m
          a(n,k+n)=a(n,k+n)/a(n+N)
          DO 6 ie=1,n-1
             i=n-ie
             ix=i+1
             DO 7 j=ix,n
                a(i,k+n)=a(i,k+n)-a(j,k+n)*a(i,j)
  7          continue
             a(i,k+n)=a(i,k+n)/a(i,i)
  6    continue
       return
     else if(abs(a(1,1)).lt.delt) then
       WRITE(*,4)
       return
     endifF
     DO 8 j=1,m
       a(1,n+j)=a(1,n+j)/a(1,1)
  8 continue
     return
     END

     SUBROUTINE datmat(N,Dy,Ar,VOL,TVOL)
c this subroutine sets the geometrical data and computes ;
c area, volume,volume for each node, depth Y from the top
c to the nodal boundary
      PRINT*, 'Enter dimensions of slab in mm'
      print*, 'length'
      read *, rlength
      print*, 'width'
      read *, W
      print*, 'thickness of each layer, mm'
      read *, y1,y2,y3
         Ar    = (W*rlength)*1E-6
      PRINT*, 'Enter nodal distance,mm'
      READ *, dynode
      l  = y1/dynode + 1
      lm = y2/dynode + 1
      n  = y3/dynode +lm
     depth = (y1+y2+y3)*1e-3
      dy   = dynode*1e-3
c dx   = dynode*1e-3
         VOL  = Ar*dy
         TVOL = Ar*depth
c
     RETURN
     END
```